Orienting Behaviours and Attentional Processes in the Mouse and Macaque: Neuroanatomy, Electrophysiology and Optogenetics

Michael Anthony Savage

Institute of Neuroscience, Newcastle University

Thesis submitted for the degree of Doctor of Philosophy

September 2016

Abstract

The neuronal basis of orienting and attentional behaviours has been widely researched in higher animals such as non-human primates (NHPs). However the organisation of these behaviours and processes in rodent models has been less well characterised. This thesis is motivated to delineate the key neuroanatomical pathways and neuronal mechanisms that account for orienting behaviours in the mouse model and compare them, in part, to those seen in the macaque. A better understanding of the processes and networks involved with attention and orienting is necessary in order to relate findings in the mouse model to those seen in humans and NHPs. Further to this, the availability of highly targeted manipulations in the mouse, such as optogenetics, requires a more detailed picture of the neurophysiology underpinning those behaviours to effectively interpret findings and design experiments to exploit these techniques and animal models for maximum benefit.

In this thesis, study one focuses on the neuroanatomical pathways that terminate in subregions of the midbrain superior colliculus (SC) in the mouse (*mus musculus*) using iontophoretic injection of the retrograde tracer fluorogold. This region has been implicated in various forms of orienting behaviours in both macaques and mice (Albano et al., 1982, Dean et al., 1988b, Felsen and Mainen, 2008). Furthermore study one examines the prefrontal connectivity that links to the SC subsections and which may govern approach and avoidance behaviours (motor cortex area 2 (M2) and cingulate area (Cg)) in the mouse via pressure injection of the anterograde tracer biotinylated dextran amine into these regions. It was found that the medial and lateral SC receive differential prefrontal input from the Cg and M2 respectively. And that these areas project to brain networks related to avoidance or approach. This section furthers our understanding of the partially segregated networks which exist in the prefrontal cortex and midbrain of the mouse, which are important in mediation of different orienting behaviours

Study two focuses on the effects of one type of orienting, namely bottom-up attention (BU) in visual areas. This exogenous (automatic) form of visual attention has been studied extensively in human psychophysics (Posner, 1980, Nakayama and Mackeben, 1989) and the areas involved in the human brain have been delineated using brain imaging (Corbetta and Shulman, 2002, Liu et al., 2005). To understand the neurophysiology involved, some electrophysiological invasive studies have been performed in the macaque monkeys,

(Luck et al., 1997, Buschman and Miller, 2007), but our understanding of the mechanisms involved is relatively sparse when compared to top-down (endogenous) attentional processing. To understand the similarities in this mechanism between macaques and mice it is therefore important to study both model systems using similar approaches. The research of this chapter aims to make direct comparisons between these two model species via electrophysiological recordings in a bottom-up attentional paradigm. It was found that in the macaque BU cues increased responses to visual stimuli in both V1 and V4, but no obvious pattern was seen in the mouse V1 and SC. This study goes some way in describing the similarities and differences in neural responses in visual areas of different species which are utilised for attention based paradigms

Finally study three focuses on linking the previous two studies. In study two we investigated bottom-up attentional processes, which are thought to involve early, fast visuomotor pathways. Whereas in study one we found that SC and V1, areas known for their involvement in and ability to coordinate rapid visuomotor responses, respectively, also receive clear and structured input from higher-level prefrontal areas. Therefore we hypothesized that stimulating these prefrontal areas could modulate bottom-up attention. This is achieved by using optogenetic stimulation of prefrontal control regions, such as Cg, identified in this research whilst preforming electrophysiological recordings in a bottom-up attentional paradigm. In V1 is was found that optogenetic stimulation had no effect on neuronal activation. However in SC optogenetic activation increased the sustained stimulus response, regardless of cuing condition. Taken together, this research further investigates some brain regions involved in orienting and attention in both mice and macaques and partially bridges the gap in understanding between these two animal models.

Acknowledgements

I would like to thank and recognise all of the people who have made it possible for me to complete this PhD. First and foremost I would like to thank my supervisors Alexander Thiele and Richard McQuade for their invaluable help, expertise and support over the course of the 4 years. They have been an amazing support and guidance in my early years in sciences. Without their advice I would not be where I am today.

I would like to thank the past and present members of the Thiele Group, Michael Boyd, Alwin Gieselmann, Christian Brandt, Helen Gray, Miguel Da Silva and Jochem van Kampen for their advice and help on every aspect of my work and much more.

I would like to thank the other members of ION, especially Zoltan Derszi and Daniel Erskine for their invaluable opinions and advice on everything. I would also like to acknowledge the help and support of the CBC staff for the technical assistance with the animals and equipment.

I would like to thank all of my friends from Newcastle and further afield for helping me enjoy myself so much in the city and for making my life so much more fun. I would especially like to mention all of the past and present members of the NUSRC, without whom Newcastle would not have felt like so much of a home for the 7 years I have been here.

I can never thank my family, my parents, Daniel, Conor, and Ash enough for the continued support and constant advice. Their enthusiasm and pride have keep me going and gave me the determination to stick it out over the course of the 4 years. And to someone was there at the start but is not here anymore, Lillian McKee, thank you for all you did.

Finally, I am eternally indebted to one particular person, Audrey. Who has put up with more than anyone should have to bear as I have worked through these 4 years. How you deal with me getting so stressed and caught up with the work I will never know. You have kept me grounded and sane more than I can ever thank you.

I set out at the beginning of this time to ‘seek the truth’ and with the help of everyone above I have accomplished that.

Table of Contents

List of Figures

List of Tables

Abbreviations List

AI	agranular insular cortex
AcbC	accumbens nucleus, core
AM	anteromedial thalamic nucleus
APT	anterior pretectal nucleus
Au1	primary auditory cortex
AVDM	anteroventral thalamic nucleus, dorsomedial part
AVVL	anteroventral thalamic nucleus, ventrolateral part
BDA	biotinylated dextran amine
BLA	basolateral amygdaloid nucleus, anterior part
Cg1	cingulate cortex, area 1
Cg2	cingulate cortex, area 2
Cl	claustrum
CL	centrolateral thalamic nucleus
CM	central medial thalamic nucleus
cp	cerebral peduncle
CPu(dl)	caudate putamen (striatum), dorsolateral
CPu(dm)	caudate putamen (striatum), dorsomedial
DLG	dorsal lateral geniculate nucleus
DP	dorsal peduncular cortex
DRV	dorsal raphe nucleus, ventral part
DTT	dorsal tenia tecta
ECIC	external cortex of the inferior colliculus
Ect	ectorhinal cortex

FG	fluorogold
GP	globus pallidus
HDB	nucleus of the horizontal limb of the diagonal band
IAD	interanterodorsal thalamic nucleus
IP	interpeduncular nucleus
LDDM	laterodorsal thalamic nucleus, dorsomedial part
LDVL	laterodorsal thalamic nucleus, ventrolateral part
LH	lateral hypothalamic area
LHb	lateral habenular nucleus
ll	lateral lemniscus
LO	lateral orbital cortex
LPLR	lateral posterior thalamic nucleus, laterorostral part
LPMR	lateral posterior thalamic nucleus, mediorostral part
LPtA	lateral parietal association cortex
LS	lateral septal nucleus
M1	primary motor cortex
M2	secondary motor cortex
MDL	mediodorsal thalamic nucleus, lateral part
MnR	median raphe nucleus
MO	medial orbital cortex
MPtA	medial parietal association cortex
mRt	mesencephalic reticular formation
MS	medial septal nucleus
PAG	periaqueductal gray
PBG	parabigeminal nucleus
PC	paracentral thalamic nucleus

PCom	nucleus of the posterior commissure
PLH	peduncular part of lateral hypothalamus
PMnR	paramedian raphe nucleus
Pn	pontine nuclei
Po	posterior thalamic nuclear group
Post	postsubiculum
PR	prerubral field
PRh	perirhinal cortex
PrL	prelimbic cortex
PT	paratenial thalamic nucleus
Re	reuniens thalamic nucleus
RSD	retrosplenial dysgranular cortex
RSG	retrosplenial granular cortex
Rt	reticular nucleus (prethalamus)
S1BF	primary somatosensory cortex, barrel field
S1FL	primary somatosensory cortex, forelimb region
S1HL	primary somatosensory cortex, hindlimb region
S1Tr	primary somatosensory cortex, trunk region
SC(l)	superior colliculus, lateral part
SC(m)	superior colliculus, medial part
SNCD	substantia nigra, compact part, dorsal tier
SNR(dl)	substantia nigra, reticular part, dorsolateral
SNR(vm)	substantia nigra, reticular part, ventromedial
STh	subthalamic nucleus
Sub	submedius thalamic nucleus
V1	primary visual cortex

V2L	secondary visual cortex, lateral area
V2ML	secondary visual cortex, mediolateral area
V2MM	secondary visual cortex, mediomedial area
VA	ventral anterior thalamic nucleus
VDB	nucleus of the vertical limb of the diagonal band
VL	ventrolateral thalamic nucleus
VM	ventromedial thalamic nucleus
VMH	ventromedial hypothalamic nucleus
VO	ventral orbital cortex
VPM	ventral posteromedial thalamic nucleus
ZID	zona incerta, dorsal part
ZIV	zona incerta, ventral part

Chapter 1. General Introduction

Neuroscience aims to understand the mechanisms the brain uses to extract information from the external world, and the mechanisms that enable subjects to act upon the external world. This task is accomplished by processing signals and cues from the environment and constructing or generating internal mental states relating to the exogenous enviroment. A central objective is the extraction of salient cues and relevant information from the overabundance of information which surrounds us. One cognitive process that performs this function is generally known as attention. Attention is one of the primary mental processes for many forms of sentient life. For example, attentional processes allow animals to hunt for prey and aid in the detection of predators in the animal's natural environment. At a higher cognitive level, attentional processes are necessary for humans to complete a plethora of everyday tasks, from brushing teeth to avoiding moving vehicles when crossing the street.

One cognitive activity heavily linked to attention is orienting. Orienting can be thought of as an externalisation of attentional processes towards stimuli and events which relate to current internal states. This thesis focuses on the role and biological basis of the different orienting behaviours which have been observed in the mouse and the comparison of neurophysiological signatures of a specific type of orienting behaviour (bottom-up attention) in mouse and macaque primary visual cortex. This work partially bridges the gap in the understanding of attention and orienting behaviours in these widely used animal models. Specifically this thesis will cover:

- The neuroanatomical basis of different orienting behaviours which have been characterised in the rodent by means of neuronal tracing of both midbrain and prefrontal areas in the mouse
- The similarities and differences in the visual cortex responses in both macaques and rodents to bottom-up attentional stimulation
- The effects of optogenetic activation of these prefrontal areas on visual responses in the mouse

The introduction covers the fundamental concepts central to this thesis, such as the descriptions of analogous orienting and attentional mechanisms in lower organisms and the nature of these behaviours in both mice and macaques. The literature regarding some of brain areas involved in the generation of orienting and attention will be examined. In addition it presents a rationale for usage and an explanation of the mechanisms of the methodologies employed, such as neuronal tracers and the use of optogenetics.

Subsequent chapters will outline the generalised methods and procedures utilised for this research, and look at the literature, results and discussion pertaining to each portion of research. This is followed by a general discussion of the findings in terms of their relation and importance to the existing literature.

1.1 Origins of Attention and Orienting: the progression from simple to complex mechanisms

1.1.1 Tropisms and Taxes in Simple Life Forms

In order to fully comprehend the importance of the study of attention and orienting in higher order animals it must be noted how wide-spread similar phenomena are in lower forms of life. Orienting towards or away from positive or negatively valenced stimulus is essential for all types of organisms. In botany these responses are referred to as ‘tropisms’, and these are responsible for a number of the characteristic reactions observed in the plant kingdom. These include the attraction of seedling shoots towards light (phototropism) (Whippo and Hangarter, 2006), or guiding root systems towards deeper ground in search of water (geotropism) (Kiss et al., 1989).

In bacterial species such as e.coli a number of ‘taxes’ have been categorised. Such taxes are distinct from tropisms due to the ability of these organisms to move in response to the stimulus. These taxes have included movement towards food sources or away from harmful stimuli (chemotaxis) (Wadhams and Armitage, 2004), movement towards or away from light (phototaxis) (Sprenger et al., 1993) and others. Both tropisms and taxes, although they seem similar to the orienting behaviours observed in higher order animals, are more akin to automatic mechanisms which occur in direct response to the stimulus properties without any internal mental representation (Pisula et al., 2013). However, they

do highlight the idea that orienting to the environment around an organism is an extremely fundamental function of any living organism.

1.1.2 Orienting Processes

Orienting behaviours in animals equipped with a cerebrum are significantly more complex, and are accompanied by greater behavioural flexibility, compared to those seen in lower organisms. But even here, at its simplest level, orientation requires stimulus evaluation in terms of its significance and valence to the animal. This requires channelling of sensory information to association areas and motor areas, thus mediating goal directed behaviours (Felsen and Mainen, 2008, Erlich et al., 2011, Felsen and Mainen, 2012, Guo et al., 2014).

Orienting behaviours were first categorised by Pavlov in his classical conditioning studies. In these experiments he noticed that the animals could get distracted by an unexpected or novel stimulus, which would elicit an orienting response or a 'Что такое?' or 'What is it?' response (Pavlov, 1927, Zernicki, 1987). Although Pavlov identified these behaviours they were not fully examined at that time. These orientation behaviours were first examined in greater detail in classical habituation experiments where a stimulus was presented to an animal without any behavioural consequences until no further overt response could be observed (Groves and Thompson, 1970). Building on this, the conditioning experiments by Thorndike examined orienting responses in terms of instrumental conditioning, whereby animals learn about the consequences of their behaviour. This technique sought to promote a relevant orienting response to a stimulus. In this manner the animal learned an association which was based on reinforcement of the correct orienting behaviours and actions towards the operant lever. He termed this process the "Law of Effect" (Thorndike, 1927).

The works of B.F. Skinner established that an animal would not only associate the primary orienting action with reward or punishment but also to any stimulus that could be associated with an experimental response. For example an animal would not only orient towards a food reward, but also to any stimulus which was associated with, and predictive of a reward. If a stimulus or action was associated with a negative effect the animals would learn escape and avoidance behaviours. The neural basis of these behaviours was then investigated in many neuroscientific studies through physical or chemical

perturbations of specific brain areas. These studies revealed midbrain and prefrontal areas in rodents to be essential in such orienting processes (Cowey and Bozek, 1974, Midgley and Tees, 1981, Sahibzada et al., 1986). These results have been matched with similar findings in the macaque (Goldberg and Wurtz, 1972a, Schiller et al., 1987, Moore and Armstrong, 2003)

Orienting responses are often dependent on attentional state and internal motivational state (Sul et al., 2011, Manita et al., 2015). Animals in decision making tasks will make an association to any stimulus correlated with upcoming reward outcomes and thus can develop complex goal directed behaviours. These goal directed actions are subject to a variety of internal states such as satiety and reward association. These processes can be flexible to shifts in saliency and are constantly evaluated to incorporate the most recent information received and behavioural outcomes (Joshua and Michael, 2007).

1.1.3 Approach vs Avoidance

Approach and avoidance occur in response to both novel/unexpected or learned stimuli which have behavioural relevance to the animal. They can be triggered by any sensory modality, e.g. the sight, sound, or smell of an approaching predator or prey.

This thesis will focus primarily on visually based orienting. In rodents this largely falls into two categories, namely positively valenced approach related and negatively valenced avoidance related behaviours. In the natural environment prey/food related cues prompt approach and feeding behaviours, while avoidance responses are elicited by noxious stimuli or stimuli signalling threat and danger. Due to the ethological niche most rodents occupy, these different behaviours are elicited by stimuli which appear in specific regions in the external environment in relation to the animal. Predators usually appear from above, and thus the upper visual field represents a region where danger lurks and stimuli there might more easily trigger avoidance responses (Wei et al., 2015). Conversely, food cues and other positive stimuli (such as pups) are more likely to appear in the lower visual field (Furigo et al., 2010, Favaro et al., 2011), and stimuli in those locations would thus more easily trigger approach responses.

Historically, the neurological and biological basis of these orienting behaviours have been examined through the use of large scale lesion and stimulation studies which identified the importance of both prefrontal areas and midbrain areas in controlling and modulating

these behaviours. Stimulation or removal/inhibition of specific prefrontal regions elicit or inhibit either approach or avoidance behaviours (Gabriel et al., 1991, Calejesan et al., 2000, Erlich et al., 2011, Guo et al., 2014). Similar procedures applied to the midbrain showed that both approach and avoidance behaviours depend on superior colliculus activity (Goodale and Murison, 1975, Sahibzada et al., 1986, Felsen and Mainen, 2012, Wei et al., 2015). The exact brain areas and mechanisms responsible for this will be covered in greater detail in Chapter 3.

1.1.4 Attention

Sensory orienting behaviours to external events often involve some form of attention, although attention is not always involved. For example an orienting reflex such as the nociceptive withdrawal reflex does not require attentional involvement, even if such orientation can be modulated by directed attention (Bjerre et al., 2011). Attentional processes simultaneously increase neuronal responses to the attended stimulus whilst inhibiting responses to other non-salient cues (Moran and Desimone, 1985). Broadly speaking there are two forms of attention which can be deployed depending on the characteristics of the situation, Exogenous (bottom-up) attention and Endogenous (top-down) attention (Posner, 1980, Nakayama and Mackeben, 1989, Theeuwes, 1991).

Bottom-up attention arises from unexpected salient cues in the external environment, i.e. a warning call, or for humans, a police siren. These cues have an unexpected onset and location, and draw attention to the point of origin in an automated manner and focus subsequent mental processing on that external location. Exogenous attention operates in a quick, bottom–up signal transmission manner, where the fast processing speed can allow an animal to make the appropriate rapid response, e.g. avoid predation (Carretie, 2014). It has a transient, short time course which decays to allow control of attention to be reasserted in top-down manner. This short time course is, in part, caused by the process of inhibition of return, which suppresses the visual response to a stimulus which is repeated or constant over a very short latency and promotes the saliency of novel stimuli (Posner and Cohen, 1984).

Conversely, top-down or endogenous attention is a central mechanism activated by goal directed behavioural processes, such as searching through a crowd for a particular face. The process originates internally, and operates in a top-down manner, whereby the current

emotional, physical, or cognitive state influences the features of the sensory field which the subject attends to. This mechanism is utilised for complex mental procedures requiring responses based on salient or non-salient cues which are differentiated from distracter cues by deploying attentional processes (Chica et al., 2013). Top-down attention can be sustained for a very long time and allows an organism to focus on the behaviourally relevant cues or stimuli in the environment and the changing nature of these cues.

The neuronal networks involved in the deployment of attention in humans and other primates are complex and are believed to arise from the coordinated activity of multiple prefrontal brain regions, which interact with more posterior cortical and primary sensory regions and sub-cortical output pathways which are routed through the midbrain and brain stem. (Schiller, 1977, Schiller et al., 1987, Tu and Keating, 2000). Top-down and bottom-up attention utilise partially overlapping, but also somewhat segregated brain networks (Corbetta and Shulman, 2002) which interact during normal vision (McMains and Kastner, 2011). Top-down attention is routed through the dorsal fronto-parietal network. As the name suggests this pathway includes prefrontal regions such as the frontal eye field (Schall, 2004), the dorsolateral prefrontal cortex (Buschman and Miller, 2007), regions of the parietal cortex such as the lateral intraparietal area (Bisley and Goldberg, 2003). A general summary of this network can be seen in Figure 1-1. This network works in a bilateral manner to analyse visual features and stimuli which are important to the current goals of the animal (Corbetta and Shulman, 2002). As such it interacts with sensory areas within the fronto-parietal network, where it alters stimulus processing. Top-down attentional modulation has, for example, been described in the striate (Roelfsema et al., 1998) and extrastriate cortex (Moran and Desimone, 1985) as well the as the midbrain Superior Colliculus (SC) (Goldberg and Wurtz, 1972a).

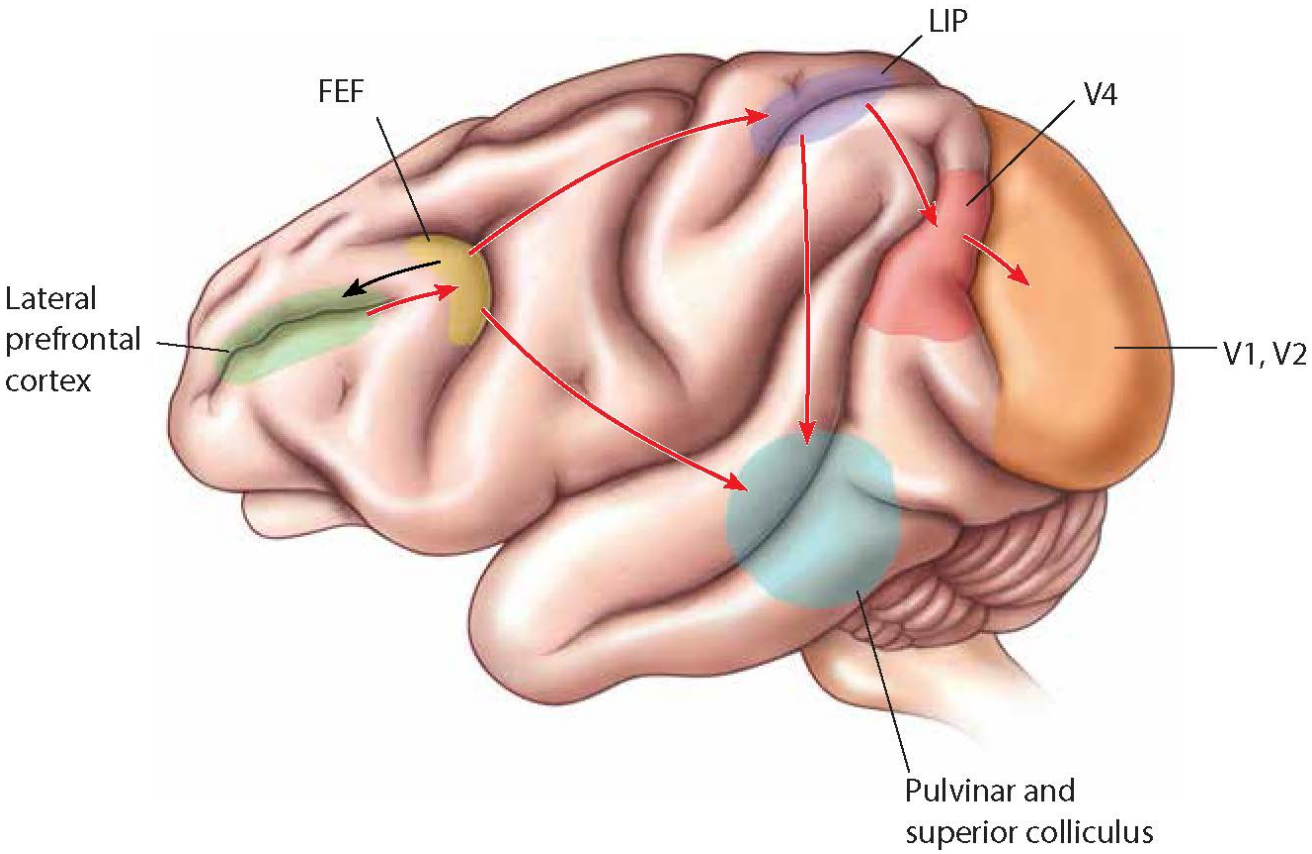

Figure 1-1. Basic Summary of the Fronto-Parietal Attentional Network in the Macaque

The frontoparietal network is a very complex arrangement of a variety of cortical and subcortical brain regions. Herein, red arrows indicate feedback signalling and black indicates feedforward signalling. However in reality this arrangement is for more complex with both feedback and feedforward signals arising from and between multiple brain regions. It must be noted that the pulvinar and superior colliculus are both subcortical areas and the teal circlar demarcation referes to the overall location underneath the cortex. Adapted from Neuroscience Exploring the Brain 4th edition.

Bottom-up attention is achieved through a somewhat different network, which is lateralised to the right hemisphere (in humans) and involves the ventral fronto-parietal network. Despite its segregation, bottom-up attention is known to interact with areas involved in top-down control (Buschman and Miller, 2007). This network includes more ventral portions of the frontal cortex such as the middle and inferior frontal gyrus

(Corbetta et al., 2008), the more lateral portions of the parietal cortex like the inferior parietal lobule and the superior temporal gyrus (Astafiev et al., 2006). This networks also interacts with regions of the striate and extrastriate cortex as well the as the SC (Luck et al., 1997, Müller et al., 2005). This network responds to unexpected exogenous stimuli which have a high likelihood of being behaviourally relevant (Corbetta and Shulman, 2002).

These partially segregated brain networks work in cooperation to produce complex attentional and sensory orienting behaviours which allow animals to act appropriately in everyday environments. This thesis will mainly focus on bottom-up attention, as it may trigger the basic orienting behaviours described above.

1.1.4.1 Overt vs Covert Attention

In addition to the distinction between top-down and bottom-up forms of attention, attention can be deployed in terms of overt and covert attention. Overt attention brings an object into optimal position for sensory evaluation, in humans and macaques this process is known as foveating (Schütz et al., 2009). Foveating is achieved via the use of discrete eye movements called visual saccades which bring a visual stimulus onto the foveal visual receptive field. The existence of saccades was first discovered in the 1800s by a number of scientists (von Helmholtz, 1867, Javal, 1879). They observed that during reading the eye did not move in a continuous fashion, but moved in discrete fast movements which were termed ‘saccades’ by Javal.

Visual saccades are defined as rapid purposeful eye movements across the visual field, which are related to current goals or behavioural contexts (Yarbus, 1967, Hoffman and Subramaniam, 1995). Saccades are a means of moving the object of interest to an area of the retina which has the highest photoreceptor density, known as the fovea in primates, (Becker, 1989, Melcher and Kowler, 2001).

However, for animals that do not have a fovea such a rodents, eye movements are not a reliable measure of overt attention. This is due to a lack of the high density of photoreceptors in their eyes. Instead, they tend to perform overt orienting actions with their whole bodies, or specific body parts such as moving their heads and torsos (Dean et al., 1986, Sahibzada et al., 1986, Dean et al., 1988a). By doing this they bring the stimulus which is the object of their attention into a more optimal position for sensory decoding, for

example more centrally for binocular viewing. The major function of eye movements in rodents has been shown to be maintenance of binocular evaluation for monocular representations which do not fuse, in the frontal and upper portions of the visual field; thereby ensuring stimuli appearing in those regions are better processed for visual evaluation and behavioural response (Wallace et al., 2013).

Brain regions that have been heavily linked to the formation and excitation of saccades and other orienting movements are the frontal eye field (FEF) and the superior colliculus (SC). In primates the SC has been shown to mediate all saccadic movements. Electrical stimulation of this region causes saccadic movements with defined endpoints, relative to a retinotopic map in the region (Schiller and Stryker, 1972). These movements can be inhibited and disrupted by pharmacological inactivation of the appropriate retinotopic locations (Hikosaka and Wurtz, 1985). In rodents similar orienting behaviours can be elicited by stimulation of prefrontal regions such as the motor cortex area 2 and the SC. These stimulations result in body orienting movements (Sinnamon and Galer, 1984, Dean et al., 1986). These regions will be covered in greater detail below.

In contrast to overt attention, covert attention does not require any specific orienting action. The ability to direct attention to areas of the visual field without eye movement was first described in the 1800s and it was shown that directing attention to one part of the visual field increased accuracy of response in that region but decreased accuracy in other regions of the visual field (von Helmholtz, 1867). This covert form of attention was examined in detail in the 1980s by Posner. He discovered that attention could be directed by both exogenous and endogenous cues when a subject was central fixating. Reaction times to detect a visual stimulus were reduced when a valid exogenous cue was given, conversely when an invalid cue was given, reaction times increased. Reaction times were also reduced when the subject was given a prompt to attend to a particular stimulus type (Posner, 1980).

One prominent theory, the premotor theory of attention, offers an explanatory framework for the linkage between covert and overt attention. This theory states that covert attentional signals are analogous to uninitiated saccade motor activity. This theory was founded on research that described saccade latencies to targets in different parts of the visual field. If, during central fixation, an invalid cue preceded visual target appearance in the opposite hemifield, the saccade latencies were longer than that of valid or invalid cues to the same hemifield. This suggested that attention prepared the motor programme for eye

movement before saccadic onset. Therefore if the motor programme was incorrect, reprogramming would be necessary, causing a higher latency (Rizzolatti et al., 1987). In addition, human subjects display reduced accuracy in saccade tasks when attention is directed towards a different part of the visual field than the saccade target (Kowler et al., 1995). These findings suggest that motor planning underpins the evolution of attentional behaviours.

Electrophysiological evidence also concurs with this theory. If one of the prefrontal attention controlling areas, the FEF is microstimulated with very low currents, covert attentional shifts will occur to a defined region of the visual field. Consequently, task accuracy will be increased in the retinotopic location of the stimulation during a target discrimination (Moore and Fallah, 2001). In addition, microstimulation of FEF will cause enhancement of visual responses in retinotopically matched V4 neurons (Moore and Armstrong, 2003). However, if the stimulation current is increased, then saccades to the retinotopic location will occur (Moore and Fallah, 2004). Similar findings have been observed in the midbrain area SC of the macaque, where accuracy of visual discrimination is increased when the subregion within the SC coding for a target location is electrically stimulated with subthreshold currents, too low for saccade initiation (Müller et al., 2005). Taken together this evidence suggests that the mechanisms which guide covert attention shifts also guide overt orienting behaviours such as saccades.

1.2 Brain Regions Involved with Orienting

As this thesis is very much concerned with the specific neuroanatomical basis and function of a number of cognitive behaviours and processes, below the key areas investigated in this work are described in terms of the brain connectivity and functional properties.

1.2.1 The Superior Colliculus

The Superior Colliculus (SC) is a multimodal sensory-motor midbrain structure, involved in visual, auditory and somatosensory triggered orienting (Stein, 1981, Westby et al., 1990, Meredith et al., 1992, Wallace et al., 1993, Thiele et al., 1996). This area is highly conserved across vertebrate species (Stein, 1981, King, 2004). In birds, reptiles, amphibians and fish, this region is known as the optic tectum. The optic tectum in these animals comprises a large portion of the brain. This is the major visually responsive area

which is intrinsically linked with visually guided and sensory orienting behaviours in birds (Knudsen et al., 1993), reptiles (Stein and Gaither, 1981), amphibians (Ingle, 1970) and fish (Meek, 1983). In these animals, which do not have a cerebral cortex, this area is the principal region for sensorimotor integration. It is vital for a range of critical orienting behaviours, such as predator evasion and predatory hunting (Ingle, 1975, Newman et al., 1980, Hoglund et al., 2005, Wylie et al., 2009).

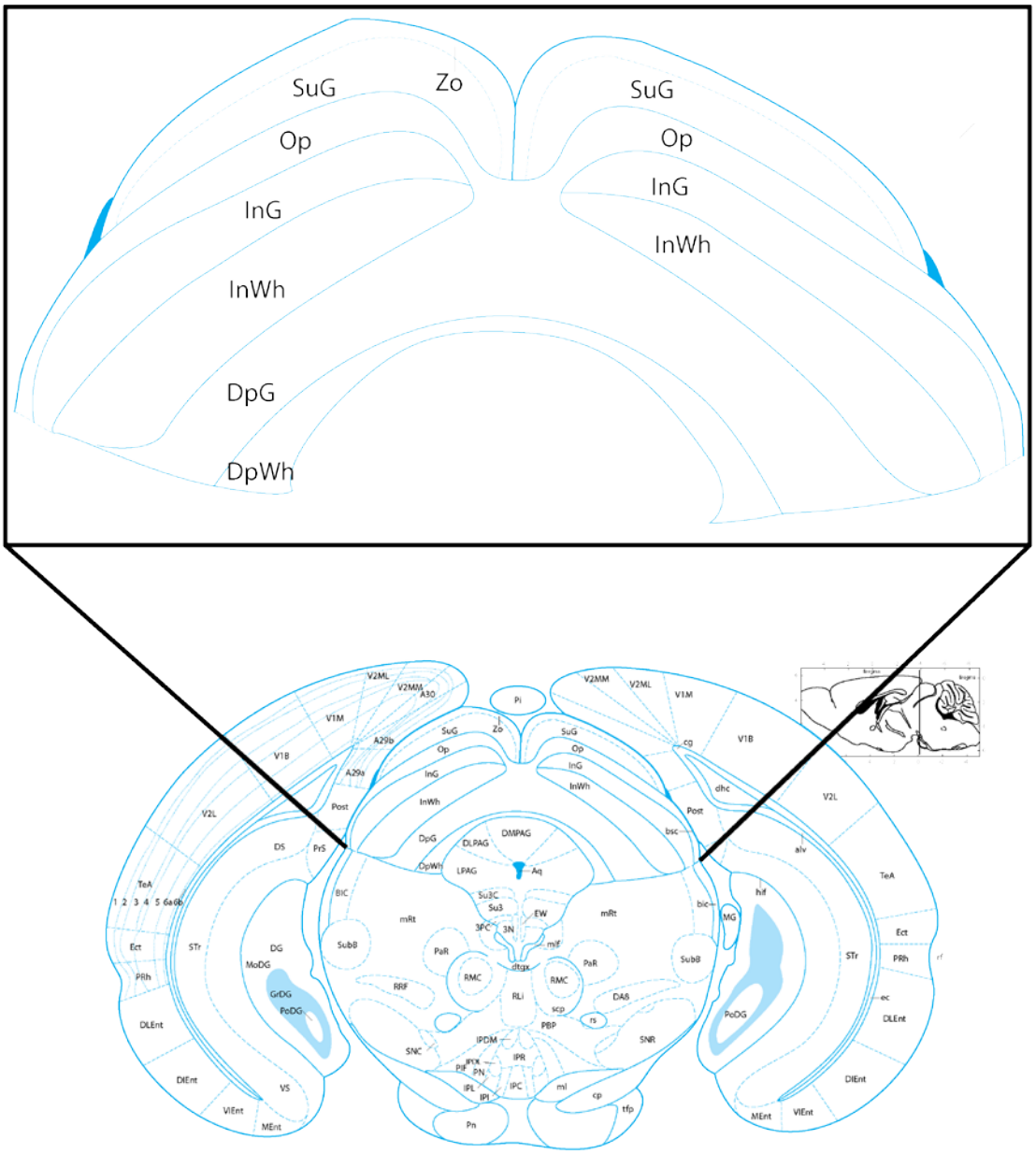

Figure 1-2. Gross Anatomy of the Murine Superior Colliculus

Stereotactic coronal view of mouse superior colliculus according to Franklin & Paxinos 2012. Zo-zonal layer of SC or stratum zonale, SuG-superficial layer of SC or stratum griseum superficiale, Op-optic nerve layer of SC or stratum opticum, InG-intermediate gray layer of the SC or stratum griseum intermediale, InW-intermediate white layer of SC or stratum album intermediale, DpG-deep gray layer of SC or stratum griseum profundum, DpWh-deep white layer of SC or stratum album profundum.

In higher animals, such as mammals, the SC is located just under the cortex in the midbrain and consists of seven layers. Each of the seven layers of the SC has a well-defined function and cortical connectivity. Functionally these layers fall into three categories; the stratum zonale, the stratum griseum superficiale and the stratum opticum form the superficial layers, the stratum griseum intermediale and the stratum album intermediale form the intermediate layers, and the stratum griseum profundum and the stratum album profundum form the deep layers of the SC which are shown in Figure 1-2. The three subdivisions receive information from all senses, barring olfaction. This sensory information is mapped onto the SC area in a topographic manner, whereby topographic maps of different sensory modalities overlap (in register) to produce a coherent representation of the sensory environment (Stein et al., 2014).

The superficial layers of the SC receive visual information through direct retinal connections. In rodents these direct retinal connections comprise 70-80% of the projections from the retina and terminate bilaterally onto the SC, with a contralateral bias (Chalupa and Thompson, 1980, Vaney et al., 1981, Hofbauer and Dräger, 1985). In macaques this percentage is far lower. Approximately 10% of retinal ganglion cells project to the SC (Perry and Cowey, 1984). In the intermediate and deep layers the sensory input becomes multimodal, with incoming signals arriving from the somatosensory, auditory areas, and motor planning areas. In fact, within the deep layers of macaque SC, a topographical motor map of movement vectors has been observed, that correlates with the visual map within the superficial layers (Goldberg and Wurtz, 1972b, Robinson, 1972, Schiller and Stryker, 1972). The motor map is related to eye and head movements in both macaques (Freedman et al., 1996) and cats (Paré et al., 1994). Additionally a gaze-related

coordinate system for reaching actions in the macaque has been identified (Stuphorn et al., 2000). No direct olfactory connections to the SC have been reported, however secondary odour areas project onto the SC (Neafsey et al., 1986).

The diverse sensory information converging onto a single area makes the SC an ideal sensory integrator. In most animals there is evidence for overlapping sensory maps throughout the layers of the SC with spatial receptive fields that are in register between sensory modalities (Meredith and Stein, 1990, Wallace et al., 1996). These overlapping sensory maps help animals to associate differing modalities of sensory cues with the corresponding objects in their environment, e.g. so that the visual picture of another animal and any noises it may make are processed as a single entity situated in the external world (Meredith et al., 1992, Wallace et al., 1993). However, in certain conditions these different sensory maps may not be fully aligned, either by deliberate experimental mismatch, or as a result of internal misalignment caused by single sensory orienting (eye or pinna movements). If there is a deliberate mismatch in either temporal or spatial field, the response to the stimuli in the SC can be reduced, conversely if they are concurrent there can be large potentiation of responsiveness (Wallace et al., 1996). However, if internal misalignment causes multisensory mismatch then other externally based senses can change receptive field conformation and bring the integrated map back into alignment (Jay and Sparks, 1987, Peck et al., 1995).

The role of the SC as a sensory integrator throughout the vertebrate kingdom makes it an ideal candidate to be involved in, or mediate, complex behaviours. A number of different methodologies have been employed to study this issue.

Microstimulation of the SC in the rat produces a variety of complex behaviours including approach, rearing behaviour and freezing-fear behaviours (Sahibzada et al., 1986). Previous research has suggested that these behaviours could be mapped to different parts of the SC; with investigative/approach behaviours arising from caudal-lateral stimulation whereas aversive/fearful behaviours from rostral-medial stimulation (Dean et al., 1986, Dean et al., 1988b). However these responses were not completely segregated within those subregions (Sahibzada et al., 1986).

Lesions of the SC in rodents and NHPs can lead to contralateral hemispatial neglect, where sensory cues do not elicit orientation behaviours (Kirvel et al., 1974, Albano et al.,

1982). Furthermore, such lesions produce deficits in approach behaviours (Goodale and Murison, 1975, Midgley and Tees, 1981) while a pharmacological blockade of the SC inhibited fear induced startle behaviours (Zhao and Davis, 2004). In addition, other lesion and inhibition studies of this brain region have produced analogous effects to those which are seen in NHP inactivation of the SC (Stryker and Schiller, 1975, Dean et al., 1986). The similarity between lesions of this midbrain region and lesions of prefrontal areas associated with goal directed orienting (frontal eye field (Schiller et al., 1987)), (frontal orienting field (Felsen and Mainen, 2008)) in both NHPs and rats suggest that certain orienting and decision making processes are routed through the SC, and therefore cannot occur when it is removed.

Electrophysiological studies have shown that SC activity can be correlated with upcoming behavioural choices in sensory discrimination tasks (Felsen and Mainen, 2012, Stubblefield et al., 2013).This indicates the importance of the SC in the recognition and response to external stimuli. One study utilising genetic based interventions has also supported these findings, confirming the role of the SC in the active perception of sensory information in space contralateral to the lesion (Stubblefield et al., 2013). All of this information, taken together, supports a strong case for the SC being intrinsically involved in the generation of decision outcomes in cognitive tasks and orienting behaviours to positively and negatively associated stimuli.

In the past, most research has focused on the SC as a whole. This approach may have obscured some critical distinctions at the subregional level. For example, recent research (Comoli et al., 2012) has shown that subregions within the rat SC may be preferentially involved with approach or avoidance behaviours. These studies suggest that the medial side is more heavily involved in fear related avoidance behaviours while the lateral side is more heavily involved in appetitive related approach behaviours. These observations make sense when considering the rodents' specific ethological niche. For most rodents, predators are more likely to occur in the upper visual field, and prey are more likely to occur in the lower visual field. This is coupled with the well documented retinotopy in the rodent SC, where the medial/anterior subregion codes for the upper visual field, and the lateral/posterior subregion codes for the lower visual field (Ahmadlou and Heimel, 2015). Furthermore there are specific neural connectivity patterns of these subdomains. For example, the ventromedial hypothalamic nuclei, involved with fear responses, project

exclusively to the medial SC, while the barrel cortex, involved in appetitive whisking projects exclusively to the lateral SC (Comoli et al., 2012). The full extent and importance of this functional segregation will be discussed later in Chapter 3.

1.2.2 Motor Cortex Area 2

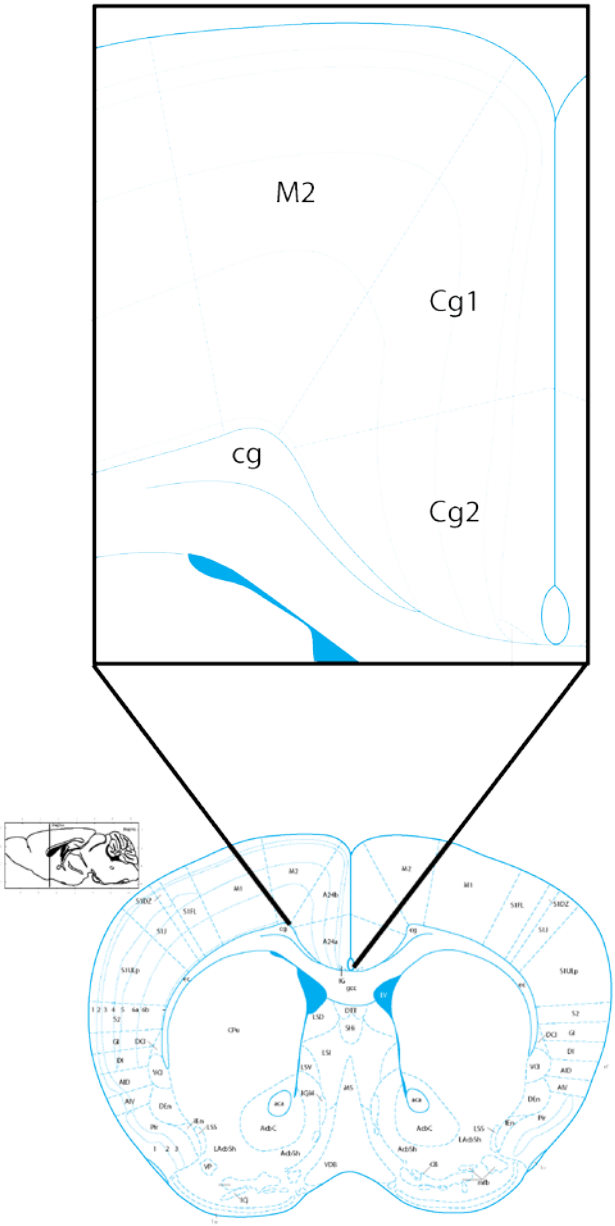

Figure 1-3. Gross Anatomy of the Murine Motor Cortex Area 2 and Cingulate Area

Stereotactic coronal view of mouse superior colliculus according to Franklin & Paxinos 2012. M2-Motor Cortex Area 2, Cg1-Cingulate Area 1, Cingulate Area 2.

The Motor Cortex Area 2 (M2) is a medial prefrontal area found in the rodent cortex. It is a preparatory motor area involved in motor planning, learning and decision related activity (Erlich et al., 2011, Sul et al., 2011, Guo et al., 2014, Manita et al., 2015). The region sits in the dorsal portion of the medial cortex and comprises five separate layers, which are shown in Figure 1-3. This region of the cortex is agranular, and therefore lacks the traditional layer 4 (Brecht et al., 2004). These layers receive and project to a diverse number of targets throughout the brain. Layer 2/3, and 5 pyramidal cells project to other regions in the cortex, layer 5 sends axons to subcortical structures such as the striatum, midbrain and the spinal cord and layer 6 pyramidal cells project to the thalamus (Thomson and Bannister, 2003, Brecht et al., 2004, Li et al., 2015, Jeong et al., 2016).

The function of this area has been under debate for some time due to the varied nature of the functional properties proposed by different investigators. These functional properties suggest roles in memory based discrimination tasks (Erlich et al., 2011), whisking and licking based decision tasks (Guo et al., 2014), and accuracy perception of somatosensory stimuli (Manita et al., 2015). The apparent complexity/diversity of properties has been further compounded by the wide diversity of taxonomy utilised to describe the same anatomical brain region in the literature (see Table 1-1) (Crowne and Pathria, 1982, Reep et al., 1987, Erlich et al., 2011, Chen et al., 2013, Guo et al., 2014, Oh et al., 2014).

This taxonomy has come about, in part, due to the variety of techniques and methodologies employed to test the functional and anatomical properties. In order to simplify this issue for present purposes the area will hereafter be referred to as Motor Cortex Area 2 (M2). This is the terminology utilised by one of the most recent anatomical mouse brain atlases (Franklin and Paxinos, 2012).

The region was first described in studies which employed large-scale lesions. These lesions caused significant deficits in fine motor control, learning, memory, and a generalised hemispatial neglect in rodents (Midgley and Tees, 1981, Crowne and Pathria, 1982, Crowne et al., 1986). Interestingly, the unilateral deficits seen from unilateral removal or inactivation of M2 have been attributed to a loss of projection neurons to the pyramidal tract (Li et al., 2015). Electrical stimulation of M2 in rodents caused movements in the fascia and the body; most prominently in the head and neck. These

observations led to the idea that M2 functions as a descending motor control area. However, further studies of M2 did not fully support this theory. Research which employed reversible inactivation such as cooling and muscimol injection discovered that inhibition of M2 does not cause major movement deficits. It did produce problems with updating motor planning and reversal learning in a variety of operant and associative learning tasks (Smith et al., 2010, Sul et al., 2011, Zagha et al., 2013). Additionally the neuronal response types which appear intermingled within M2, have been described. These include i) cells which show increased firing over time during cognitive task such a delayed odour discrimination, regardless of response, ii) cells which ramped up activity during a cue or sampling period, and iii) cells which were associated with motor response output (Erlich et al., 2011, Guo et al., 2014, Kopec et al., 2015). In addition, more anterior parts of M2 have been associated with learning induced improvements in somatosensory whisker discrimination tasks which were accompanied by increased encoding of whisker kinematics in somatosensory neurons projection to M2 (Chen et al., 2015). This enhancement of functional connectivity may allow for a better representation of the location of stimuli in space (Chen et al., 2013). Neurons in M2 cluster in both spatial and temporal terms in order to form functional ensembles which can represent a variety of different motor task including fine active perception of somatosensory stimuli, whisker stimuli, and motor response in rodents (Ferezou et al., 2007, Huber et al., 2012, Manita et al., 2015). Taken together, this information builds a picture of M2 as being involved in the origination and refinement of motor responses and goal directed planning. Furthermore, this brain region presents itself as an ideal location for experimental manipulation to uncover the neuronal basis of these basic orienting/attentional processes in the mouse.

1.2.3 Cingulate Area

The cingulate area (Cg) is a medial prefrontal region which is found in mammals. It has been linked to a variety of different behavioural processes, including nociception and aversion learning, and orienting behaviours (Gabriel et al., 1991, Calejesan et al., 2000, Kvitsiani et al., 2013). In rodents the Cg is located in the medial wall of the cortex, ventral to M2. It is a long strip of cortex spanning a large portion of the rostro-caudal length of the brain. Specifically it runs from approximately 2mm anterior to bregma to 1mm posterior to bregma. This brain area can be seen in Figure 1-3. Large scale lesions of Cg in rodents cause changes in orienting behaviours, and can lead to increases in anticipatory responses

in delayed operant tasks which indicates a role for Cg in inhibitory control (Muir et al., 1996). Furthermore, Cg has been implicated in foraging decisions in both rodents and primates. In macaques, the anterior cingulate cortex (ACC) has been shown to track reward probability values and to be involved in task switching (Blanchard and Hayden, 2014). In mice, the activity of Cg has been very closely linked to stay/go decisions in rewarded vs unrewarded environments (Kvitsiani et al., 2013). The interaction between effort and reward and risk and reward has been shown to be affected by Cg lesions. Lesioned animals are less likely to make high risk/high reward or high effort/high reward choices (Rudebeck et al., 2006).

One of the most well documented functions of Cg is its involvement in pain processing and avoidance behaviours. A number of studies have found that pain responsive neurons within Cg respond to a variety of pain types directed at both the skin and viscera (Sikes and Vogt, 1992, Yamamura et al., 1996, Shyu et al., 2008, Sikes et al., 2008). Removal of Cg also impairs avoidance reflexes elicited by noxious heat stimuli (Pastoriza et al., 1996). Furthermore, lesions of Cg block responses to inflammatory pain (Donahue et al., 2001, Johansen et al., 2001). Cg removal results in a deficit in avoidance learning in rabbits without affecting normal motor function, further highlighting the importance of this area in aversive orienting behaviours (Gabriel et al., 1991). Interestingly, inhibition of the Cg via muscimol during fear conditioning inhibited freezing responses in negatively associated locations, and to conditioned aversive stimuli (Tang et al., 2005). Neurochemical excitation of the Cg can cause facilitation of the tail-flick reflex in rats (Calejesan et al., 2000). This highlights the role of the Cg in the top-down modulation of aversive orienting reflexes. In addition, direct electrical and chemical stimulation of Cg causes or potentiates freezing and avoidance behaviour as well as conditioned fear memory (Johansen and Fields, 2004, Tang et al., 2005). Taken together, these experimental findings suggests that the Cg is intrinsically involved in the top-down control or modulation of responses to negatively associated events or locations.

1.2.4 Primary Visual Cortex

The primary visual cortex (V1) sits at the caudal end of the cortex. This region is the major neocortical target for visual information coming from the retina, by way of relay through the lateral geniculate nucleus of the thalamus (LGN). This region contains a

retinotopic representation of the visual world with a partial hemispheric decussation in rodents. In other words, the majority signals from the contralateral eye travel to V1 which builds a picture of the contralateral visual field, with some crossover in the nasal/central part of vision (Coleman et al., 2009). However in macaques and humans there is a complete crossover of visual information, meaning that there is a full segregation of ipsi- vs. contralateral visual field representation (Petros et al., 2008).

This region was first identified as being involved in vision by unilateral blinding of animals and study of the neural degeneration in the brain. An Italian anatomist, Bartolomeo Panizza was responsible for this discovery (Panizza, 1855) but it was not until the advent of electrophysiology that the fine structure and function of V1 was resolved. Studies conducted in the cat visual cortex uncovered the existence of neurons responsive to stimulation in specific parts of the visual field (Hubel and Wiesel, 1959). In addition, cells which displayed orientation and movement direction selectivity were described (Hubel and Wiesel, 1959, Hubel and Wiesel, 1962). The studies formed the basis for the expansion of visual based research into other animals and more complex experimental designs and allowed the intricate picture of V1 organisation to unfold.

At its simplest level, V1 is composed of 6 cortical layers. The LGN, which is the main bottom-up input to V1 feeds visual information to layer 4C and layer 6 through magnocellular and parvocellular pathways and to layers 1, and 2/3 through the koniocellular pathway (Hubel and Wiesel, 1972, Hendrickson et al., 1978, Livingstone and Hubel, 1982, Blasdel and Lund, 1983). These different retinal ganglion cell pathways originate from different cell types which have specificity for different visual stimulus properties. The magnocellular pathway is specialised to detect large, fast moving, low contrast stimuli. The parvocellular pathway is adapted for small stimuli and detecting fine detail in stimuli (Callaway, 1998). Finally the koniocellular pathway is still relatively unclassified but is responsive to short wavelength light, and is involved in modulating V1 layer 1-3 activity (Klein et al., 2016). Once the LGN information arrives at V1 through layers 4C and 6 (which themselves are reciprocally connected). Layer 4C then projects to layers 2-4B and layer 5 (which are reciprocally connected). Layers 2-4B then project to the other the higher cortical visual areas, while layer 4C then projects back to the LGN (Callaway, 1998).

1.2.4.1 Macaque

The organisation of the macaque V1 is widely thought to be one of the closest correlates to that which is seen in the human V1. Visual information is processed and organised in various overlapping maps which hold different types of representations of the visual field. There is a retinotopic map of the external world, which means that a particular location in V1 codes the spatial information from a specified region of the retina, whereby neighbouring neurons represent neighbouring parts of the external visual world. This builds up a picture of the external environment in the contralateral hemifield, even if in a distorted manner, as retinal cell densities, and thus resolution in the cortex differ in a systematic manner. In the macaque, and human to some extent, this map is organised such that the more central or foveal representation is located in the more lateral portion of the region; the peripheral spatial locations are found in the more medial portion of the brain region and the inside bank of the cortex. Furthermore, the upper and lower visual fields are flipped so that the upper part of the area represents the lower visual field (Tootell et al., 1988).

Concurrent to that retinotopic map, ocular dominance columns exist within layer 4C, which are strips of cortex which lay in parallel over the cortical surface, receive visual information from a single eye (LeVay et al., 1975, Callaway, 1998). A further organisation in primate V1 is based on the existence of orientation columns, which run vertically through the cortex, and have preferences for specific orientations. These build into orientation preference regions are selective for the same orientations. These bands are then arranged in a pin-wheel like fashion, where transition in a clockwise or anticlockwise manner produces changes in preference which cover the orientation space (Bartfeld and Grinvald, 1992). Finally, there are cytochrome oxidase positive blob structures which code for various stimulus features such as colour or spatial frequency (Livingstone and Hubel, 1984, Johnson et al., 2001). All of these various maps and preference arrangements are constructed in V1 to produce overlapping mosaics of all three visual features (retinotopy, orientation, and colour), which allows for complete processing of visual stimulus details (Bartfeld and Grinvald, 1992).

1.2.4.2 Mouse

The organisation of rodent V1 differs from that of the macaque and human. The retinotopic mapping of this region show that the most anterior part encodes the lower visual field and the most medial part codes for lateral portion of the visual field. The azimuth and elevation are represented in orthogonal bands (Wagor et al., 1980, Ji et al., 2015). Classically, beyond the retinotopy, the structure of mouse V1 has been described as 'salt and pepper'. In essence this relates to the lack of orientation columns and the intermixing of neurons of different orientation preferences throughout V1 (Ohki and Reid, 2007). However, more recent studies have uncovered a finer scale organisation within this area. In addition to terminating in layer 4, the LGN projects to mouse V1 layer 1 in a patchy manner, i.e. to patches which contain high concentrations of muscarinic receptor 2 (M2). These patches have higher spatial acuity, whereas the interpatch regions have higher temporal acuity (Ji et al., 2015). Furthermore, spatial clustering of parvalbumin (PV) positive neurons has been shown to correlate with similarity of orientation preference (Runyan and Sur, 2013). In contrast to the 'salt and pepper' theory, a recent study has also shown that orientation microcolumns can be seen in mouse V1 (Ringach et al., 2016). This results in similar orientation preferences of neurons in regions of 50 μm dimeter. Re-analysis of previous work by Ohki & Reid demonstrated that this spatial clustering could be observed in the original data. Taken together, this research proposes a strong case for the organisation of rodent V1 to include some form of orientation preference clustering, even if this differs from the organization found in primates.

1.2.5 Visual Area 4

Visual Area 4 is one of the higher visual areas of the human and macaque brain, which interacts with lower visual areas and higher order attentional regions. This region is involved in multiple parts of visual stimulus processing, including orientation, colour and spatial feature selectivity. This region receives a variety of feedforward and feedback connections from different visual and attentional regions. The main feedforward visual projections occur from visual area 2 (V2) and visual area 3 (V3) (Shipp and Zeki, 1985, Felleman et al., 1997). Although there is also direct thalamic input from the LGN (Hendry and Reid, 2000), V4 receives a greater diversity of reciprocal connections from higher visual and cognitive brain regions than V1 does. These include the lateral intraparietal area

(LIP), the anterior temporal cortex (TEa), the medial temporal area (MT), the superior temporal sulcus (STS) and the FEF (Ungerleider et al., 2008).

The connections with the FEF have been shown to be one of the main pathways for attentional modulation. If FEF cells, which project to V4, are microstimulated, both the visual selectivity of cells in V4 and an animal's accuracy in a contrast discrimination task are increased (Moore and Armstrong, 2003, Moore and Fallah, 2004).

1.3 Principals of the Methodology Employed in this Work

1.3.1 Neuroanatomy and Neural Tracing

A large proportion of the techniques used in modern neuroscience, such as neuroanatomical tract tracing, are underpinned by the discoveries of Camillo Golgi and Santiago Ramon y Cajal (1909). Their pioneering work of neural tissue staining work first revealed the existence of discrete neuronal types which had their own particular morphology and organisation. This lead to the formation of the *Neuron Doctrine*, which states that the brain is composed of discrete cells rather than being a synctitium (Jones et al 1999). This breakthrough led to the idea that the multitude and variety of behavioural processes which occur in the brain are enacted through the coordinated activity and properties of single cells (Cajal, 1909, Yuste, 2015). Subsequent work discovered that it was not just the morphological properties of these neurons which indicated their function, but also their specific connectivity within the brain. Thus the idea developed of specific networks which mediate a particular cognitive task or behaviour.

The stain that was utilised by Golgi and Cajal was based on silver impregnation of the neurons using a silver nitrate and potassium dichromate reaction. The mechanism underpinning this method is still largely unknown, as the neurons they identified are labelled in a random manner (Pannese 1999).

In more recent years neural tracers have been developed, which not only stain the local area of neurons, but trace their connectivity in either a retrograde or anterograde fashion. This allows a picture of the connectivity of different brain areas and subregions to be constructed. Two such tracers employed in the current experiments are the retrograde tracer fluorogold (FG), otherwise known as hydroxystilbamidine, and the anterograde tracer biotinylated dextran amine (BDA). This research makes use of these more modern tracers to uncover the fine scale connectivity of multiple brain regions in the mouse.

1.3.2 Electrophysiology

Another investigative technique which was established to examine the properties of the brain is electrophysiology. This technique was again based on the idea that single neurons fulfil specific roles within the brain. This method relies on the idea that neurons use electrical signals to integrate and code information, which then is transformed into a chemical signal to communicate the coded information to other cells. There is however, another form of neuronal communication which is not covered by this thesis, Ephaptic Coupling. This uses chemical signalling through gap junctions to send information around the brain (Anastassiou et al., 2011). The first occurrence of electrophysiology in the literature was conducted by Edgar Adrian. He observed electrical discharges in single nerve fibres which were produced by a variety of manipulations. These included tension on muscle tissue, and pressure, touch, or movement on skin (Adrian, 1928). These recordings were conducted with simple single electrodes, which are very thin pieces of insulated metallic wire that are inserted into the tissue. Since that time there have been major technological advances in the methods of recording from neurons, in terms of the actual electrodes and the amplification of the signal. In this thesis, the recordings conducted used laminar multielectrodes. These are compact devices which contain multiple electrode contacts along its length. The advantage of laminar electrodes is two-fold. Firstly, it increases the amount of data that can be collected from a single recording. Secondly the laminar spacing of the contacts on a single electrode allows the measurement and investigation of the roles of different layers of cortical areas. It is for these reasons that laminar electrodes are employed throughout the electrophysiological portions of this work.

1.3.3 Optogenetics

The final methodology employed in this work is also the most modern, i.e. optogenetics. This technique allows for the control of neural circuits and behaviour through optical stimulation. This is achieved through the transfection of neural tissue with a virus, or genetic encoding, which produces a light sensitive opsin. These opsins are photoreactive and can be coupled to a variety of second messenger apparatus such as ion channels and g-coupled receptors. Depending on the configuration of these, activation of the opsin can cause stimulation or inhibition of cells. This technique was first employed in cell culture

by the transfection of drosophila rhodopsin (Zemelman et al., 2002). Once the principle was established a number of different opsins were adapted for this purpose, such as the channelrhodopsin (Nagel et al., 2003) and halorhodopsin (Zhang et al., 2007). These opsins have been shown to both modulate the activity of neuronal populations as well as to have measureable effects at a behavioural level. For this reason this is a perfect tool to investigate the specific function of particular brain regions in the wider context of behaviour.

1.4 Outstanding Research Questions

This chapter outlines the fundamental concepts, background literature, and brain regions central to this thesis. More specifically this section concerns visual attention and orienting in both mice and macaques. This chapter details the current understanding of these cognitive processes and functionality of specific brain areas in these processes. However, there remain a number of issues highlighted through the introduction which have not been fully examined within the literature. This thesis addresses a variety of these outstanding issues in order to positively contribute to the field.

With regard to the specific neuroanatomical pathways which may underpin orienting in rodents, until recently this has been largely focused on the rat model. It has widely been assumed that rats and mice have very similar neuroanatomy and cognitive functioning. This thesis specifically examines the neuroanatomical pathways which exist in the mouse in order to address this deficit.

Furthermore, another overarching theme of this thesis is the relation between specific forms automatic visual attentional processing in the macaque and the mouse. As stated previously, there has been an increase in the use of rodent models to investigate behaviours and cognitive processes which have been defined in the macaque. However, very few studies are able to make direct comparisons between these two animal models. This thesis addresses this issue by using directly comparable experimental designs in the macaque and mouse to investigate the mechanisms of bottom-up exogenous attention processing in a variety of visual areas.

One of the major reasons for this increase in usage of the mouse model has been the creation of highly targeted genetically based techniques such as optogenetics. Until very recently these techniques have been utilised to study the effects of optogenetic

manipulation at a behavioural level or within the brain regions which have been transfected with the optogenetic construct. Very few studies have examined the effects manipulation of projections from one brain region to another, especially within awake animals. This thesis aims to add to the existing literature by exploiting optogenetics to manipulate some of the projections characterises in the previous chapter. Namely the prefrontal projections to visual areas in the mouse with an excitatory construct during the bottom-up attentional paradigm previously explored. This should produce a more detailed understanding of the functional properties of top-down long range projections in mouse prefrontal cortex.

Taken together this thesis aims to add to the existing understanding of a variety of different fields related to the anatomy of and mechanisms responsible for attention and orienting in both mice and macaques.

Table 1-1. Different terminology within the literature for the rodent M2 and methodology employed for the research

Brain Area Name	Species	Authors	Stereotactic Coordinates (Bregma = (0, 0))	Methodology
Agranular Medial Cortex	Rat	(Hoover and Vertes, 2007)	+3.7 mm AP, +1.5mm ML	Retrograde neural labelling using iontophoretic injections of Fluorogold into the mPFC
Anterior Lateral Motor Cortex	Mouse	(Guo et al., 2014)	+2.5 mm AP, + 1.5 mm ML	Electrophysiological recordings and optogenetic inactivation of area
Anteromedial Cortex	Rat	(Crowne et al., 1986)	+4- -2mm AP,+ 0-2mm ML	Unilateral lesions of the anteromedial cortex and sensory cued behavioural training Electrical stimulation of the area produces head movements
Area 6/8	Rat	(Miller, 1987)	+2.2 mm AP, + 1.5 mm ML	Retrograde neural labelling using horseradish peroxidase injections into the spinal cord
Dorsomedial Prefrontal Cortex	Rat	(Cowey and Bozek, 1974)	+5.2-1mm AP, +1.5 mm ML	Unilateral lesions of the area, followed by recording of behavioural choice in Y-maze
Fr2	Rat	(Zilles, 1985)	+5.2- -3.3mm AP +1.5mm ML	Anatomical and histological staining and systematic sectioning of brain tissue

Frontal Orienting Field	Rat	(Erlich et al., 2011)	+2 mm AP, ± 1.3 ML	Electrophysiological activity and pharmacological inactivation recorded during delay period of auditory cued forced choice task
Medial Agranular Cortex	Rat	(Reep et al., 1987)	+4-1.7mm AP, + 1mm ML	Unilateral lesions of AGm, anterograde neural labelling after tracer injection into AGm
Medial Precentral Cortex	Rat	(Reep et al., 1984)	+2.7mm AP, +1mm ML	Anterograde neural tracing of brain after injection into area
Medial Frontal Cortex	Rat	(Guandalini, 1998)	+1.7-0 mm AP, +1mm ML	Microelectrode stimulation of the area, coupled with anterograde tracer injection
Motor Cortex 1	Mouse	(Chen et al., 2013)	+1.2 mm AP, + 0.6 mm ML	Electrophysiological recordings in S1 and optogenetic activation of the region
Motor Cortex 2	Rat/Mouse	(Paxinos and Watson, 1986, Franklin and Paxinos, 2008)	+4.2- -3mm AP, +1-1.5mm ML (Rat) +2.5 mm- -1.3mm AP, +0.5-1.5mm ML (Mouse)	Anatomical and histological staining and systematic sectioning of brain tissue
Vibrissal Primary Motor Cortex	Mouse	(Zagha et al., 2013)	+1 mm AP, + 1 mm ML	Electrophysiological recordings and optogenetic activation of the region

Whisker Motor Cortex	Rat	(Hill et al., 2011)	+2.5 mm AP, + 1.5mm ML	Electrophysiological recordings of the area correlated with whisker movement dynamics in free moving and head fixed rats
Rat Frontal Eye Field	Rat	(Neafsey et al., 1986)	+2 mm AP, + 1mm ML	Retrograde neural tracing after injection into the SC and PAG
Secondary Motor Area	Mouse	(Oh et al., 2014)	+2.95-0.26mm AP, 0.2-1.5mm ML	Anterograde viral vector tracing

Chapter 2. General Methodology

2.1 Experimental Subjects

All experiments were carried out in accordance with the European Communities Council Directive 1986 (86/609/EEC), the US National Institutes of Health Guidelines for the Care and Use of Animals for Experimental Procedures, and the UK Animals Scientific Procedures Act.

2.1.1 Mice

Animals involved in this study were C57BL6 mice obtained from Harlan Laboratories. Mice utilised for the tracing studies were housed in standardised cages with ad libitum access to food and water.

2.1.2 Macaque

The animal involved in the study (monkey 1) was obtained from the Medical Research Council Centre for Macaques Porton Down.

2.2 Surgical Procedures

2.2.1 Tracer Injection surgeries

Animals were anaesthetised using a mixture of 1mg/kg medetomidine and 50mg/kg ketamine. The animals' heads were shaved and cleaned. Animals were placed in a motorized stereotax (Stoelting, Germany), which was controlled via a joystick with custom written scripts to interact with the StereoDrive software. Body temperature was maintained at ~37˚C using a thermostatic heating blanket (Harvard Apparatus). The animals' eyes were protected from drying out using optic drops (Carbomer 0.2%). An incision was made with a scalpel along the midline of the scalp to expose the skull. A craniotomy was then performed (0.7mm or 0.5mm) over the stereotactically measured target location (see Table 2-1).

The tracer injection protocol was then conducted (see below). After removal of the probe, the incision was sutured and the animal was given postoperative analgesia (non-steroidal anti-inflammatory analgesic meloxicam (10mg/kg s.c) and medetomidine anaesthetic was reversed by administration of atipamezole (1mg/kg s.c.)). The animals were then allowed to recover in a temperature controlled unit to minimise postoperative recovery time.

2.2.2 Viral Vector Injection

Initially, animals were placed in an induction chamber and anaesthesia was induced by isoflurane administration. Isoflurane administration was done with 3l/min oxygen and 5% flow rate. Once anaesthetised, the heads of the animals were shaved to remove excess hair. Animals were then transferred to the motorised stereotax with a mouse volatile anaesthetic attachment for isoflurane to allow for continuous anaesthesia at a maintenance level of 1l/m oxygen and 1.5-3% flow rate. The rest of the hair on the cranium was removed using hair removal cream (Boots, UK). Animals were kept at 37˚C using a thermostatic heating blanket (Harvard Apparatus). Animals were given meloxicam (10 mg/kg s.c) for analgesia after initial anaesthesia. The animals' eyes were protected from drying out using optic drops (Carbomer 0.2%). An incision was made with a scalpel along the midline of the scalp to expose the skull. A craniotomy was then performed (0.7mm or 0.5mm) over the stereotactically measured target location in either Motor Cortex Area 2 or Cingulate Area (see Table 2-1). The virus was then placed in a pressure injection pipette and once the micropipette was advanced to the chosen location (two injection sites within the tract down the cortical column, approximately at 700µm and 300µm depth) a volume of 66nl per site was injected over a period of 5 minutes.

2.2.3 Cranial implant Surgeries

2.2.3.1 Mouse

In order to perform awake behaving electrophysiological recordings in the mouse brain, a head-post and cranial chambers were implanted. Animals were sedated and prepared as described above for viral vector injection. A midline incision was made onto the scalp and excess tissue was removed from the bone. The tissue margin was then secured around the area of the implant with tissue glue (cyanoacrylic, Homebase UK). The exposed bone was prepared for the dental acrylic implant via the application of a UV light curable etching

solution (iBOND Total Etch, Heraeus Kulzer) to aid adhesion. The location of bregma was identified and marked for future reference and chamber implantation. The acrylic head implant was constructed first from using a small ball of UV light curable acrylic (Charisma, Heraeus Kulzer), rolled out to an extended 'rod like' shape (~0.5-1mm*20mm), which was placed next to the tissue margin, and gently pushed against it to obtain a good seal between the tissue glue at the tissue margin and the Charisma. Once in place it was cured by application of UV light (Demi Kerr Plus, ~20 sec). This left a central part of the cranium visible (covered and sealed by the cured total etch), which could be filled as needed with additional (less viscous) UV curable acrylic (Tetric Evoflow, Heraeus Kulzer). The latter was also used to secure the custom made implants to the bone. Following implant surgery, animals were allowed to fully recover.

In the days before, or on the day when electrophysiological recordings were started animals were anaesthetised with isoflurane again and small (~0.5-1mm diameter) craniotomies were performed over areas of interest using stereotactic coordinates. Custom-made recording chambers were implanted over the craniotomies to keep them clean when animals returned to the home cage.

2.2.3.2 Macaque

The animal (macaca mulatta, male, 9 years old, weight ~10kg) was implanted with a headpost under sterile surgical conditions (Thiele et al., 2006). Furthermore two chambers, one over V1 and one over V4 were implanted on the right hemisphere of the animal. Both the headpost and chambers were composted of PEEK (polyether ether ketone).

2.2.4 Cranial Window Implantation

To allow repeated optical stimulation of the transfected brain region in the mouse, a cranial window was implanted over the injected area. This involved sedation of the animal with isoflurane as described above for viral injection procedure. Once the animal was sedated and prepared as previously described a 3 or 4mm diameter region was demarked on the skull with a biopsy punch. This bone area was then removed using a dental drill. These procedures caused small amount of bleeding which can cloud the cranial window unless removed extremely gently and carefully. This was achieved by gently wiping the dura mater with gel foam soaked in saline. Once adequately cleaned a glass coverslip was

placed onto the brain and cemented in with dental acrylic. This window was then utilised to allow for light induced excitation of affected cells.

Animals were then allowed to fully recover. A few days before electrophysiological recording animals were anaesthetised again and craniotomies were performed over areas of interest using stereotactic coordinates (see Table 2-1). These regions were uncovered and then a custom-made recording chambers were implanted over the areas to allow for electrode placement.

2.3 Neuroanatomy and Tract Tracing

2.3.1 Tracers and injection apparatus

2.3.1.1 Retrograde Tracing

The tracer utilised for retrograde tracing was fluorogold (FG) (Life Technologies). A custom made two barrelled iontophoresis pipette with a tungsten microelectrode (tip 10-20 microns) (Thiele et al., 2006) was filled with a 3% (in saline) solution of the tracer. The pipette was attached to a Harvard Neurphore BH-2. The pipette was advanced to the chosen location with a hold current of -500nA. Once at the target location, the tracer was iontophoresed at +500nA for 30 minutes (Schmued and Heimer, 1990). After this the current was changed to a hold current of -500nA for removal of the probe. The pipette was left at its injection location for 20 minutes after injection to allow for best diffusion of the tracer into the tissue before removal.

2.3.1.2 Anterograde Tracing

The tracer utilised for anterograde tracing was Biotinylated Dextran Amine MW-10,000 (BDA) (Life Technologies) (in saline). A calibrated air pressure micropipette was filled with 15% of the tracer. The micropipette was attached to a custom air-pressure system and filled. Once the micropipette was advanced to the chosen location a volume of 66nl was injected over a period of 5 minutes. The pipette was left in place after injection for 20 minutes to allow for best diffusion of the tracer into the tissue before removal.

2.3.2 Brain recovery

After a 3-4 day recovery period following tracer injection, animals were given an overdose of sodium pentobarbital (0.3ml 200mg/ml ip). Then they were transcardially perfused with an initial injection of 1ml heparin sulphate (5,000 I.U./ml), before a 4% paraformaldehyde in phosphate buffer solution (PBS) solution with 20% sucrose for 30 minutes at 1ml/minute. Post perfusion, brains were removed and placed in the paraformaldehyde solution to post-fix for 24 hours. After post-fixing the brains were cryo-protected in a 30% sucrose solution for another 24 hour period.

2.3.3 Histology

2.3.3.1 Retrograde FG Tracing

After cryoprotection, serial coronal free floating sections (40µm) were taken (Microm cryostat, HM500 OM) from the start of frontal cortex up to the inferior colliculus and placed in 4% phosphate buffer solution (PBS). Every 4th section was taken for further analysis. The remaining sections were placed in a cryoprotectant solution (one liter of cryoprotectant solution consists of 500 ml 0.1M phosphate buffer, 300g sucrose (30% w/v), 10g polyvinylpyrolidone (1% w/v; PVP-40), 300 ml ethylene glycol (30% v/v)) (Watson Jr et al., 1986, Hoffman and Le, 2004) and stored at -20C. The sections for analysis went through an initial autofluorescence quenching step (20 minute 1% sodium borohydride wash, followed by a 20 minute wash with 5 mM Glycine) and PBS washes (3x10 min). Sections were then mounted onto microscope slides with a propidium iodide (PI) medium (Vectashield H-1300) or a DAPI medium (Vectashield H-1500).

2.3.3.2 Anterograde BDA Tracing

After cryoprotection, serial coronal free floating sections (40 µm) were taken (Microm cryostat, HM500 OM) from the start of frontal cortex up to the inferior colliculus and placed in 4% phosphate buffer solution (PBS). Every 4th section was taken for further analysis. The remaining sections were placed in a cryoprotectant solution (Hoffman and Le, 2004) and stored at -20C. The sections for analysis went through an initial autofluorescence quenching step (20 minute 1% sodium borohydride wash, followed by a 20 minute wash with 5mM Glycine) and PBS washes (3x10 min). Sections were incubated

for 2 hours in streptavidin-Alexa 488 (1:500 in 1% normal bovine serum, 0.2% triton X, 0.1% gelatine in PBS) at room temperature followed by PBS washes (3x10 min). Sections were then mounted onto microscope slides with a DAPI medium (Vectashield H-1500).

2.3.4 Fluorescence Microscopy

For the retrograde experiments with unamplified fluorescence, sections were examined under a fluorescence microscope (Leica DM LB 100T), at an excitation wavelength of 350 nm to illuminate endogenous FG fluorescence. Excitation at 530 nm was utilized to highlight nuclei with the propidium iodide (PI) staining and co-locate with the tracer signal. Digital images were acquired using 'MicroFire' optics.

Sections from the anterograde tracing, which had undergone immunohistochemical amplification were examined under a fluorescence microscope (Zeiss Axioimager II). Projection patterns were visualized with excitation at 500 nm; nuclei counterstains were visualized with either 530 nm excitation (PI) or 350 nm (DAPI). Photo-merges were taken of stained areas for further qualitative and quantitative analysis using AxioVision software. For illustrative purposes photomicrographs were processed for brightness and contrast and gray-scaled using Adobe Photoshop CS6.

2.3.5 Analysis of tracer

2.3.5.1 Contour Plots of Injection Sites

In order to display the extent of our injections, photomicrographs of each injection case were taken for each animals. These were then processed using ImageJ to remove background luminance and thresholded. This was achieved through custom scripts which calculate the thresholding value (L_{sub}) according to the following formula:

$$L_{sub} = L_{mean}(ROI) + L_{\sigma^2}(ROI)$$

where L_{mean}corresponds to the mean luminance across the region of interest (ROI), and L_{σ^2} corresponds to the variance of the luminance across the ROI. The ROI chosen for the luminance subtraction was taken from the non labelled region of the photomicrograph. This produced a binary image, where values of 1 displayed the extent of tracer injection. From these images a contour describing the extent of labelling was produced by demarcating the

limits of the binary signal. These contours were then imported into a vector graphics program and transposed onto representative brain atlas slides (Franklin and Paxinos, 2012).

2.3.5.2 Retrograde

For quantitative analysis of the retrograde tracing study, images were processed with ImageJ 2 (Schindelin et al., 2012). For this we wrote script which performed a Gaussian Convoluted Background Subtraction (sigma = 20) to remove biological artefacts, and to filter and grayscale the images. ROIs for brain regions were defined and demarcated on nuclear counterstained images (DAPI, PI) using the mouse brain atlas as reference (Franklin & Paxinos 2012). Images underwent semi-automated cell counting for each injection case. Based on these numbers, we calculated the proportion of cells labelled in any brain area (from all cells labelled across the brain of a given experimental animal), and used these to calculate proportions across our experimental animals. To simplify the presentation and classification we decided on 5 categories of connectivity strength, whereby areas to have no input to the SC were labelled with a '-', low (<2.5%), input with '+', medium (<5%), input with a '++', high input (5-7.5%) with a '+++', and very high input (>7.5% of cells labelled (from all cells labelled) as '++++' which are displayed in Table 1.

Examples of each of level of labelling are shown below from representative cases for retrograde Fluorogold transport (Figure 2-1).

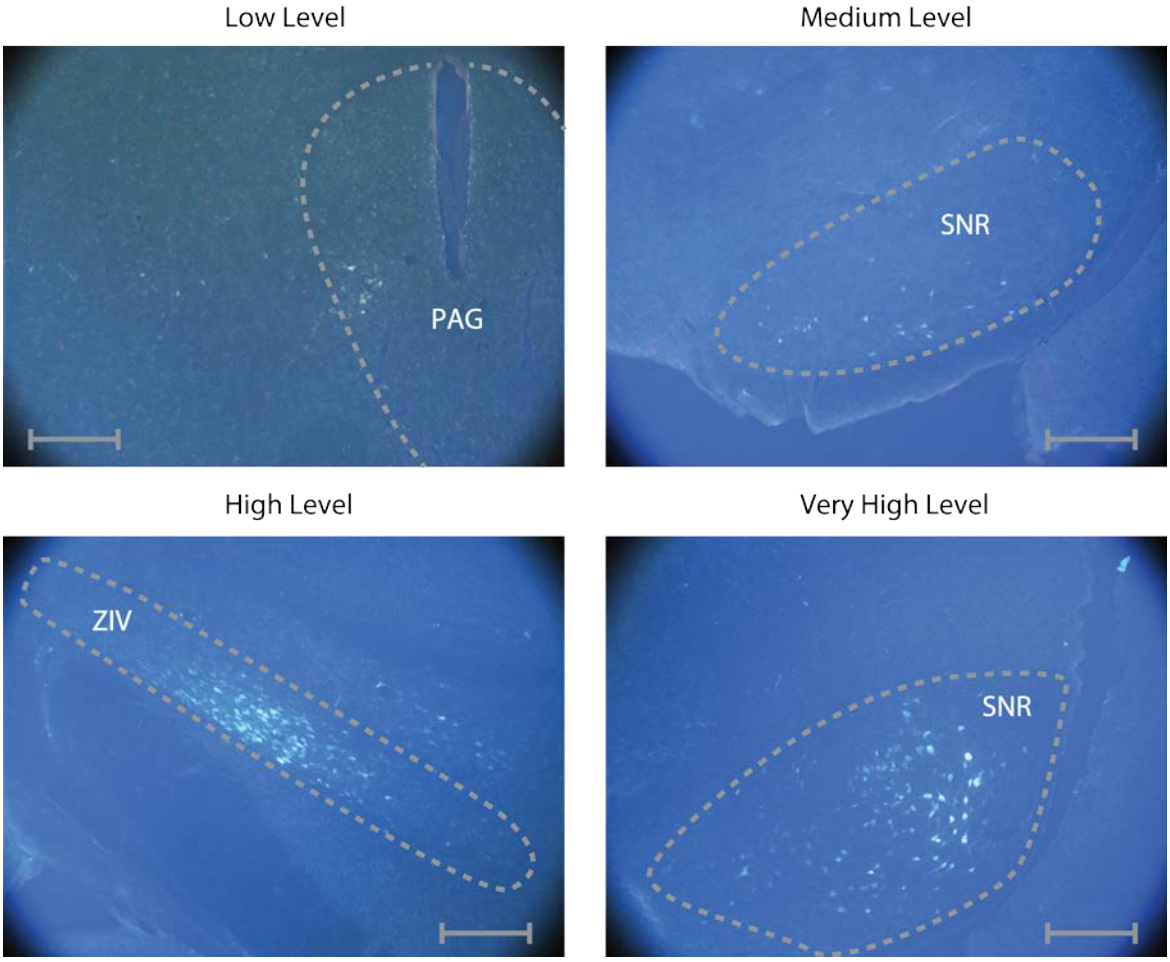

Figure 2-1. Example Photomicrographs of Each Level of Retrograde Tracing

Photomicrographs illustrating each level of retrograde Fluorogold labelling after injections in the SC. Scale bar equates to 250µm. PAG-periaquaductal grey, ZIV-zona incerta ventral part, SNR-substantia nigra pars compacta.

2.3.5.3 Anterograde

For representation of the anterograde tracing data in table 2 the images underwent qualitative visual inspection and were classified into one of five signal strengths , none '-', low '+', medium '++', high '+++', and very high '++++'. Examples of each of level of labelling are shown below from representative cases for anterograde BDA transport (Figure 2-2).

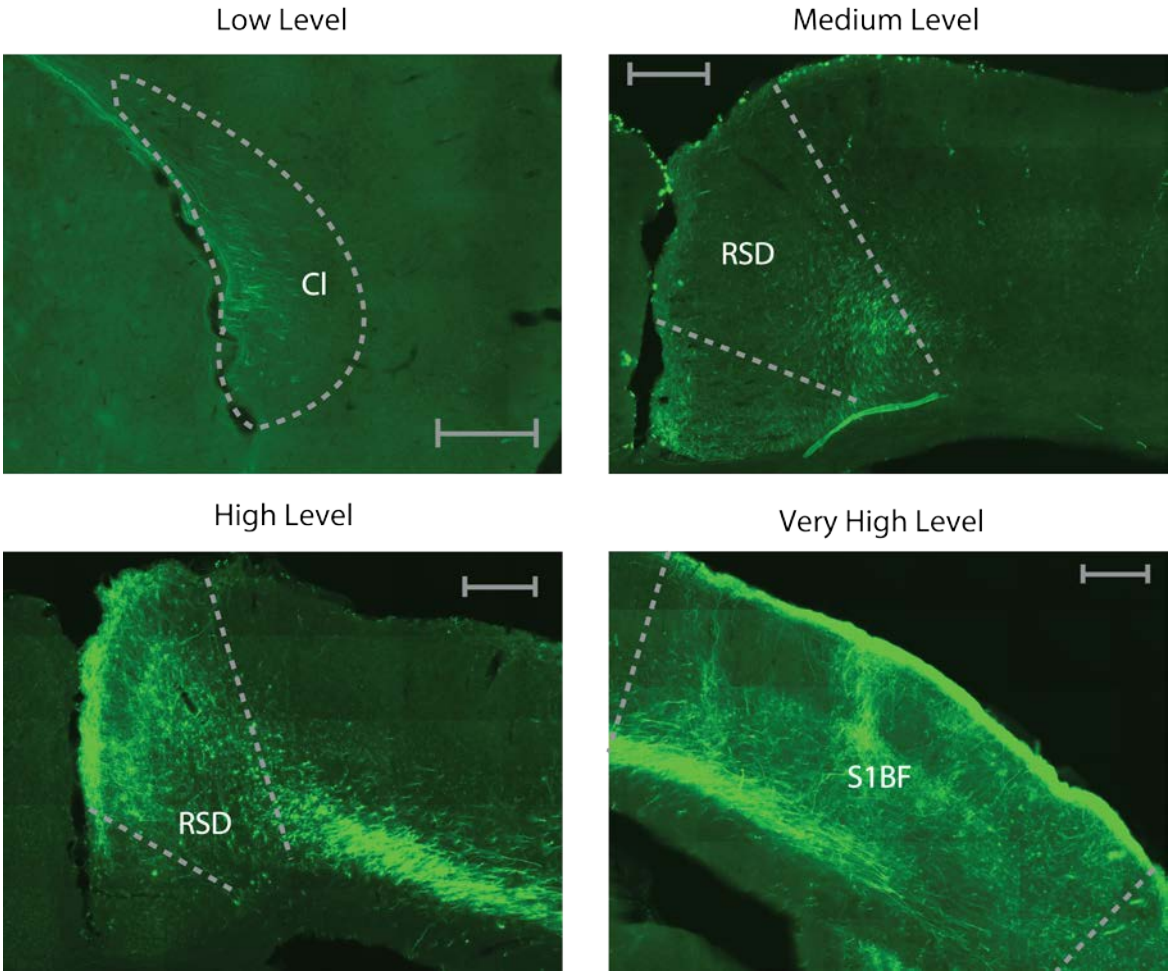

Figure 2-2. Example Photomicrographs of Each Level of Anterograde Tracing

Photomicrographs illustrating each level of anterograde BDA labelling after injections in the Motor Cortex Area 2 and Cingulate Area. Scale bar equates to 250µm. Cl-claustrum, RSD- retrosplenial cortex, dysgranular, S1BF-primary somatosensory cortex, barrel field.

2.3.5.4 Quantitative Analysis

For both retrograde and anterograde conditions, images were processed with ImageJ 2 software (Schindelin et al., 2012). This entailed Gaussian filtering (sigma = 3.5) to remove acquisition and biological artefacts. Images were then converted to grayscale and background luminance removal and thresholding was conducted. This was achieved through custom scripts which calculate the thresholding value (L_{sub}) according to the following formula:

$$L_{sub} = L_{mean}(ROI) + L_{\sigma^2}(ROI)$$

were L_{mean} corresponds to the mean luminance across the region of interest (ROI), and L_{σ^2} corresponds to the variance of the luminance across the ROI. ROIs were defined and demarcated on nuclear counterstained images (DAPI, PI) using the mouse brain atlas as reference (Franklin & Paxinos 2012). The tracer signals within the ROI were then quantified by automated cell counts/area (retrograde tracing) or percentage area expressing the tracer signal (anterograde tracing). A flow diagram of this process can be seen in Figure 2-3. Preferential connectivity of a particular injection site to different ROIs was determined by calculating the modulation index (MI) of connectivity which was calculated as:

$$MI = \frac{Q(ROIa) - Q(ROIb)}{Q(ROIa) + Q(ROIb)}$$

where $Q(ROIa)$ corresponds to the quantified amount of tracer in a particular region of interest, and $Q(ROIb)$ corresponds to the quantified amount of tracer in a complementary region. A preference in connectivity for $ROIa$ would yield a positive number between 0-1, a preference for $ROIb$ would yield a negative number between 0-1. The code for all of the analysis is available online (https://github.com/GrimmSnark/Image_analysis_fiji). Significant differences between the MIs for the particular injection site were tested by a Mann-Whitney U test, alpha value = 0.05.

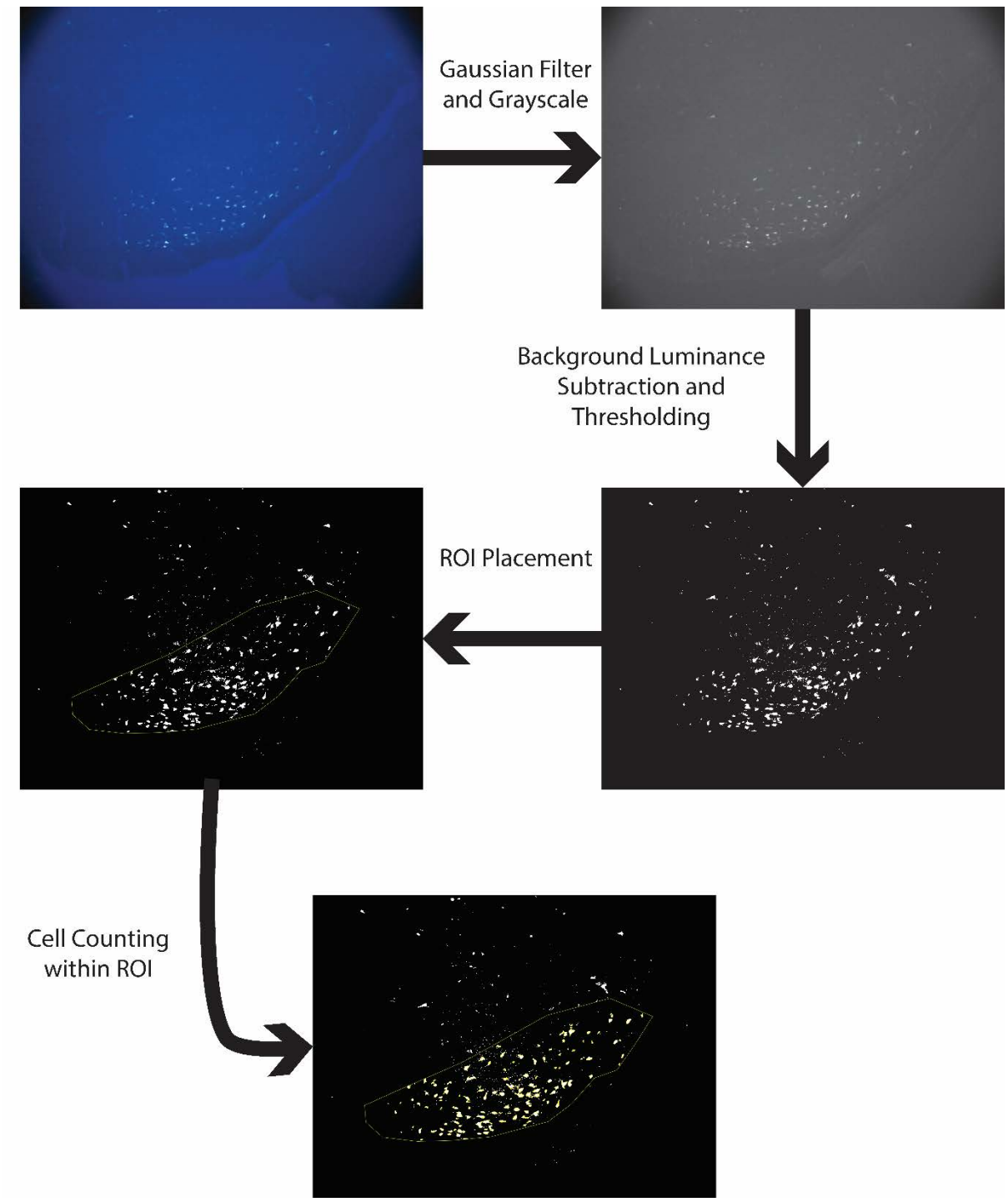

Figure 2-3. Processing Pipeline for Quantitative Measurement of Connection Preference

This process allowed for the semi-automated quantification and analysis of the tracing data in Chapter 3. Images were Gaussian filtered, then converted to grayscale 16bit format. Background luminance subtraction was based on manual sampling of background luminance through an ROI and then the images were binary thresholded. Automated cell counting was conducted on specific ROIs for brain regions or subregions

2.4 Electrophysiology

2.4.1 Electrophysiological Setup

2.4.1.1 Mice

The electrophysiological responses in V1 were recorded using 16 contact laminar electrodes (Atlas Neuroengineering) with a spacing of 50 (E16-50-S1-L8), 150 (E16-150-S1-L7), or 250µm (E16-250-S1-L8). Data were acquired with a Neuralynx LynxSX recording system and the Cheetah software package (Neuralynx, Bozeman, MT, USA). This was interlinked with the presentation software Cortex 5.95 (http://www.nimh.nih.gov/labs-at-nimh/research-areas/clinics-and-labs/ln/shn/software-projects.shtml) to collect the experimental data. The sample periods utilised for analysis were the spontaneous firing period (256ms before stimulus onset) and the entire period of stimulus presentation (from pre-cue onset to post-cue offset 550ms).

2.4.1.2 Macaques

The electrophysiological responses in V1 were recorded using 16 contact laminar electrodes (Plexon U probes) with a spacing of 150 um. Data were acquired with a Neuralynx Digital Lynx recording system and the Cheetah software package (Neuralynx, Bozeman, MT, USA). This was interlinked with the presentation software Cortex 5.95 (http://www.nimh.nih.gov/labs-at-nimh/research-areas/clinics-and-labs/ln/shn/software-projects.shtml) to collect the experimental data. The sample periods utilised for analysis were the spontaneous firing period (256ms before stimulus onset) and the entire period of stimulus presentation (from pre-cue onset to post-cue offset 550ms).

The eye position for the experiments was mapped onto the cortex program with a 120Hz infa-red camera and the TRec Eye Tracking software (Thomas Recording, Germany).

2.4.2 Receptive Field Mapping Paradigm

2.4.2.1 Mouse

Visual receptive field (RF) mapping was achieved through a reverse correlation paradigm (Gieselmann and Thiele, 2008). The stimuli were presented on a 24 inch CRT monitor at

120Hz refresh rate. 108 black squares, which measured either 11.1 or 8 degree of visual angle (DVA), were presented to the animal in a continuous random sequence for 150ms each. The 11.1 DVA squares were used to cover the entire presentation screen. The smaller 8 DVA squares were used to hone in on the RF, and obtain a finer grained representation.

2.4.2.2 Macaque

The visual receptive field mapping paradigm employed for the macaque was almost identical to the mouse. The stimuli were presented on a 24 inch CRT monitor at 110Hz refresh rate. However, due to the increased visual acuity and decreased RF sizes in this animal the sizes of the stimuli were reduced to 0.25- 2 DVA. Furthermore, there was no optogenetic stimulation as the animal had not been transfected.

2.4.3 Visual Stimulation Paradigm

2.4.3.1 Mouse

To analyse effects of bottom-up attention in a passive viewing paradigm, the following visual experimental protocol was employed. The placement of the stimuli entailed two sinusoidal gratings (vertical and horizontal orientation, spatial frequency (sf)-0.2cpd, 80% contrast, 30 DVA diameter) at either the RF location or a location at the identical elevation, but on the opposite azimuth position relative to the CRT screen midline. The animal faced the screen in a manner such that the visual receptive field(s) of the recorded neuron(s) would not extend beyond the CRT screen midline ensuring it would not be covered by both visual stimuli. The experiment involved a design which yielded eight conditions which were determined as follows:

- The presence of either the vertical ‘target’ grating or the ‘horizontal ‘distractor’ grating in the receptive field location (note, that the terminology of target and distractor is derived from the macaque experiments, as the macaque was engaged in an active task on some recording days where he had to detect and report the location the vertical grating).
- The presence of either a pre-cue or a post-cue above/below the receptive field location or above/below the non-RF location

This resulted in the following 8 conditions, i.e. pre-cue RF with the vertical grating on the RF, pre-cue non-RF with the vertical grating on the RF, post-cue RF with the vertical grating on the RF, and post-cue non-RF with the vertical grating on the RF, pre-cue RF with the horizontal grating on the RF, pre-cue non-RF with the horizontal grating on the RF, post-cue RF with the horizontal grating on the RF, and post-cue non-RF with the horizontal grating on the RF.

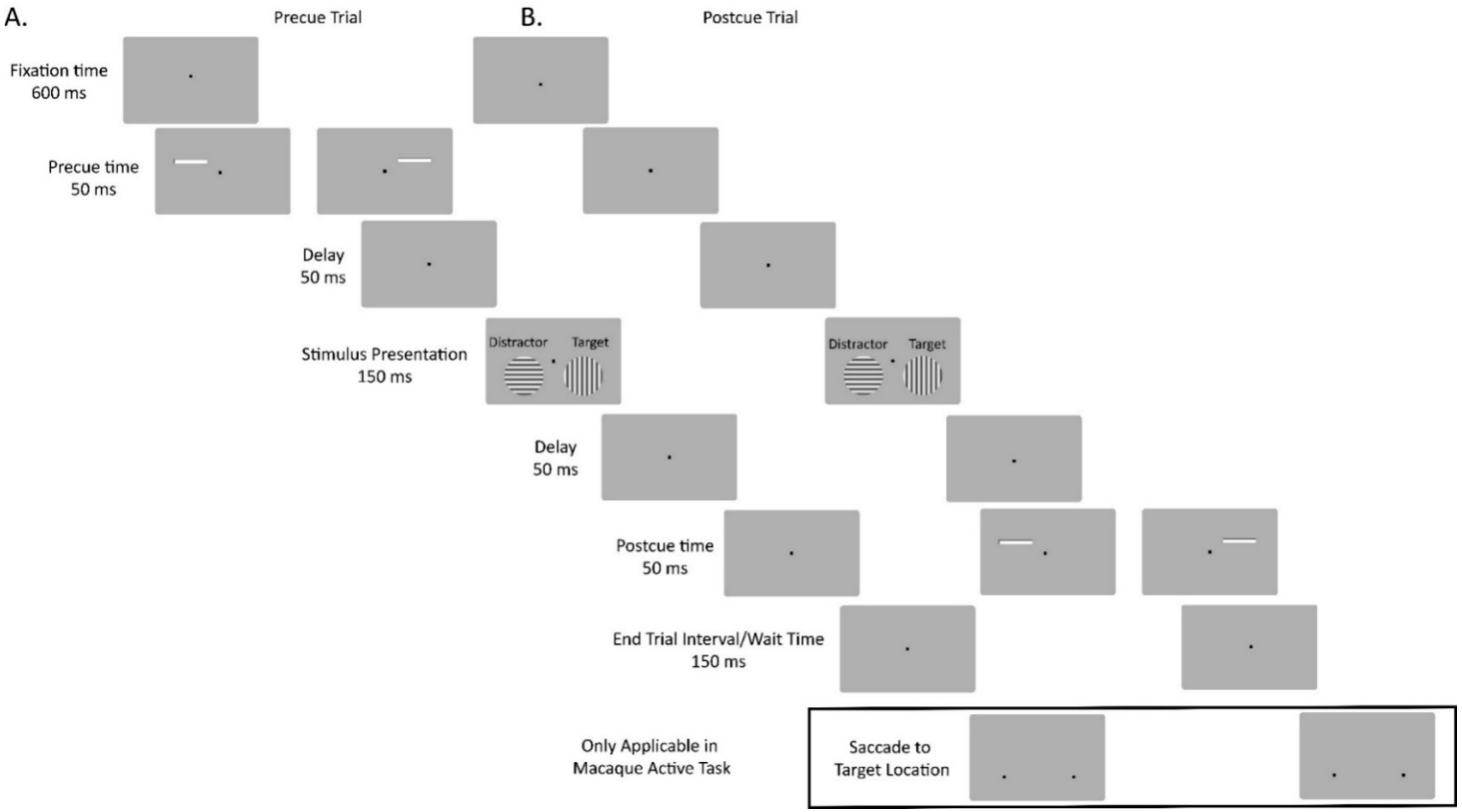

Figure 2-4. Trial Structure Utilised for Bottom-Up Attention Studies in both Macaque and Mouse

Trials started with a prestimulus/fixation time. Then depending on the condition a pre-cue could be presented followed by a delay period. The two stimuli were then presented (Vertical 'Target' and Horizontal 'Distractor' gratings), so that one grating fell on the RF of the recorded neurons. The other grating was presented in the opposite half of the screen (opposite relative to the vertical [azimuth] midline). Following grating presentation a delay period of 50 ms occurred. Thereafter, either a further delay period occurred (50ms) or or post-cue was presented (50 ms) depending on the condition. Finally after another delay of 150ms the trial ended. In the macaque, we additionally employed an active saccade paradigm, which required the animal to saccade to the location of the previous 'Target' grating.

Furthermore on certain recording days, optogenetic stimulation of prefrontal regions (transfected with channel rhodopsin 2) was implemented for the entire pre-cue onset to post-cue offset period on 50% of the trials. This then yielded 16 conditions, i.e. the original 8 doubled to be with and without optogenetic stimulation.

A trial started after a variable prestimulus time between 600-1200ms. In 4/8 conditions a pre-cue would be presented for 50ms, above (or below) either the RF location or in the opposite hemifield/screen location, followed by a 50ms interstimulus time. Thereafter two gratings (one with horizontal orientation, the other with vertical orientation sf-0.2cpd, 80% contrast (Michelson contrast), 30 DVA diameter) were presented for 150ms, with a 50% probability of one or the other being placed in the RF. In the remaining 4/8 conditions, the gratings were followed by a 50ms interstimulus time and then a post-cue for 50ms above or below either the RF or non-RF side, i.e. the opposite screen half for the mouse recordings. Note that only one cue was presented per trial (see Figure 2-4). The pre/post-cues were horizontal bars (15 degrees length, 2 degrees wide). The pre/post-cue location was set to be above or below the visual receptive field of the recording area depending on the RF location on the screen. The average distance from the centre of the RF was 19 degrees. The cue appeared in either of the 4 locations (i.e. pre-cue RF, pre-cue non-RF, post cue RF, post cue non-RF) on an even probability basis.

2.4.3.2 Macaque

The visual stimulation paradigm utilised for the macaque was very similar to that used for the mouse. The trial structure was identical, apart from of the following factors. The stimuli were of a different size, spatial frequency, and contrast. The spatial frequency was 5cpd, the contrast was 48% (Michelson contrast), and they were of 3 or 8 DVA diameter. Due to the changes in stimulus size the cue size and position was modified (for 3 degree gratings, the cue size was 2.62 DVA long and 0.33 DVA wide, for the 8 DVA gratings, the cue size was 8 DVA long and 1 DVA wide). Moreover, due to the fact that the monkey fixated centrally on the screen, the non-RF stimulus was placed in the opposite hemifield with equal eccentricity relative to the fixation spot. Throughout the entire duration of the pre-cue to post-cue phase the monkey was centrally fixated by keeping its eye focused in a 2 DVA window around the fixation spot. There was no optogenetic stimulation in the

macaque, which meant that the simpler 2x4 design was employed. Finally, there were two versions of the task, a Passive Fixation paradigm (similar to the mouse paradigm, no active response was required) and a Saccade based paradigm, where the monkey had to detect the location of the vertical grating and report it via a saccadic eye movement at the end of the trial. This active version therefore differed insofar that it required the presentation of 2 saccade targets at the end of the trial and an active response (saccade to one of the targets). The saccade targets were presented with a 200ms delay after the post-cue offset time. They appeared at exactly the center locations of previously presented gratings. The monkey had to saccade to the target where the vertically orientated grating had been (see Figure 2-4).

2.5 Optogenetics

2.5.1 Viral Constructs

The viral construct used in this research was based on the adenosine associated virus serotype 5 with different promotors and expression of optogenetic channels. The construct causes excitatory neurons to express channel rhodopsin 2 under a calmodulin-dependent kinase II promotor with a yellow florescent protein marker (AAV5-CamKII-ChR2-eYFP, Penn Vector Core, USA). This non-specifically transfects excitatory projection neurons within the injection site and allows their activity to be driven by blue light excitation of 490nm.

2.5.2 Optical Stimulation

The optical stimulation of the transfected regions was achieved using an optical fibre placed above the cranial widow. The wavelength used for channelrhodopsin 2 activation was 470nm. There were two different light sources and fibres utilised in this study. The details for this are summarised in Table 2-2.

2.5.3 Efficacy of Viral Transfection

The efficacy of the viral transfection in the mouse brain was assessed in a number of ways. Firstly, since the construct causes the expression of yellow fluorescent protein, a visual inspection of the injection site was conducted after the skull was thinned. A UV light was used as optical stimulation (~490nm, Kerr Demi Plus light curer) coupled with protective

laser light glasses as a filter (filtered 180 to 532 nm). This allowed for a general estimation of expression whilst the animal was still alive. Once this first assessment was conducted, a more detailed quantification of the functional expression of the viral constructs was attempted.

Before cranial window implantation, the efficacy of viral transfection in the injection site was analysed. To do this the animal was sedated as previously described, and a craniotomy (approximately 1-2 mm diameter) was performed over the previous viral injection site. A laminar electrode was lowered and an optic fibre was placed above the craniotomy. The region was stimulated with light, with either long activation times or various pulse trains, depending on the recording day. Rasters and PSTHs were produced for individual cells or multi-units per electrode contact. Efficacy of light presentation was tested with Wilcoxon Signed Rank test, whereby firing rates (spikes per second) for periods of optogenetic stimulation were compared to rates during periods without stimulation. For comparison, this test was compared to control condition in which sham (no stimulation) was present.

2.5.4 Electrophysiological Setup

The electrophysiological setup utilised for the optogenetic experiments was the same as previously mentioned for the bottom-up attentional paradigm for the mouse.

2.6 Electrophysiological Data Analysis

2.6.1 Precuing and Optogenetic Stimulation General Analysis

To examine how the different forms of (pre/post)-cuing, grating (vertical/horizontal), and optogenetic stimulation (presence/absence) conditions affected neuronal activity in the bottom-up attentional paradigm a repeated measures multi-factorial 2x3x4 ANOVA was conducted on both the spiking activity and the MUAe.

For single contacts in the macaque and mouse bottom-up attentional data the activity for each of the 8 experimental conditions in three different trial time periods (pre-cue, grating stimulus, and post-cue time windows) was calculated for contacts with a z-score > 3 to the grating stimulus presentation. The z-score was calculated as shown below:

$$zscore = \frac{X - \mu}{\sigma}$$

The mean stimulus grating response (X) was taken and the mean (μ) of the whole spontaneous trial period. This was then divided by the standard deviation (σ) over all of the trials.

These cohorts were then run through a 2x4x4 way ANOVA, where the factors tested were grating type (vertical 'target' or horizontal 'distractor'), time window (4 levels-pre-cue, stimulus, post-cue, and whole pre-cue on to post-cue off) and cuing condition (pre-cue RF, pre-cue non-RF, post-cue-RF, post-cue non-RF).

For the optogenetic mouse experiments the ANOVA was adapted to be a 2x2x4x4 way ANOVA, which was the same as the previous analysis with an added factor of optogenetic stimulation (presence or absence).

A population average was then obtained separately across all the experiments for these contacts. The ANOVA used for the population analysis to test the significance of different factors and interactions.

Any significant factor or interaction was further tested with post hoc Wilcoxon Signed Rank tests, which were FDR corrected for account for multiple comparisons (Benjamini and Hochberg, 1995).

2.6.2 Spiking Data

Spiking data was collected from the electrodes in both the macaque and mouse at 32kHz and bandpass filtered from 600-9000Hz. The data for each contact was then thresholded using the Spike Sort 3D program (http://neuralynx.com/research_software/spike_sort_3d) with individualised manual waveform clustering. The data for each contact was then aligned to the experimental stimuli events for further analysis.

2.6.2.1 Raster Plots

Raster plots for individual recording locations for each experiment were produced by aligning spike events over time for each trial. Example contacts were then taken for illustrative purposes within specific results sections.

2.6.2.2 Peri-stimulus Time Histograms (PSTHs)

For individual recording contacts, the spiking activity for each trial was calculated. This was then averaged and normalised to the maximum activity per channel per recording. This trace was then Gaussian filtered and plotted for individual recordings. Grand averages for each brain area were calculated by including contacts where visual responses (to the gratings) compared to baseline activity achieved a z-score of z-score > 3, regardless of cuing condition. This population of normalised responses was then averaged and plotted for each the conditions.

2.6.3 Multi-Unit Activity Envelope (MUAe)

Continuously sampled data was processed to obtain the envelope multiunit activity (MUAe) utilising a technique adapted from the literature (Super and Roelfsema, 2005). This entailed collecting the data at 32kHz and bandpass filtering it between 600-9000Hz, followed by rectification of the signal. It was then low-pass filtered at 200Hz and down-sampled to 1kHz for further analysis. The MUAe activity was then aligned to the experiment per trial and averaged. This resultant average was then smoothed with a Gaussian filter. A z-score for the visual induced activity was calculated and channels with a z-score > 3 were included for further analysis.

To generate grand average plots for each area, the signals from contacts with a stimulus z-score > 3 were averaged. This was then plotted along with the standard error of the mean (SEMs) across each condition. In addition to this the cumulative normalised activity was calculated across the conditions for the trial length and tested for significant differences with Wilcoxon Signed Rank tests.

2.6.4 Local Field Potential Analysis

The LFP for this analysis was recorded at 32kHz and then down-sampled to 1kHz for further analysis. It was aligned to trial events for each electrode contact for each experiment in all animals. This was then put through a matching pursuit analysis program which was adapted from previous literature (Chandran Ks et al., 2016). This entailed an initial 50Hz filter to remove any line noise. Then a 1024ms time window was taken

around the stimulus onset for processing with the matching pursuit algorithm. The scripts for this analysis were supplied by the creator Supratim Ray (https://github.com/supratimray/MP). This resulted in a matrix of time frequencies modulations for each channel. This was then collated and averaged for all channels with a MUAe stimulus induced activity of z-score > 3. Difference plots for conditions were calculated by subtracting the time frequency grand average matrixes for each conditions to result in plots for pre-cue RF minus pre-cue non-RF, pre-cue RF minus post-cue-RF for each of the two grating stimuli. The uncorrected frequency differences were then plotted. Additionally, a t-test was then run to test significance changes in frequency over time for each condition. The resulting p-values were then FDR corrected to account for multiple comparisons. These significance values were then used to threshold the frequency time plots to significant differences.

This matching pursuit design was employed as this algorithm, although being computationally intensive has a number of advantages over other ways of analysis. The most important of which is that due to the specifics of the time frequency windowing (not covered herein, see (Chandran Ks et al., 2016). This allows for good decoding of LFP spectral frequency content, while still having good temporal specificity. This is in contrast to other methods of analysis such as fast Fourier transform.

Table 2-1. Summary of the Injection and Recording Chamber Locations Utilised in Mice

Brain Area Name	Tracing Injection Coordinates (Bregma = (0, 0))	Virus Injection Coordinates (Bregma = (0, 0))	Recording Coordinates (Bregma = (0, 0))
Cingulate Area	+1.1 mm AP, +0.3mm ML, DV 1.3mm	+1.1 mm AP, +0.3mm ML, DV 1.3, 0.9mm	+1.1 mm AP, +0.3mm ML, DV 1.3mm
Motor Cortex Area 2	+1.1 mm AP, +0.3mm ML, DV 0.8mm	+1.1 mm AP, +0.3mm ML, DV 0.8, 0.3mm	+1.1 mm AP, +0.3mm ML, DV 0.8mm
Primary Visual Cortex			-2 mm AP, +2mm ML -3.5 mm AP, +2mm ML
Superior Colliculus Medial	-3.7 mm AP, +0.3mm ML, DV 1.3mm		-3.5 mm AP, +0.8mm ML
Superior Colliculus Lateral	-3.7 mm AP, +1.3mm ML, DV 2.2mm		-3.5 mm AP, +0.8mm ML

Table 2-2. Summary of the LED Light Sources and Optical Fibre Powers Utilised

LED Light Source	Source Power	Optical Fibre Diameter	Power Output from Fibre
TRec	9mW	TRec-125um diamete	0.3mW
CoolLED- pE100	90mW	Thorlabs- Custom 1.5mm diameter	87mW

Chapter 3. The Neuroanatomical Connectivity Underlying Orienting in the Mouse

3.1 Introduction

The Superior Colliculus (SC) is a multimodal sensory-motor midbrain structure, involved in visual, auditory and somatosensory triggered orienting (Stein, 1981, Westby et al., 1990, Meredith et al., 1992, Wallace et al., 1993, Thiele et al., 1996). In most species the spatial representation of sensory inputs are aligned to the retinotopic organization of the superficial layers where the central or frontal field/space is represented in the anterior SC, the upper visual hemi-field in the medial SC, and the lower visual hemi-field in the lateral SC (Goldberg and Wurtz, 1972b, Drager and Hubel, 1976, Meredith and Stein, 1990, Thiele et al., 1991). Multimodal sensory processing occurs in the intermediate and lower layers where sensory neurons are intermixed with sensory-motor responses coding for eye (Wurtz and Albano, 1980), head (Harris, 1980), pinnae (Stein and Clamann, 1981), and whisker movements (Bezdudnaya and Castro-Alamancos, 2014). In primates electrical microstimulation in intermediate and deep layers of SC results in defined saccadic eye-movements, with endpoints in the visual receptive field locations of the stimulation sites (Stryker and Schiller, 1975). This suggests that sensorimotor integration in the SC invariably triggers orienting responses towards the object of interest. However, in rats, stimulation of the SC can elicit orienting responses towards the visual field representation at the stimulation site, and result in defensive behaviours such as freezing, or orienting movements away from the visual field region (Dean et al., 1988b, Dean et al., 1989). These different types of behaviour are, at least to some extent, mediated by two separate output pathways from the intermediate and deep layers of the SC. The crossed descending tecto-reticulo-spinal projection, which preferentially arises from the lateral SC (Redgrave et al., 1986), is speculated to be involved in approach movements towards novel stimuli, whereas the uncrossed ipsilateral pathway, of which certain parts arise in the medial SC, is likely involved in avoidance and escape-like behaviour (Westby et al., 1990). This view is in accord with the ecological niches which rodents occupy, where predators most likely appear in the upper visual field, represented medially in the SC, while prey most likely appear in the lower visual field where they can also be detected by the whisker system (Westby et al., 1990, Furigo et al., 2010), represented

preferentially in the lateral SC (Favaro et al., 2011). In line with this, inputs to the medial and the lateral parts of the SC in the rat show an anatomical segregation of inputs from subcortical and from cortical sources which may feed into the avoidance and approach related pathways (Comoli et al., 2012). It is currently unknown whether this distinction holds for the mouse SC, although a recent study has dissected a pathway originating in the intermediate layers of the medial SC. This is involved in defensive behaviour, and provides a short latency route through the lateral posterior thalamus to the lateral amygdala (Wei et al., 2015). Beyond the level of the SC, the larger scale cortical and subcortical anatomical networks involved in approach and avoidance behaviour in rodents have not been delineated in great detail. In pursuit of this goal, retrograde tracers were injected into the medial or lateral parts of the murine SC (SCm, SCl) to determine their specific input connections. We found that SCl and SCm receive inputs from shared, but also largely distinct sources. The major cortical source of input to SCl originated from Motor Cortex Area 2 (M2) (which in rats has been labelled the Frontal Orienting Field (FOF) (Erlich et al., 2011)), while a major cortical input to SCm arises in the Cingulate Area (Cg). Anterograde injections into M2 and the Cg, reveal output selectivity, which is not limited to the SC. M2 has descending control over a network of areas involved in somatosensation and appetitive behaviours, while Cg has descending control over a network of areas involved in analysis of far sensory processing (vision, audition), and avoidance behaviours.

3.2 Methodology

The methodology utilised for this section has been described previously in detail (see Chapter 2.2 & 2.3). In brief, retrograde and anterograde tracing was conducted in a number of different brain regions in the mouse brain. For the retrograde tracing the medial (n=5) and lateral (n=4) SC were chosen for iontophoretic injection of fluorogold (FG) (3% in saline, +500nA for 30 minutes). For the anterograde tracing, the motor cortex area 2 (M2) (n=5) and cingulate region (n=4) were chosen for pressure injection of biotinylated dextran amine MW 10,000 (BDA) (3% in saline, 66nl volume). The exact coordinates of injection locations are listed in Table 2-1.

After a short post-injection survival period, the animal were transcardially perfused with paraformaldehyde and the brains were removed, cryoprotected and sectioned at 40µm on a

cryostat. The sections were then analysed for innate fluorescence signal or processed to increase the labelling signal. In the retrograde condition the brain slices underwent cell counting with ImageJ and were quantified in terms of percentage of total labelled cells per animal. These values were then averaged for brain regions which displayed labelled cells across the entire experimental cohort. These averages were then placed into graphical and tabular forms. Any variance present in the results was examined in terms of confidence intervals which were used to inform the histograms which can be seen below.

The anterograde conditions underwent qualitative visual assessment to produce a table of relative labelling densities for each brain region with visible label. These values were then placed into graphical and tabular forms for brain regions which displayed labelled cells across the entire cohort

Certain regions of interest in both the retrograde and anterograde labelling underwent a further quantification to test for significant differences in labelling preference between the injection conditions. A modulation index for was calculated and a Mann-Whitney test was used for significance testing. A full description of the methodology employed to achieve this is detailed in Chapter 2.3.

3.3 Results

The retrograde tracer FG was iontophoretically injected into the SCm or SCl, and injections of the anterograde tracer BDA were completed into the two main cortical SC input structures which are assumed to be key structures involved in top down behavioural control, namely the Cg or M2. It was found that the intermediate and deep layers of the SCl and SCm showed a segregation with respect to specific cortical and subcortical afferents. Moreover, Cg and M2 showed equally substantial segregation regarding their projection sites. The specificity of these connections supports the hypothesis that the medial SC and the Cg are involved in avoidance (aversive) behaviour, while SCl and M2 are involved in approach (appetitive) behaviour.

To begin, the results from the experiments where retrograde tracers were injected into the SC will be discussed, followed by the results where anterograde tracers were injected into M2 and Cg, respectively.

3.3.1 Retrograde Tracing

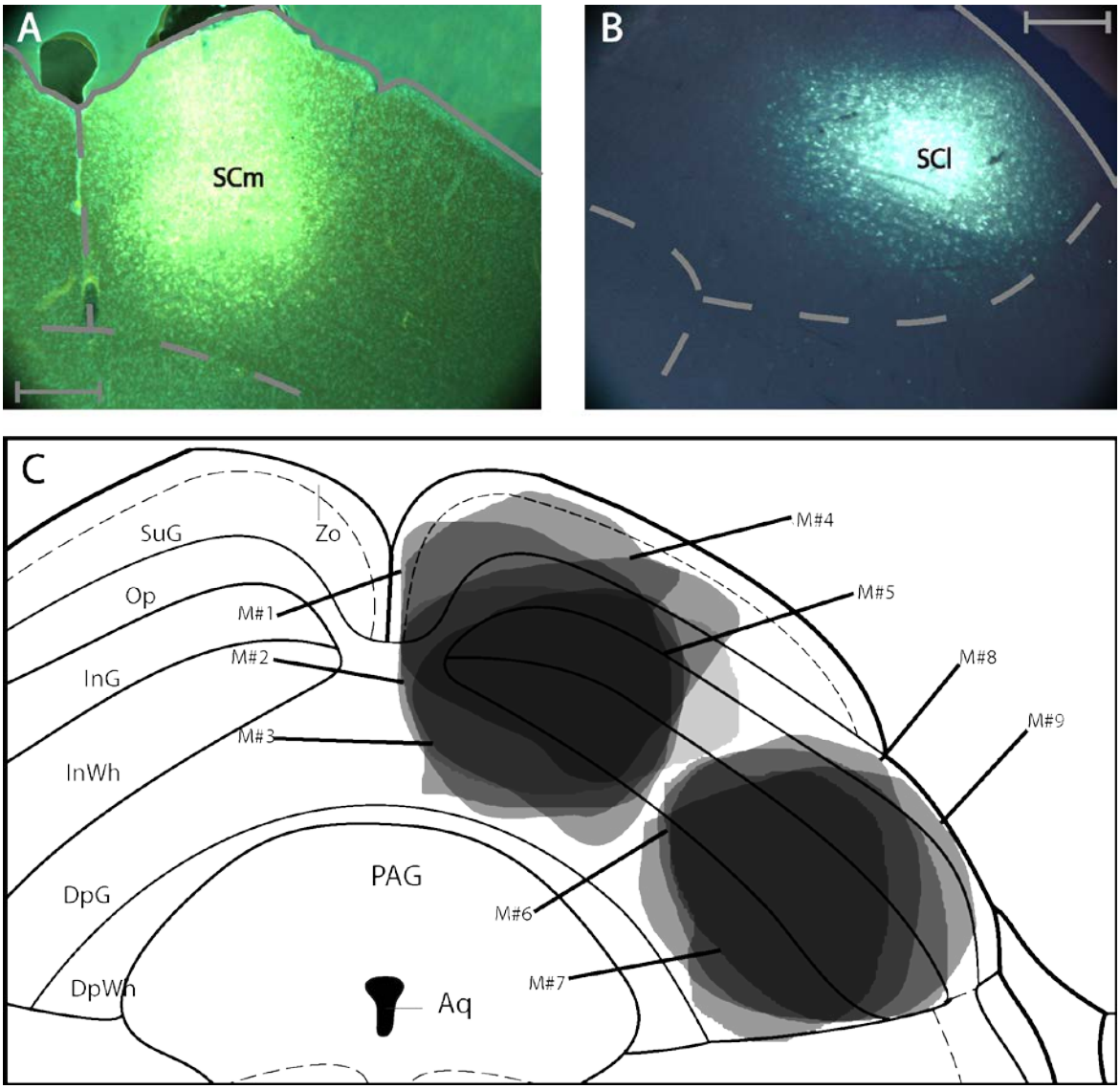

Figure 3-1. Retrograde Tracer Injections in the Mouse Superior Colliculus

A. Photomicrograph of fluorogold injection into the medial superior colliculus. **B.** Photomicrograph of fluorogold injection into the lateral superior colliculus. All scale bars equate to 250µm. **C.** Summary of injections. Each shaded area represents the extent of the labelled injection site for both medial and lateral SC conditions. The darker shading indicates overlap of injection volume. Nomenclature is derived from Franklin, K.B.J. & Paxinos, G. 2012. For abbreviations see list.

5 medial and 4 lateral injections were performed for retrograde tracing in the mouse SC. Local spread of tracer in all of these cases was confined to the target sites in the SC, i.e. lateral injections did not spread into medial parts and vice versa. The injections also did not spread into neighbouring brain areas such as the periaqueductal gray (PAG) or the mesencephalic reticular formation (mRt) (Figure 3-1, A-C). There was some variation in the anterior-posterior extent of the injection sites, which was caused by slight differences in overall bregma localisation, probe placement and brain size. This may have caused differences in the brain region and subregional origin of retrogradely labelled cells. However any differences were mitigated by the strict inclusion criterion. Namely, that any brain region and subregional labelling bias/separation must have been present throughout all cohort cases to be included in the results. Retrogradely labelled cells usually arose from areas located ipsilateral to the injection site, but occasionally also from areas contralateral to the injection site. These two areas will be further delineated by the use of the terms ‘ipsilateral’, ‘contralateral’, and ‘bilateral’. First, the cortical areas, where retrograde label was found will be described, followed by a description of subcortical areas where retrograde label was identified. Descriptions will start with those areas that project exclusively to either the SCl or the SCm, followed by a description of areas that project to both SC subdivisions, with a focus on areas where retrograde label was medium to strong. A complete list of all structures that showed retrograde label after SC injections is given in Table 3-1, Figure 3-2, Figure 3-3, and Figure 3-4. Furthermore to aid in representation of the data, labelling from both the SCl and SCm is presented schematically in serial atlas sections for example cases, see Figure 3-5 and Figure 3-6.

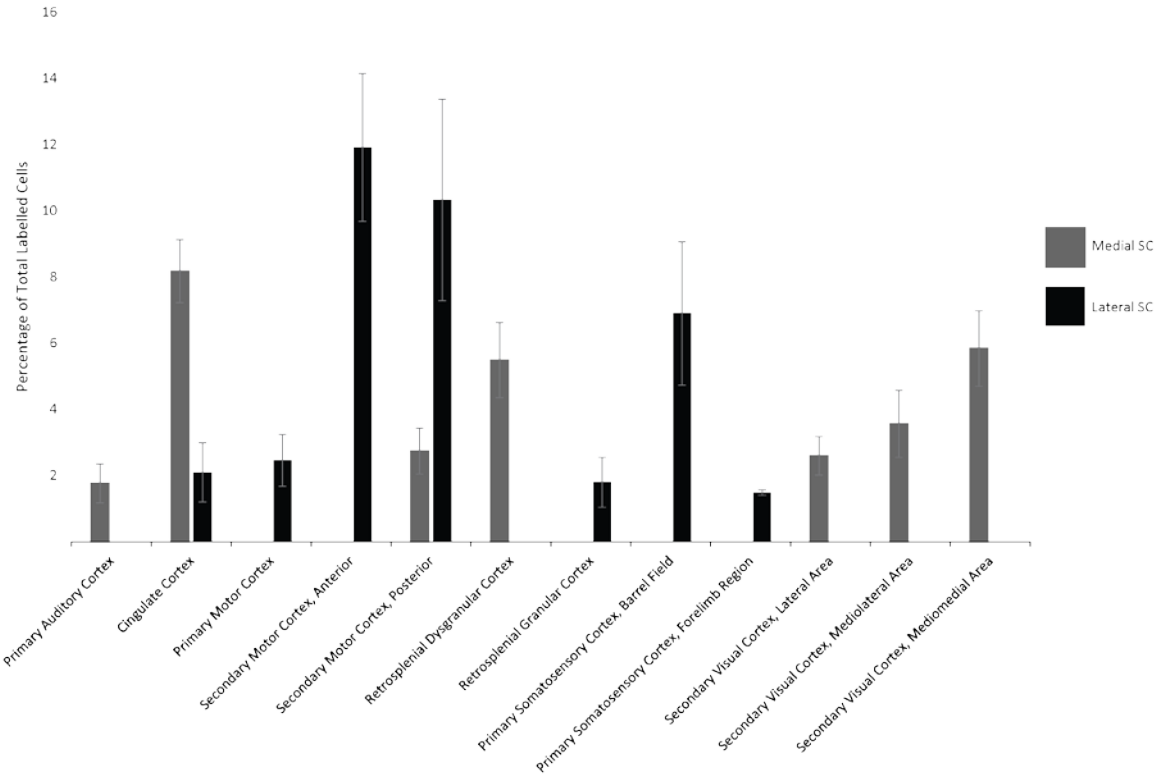

Figure 3-2. Summary of Average Percentage of Total Labelled Cells in the Cortex for Ipsilateral Brain Areas after Injections of Fluorogold into the Medial (Gray) and Lateral (Black) Superior Colliculus.

Histograms represent percentage of total labelled neurons found in each area. Error bar represent 95% confidence intervals for the population of injection cases.

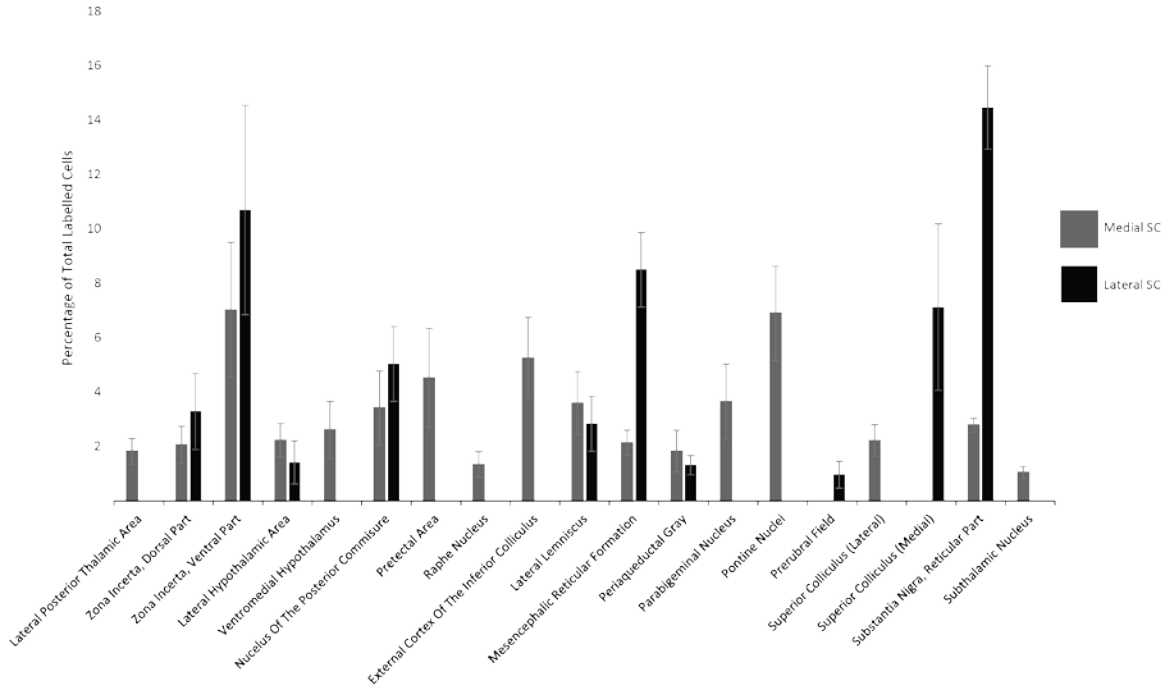

Figure 3-3. Summary of Average Percentage of Total Labelled Cells in the Subcortex for Ipsilateral Brain Areas after Injections of Fluorogold into the Medial (Gray) and Lateral (Black) Superior Colliculus.

Histograms represent percentage of total labelled neurons found in each area. Error bar represent 95% confidence intervals for the population of injection cases.

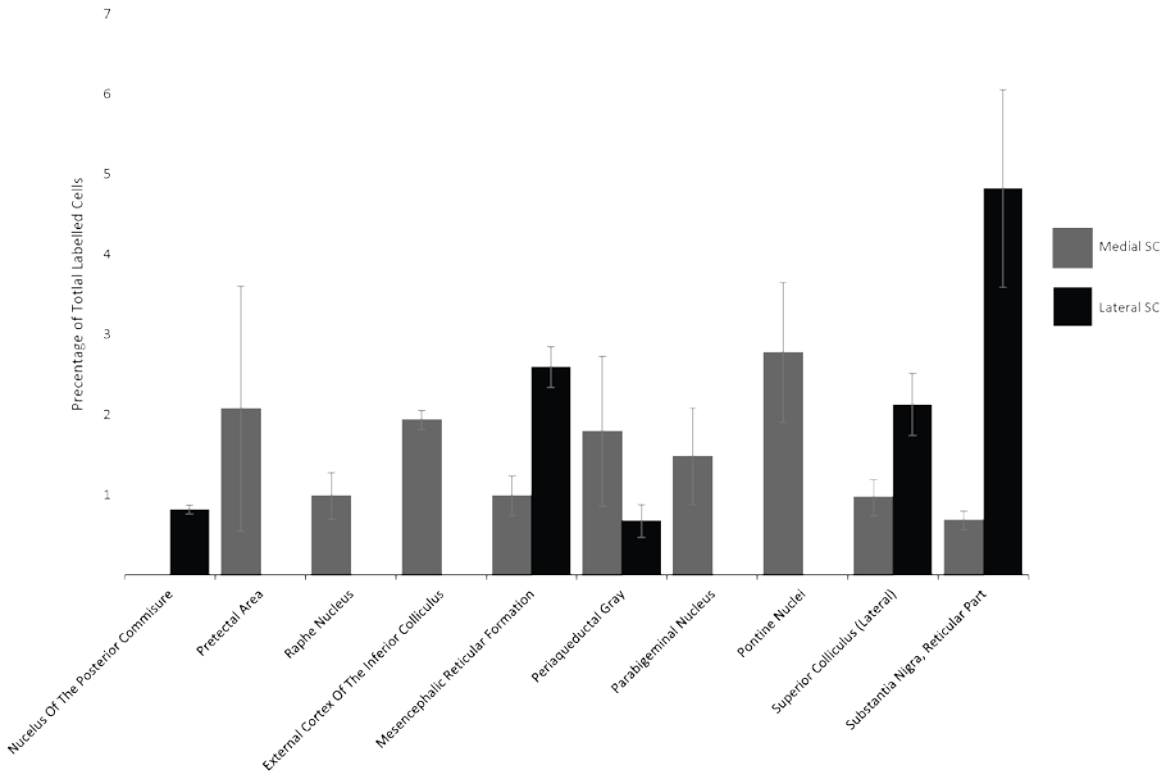

Figure 3-4. Summary of Average Percentage of Total Labelled Cells for Contralateral Brain Areas after Injections of Fluorogold into the Medial (Gray) and Lateral (Black) Superior Colliculus.

Histograms represent percentage of total labelled neurons found in each area. Error bar represent 95% confidence intervals for the population of injection cases.

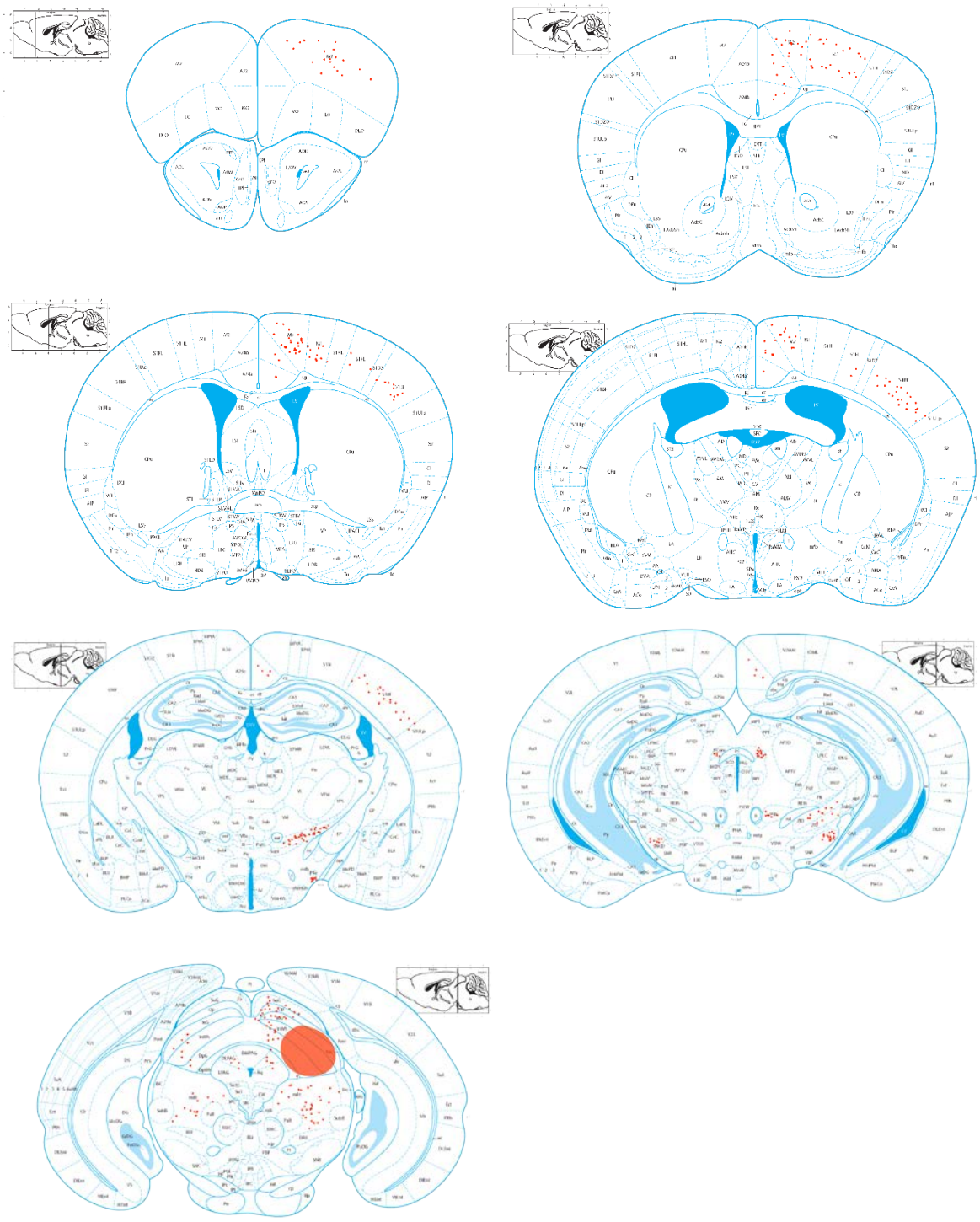

Figure 3-5. Schematic Representation of Retrograde Neuronal Labelling After Injection of Fluorogold into the Lateral Superior Colliculus in Single Case

Each red dot represents a single labelled neuron. Red shaded areas represents injection site extent. Atlas sections adapted from Paxinos and Watson 2012.

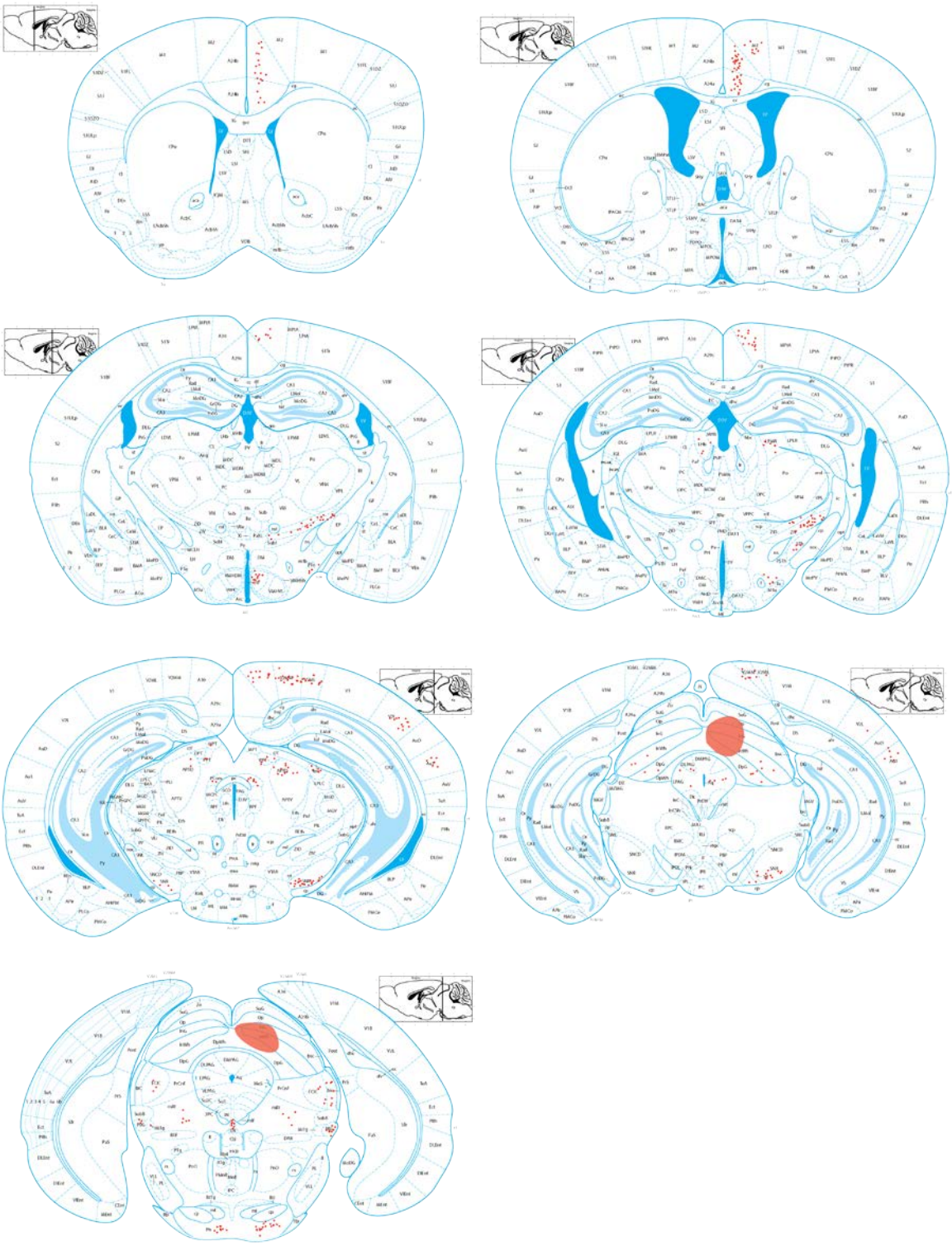

Figure 3-6. Schematic Representation of Retrograde Neuronal Labelling After Injection of Fluorogold into the Medial Superior Colliculus in Single Case

Each red dot represents a single labelled neuron. Red shaded areas represents injection site extent. Atlas sections adapted from Paxinos and Watson 2012.

Table 3-1. Qualitative Densities of Retrogradely Labelled Brain Areas after Injection of Fluorogold in the Medial and Lateral Superior Colliculus

Relative cell count densities were assigned one of five levels via quantitative assessment of percentage of total cells labelled in each injected animal. The percentages were then averaged across the entire experimental cohort (none '-' 0%, low '+' < 2.5%, medium '++' <5%, high '+++' <7.5% and very high '++++'>7.5%). See methods for more details. Injection sites could not be quantified in this manner due to tracer spread and were therefore marked with N/A.

		SC (m)		SC(l)	
		Ipsi	Contra	Ipsi	Contra
Cortex					
Prefrontal					
Cg	cingulate cortex	++++	-	+	-
M1 (An)	primary motor cortex	-	-	+	-
M2 (An)	secondary motor cortex	-	-	++++	-
M2 (Pos)	secondary motor cortex	++	-	++++	-
Sensory					
Au1	primary auditory cortex	+	-	-	-
RSD	retrosplenial dysgranular cortex	+++	-	-	-
RSG	retrosplenial granular cortex	-	-	+	-
S1BF	primary somatosensory cortex, barrel field	-	-	+++	-
S1FL	primary somatosensory cortex, forelimb region	-	-	+	-
V2L	secondary visual cortex, lateral area	++	-	-	-

V2ML	secondary visual cortex, mediolateral area	++	-	-	-
V2MM	secondary visual cortex, mediomedial area	+++	-	-	-
Thalamus					
LPMR	lateral posterior thalamic nucleus, mediorostral part	+	-	-	-
ZID	zona incerta, dorsal part	+	-	++	-
ZIV	zona incerta, ventral part	+++	-	++++	-
Hypothalamus					
LH	lateral hypothalamic area	+	-	+	-
VMH	ventromedial hypothalamus	++	-	-	-
Pretectum					
PCom	nucelus of the posterior commissure	++	-	+++	+
PT	pretectal area	++	+	-	-
Midbrain					
DRV	dorsal raphe nucleus	+	+	-	-
ECIC	external cortex of the inferior colliculus	+++	+	-	-
ll	lateral lemniscus	++	-	++	-
mRt	mesencephalic reticular formation	+	+	++++	++
PAG	periaqueductal gray	+	+	+	+
PBG	parabigeminal nucleus	++	+	-	-
Pn	pontine nuclei	+++	++	-	-

PR	prerubral field	-	-	+	-
SC (l)	superior colliculus (lateral)	+	+	N/A	+
SC (m)	superior colliculus (medial)	N/A	-	+++	-
SNR	substantia nigra, reticular part	++	+	++++	++
STh	subthalamic nucleus	+	-	-	-

3.3.1.1 Cortex

Retrogradely labelled cell populations in the neocortex, after injection into the two different subdivision of the SC, were remarkably segregated. As expected, retrogradely labelled cells in the cortex were confined to layer 5B.

The secondary visual cortex (V2MM, V2ML, V2L, ipsilateral) (Figure 3-7A), the primary auditory cortex (Au1, ipsilateral) (Figure 3-7B), as well as the dysgranular portion of the retrosplenial cortex (RSD, ipsilateral) Figure 3-7C) showed retrograde labelling only after SCm injections.

Conversely, the somatosensory areas, specifically S1, the barrel field (S1BF, ipsilateral) (Figure 3-8A), the flank region (S1FL, ipsilateral), the primary motor cortex (M1, ipsilateral) Figure 3-8B), as well as the granular portion of the retrosplenial cortex (RSG, ipsilateral) (Figure 3-8C) showed retrograde labelling exclusively after SCl injections.

There was a separation of labelled RSD and RSG cells for the SCm and SCl injection, with SCm receiving input mostly from RSD, and SCl receiving input mostly from RSG, even if labelled RSG neurons were found in two of the six SCm injection cases.

Retrogradely labelled cells after SCm and SCl injections were found in the M2 (ipsilateral), and in the Cg (ipsilateral). While these two areas showed retrogradely labelled cells after both, SCl and SCm injections, they did so to different degrees. The SCm injections resulted in higher numbers of labelled cells in the Cg (Figure 3-7D). Conversely, the SCl injections resulted in higher numbers of retrogradely labelled neurons in M2 (Figure 3-8D). This bias in connectivity for Cg and M2 was significant

(p=0.016, Mann-Whitney U-Test, Figure 3-11A left). Cells from both these regions are shown in higher magnification in Figure 3-9, and Figure 3-10.

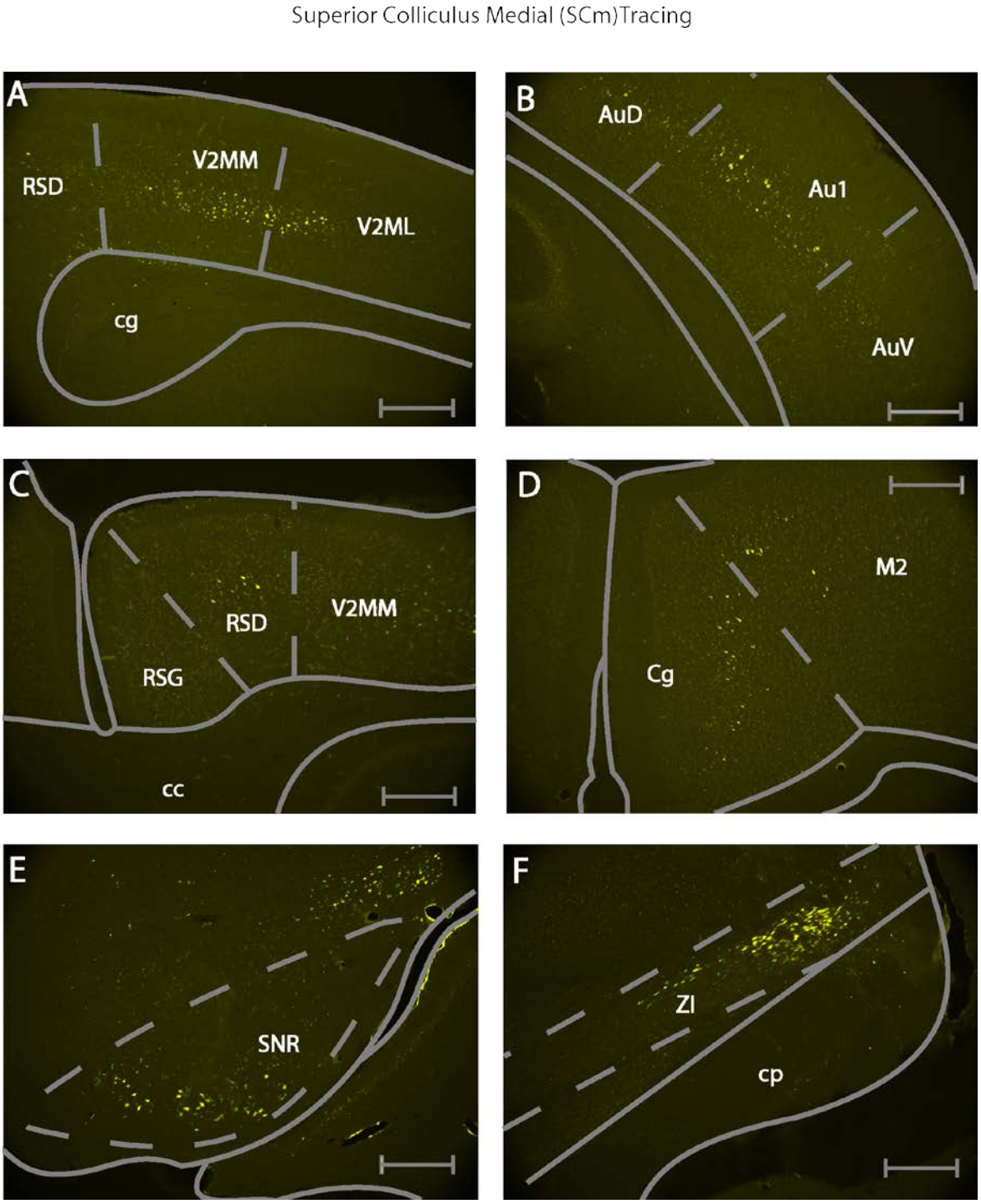

Figure 3-7. Example Photomicrographs of Retrogradely Labelled Brain Areas after Injection of Fluorogold into the Medial Superior Colliculus.

A. Labelling seen in the secondary visual cortex (V2MM/V2ML), cg- cingulum. **B.** Labelling seen in the primary auditory cortex (Au1). **C.** Labelling seen in the dysgranular retrospenial cortex (RSD), cc- corpus callosum. **D.** Labelling seen in the cingulate area (Cg) and motor cortex area 2 (M2). **E.** Labelling seen in the ventromedial substantia nigra (SNR[vm]). **F.** Labelling seen in the dorsolateral zona incerta (ZI), cp- cerebral peduncule. All scale bars equate to 250µm. Nomenclature is derived from Franklin, K.B.J. & Paxinos, G. 2012. For abbreviations see list.

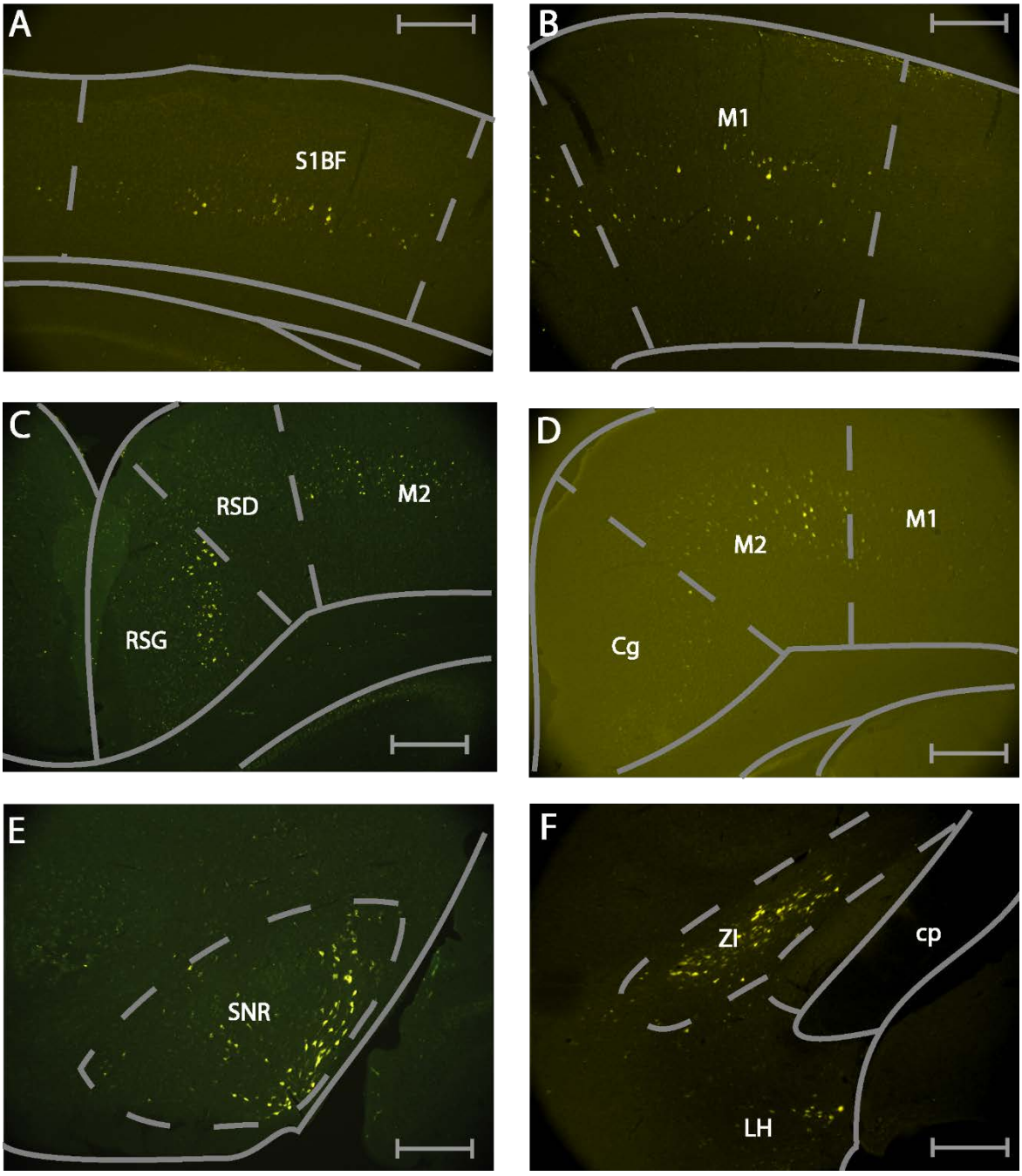

Figure 3-8. Example Photomicrographs of Retrogradely Labelled Brain Areas After Injection of Fluorogold into the Lateral Superior Colliculus.

A. Labelling seen in the primary somatosensory area (S1BF). **B.** Labelling seen in the primary motor cortex (M1). **C.** Labelling seen in the granular retrospenial cortex (RSG). **D.** Labelling seen in the Cg and M2. **E.** Labelling seen in the dorsolateral SNR. **F.** Labelling seen in the ventromedial ZI. All scale bars equate to 250µm. Nomenclature is derived from Franklin, K.B.J. & Paxinos, G. 2012. For abbreviations see list.

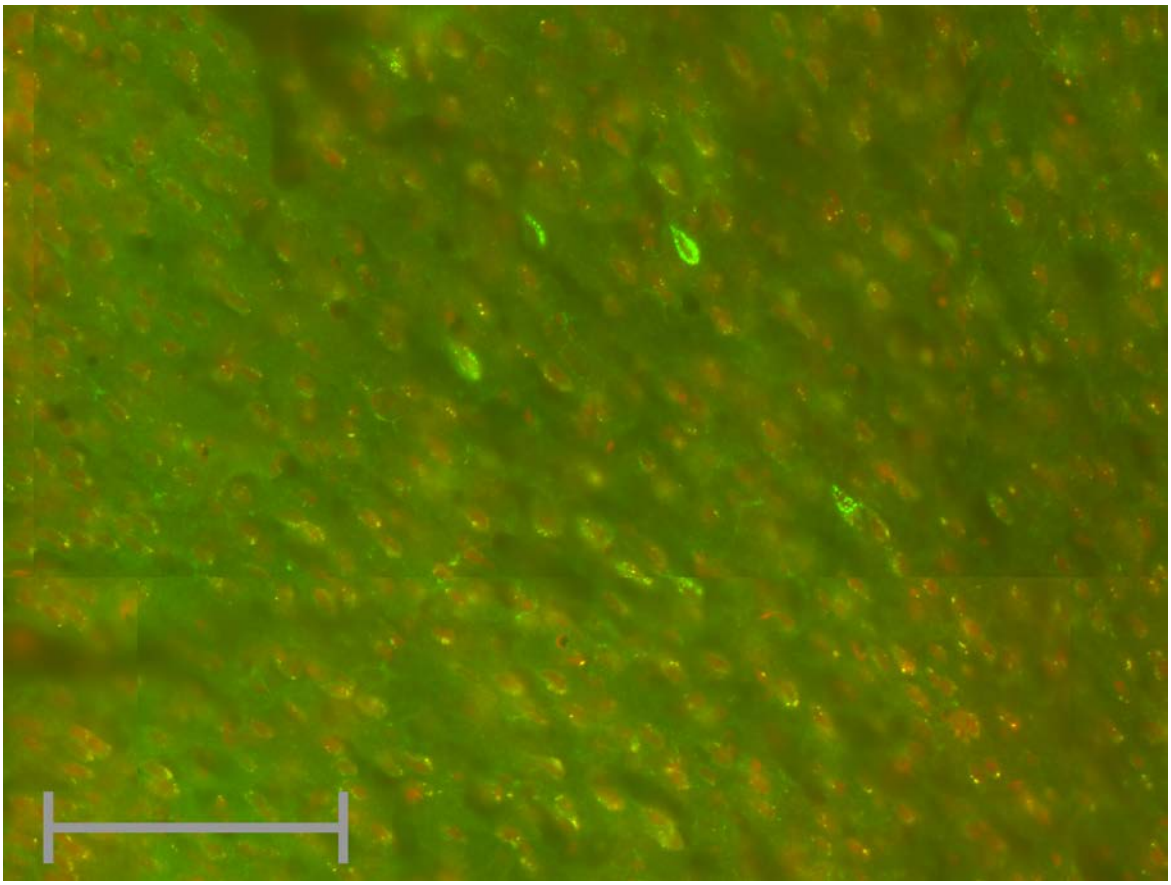

Figure 3-9. Example of Retrograde Labelled Neurons in the Cingulate Area After Injection of the Retrograde Tracer Fluorogold into the Medial Superior Colliculus

Scale bar equates to 200µm. Green represents fluorogold labelling, red represents propridum iodine nuclei staining.

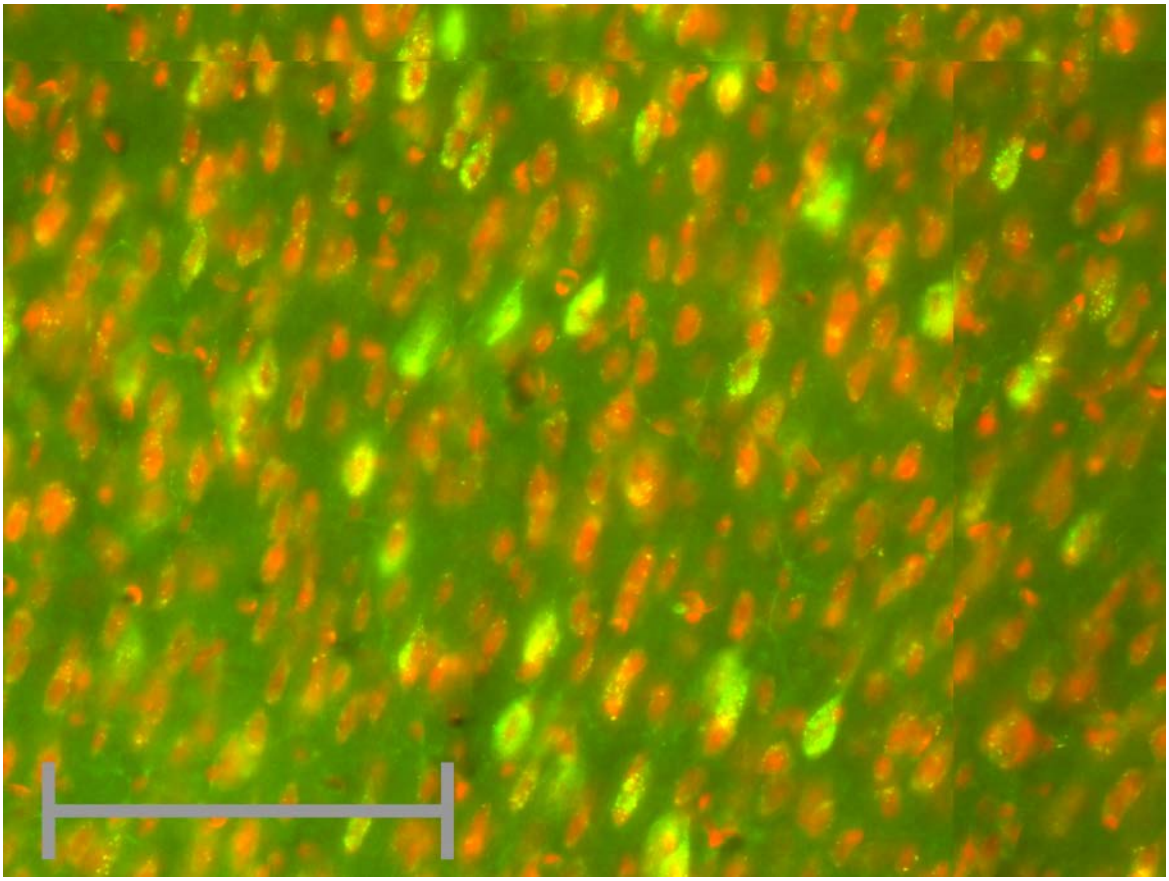

Figure 3-10. Example of Retrograde Labelled Neurons in the Motor Cortex Area 2 After Injection of the Retrograde Tracer Fluorogold into the Lateral Superior Colliculus

Scale bar equates to 200µm. Green represents fluorogold labelling, red represents propridum iodine nuclei staining.

3.3.1.2 Midbrain

Regions with retrogradely labelled cells, only after SCm injections, included the subthalamic nucleus (STh, ipsilateral), the dorsal raphe (DRV, bilateral), the external cortex of the inferior colliculus (ECIC, bilateral), the parabigeminal nucleus (PBG, bilateral) and the pontine nucleus (Pn, bilateral).

The prerubral field (PR, ipsilateral) showed retrogradely labelled cells exclusively after SCl injections.

A number of midbrain regions contained retrogradely labelled neurons after injections of tracer into either subdivision of the SC. These included the lateral lemniscus (ll,

ipsilateral), the PAG (bilateral), the mRt (bilateral), the substantia nigra (SNR, bilateral), and the SC (bilateral). The ll and the PAG showed similar density of retrogradely labelled cells, regardless of the injection site. The SC, mRt and SNR had differential numbers of retrogradely labelled cells following injection into the two subdivisions of the SC. The contralateral SCl was retrogradely labelled following injections into the SCm and the SCl. The mRt (ipsilateral) showed a higher number of retrogradely labelled cells after SCl than after SCm injections. The SNR equally showed larger numbers of retrogradely labelled cells following SCl injection when compared to SCm injections. In addition, there was a significant ($p = 0.016$, Mann-Whitney U-Test) preference for the ventromedial SNR to show retrogradely labelled cells following SCm injections and for the dorsolateral SNR to show retrogradely labelled cells following SCl injections (Figure 3-7E, Figure 3-8A, Figure 3-11A right).

3.3.1.3 Thalamic and Hypothalamic Areas

Retrogradely labelled cells after SCm, but not after SCl injections, were found in the lateral posterior thalamic nucleus, mediorostral part (LPMR, ipsilateral) and the ventromedial hypothalamic nucleus (VMH, ipsilateral).

SCl injections did not result in exclusive retrograde label in the thalamus or hypothalamus.

A number of thalamic and hypothalamic regions contained retrogradely labelled neurons after both SCm, and SCl injections. The zona incerta ventral part (ZIV, ipsilateral) and dorsal part (ZID, ipsilateral) displayed retrograde neuronal labelling after injection into SCm and SCl. The ZIV was more strongly connected to the SC (l and m) than the ZID. Moreover, the neuronal projections from the ZI were spatially segregated, with the population projecting to the SCm being located in the dorsolateral region bordering on the dorsal lateral geniculate nucleus (DLG). The population projecting to the SCl was found in the ventromedial portion of ZI (Figure 3-7F, Figure 3-8F).

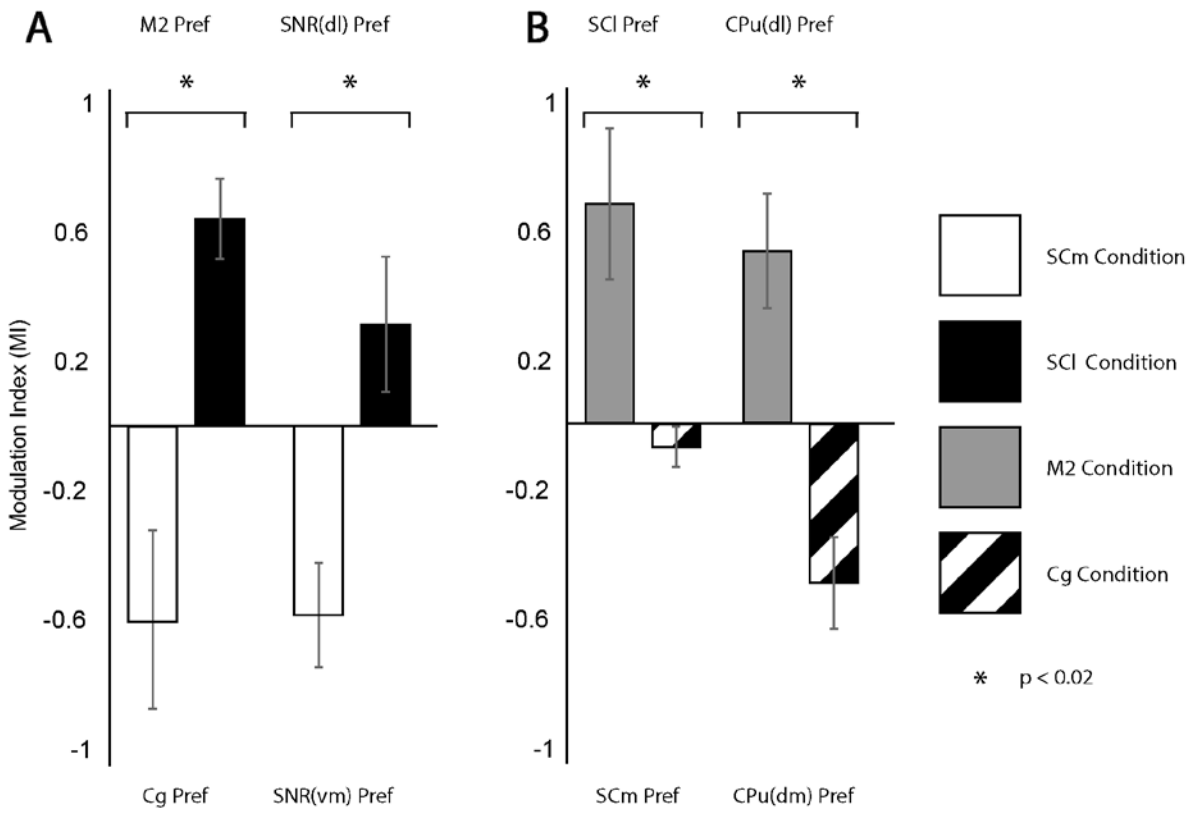

Figure 3-11. Modulation Indices (MIs) for Tracing Data.

A. MIs of retrograde labelling in M2 vs. Cg (left) and SNR(dl) vs. SNR(vm) (right). **B.** MIs of anterograde labelling in SCm vs. SCl (left) and CPu(dm) vs. CPu(dl) (right). White bars indicate MIs after SCm injections, black bars indicate MIs after SCl injections, gray bars indicate MIs after M2 injections , and dashed bars MIs after Cg injections) '*' represents p< 0.02. Nomenclature is derived from Franklin, K.B.J. & Paxinos, G. 2012. For abbreviations see list.

3.3.1.4 Pretectum

The pretectal area (PT, ipsilateral) was retrogradely labelled only after SCm injections.

Retrogradely labelled cells were found in the nucleus of the posterior commissure (PCom, ipsilateral) after both SCm and SCl injections, while the PCom (contralateral) only sends efferents to the SCl.

To provide a general overview of input to the SC from the entire brain, a flatmap connection diagram of the areas which exhibited retrogradely labelled cells after SCm and SCl injections were generated (see Figure 3-12).

3.3.2 Anterograde Tracing

The anterograde procedure involved 5 M2 and 4 Cg injections with the BDA tracer. The tracer in all cases was confined to the target area and did not leak into neighbouring brain regions such as the corpus callosum (cc) or the third ventricle (Figure 3-13A-C). There was some variation in the anterior-posterior extent of the injection sites, which was caused by slight differences in overall bregma localisation, probe placement and brain size. This may have caused differences in the brain region and subregional origin of anterogradely labelled fibres. However any differences were mitigated by the strict inclusion criterion. Namely, that any brain region and subregional labelling bias/separation must have been present throughout all cohort cases to be included in the results. Based on this method, we will first describe cortical areas, where anterograde label was found exclusively after M2 injections, followed by a description of cortical areas where anterograde label was found exclusively after Cg injections. Thereafter, cortical areas will be described where anterograde label was found after both, M2 and Cg injections. This schema of description will be repeated for subcortical areas where anterograde label was found, focusing on areas where anterograde label was medium to strong. A complete list of all structures that showed anterograde label after M2 and Cg injections is given in Table 3-2. Flatfield connectivity maps for both of the anterograde tracing conditions were completed to better visualize the extent of labelling throughout the brain (Figure 3-14, Figure 3-15). Both regions predominantly projected ipsilateral, however a few regions also showed anterograde label contralateral to the injection site.

Furthermore to aid in representation of the data, labelling from both the M2 and Cg is presented schematically in serial atlas sections for example cases, see Figure 3-16, and Figure 3-17.

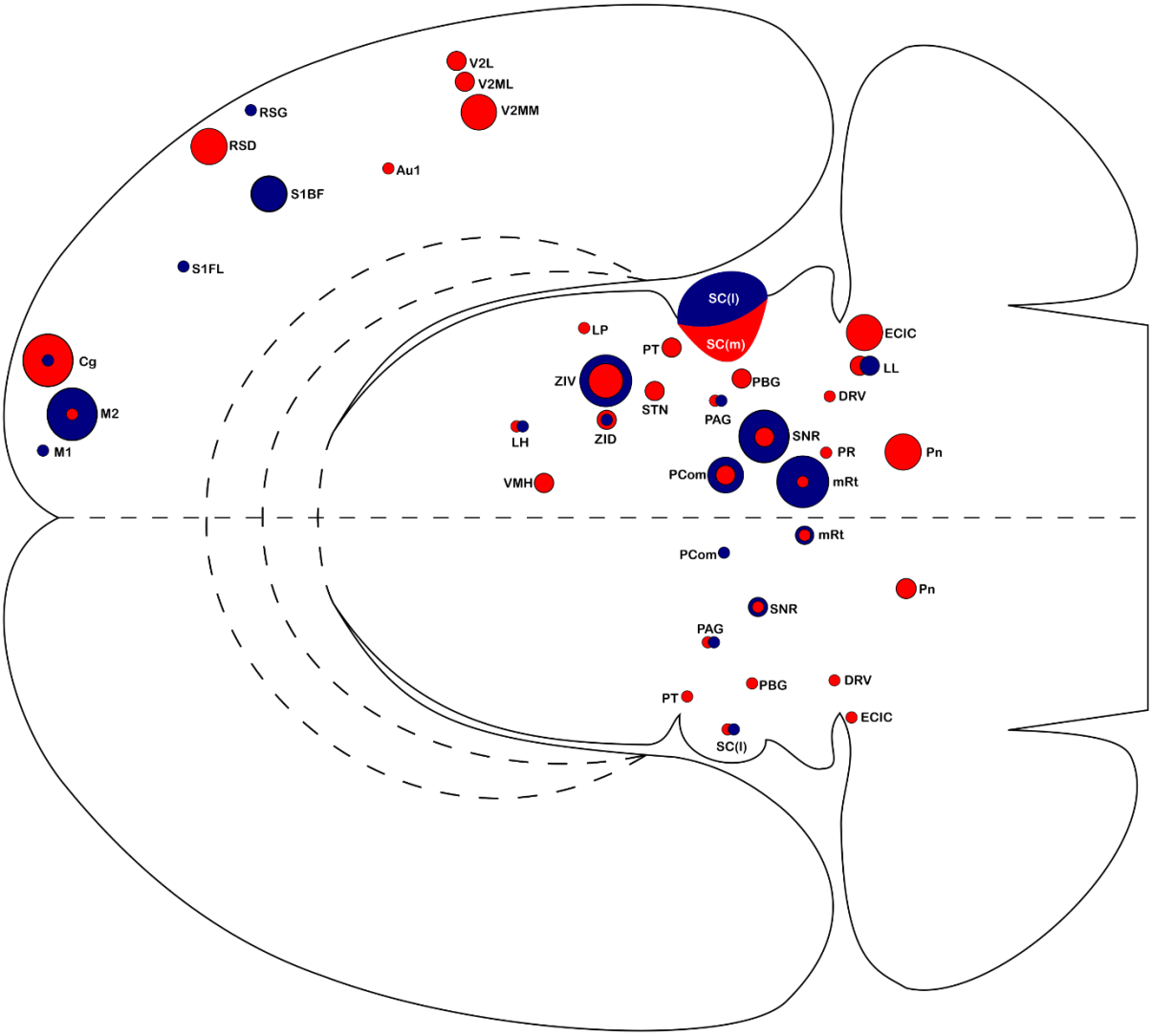

Figure 3-12. Flatfield Map Summarising Retrograde Connectivity Patterns after Injection of Fluorogold into the Medial and Lateral Superior Colliculus

Connectivity is displayed in four levels, low, medium, high and very high which is represented by the size of the circle. Red indicates medial SC retrograde connectivity, blue indicates lateral SC retrograde connectivity. Nomenclature is derived from Franklin, K.B.J. & Paxinos, G. 2012. For abbreviations see list.

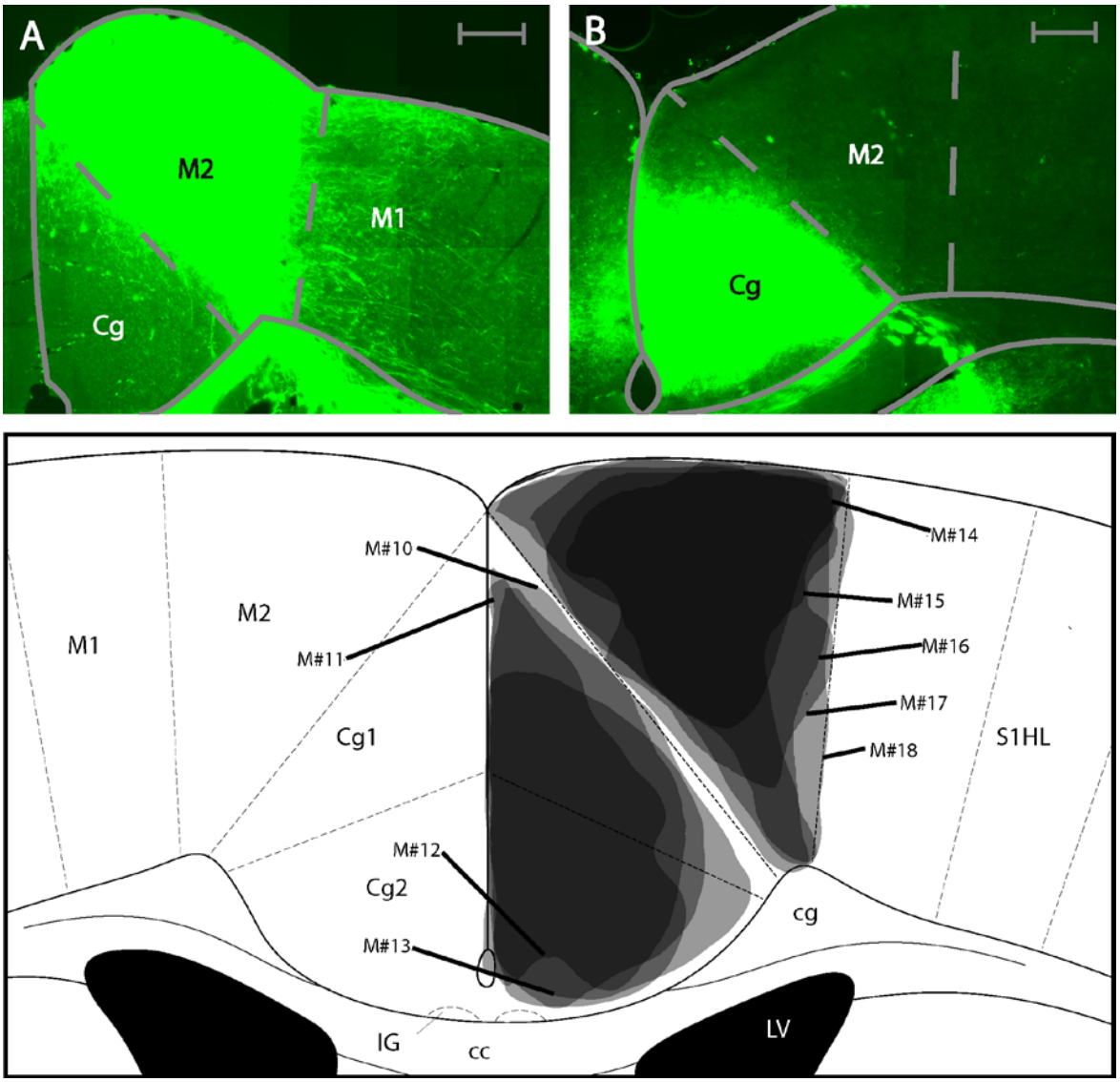

Figure 3-13. Injections sites for Anterograde Tracing.

A. Photomicrograph of biotinylated dextran anime injection into the M2. **B.** Photomicrograph of biotinylated dextran amine injection into the Cg. All scale bars equate to 250µm. **C.** Summary of injection sites for all cases in the anterograde tracing in the Cg and M2. Each shaded area represents the extent of the labelled injection site for both the Cg and M2. The darker shading indicates overlap of injection volume. Nomenclature is derived from Franklin, K.B.J. & Paxinos, G. 2012. For abbreviations see list.

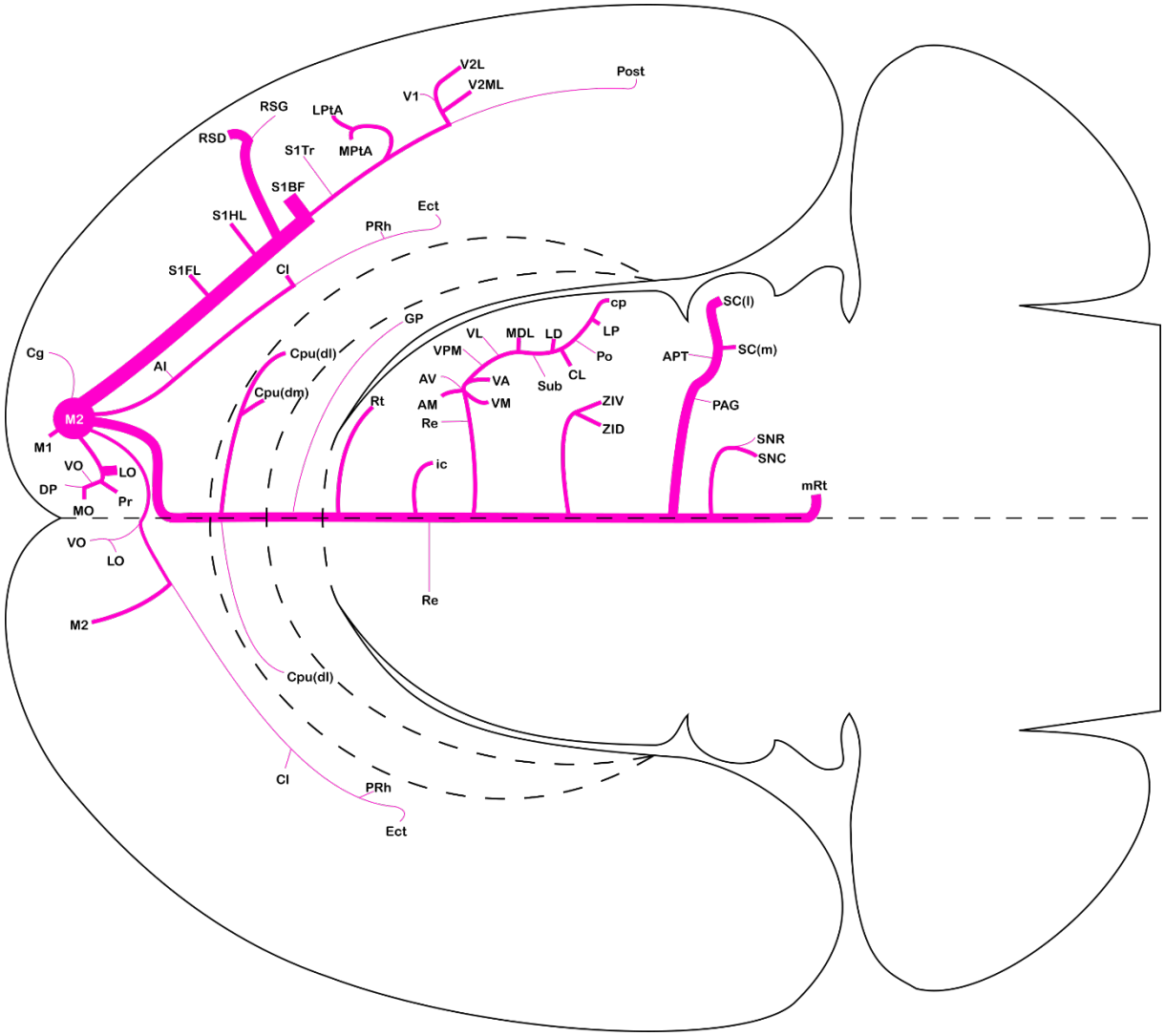

Figure 3-14. Flatfield Map Summarising Anterograde Connectivity Patterns after Injection of BDA into the Motor Cortex Area 2

Connectivity is displayed in four levels, low, medium, high and very high indicated by the thickness of the lines. Nomenclature is derived from Franklin, K.B.J. & Paxinos, G. 2012.

For abbreviations see list

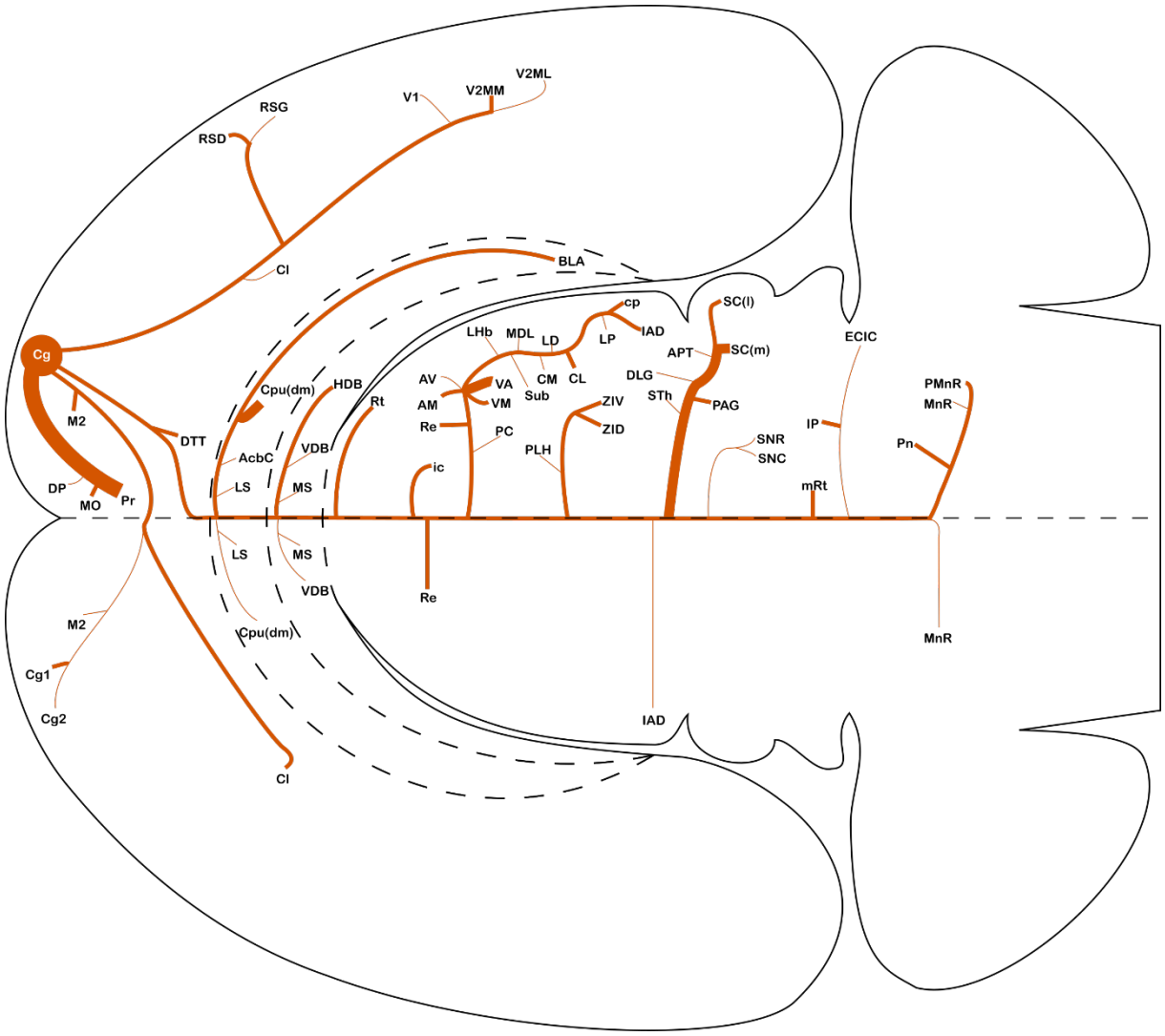

Figure 3-15. Flatfield Map Summarising Anterograde Connectivity Patterns after Injection of BDA into the Cingulate Area

Connectivity is displayed in four levels, low, medium, high and very high indicated by the thickness of the lines. Nomenclature is derived from Franklin, K.B.J. & Paxinos, G. 2012. For abbreviations see list.

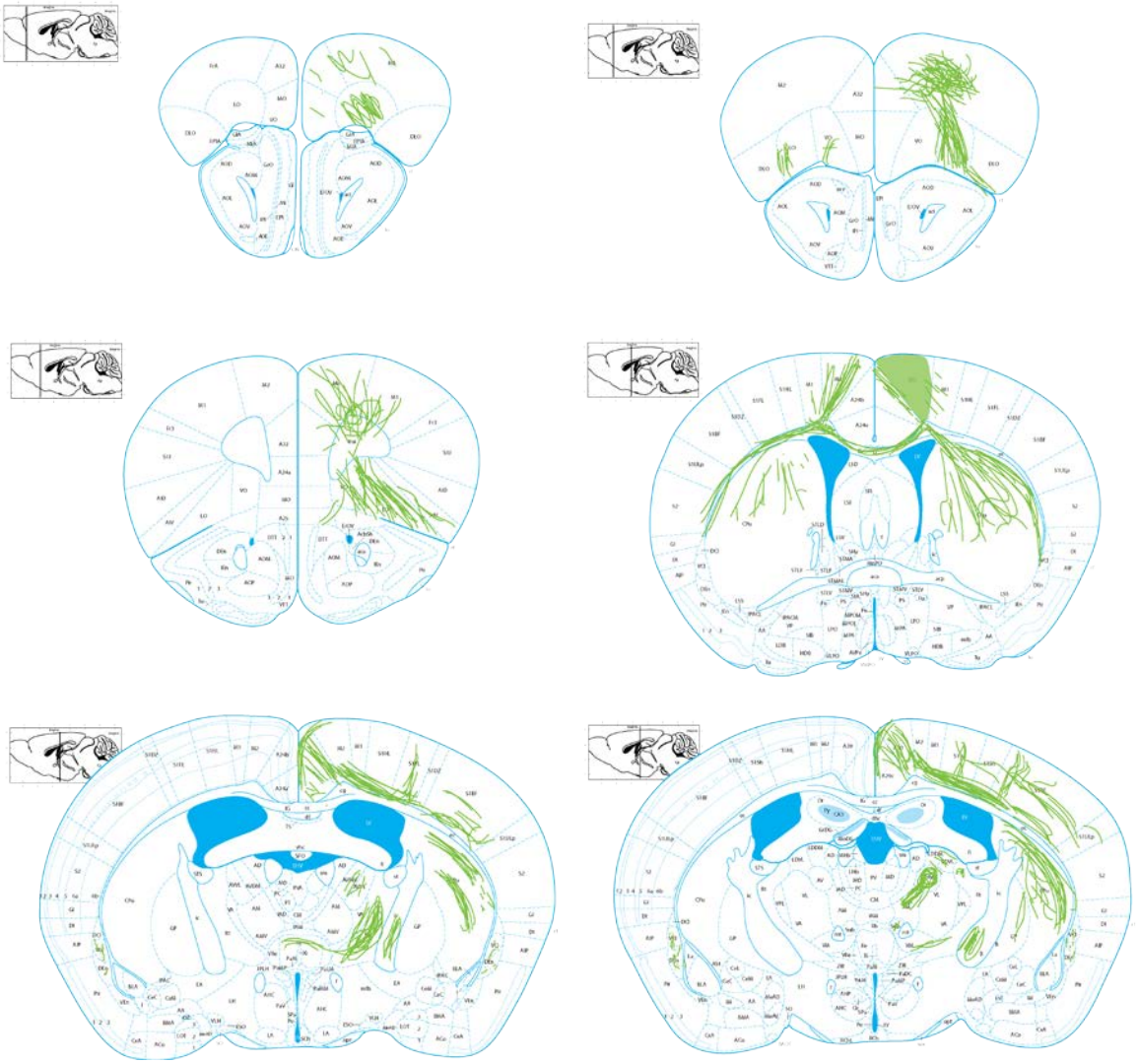

Figure 3-16 (see below)

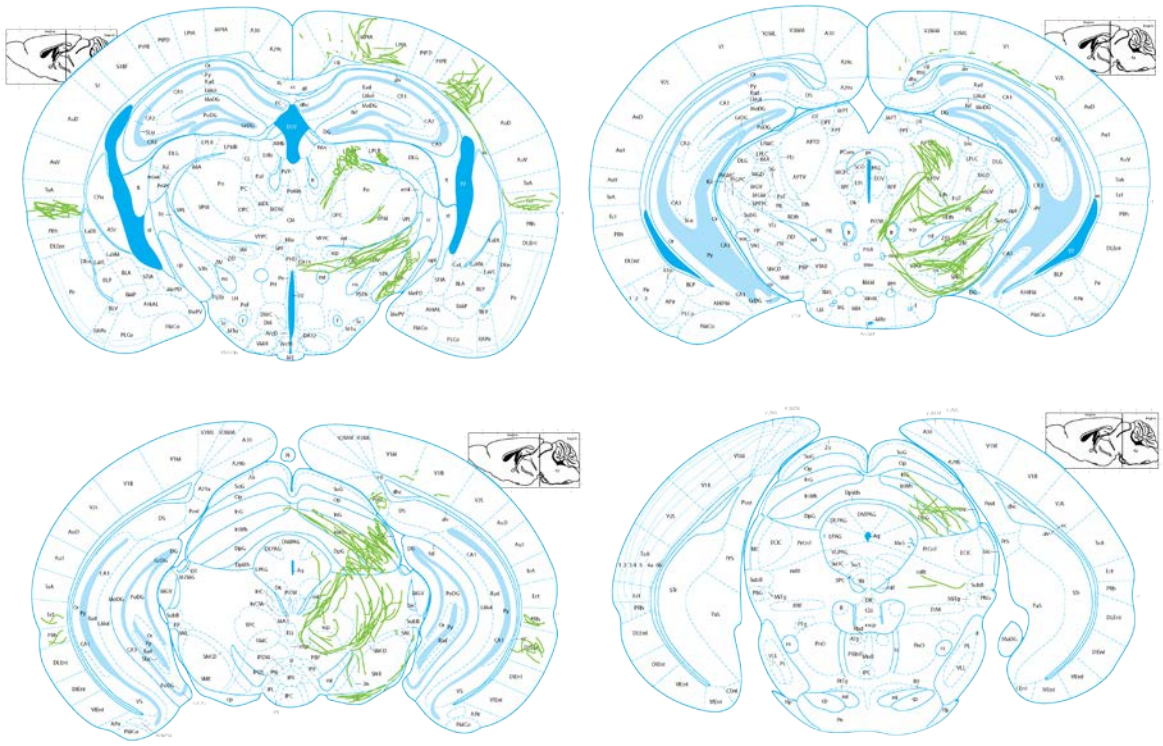

Figure 3-16. Schematic Representation of Anterograde Neuronal Labelling After Injection of Biotinylated Dextran Amine into the Motor Cortex Area 2 in Single Case

Green lines represent labelled fibres. Green shaded areas represents injection site extent. Atlas sections adapted from Paxinos and Watson 2012.

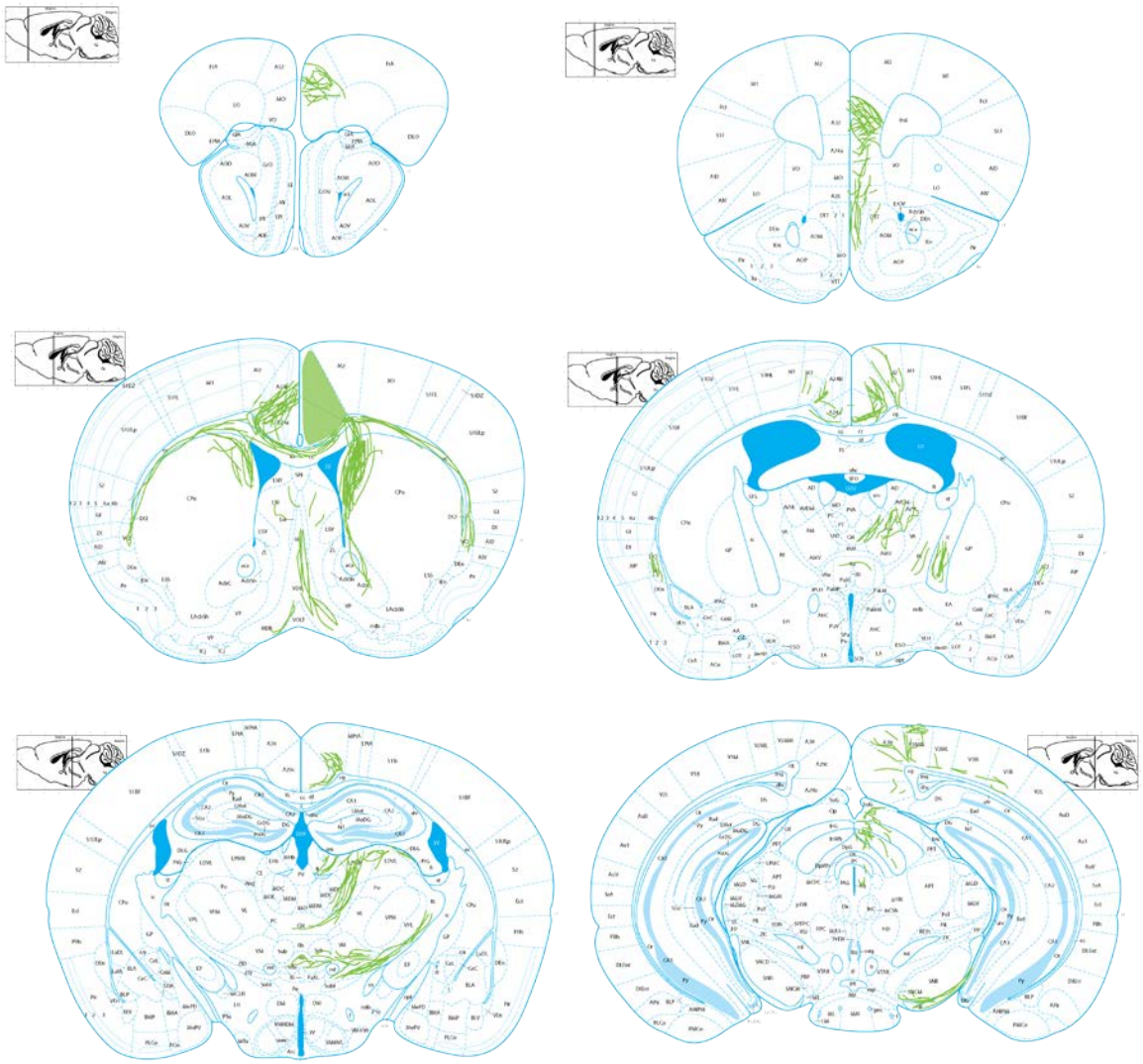

Figure 3-17 (see below)

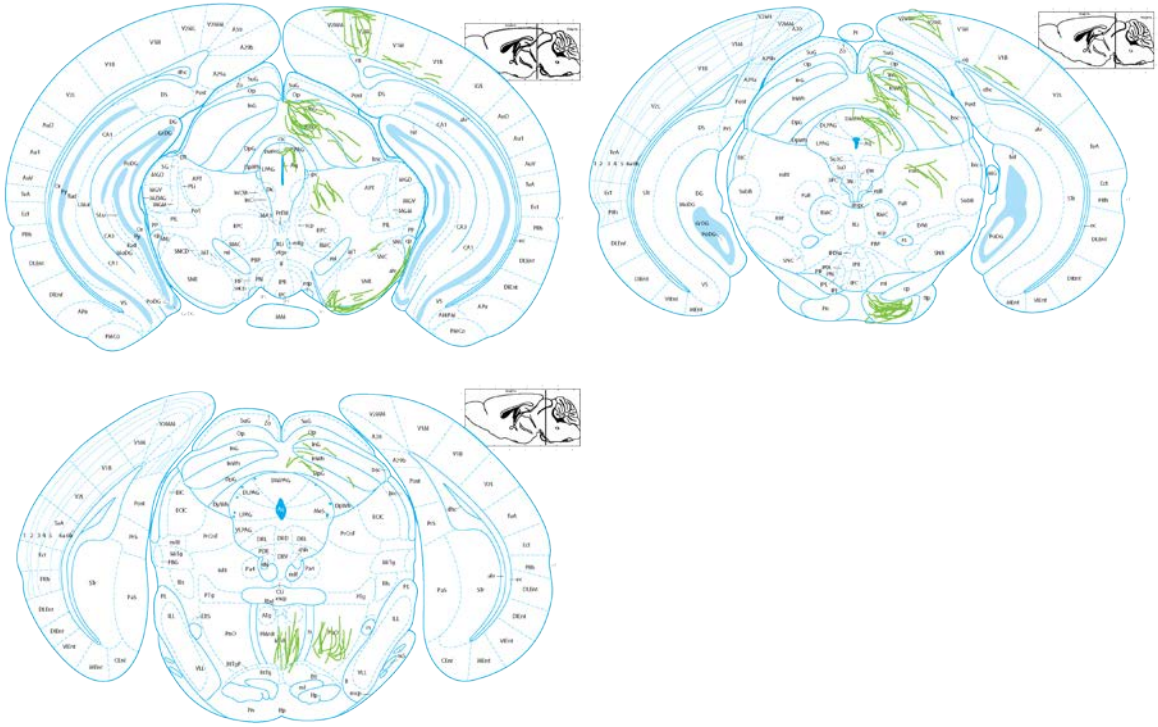

Figure 3-17. Schematic Representation of Anterograde Neuronal Labelling After Injection of Biotinylated Dextran Amine into the Cingulate Area in Single Case

Green lines represent labelled fibres. Green shaded areas represents injection site extent. Atlas sections adapted from Paxinos and Watson 2012.

3.3.2.1 Cortex

The prefrontal cortex, the orbital cortex, lateral (LO, bilateral) and ventral (VO, bilateral) showed anterograde label exclusively after M2 injections. Anterograde label following M2 injections was found in virtually all primary somatosensory areas with stronger label in the barrel field (S1BF, ipsilateral) Figure 3-18A), than the limb (S1FL, ipsilateral, S1HL, ipsilateral), as well as trunk regions (S1Tr, ipsilateral, Figure 3-18B). A noticeable difference was found between the laminar connectivity profiles to S1BF and the rest of S1. In the S1BF anterograde labelling was concentrated in layer 1, 4 and 6, whereas for the other S1 regions, anterograde labelling was located in layer 5 and 6.

In addition the ipsilateral primary motor cortex (M1, ipsilateral, layer 1, 5, 6, Figure 3-13A, Figure 3-18B), visual cortex V2L (ipsilateral across layers 1, 4 and 5), the parietal cortex (MPtA, ipsilateral, LPtA, ipsilateral, with preferential labelling in layers 5 and 6),

the agranular insular cortex (AI, bilateral), the ectorhinal cortex (Ect, bilateral), postsubiculum (Post, ipsilateral), and the perirhinal cortex (PRh, bilateral) were anterogradely labelled exclusively after M2 injections.

Within the prefrontal cortex, the only area with exclusive anterograde labelling after Cg injections was the dorsal tenia tecta (DTT, ipsilateral). V2ML was the only sensory area with exclusive anterograde label after Cg injections (ipsilateral, Figure 3-19A across layers 1-5). In addition the contralateral Cg showed anterograde label after Cg injections.

Cortical areas anterogradely labelled after injections into M2 and Cg included the dorsal peduncular cortex (DP, ipsilateral and biased towards the caudal end), the claustrum (Cl, bilateral, with a bias to the contralateral side), the primary visual cortex (V1, ipsilateral), the V2MM (ipsilateral), the prelimbic cortex (PrL, ipsilateral), the medial orbital cortex (MO, ipsilateral), RSD (ipsilateral, Figure 3-18B, Figure 3-19B) and RSG, (ipsilateral, Figure 3-18B, Figure 3-19B).

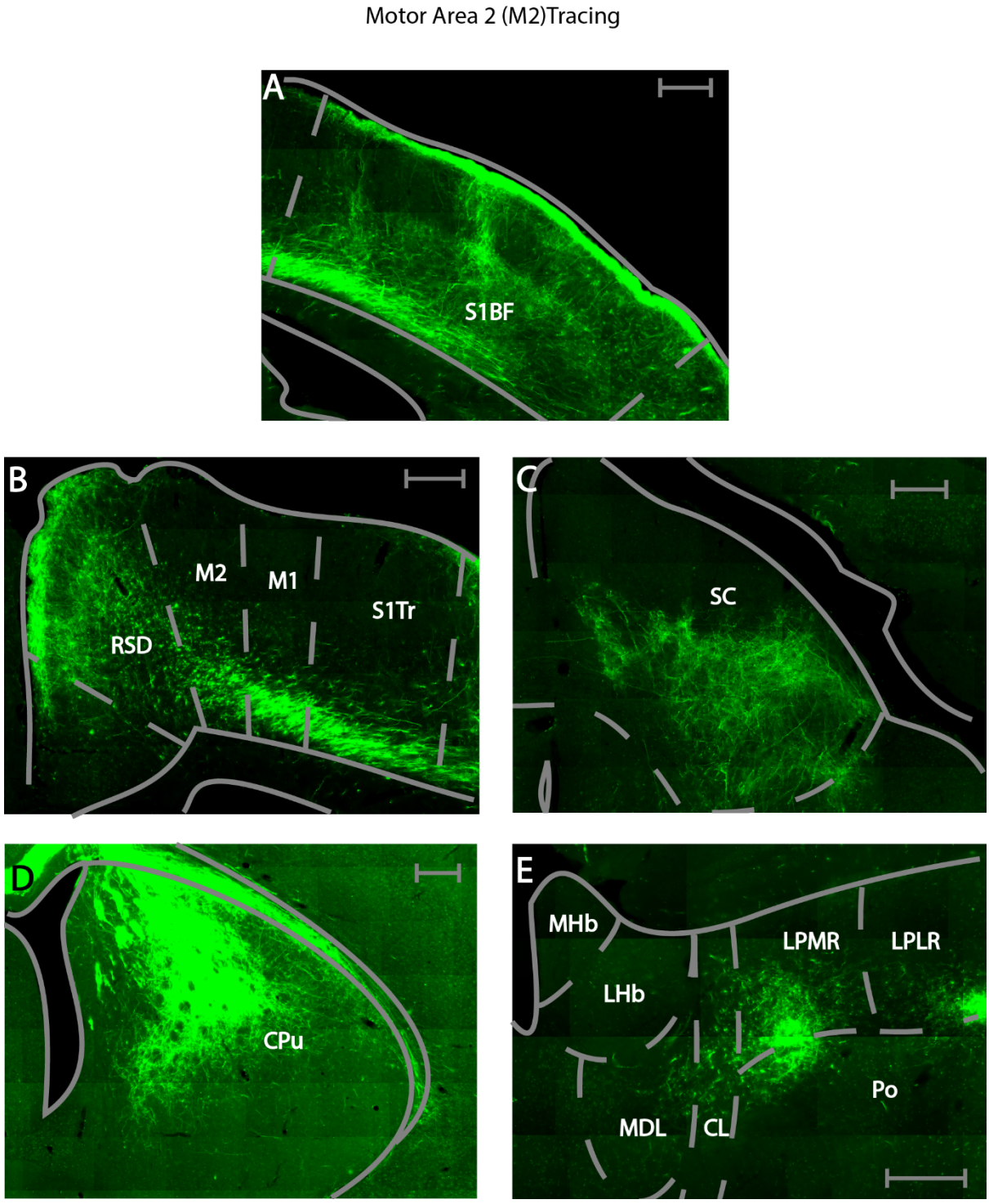

Figure 3-18. Example Photomicrographs of Anterogradely Labelled Brain Areas after Injection of BDA into the M2.

A. Labelling seen in the primary somatosensory area (S1BF). **B.** Labelling seen throughout the RSD, M2, primary motor cortex (M1) and S1. **C.** Labelling seen in the lateral portion of the superior colliculus (SCl). **D.** Labelling seen in the dorsolateral striatum (CPu[dl]). **E.** Labelling seen in the thalamus, namely the lateral posterior

mediorostral and laterorostral part (LPLR, LPMR), the mediodorsal (MDL), the central lateral (CL) and the posterior (Po). All scale bars equate to 250µm. Nomenclature is derived from Franklin, K.B.J. & Paxinos, G. 2012. For abbreviations see list.

Despite the shared input of the above areas from Cg and M2, some biases or subregional differences were observed. PrL was more strongly connected to Cg than M2, ipsilaterally. M2 projected to more anterior locations in MO than Cg. Following M2 and Cg injections, the retrosplenial cortex showed anterograde label mostly in the RSD subdivision. This was stronger after M2 injections (compared to Cg injections). Moreover, M2 injections resulted in anterograde labelling in the upper layers of RSD (layer 1-3, Figure 3-18B), whereas the Cg injections resulted in anterograde label in the lower cortical layers of RSD (layer 5-6, Figure 3-19B). V2MM received more input from M2 than Cg.

3.3.2.2 Midbrain

All of the midbrain areas that received input from M2, also received input from Cg, while the opposite was not the case (see below).

Midbrain areas with anterograde label after Cg, but not M2 injections, were the ECIC, (ipsilateral), the STh (ipsilateral), the interpeduncular nucleus (IP, ipsilateral), the paramedian raphe nucleus (PMnR, ipsilateral), the median raphe nucleus (MnR, bilateral), and the Pn (ipsilateral).

Anterograde label in the midbrain after both M2 and Cg injections, was found in the cerebral peduncle (cp, ipsilateral), the SNR (ipsilateral), the substantia nigra pars compacta (SNC, ipsilateral), the dorsolateral and ventrolateral PAG (DLPAG, ipsilateral, VLPAG, ipsilateral), mRt (ipsilateral), the SCl (ipsilateral), and SCm (ipsilateral).

Despite the fact that the above areas showed anterograde label after either injection, some areas showed a spatial preference of anterograde labelling within their subdivisions. The PAG was more strongly labelled in the dorso-lateral part (DLPAG) after Cg injections, while it was more strongly labelled in the ventro-lateral part (VLPAG) following M2 injections. The substantia nigra, while receiving input from both areas, did so in a

topographically biased manner. The SNR received connections from both the Cg and M2 which terminated onto the ventromedial part of the area. The SNC received sparse connections from the Cg and more abundant connections from M2.

Other midbrain regions received stronger input from one of the two areas. The mRt showed more anterograde label after M2 than after Cg injections. The SCl showed more anterograde label than SCm after M2 injections, whilst the opposite was the case after Cg injections (Figure 3-18C, Figure 3-19C). This preference was significant (p= 0.016, Mann-Whitney U-Test) (Figure 3-11B left). Additionally, anterograde label from the Cg was found in more anterior parts of the SC than that arising from M2.

3.3.2.3 Basal Forebrain

The basal forebrain did not show anterograde label after M2 injections. Anterograde label was found in parts of the medial basal forebrain after Cg injections. Specifically, the medial septal nuclei (MS, bilateral), the lateral septal nuclei (LS, bilateral), the diagonal band, vertical limb (VDB, bilateral), and the diagonal band, horizontal limb (HDB, bilateral) showed anterograde label. The HDB connections expressed a bias for ipsilateral over contralateral connectivity.

3.3.2.4 Basal Ganglia

The globus pallidus (GP, ipsilateral) was anterogradely labelled only after M2, not after Cg injections. No parts of the basal ganglia were exclusively labelled after Cg injections. Furthermore the core of the nucleus accumbens (AcbC, ipsilateral) received low levels of input from Cg.

The striatum showed anterograde label after either M2 or Cg injections, albeit in a topographically segregated manner. The dorsolateral striatum (CPu[dl], ipsilateral) was more strongly labelled after M2 injections. Conversely, the dorsomedial striatum (CPu[dm], ipsilateral) was more strongly labelled following Cg injections (Figure 3-18D, Figure 3-19D). This topographical difference was significant (p = 0.016, Mann-Whitney U-Test) (Figure 3-11 right). Contralaterally, the CPu(dl) received few projections from M2, while the CPu(dm) received few projections from the Cg.

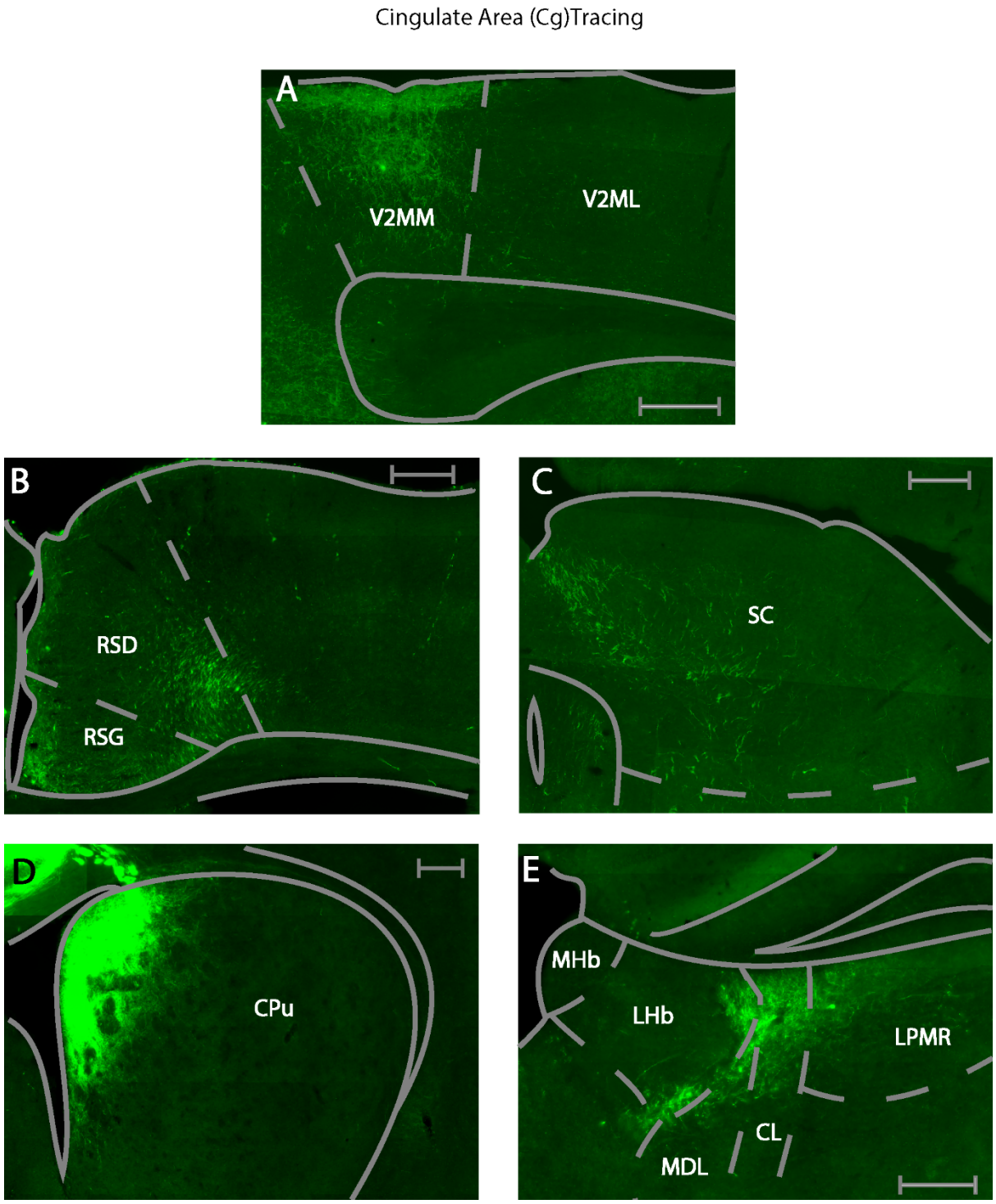

Figure 3-19. Example Photomicrographs of Anterogradely Labelled Brain Areas after Injection of BDA into the Cingulate Area.

A. Labelling seen in the secondary visual cortex (V2MM, V2ML). **B.** Labelling seen throughout the RSG. **C.** Labelling seen in the medial portion of the superior colliculus (SCm). **D.** Labelling seen in the dorsomedial striatum (CPu[dm]). **E.** Labelling seen in the thalamus, namely the LPMR, the MDL, the CL and the Po and the lateral habenula

(LHb). All scale bars equate to 250µm. Nomenclature is derived from Franklin, K.B.J. & Paxinos, G. 2012. For abbreviations see list.

3.3.2.5 Thalamic and Hypothalamic Areas

Anterograde labelling was observed only after M2 injections in the lateral posterior thalamic nucleus, laterorostral part (LPLR, ipsilateral, Figure 3-18E), the dorsal portion of the posterior thalamic nuclear group (Po, ipsilateral, Figure 3-18E), the laterodorsal thalamic nucleus, dorsomedial part (LDDM, ipsilateral), and the ventrolateral thalamic nucleus (VL, ipsilateral, dorsal portion).

The Cg projects to a larger number of thalamic nuclei, which were not matched by projections from M2. Exclusive anterograde label following Cg injections was found in the paracentral thalamic nuclei (PC, ipsilateral), the central medial thalamic nuclei (CM, bilateral), and the lateral habenular nucleus (LHb, ipsilateral, Figure 3-19E). Projections from Cg targeted the interanterodorsal thalamus (IAD, bilateral), with an ipsilateral bias. Cg projections to the dorsal lateral geniculate nucleus (DLG, ipsilateral) were found in the dorsolateral part of the area. Selective projections to the hypothalamus were restricted to the peduncular part of the lateral hypothalamus (PLH, ipsilateral).

Areas with anterograde label after both, M2 and Cg injections included the anteroventral thalamus, dorsomedial (AVDM, ipsilateral) and ventrolateral (AVVL, ipsilateral), the submedius thalamic nucleus (Sub, ipsilateral), the reticular nucleus (Rt, ipsilateral), the zona incerta, dorsal (ZID, ipsilateral) and ventral (ZIV, ipsilateral) portions, the ventromedial thalamic nucleus (VM, ipsilateral), the central lateral nucleus (CL, ipsilateral, Figure 3-18E, Figure 3-19E), anteromedial thalamic nucleus (AM, ipsilateral), the laterodorsal thalamic nucleus, ventrolateral part (LDVL, ipsilateral), the mediodorsal thalamic nucleus, lateral part (MDL, ipsilateral), and the lateral posterior thalamic nucleus, mediorostral part (LPMR, ipsilateral, Figure 3-18E, Figure 3-19E), the ventral anterior thalamic nucleus (VA, ipsilateral), and the reuniens thalamus (Re, bilateral).

A few thalamic areas showed partial topographical label segregation after M2 and Cg injections. In VM, anterograde label following Cg injections occurred throughout the

area, whereas anterograde label following M2 injections was restricted to the ventral region. In CL, anterograde label following Cg injections was restricted to the dorsal portion of the area, while input from the M2 was found further down the dorsal-ventral axis (Figure 3-18E, Figure 3-19E).

In addition, anterograde label strength in some areas differed depending on the injection site. The AM, LDVL, MDL, and the LPMR showed more anterograde label after M2, than after Cg injections (Figure 3-18E, Figure 3-19E). All of these areas displayed a topographical preference in their labelling pattern. Label in AM, regardless of injection site (M2, Cg), was found in the lateral part. Label in LDVL after M2 injections was found more in the ventral part; whereas no preference was found following Cg injections. M2 injections resulted in preferential anterograde label in the lateral portion of the MDL, while Cg injections resulted in preferential anterograde label in dorsal portion of MDL. M2 originating label in LPMR occurred more ventromedially, while Cg originating label occurred more dorsomedially (Figure 3-18E, Figure 3-19E). The Cg projected more heavily to VA and Re, than M2 did.

3.3.2.6 Amygdala

Anterograde label was found in the basolateral amygdaloid nucleus, anterior part (BLA, ipsilateral) following Cg injections, but not M2 injections.

3.3.2.7 Pretectum

The anterior pretectal nucleus (APT, ipsilateral) showed anterograde label following Cg and M2 injections.

Table 3-2. Qualitative Densities of Anterogradely Labelled Brain Areas After Injection of BDA in the Cingulate Area of Motor Cortex Area 2

Relative percentage area coverage measured in five levels (none '-', low '+', medium '++', high '+++' and very high '++++') for anterogradely traced brain regions averaged across the experimental cohort. These measures were assigned via non-quantitative visual assessment.

		M2		Cg	
		Ipsi	Contra	Ipsi	Contra
Cortex					
Association/ multimodal					
Cl	claustrum	+	++	+	++
Ect	ectorhinal cortex	+	+	-	-
M1 (Pos)	primary motor cortex	++	-	-	-
M2 (An)	secondary motor cortex	++	+	-	-
M2 (Pos)	secondary motor cortex	+++	++	++	+
Post	postsubiculum	+	-	-	-
PRh	perirhinal cortex	+	+	-	-
RSD	retrosplenial dysgranular cortex	+++	-	++	-
RSG	retrosplenial granular cortex	+	-	+	-
Parietal					
LPtA	lateral parietal association cortex	++	-	-	-
MPtA	medial parietal association cortex	++	-	-	-
Prefrontal					
AI	agranular insular cortex	+	-	-	-
Cg1 (An)	cingulate cortex, area 1	+	-	++	-

Cg1 (Pos)	cingulate cortex, area 1	-	-	+++	++
Cg2 (An)	cingulate cortex, area 2	-	-	++	+
DP	dorsal peduncular cortex	+	-	+	-
DTT	dorsal tenia tecta	-	-	++	-
LO	lateral orbital cortex	+++	+	-	-
MO	medial orbital cortex	++	-	++	-
				+++	
PrL	prelimbic cortex	++	-	+	-
VO	ventral orbital cortex	+	+	-	-
Sensory					
S1BF	primary somatosensory cortex, barrel field	++++	-	-	-
S1FL	primary somatosensory cortex, forelimb region	++	-	-	-
S1HL	primary somatosensory cortex, hindlimb region	++	-	-	-
S1Tr	primary somatosensory cortex, trunk region	+	-	-	-
V1	primary visual cortex	+	-	+	-
V2L	secondary visual cortex, lateral area	++	-	-	-
V2ML	secondary visual cortex, mediolateral area	-	-	+	-
V2MM	secondary visual cortex, mediomedial area	++	-	+	-
Basal Ganglia					

Cpu (dl)	caudate putamen (striatum), dorsolateral	++	+	-	-
Cpu (dm)	caudate putamen (striatum), dorsomedial	++	-	+++	+
GP	globus pallidus	+	-	-	-
Basal Forebrain					
AcbC	accumbens nucleus, core	-	-	+	-
HBO	horizontal limb diagonal band	-	-	++	-
LS	lateral septal	-	-	+	+
MS	medial septal	-	-	+	+
VBD	nucleus of the vertical limb of the diagonal band	-	-	+	+
Thalamus					
AM	anteromedial thalamic nucleus	++	-	+	-
AVDM	anteroventral thalamic nucleus, dorsomedial part	+	-	+	-
AVVL	anteroventral thalamic nucleus, ventrolateral part	+	-	+	-
CL	centrolateral thalamic nucleus	++	-	++	-
CM	central medial thalamic nucleus	-	-	+	-
DLG	dorsal lateral geniculate nucleus	-	-	+	-
IAD	interanterodorsal thalamic nucleus	-	-	++	+
LDDM	laterodorsal thalamic nucleus, dorsomedial part	++	-	-	-
LDVL	laterodorsal thalamic nucleus, ventrolateral part	++	-	+	-

LHb	lateral habenular nucleus	-	-	++	-
LPMR	lateral posterior thalamic nucleus, mediorostral part	++	-	+	-
LPLR	lateral posterior thalamic nucleus, laterorostral part	+	-	-	-
MDL	mediodorsal thalamic nucleus, lateral part	++	-	+	-
PC	paracentral thalamic nucleus	-	-	+	-
Po	posterior thalamic nuclear group	+	-	-	-
Re	reuniens thalamic nucleus	+	+	++	++
Rt	reticular nucleus (prethalamus)	++	-	++	-
Sub	submedius thalamic nucleus	+	-	+	-
VA	ventral anterior thalamic nucleus	++	-	+++	-
VM	ventromedial thalamic nucleus	++	-	++	-
VL	ventrolateral thalamic nucleus	+	-	-	-
VPM	ventral posteromedial nucleus	+	-	-	-
ZID	zona incerta, dorsal part	++	-	++	-
ZIV	zona incerta, ventral part	++	-	++	-
Midbrain					
ECIC	external cortex of the inferior colliculus	-	-	+	-
IP	interpeduncular nucleus	-	-	++	-
MnR	median raphe nucleus	-	-	+	+
mRt	mesencephalic reticular formation	+++	-	++	-
PAG	periaqueductal gray	+	-	++	-
PMnR	paramedian raphe nucleus	-	-	++	-

Pn	pontine nuclei	-	-	++	-
SC (l)	superior colliculus (lateral part)	++++	-	++	-
SC (m)	superior colliculus (medial part)	++	-	+++	-
SNCD	substantia nigra, compact part, dorsal tier	++	-	+	-
SNR	substantia nigra, reticular part	+	-	+	-
STh	subthalamic nucleus	-	-	+	-
Hypothalamus					
PLH	peduncular part of lateral hypothalamus	-	-	+	-
Pretectum					
APT	anterior pretectal nucleus	+	-	+	-
Amygdala					
BLA	basolateral amygdaloid nucleus, anterior part	-	-	++	-

3.4 Discussion

These experiments delineated the main cortical and subcortical inputs to the medial and lateral SC of the mouse, as well as the target areas of two key frontal areas providing strong preferential input to these SC subdivisions.

A limited overlap in the cortical and subcortical afferents to the SCm and SCl was found. The majority of regions which project to the SCm have visual, extra-personal (far) space and negative affective state related functionality. The majority of regions which project to the SCl have somato-motor, peri-personal (near) space related functionality. Areas which were labelled after injection into either of the two subdivisions of the SC, often showed topographically segregated cell populations with limited spatial overlap.

The main prefrontal areas providing segregated inputs to middle and lower layers of the SC, Cg and M2, equally target functionally segregated networks. Areas which received

input solely from the Cg are functionally related to vision, emotional state and avoidance behaviours. Areas which received input solely from M2 are functionally related to somato-sensation, gustation and approach behaviours. Areas which received projections from both Cg and M2 often had a tendency to have topographical segregation, suggesting that functional specialization in these areas exists at the level of subpopulations.

3.4.1 Relations to previous literature

3.4.1.1 SC Retrograde Tracing

The retrograde tracing data herein are largely consistent with the existing literature (Taylor et al., 1986). However, the differential connectivity between the SCm and SCl, while largely in agreement with the respective analysis in the rat (Comoli et al., 2012), shows some discrepancies. Furthermore, additional discrepancies exist when compared to the whole brain imaging project (Oh et al., 2014).

Comoli et al. (2012) reported retrograde labelling in the ectorhinal, infralimbic, prelimbic cortices, the parietal region, the temporal association area (TEa), the postsubiculum, the premamillary nucleus, and the LGN after injections into the SCm, which we did not find. Following SCl injections, retrograde label was not found in the insular cortex in our study, while it was reported by Comoli et al (2012).

Some of these discrepancies can be resolved, for example the parietal region uncovered to project to SCm by Comoli et al (2012), is likely to be equivalent to the region termed the secondary visual cortex in our work, a consequence of the sometimes variable use of nomenclature in relation to mouse cortical areas (Harvey et al., 2012, Guo et al., 2014). Oh et al. (2014) reported retrogradely labelled cells in a variety of regions which were not labelled in our data. These included projections to both the SCm and SCl from the prefrontal orbital cortex, primary sensory areas the AuD, thalamic and hypothalamic areas (LGN, Po, VM, anterior hypothalamic nucleus, dorsomedial nucleus of the hypothalamus (DMH), posterior hypothalamic nucleus, parafascicular nucleus), the amygdala, and the midbrain (the mammillary nucleus, pedunculopontine nucleus, ventral tegemental area (VTA), red nucleus).

Furthermore their data uncovered areas which connected solely to the SCm which were not found in our results, e.g. such as the prefrontal area IL, primary sensory areas (V1,

S1), cortical areas (Ect, TEa, postrhinal area, subiculum, postsubiculum), the amygdala and the hippocampus.

Brain regions found to connect only to the SCl in the Oh et al 2014 paper and not our data included prefrontal (AI), sensory (V2, S2), thalamus and hypothalamus (MDL, VPM, arcuate hypothalamic nucleus, VMH), and the midbrain (anterior pretectal nucleus, intermediate reticular nucleus, Pn, DRV) (Oh et al., 2014).

In addition, retrogradely labelled cells were found in areas, which were not reported by Comoli et al (2012). These included the external cortex of the inferior colliculus (ECIC), the PBG, the Pn and the prerubral field. The input from the PBG and the ECIC to the rat SC, however, has been shown previously (Taylor et al., 1986). The differences observed between the results presented here and the Comoli paper may reflect species specific connectivity and/or differences in relative injection site.

3.4.1.2 M2/Cg Anterograde Tracing

In general the projections identified from Cg and M2 mouse cortical and subcortical targets are similar to those found previously in the rat (Domesick, 1969, Vogt and Miller, 1983, Reep et al., 1987, Gabbott et al., 2005). However, in comparison with more recent brain mapping studies, some discrepancies were found (Oh et al., 2014, Zingg et al., 2014).

For example, a number of target areas were found by Oh et al (2014) as well as Zingg et al. (2014) studies after injections of anterograde tracer in Cg and M2 which were not uncovered in our results. These included the prefrontal region the frontal pole, the sensory related area area AuD, cortical area the areas (piriform cortex,), the basal forebrain (substantia innominata), the thalamus and hypothalamus (AD, paraventricular thalamic area, DMH, preoptic area), and the midbrain (mammillary nucleus, VTA, central raphe nucleus).

Following injections into Cg Oh et al. (2014) found projections to prefrontal areas (AI, IL, orbital), primary sensory areas (M1), cortical areas (entorhinal cortex, ECT, TEa, endopiriform cortex, POST), the thalamus and hypothalamus (Po, anterior hypothalamic nucleus, paraventricular hypothalamus) the midbrain (pretectal nucleus, PCom), and the hippocampus. Our injections did not show label in these areas.

Additionally, following injection into M2 they (Oh et al. 2014) reported anterograde connections with the gustatory region, the perirhinal cortex, the parafascicular thalamic nucleus, the AbC, the midbrain (APT, PBG, tegmental reticular nucleus) and the amygdala, which we equally did not find.

Furthermore following M2 injections we did not find anterograde labelling in the PC, the STh, and the dorsal raphe nucleus, unlike previous reports. Moreover, we found anterograde label in the SNC and the AV after M2 injections, which were not reported in previous studies in the rat. Again these difference may be species specific, or could result from differences in injection sites and labelling techniques.

3.4.2 Functional implications

3.4.2.1 Relation of Anatomical Visual Connectivity to Functionally Defined Visual Regions

This work has identified a number of differing connectivity patterns from secondary visual areas onto the SC and from the prefrontal areas (Cg, M2) to those secondary visual areas. Due to the increased focus in the literature on functionally defined higher visual areas, it is important to relate any anatomical patterns in these functional terms (Wang and Burkhalter, 2007, Marshel et al., 2011, Garrett et al., 2014).

In the SCm cohort, labelling was found in all parts of the secondary visual cortex. From the pattern of labelled cells this may equated to connectivity from a number of functionally defined visual regions, i.e. the anteromedial area (AM), rostrolateral area (RL) and posteromedial (PM) (Wang and Burkhalter, 2007).). AM has a high temporal frequency preference which may aid an animal in detecting fast moving stimuli such as predators (Marshel et al., 2011). PM has a higher spatial frequency preference which may aid in identification of the object in the visual environment. Furthermore, the more medial areas AM and PM respond to stimuli in the peripheral visual field (Marshel et al., 2011, Garrett et al., 2014). Similarly, the visual projections of Cg terminate in V2MM and V2ML, which may match the functionally defined areas AM and PM. This suggests that AM and PM receive innervation from Cg, which provide the SCm with information regarding the location and spatial features of visual stimuli in the upper/peripheral visual field. This may be important to the development of upcoming avoidance behaviours to predators.

The visual projections from M2 terminate in the V2L region, which, as defined in this study, may match a number of functionally defined visual areas such as laterointermediate area (LI), rostrolateral area (RL) and PM (Wang and Burkhalter, 2007). LI, similarly to PM, has a higher spatial frequency preference than other higher visual areas and may be related to object recognition/classification. The functional region RL has been previously localized in the parietal region of the mouse cortex and has been implicated in visual and whisker multisensory integration (Olcese et al., 2013). RL has a preference for high temporal frequency stimuli and represents the lower central visual field (Marshel et al., 2011, Garrett et al., 2014). In conjunction with our data this suggests that RL may be linked in guiding the sensory information regarding stimuli in the lower visual field to aid orienting behaviours.

3.4.2.2 SCm and avoidance behaviours

The SCm contains a retinotopic map of the upper visual space, via projections from the retina, primary and secondary visual areas (V1, V2MM, V2ML, V2L) (Ahmadlou and Heimel, 2015). Looming stimuli in the upper visual field elicits fear responses that are mediated from the SC through the LP to the amygdala (Wei et al., 2015). Furthermore, optogenetic stimulation of SCm elicits the upper visual field avoidance behaviours which are initiated via the PBG and the Pn (Shang et al., 2015). Reciprocal connectivity to the SCm from LP, a possible rodent homologue of the pulvinar, may deliver information to guide orienting behaviours (Wei et al., 2015). Finally, areas directly involved in fear processing such as the VMH and the PAG may conduct fear-state information to the SC (Dielenberg et al., 2001). Once the avoidance sensorimotor transduction has been processed in the SCm, signals can be sent through the uncrossed tecto-reticulo-spinal tract which mediates the avoidance related motor output (Redgrave et al., 1988).

3.4.2.3 SCl and approach behaviours

The SCl is retinotopically mapped to the lower visual space, where appetitive stimuli, such as prey or offspring are likely to occur, both of which require approach-orienting responses, (Ahmadlou and Heimel, 2015). In rats, appetitive hunting and whisking behaviour results in increased c-FOS expression within the SCl, and lesions of the SCl decrease predatory orienting behaviours (Furigo et al., 2010, Favaro et al., 2011).

Research groups which investigate auditory or odor cued orienting responses in the SC often place probes (electrodes, optrodes) in the lateral portion of the SC (Felsen and Mainen, 2012, Stubblefield et al., 2013, Duan et al., 2015), and thus our knowledge regarding stimulus processing in the mouse SC might be biased towards appetitive stimulus types. Once processed, the SCl sends the information through the crossed tecto-reticulo-spinal tract to brain stem motor nuclei to initiate approach behaviour (Redgrave et al., 1990).

Although this research has highlighted an existing dichotomy in the separation of approach and avoidance behaviours regarding the location of stimuli in the visual field, it must be noted that this segregation is not complete. Studies have used visually stimuli in the upper visual field which require approach behaviours (Harvey et al., 2009, Scott et al., 2015) conversely studies have employed stimuli which occur in the lower visual field which require avoidance behaviours (Ho et al., 2015, Manita et al., 2015). However in these studies the stimuli have usually been presented a large number of times and have been associated with either a positive or negative outcome. This associative learning may then override the innate visual field associated orienting biases that are normally present.

3.4.2.4 Cortical control of orienting behaviour

M2 and Cg innervate different sections of the SC which suggests that they control separate types of orienting behaviour. If so, it should be reflected in their cortical and subcortical efferent projections. This was investigated by anterograde tract tracing, and indeed uncovered a difference in projection patterns.

M2 mostly sends efferents to SCl and somatosensory cortical areas. M2 in the mouse may be the homolog to Frontal Orienting Field (FOF) in rats (Erlich et al., 2011). Behaviourally, M2 has been implicated in top-down modulation of somatosensory based orienting and appetitive approach behaviours (Erlich et al., 2011, Guo et al., 2014). Additionally, M2 projects to parietal regions (MPtA, LPtA), which are involved in evidence accumulation and decision formation (Hanks et al., 2015). M2 neurons encode a categorical classification of evidence in decision making, while parietal neurons encode a more continuous representation of accumulated evidence (Hanks et al., 2015). The connection from M2 to MPtA and LPtA suggests that parietal cortex and frontal cortex interact in a reciprocal manner, rather than in a simple feed-forward scheme where

accumulated evidence in one area is converted into a categorical representation at a higher level. Lesions of M2 in rats cause a deficit in orienting, while microstimulation elicits orienting type behaviours (Cowey and Bozek, 1974, Sinnamon and Galer, 1984). A recent study has indicated that both the M2 and the SCl are involved in the generation of short term memory representations which are required for sensory orienting (Kopec et al., 2015). Taken together this information lends weight to the role of the M2 area in guiding orienting approach related behaviours which are mediated via the SCl.

The Cg is the major source of prefrontal input into the intermediate and lower layers of the SCm. Behaviourally, it has been implicated in top-down modulation of aversion related behaviours. Lesions of the Cg in rabbits reduces avoidance behaviours in relation to noxious stimuli (Gabriel et al., 1991). Furthermore, Cg activity can precede aversion responses to pain (Freeman Jr et al., 1996). Indeed, stimulation of Cg in rodents facilitates nociceptive reflexes (Calejesan et al., 2000). The Cg is heavily interconnected with regions involved in pain and fear processing (MD, amygdala, and hypothalamus). Cg projects to a number of areas in the basal forebrain which are part of the arousal/attention network. Activation of the Cg could thus result in heightened states of arousal, through activation of those pathways. Taken together this indicates the role of the Cg in pain and fear processing, which would result in the planning of avoidance behaviours, and which can be mediated via the SCm.

In conclusion, this study has revealed anatomically segregated circuits in the mouse brain that likely orchestrate approach and avoidance behaviour, respectively. Avoidance behaviour is likely sub-served by Cg, secondary visual cortices, auditory areas, and the dysgranular retrospenial cortex in conjunction with SCm. Conversely, approach/appetitive behaviours is likely subserved by M2, somatosensory cortex, and the granular retrospenial cortex in conjunction with the SCl.

Chapter 4. Comparison of Visual Bottom-up Attention in the Macaque and Mouse Primary Visual Cortex

4.1 Introduction

The central focus of this thesis has been how two different basic orienting responses could map onto (partially) segregated neuroanatomical circuits in the mouse. Both of the orienting responses considered, namely approach and avoidance, can be triggered by unexpected salient stimuli in the external world, activating a form of bottom-up (BU) attentional processing. To investigate the neural signatures of this, a comparison of bottom-up attentional processing in the primary visual cortex in the mouse and the macaque is the topic of the current chapter. BU attention has been previously described in Chapter 1. To briefly reiterate, BU attention is triggered by unexpected salient stimuli. This could be a brief high contrast visual stimulus which appears in the visual field, unexpected salient sounds, somatosensory stimuli, and even odours and tastes. Such a stimulus, in turn, elicits an overt orienting action, like a saccade in macaques or a head/body movement in rodents; or it can focus attention to the cued location without any external movement (Posner, 1980, Nakayama and Mackeben, 1989, Wang et al., 2015). The neurophysiological signatures underlying this form of orienting is the topic in this chapter.

The effects of attentional (external) cueing of potentially relevant stimulus locations has been reported previously (Posner, 1980, Corbetta and Shulman, 2002). This was first examined in human psychophysics through the use of central or peripheral cues which preceded a visual stimulus at a peripheral visual location (Posner, 1980). It was found that cueing the upcoming stimulus location could increase accuracy in the task, and decrease reaction times. Further studies disentangled the effects of central vs peripheral cueing, and showed that central cues would elicit top-down attentional modulation, whereas peripheral cues could elicit a transient BU modulation (Nakayama and Mackeben, 1989). BU attentional modulation has been shown to increase contrast sensitivity, and spatial acuity at a behavioural level (Lu and Dosher, 1998, Carrasco et al., 2000, Liu et al., 2005).

At the neuronal level BU attention has been shown to increase firing rates in the parietal cortex, prefrontal cortex and V1 to spatial locations and stimuli where attention is directed (Gottlieb et al., 1998, Bisley and Goldberg, 2003, Katsuki and Constantinidis, 2012, Wang

et al., 2015). These studies have shed some light on the neuronal basis of BU attention in macaques, but very little is known about these processes in rodents. However, orienting behaviours which require attention have been studied in rodents (Wallace et al., 1993, Erlich et al., 2011, Felsen and Mainen, 2012, Guo et al., 2014). These have usually been studied in animals which were freely moving and therefore showed overt orienting action (Felsen and Mainen, 2012). Moreover, some of these will have required top-down attention, or a combination of bottom-up and top-down attention. Even studies that focused on headfixed animals used visual stimuli without pre-cueing, and thus do not allow for immediate comparison to data from macaque electrophysiology. To address these deficits, and compare processing in two different key animal models used in neuroscientific research we decided to perform matched experiments which trigger BU attention mechanisms in humans and in non-human primates.

These experiments used a paradigm similar to that used in human attentional studies to investigate the neural responses to BU attention in the macaque and the mouse. The paradigm is adapted from a previous human fMRI study (Liu et al., 2005).The use of the same experimental paradigm in both model species allows for detailed comparative analysis to be made regarding the fundamental processing on attentional signals in such animals.

4.2 Methodology

4.2.1 Data Analysis

The detailed data analysis has been described previously (see section 2.6). In brief the spiking, multiunit envelope and LFP data were all examined in this section. They were aligned to the trial events on the recording day and averaged across trials and the entire experiment for the different stimulus and cuing conditions. To analyse the data a number of techniques were used. Firstly a mixed model repeated measure multi-factor ANOVA was conducted on the single electrode contacts for both the spiking and MUAe data. This was used to inform the further analysis. The grand averages for the entire recording populations in the different visual areas of the animals (V1 and V4 for macaque, and V1 and SC for the mouse) were compiled for contacts with a z-score of stimulus induced activity over spontaneous activity of above 3. This informed further descriptive analysis and post-hoc analysis through the use of Wilcoxon Rank Sign Tests. Furthermore the LFP

was analysed with a matching pursuit algorithm to complete a time frequency analysis on the data to uncover differences in the spectral power in response to different stimulus and cuing conditions.

4.3 Results

4.3.1 Electrophysiology

4.3.1.1 Macaque

The procedure involved 41 laminar (16 contact) electrode recordings in one animal. These consisted of passive (n=16) and active (n=25) task dataset (recordings from a laminar electrode), as detailed above in section 2.4. The passive recordings were conducted prior to the active task. This was done to ensure that during the passive task the animal experienced no reward associations with the stimuli, and thus would not perform the task covertly even though no response was required. The passive task contained 8 V1 and 8 V4 recordings which were done in separate sessions. For the active task there were a mixture of V1 (n=1), V4 (n=4) and simultaneous V1 and V4 recordings (n=10) completed on separate sessions. I investigated whether the cuing conditions differently affected neuronal activity in the passive vs. the active task. This was done for the pre-cue and the stimulus time period, using the MUAe signal. There were no significant differences between the active and passive bottom-up paradigm during either the cuing or stimulus time periods. This allowed the data from the two tasks to be pooled to increase statistical power for the rest of the analysis.

4.3.1.1.1 Spiking Data

4.3.1.1.1.1 Overall Effects of Precuing

To test whether different forms of (pre/post)-cuing and grating (vertical/horizontal) conditions affected neuronal spiking activity at the single contact (unit) level, a multi-factor 2x4x4 ANOVA (factors: grating type [2 levels], cue [4 levels], time period analysed [4 levels]) was used, as described in section 2.6.1. Activity (sp/sec) in different time periods of single trials (pre-cue, stimulus, post-cue and pre-cue on to post-cue off) were the measured variables. Based on the signal to noise ratio criterion employed (z-score > 3

for stimulus related time period over spontaneous activity), the analysis was conducted on spiking activity from 21 contacts in V1 and 36 contacts from V4.

4.3.1.1.1.2 Cueing Effects at the Level of Single Cells (Contact)

In V1 significant effects of time window were found on all contacts, ($n=21/21$, $p<0.001$, RM- mixed model ANOVA). This result was expected and not particularly interesting, as stimulus presentation in the RF should increase firing rates. 13/21 of the contacts showed a significant effect of grating type ($p<0.001$), i.e. an orientation preference. 2/21 of the contacts exhibited a significant effect of cuing condition ($p<0.05$). When examining interactions, 12/21 contacts had a significant interaction between the grating type and the time window ($p<0.05$). 3/21 contacts showed a significant cue condition and time window interaction ($p<0.05$). Finally, one contact showed a significant interaction of grating type, cueing condition, and experimental time period ($p<0.05$). An illustrative example of a single responsive neuron in V1 is shown below (Figure 4-1).

Important differences were found for the V4 recordings, when compared to the V1 recordings. Significant effects of the time window were found in all V4 contacts, ($n=37/37$, $p<0.001$, RM- mixed model ANOVA). However, the cuing conditions induced significant changes in firing rate on 16/37 V4 contacts ($p<0.001$, ANOVA). Different firing rates due to grating type occurred on 11/37 V4 contacts ($p<0.05$, ANOVA). 32/37 V4 contacts showed a significant interaction ($p<0.05$) between the cuing conditions and the time window. 10/37 V4 contacts showed a significant interaction between the grating type and the time window, ($p<0.05$). 4/37 V4 contacts showed significant interaction between the grating type and the cuing condition ($p<0.05$). Finally, a single V4 contact had a significant three way interaction between the grating type, the cuing condition and the time window. An illustrative example of a single responsive neuron in V1 is shown below (Figure 4-2).

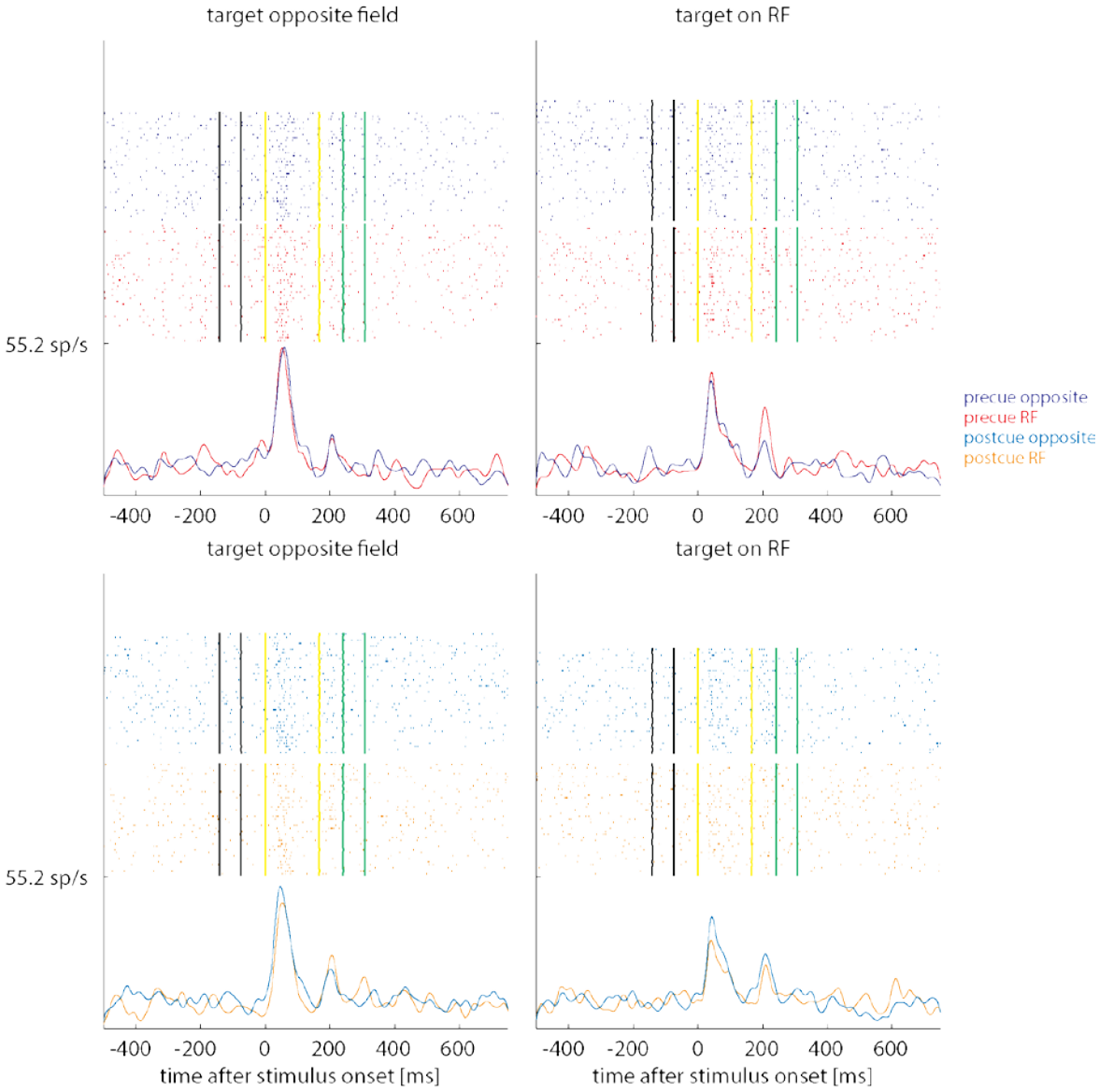

Figure 4-1. Raster Plots and Peristimulus Time Histograms for an Example Neuron in Macaque V1

Raster plots (upper panels) and histograms (lower panels) for the two grating types (horizontal [left] and vertical [right] grating) for a V1 neuron. Red ticks/trace equate to pre-cue RF condition, dark blue ticks/trace equate to pre-cue non-RF condition, orange ticks/trace equate to post-cue RF condition, light blue ticks/trace equate to post-cue non-RF condition. X-axis shows time relative to stimulus onset (time 0). The different cuing, and stimulus analysis periods are shown by vertical lines, demarcating precue onset and offset (black), stimulus onset and offset (yellow), post-cue onset and offset (green) respectively. Solid lines of the histograms show means.

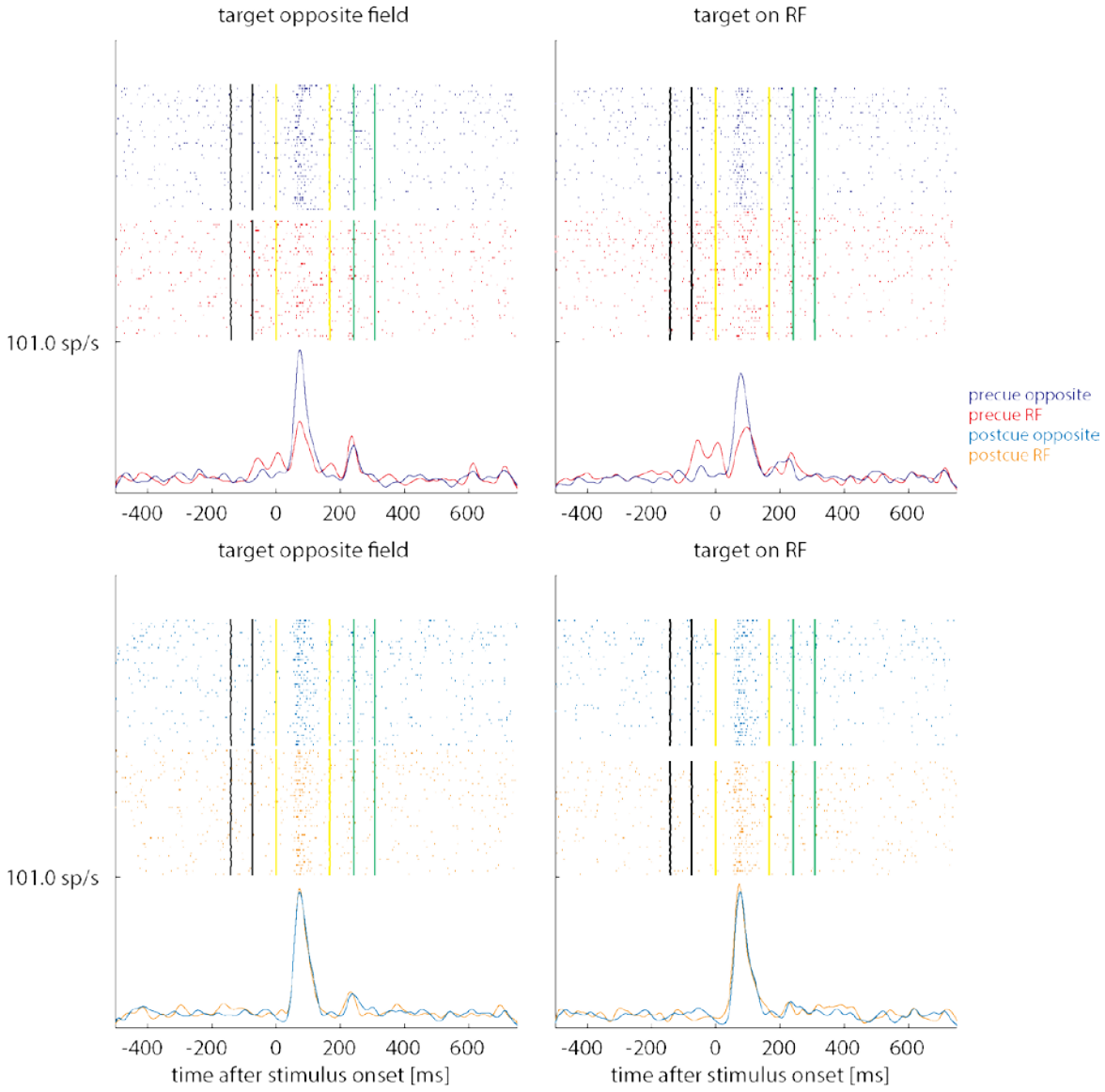

Figure 4-2. Raster Plots and Peristimulus Time Histograms for an Example Neuron in Macaque V4

Raster plots (upper panels) and histograms (lower panels) for the two grating types (horizontal [left] and vertical [right] grating) for a V4 neuron. Red ticks/trace equate to pre-cue RF condition, dark blue ticks/trace equate to pre-cue non-RF condition, orange ticks/trace equate to post-cue RF condition, light blue ticks/trace equate to post-cue non-RF condition. X-axis shows time relative to stimulus onset (time 0). The different cuing, and stimulus analysis periods are shown by vertical lines, demarcating precue onset and offset (black), stimulus onset and offset (yellow), post-cue onset and offset (green) respectively. Solid lines of the histograms show means.

4.3.1.1.1.3 Cueing Effects at the Population Level

The population PSTHs are shown in Figure 4-3 and Figure 4-4. Some features of these PSTHs are described below descriptively, as these will inform the more quantitative analysis that follows thereafter.

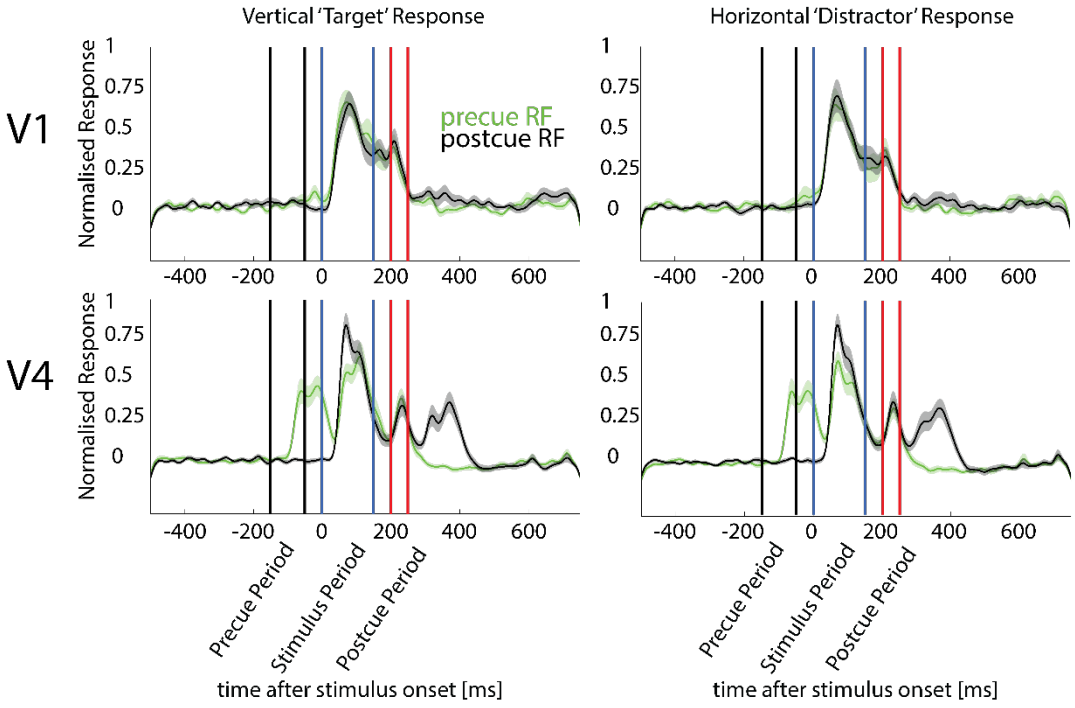

Figure 4-3. Average Normalised Population Firing Rates in Macaque V1 and V4 for Pre-cue RF vs Post-cue RF Conditions.

Population histograms for the two grating types (vertical [left] and horizontal [right] grating) for V1 (upper row) and V4 (lower row). Green histograms show the pre-cue RF conditions. Black histograms show the post-cue RF conditions. X-axis shows time relative to stimulus onset (time 0). Y-axis shows normalised averaged spiking activity. The different cuing, and stimulus analysis periods are shown by vertical lines, demarcating onset and offset respectively. Solid lines of the histograms show means, shaded areas show S.E.M (if not visible then S.E.M are too small to show).

The V1 activity population activity shows very little (if any) differences between the different cuing conditions (Figure 4-3). If differences occurred, they would most likely be present in the periods where neither cue nor grating stimuli were present (see the small differences following the pre-cue period for example). Conversely, substantial differences are apparent for the V4 data. The pre-cue RF condition elicited relatively large responses during and after the pre-cue period. This, however, also resulted in diminished stimulus induced responses, particularly during the initial response transient. Conversely, the post-cue RF condition resulted in larger responses during and following the post-cue period.

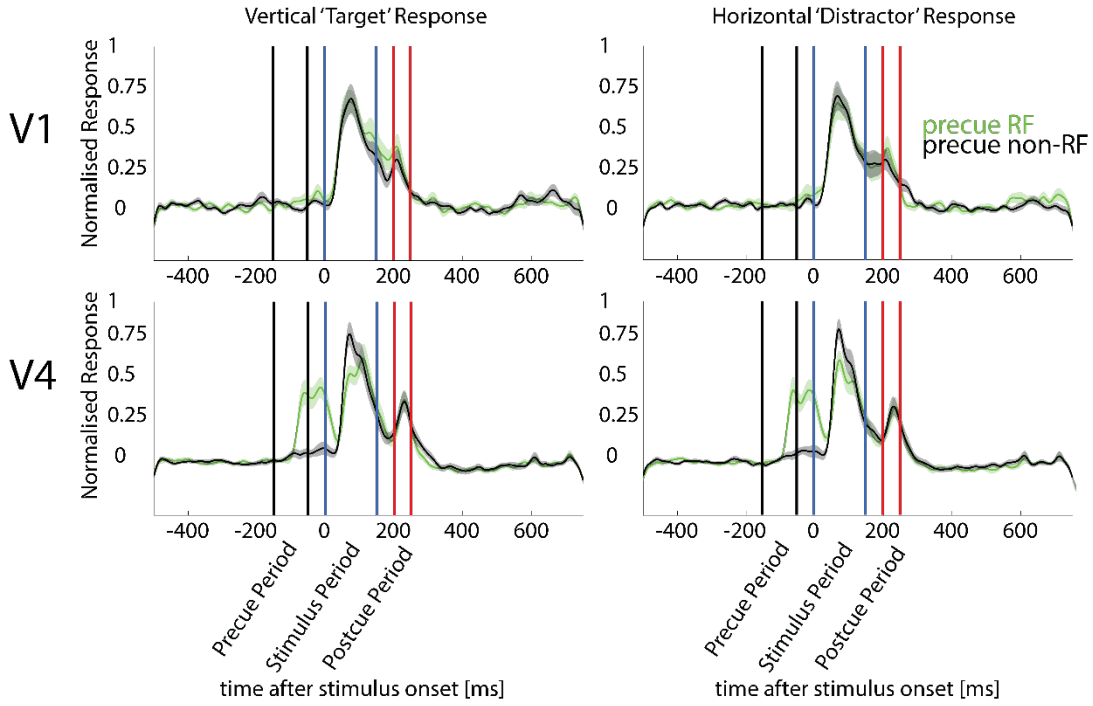

Figure 4-4. Average Normalised Population Firing Rates in Macaque V1 and V4 for the Pre-cue RF vs Pre-cue non-RF Conditions.

Population histograms for the two grating types (vertical [left] and horizontal [right] grating) for V1 (upper row) and V4 (lower row) data. Green histograms show the pre-cue RF conditions. Black histograms show the pre-cue non-RF conditions. X-axis shows time relative to stimulus onset (time 0). Y-axis shows normalised activity. The different cuing, and stimulus analysis periods are shown by vertical lines, demarcating onset and offset respectively. Solid lines of the histograms show means, shaded areas show S.E.M.

A similar result was obtained when comparing pre-cue RF vs. pre-cue non (opposite) RF conditions (Figure 4-4). Again, the V1 activity population activity showed very little (if any) differences between the two conditions (Figure 4-4). For this comparison, there might have been some small differences during the sustained response when the vertical grating had been present, but these were not present when the horizontal grating had been presented. Substantial differences were apparent for the V4 data. As described before, the pre-cue RF condition elicited relatively large responses during and after the pre-cue period, which were not present for pre-cue non-RF stimuli. These increased responses resulted in the previously described diminished stimulus induced responses, which were not present for the pre-cue non-RF condition. No obvious differences occurred during the sustained stimulus response, or following response offset.

To analyse the effects of cuing at the population level quantitatively, a repeated measures (RM) mixed model multi-factor 2x4x4 ANOVA (factors: cue [4 level], grating type [2 level], time period analysed [4 level, pre-cue, stimulus, post cue, time from pre-cue to end of post-cue]) was used. Average firing rates (sp/sec) over the relevant time periods from single contacts (cells) were the measured variables.

4.3.1.1.1.3.1 V1 Population Spiking Data

Significant effect of time window on the population activity (Table 4-1 for exact p-values) were found. There were no significant interactions between any of the factors, as already suggested by the qualitative description of the V1 population histograms.

Table 4-1. Repeated Measures Mixed Model Multi Factor ANOVA for the Population of Spiking Activity in Macaque V1

Term (Factor)	FStat	DF1	DF2	pValue
Cuing Condition	1.148	3	640	0.328
Grating Type	0.476	1	640	0.490
Time Window	40.868	3	640	<0.001
Cuing Cnd*Grating Type	1.705	3	640	0.164

Cuing Cnd*Time Window	1.262	9	640	0.254
Grating Type*Time Window	0.773	3	640	0.509
Grating Type*Cuing Cnd*Time Window	1.202	9	640	0.290

The significant effects of time window are trivial, as only the second time window contains the stimulus being displayed in the RF. The absence of a systematic grating type effects indicates that we did not have a bias in the sampling of orientation preferences for either horizontal or vertical in our population of cells. The main variable of interest, cuing condition, did not yield significant main effects, or interactions. Thus, different cueing conditions do not affect firing rates in macaque area V1, when analysed at the thresholded/spike sorted spiking level. A more detailed analysis of the pairwise effects (or absence thereof) is shown in Figure 4-5 and Figure 4-6.

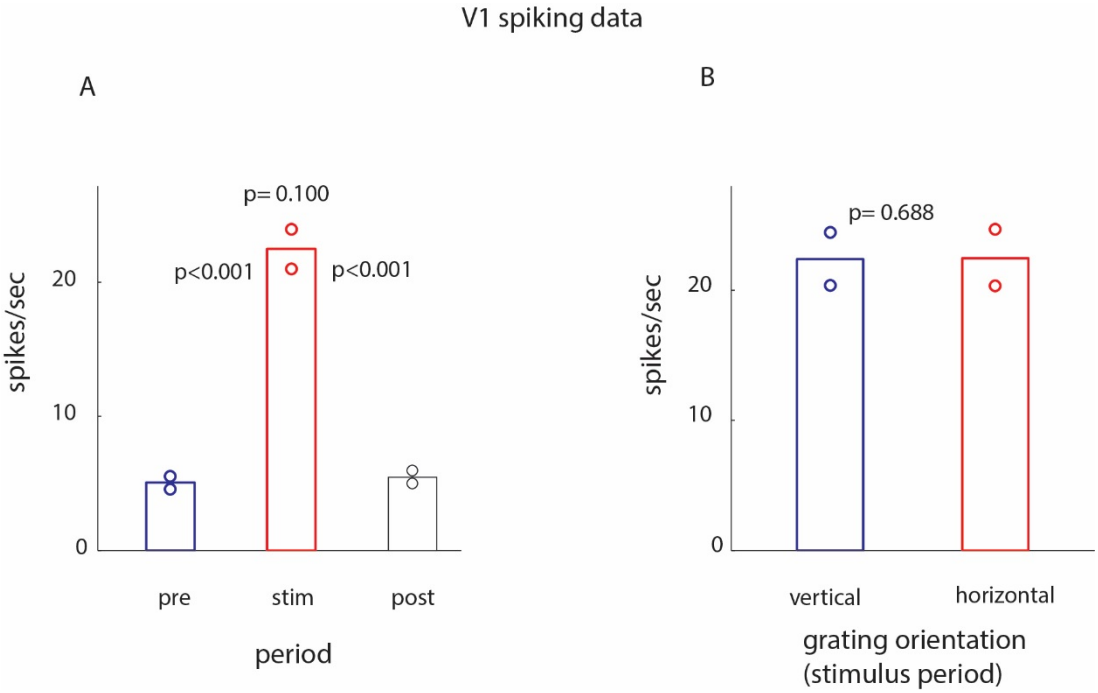

Figure 4-5. Comparison of Firing Rates for the Different Time Periods and the Two Grating Orientations in the Macaque V1

A. Mean firing rates for the population of V1 cells, during the different time periods (pre-cue [pre], stimulus [stim], and post-cue [post]). **B.** Mean firing rates for the population of V1 cells for the two different gratings, measured during the stimulus time period. P-values indicate pair wise differences (Wilcoxon Signed Rank test). Bars show mean activity, associated circles indicate 95% confidence intervals.

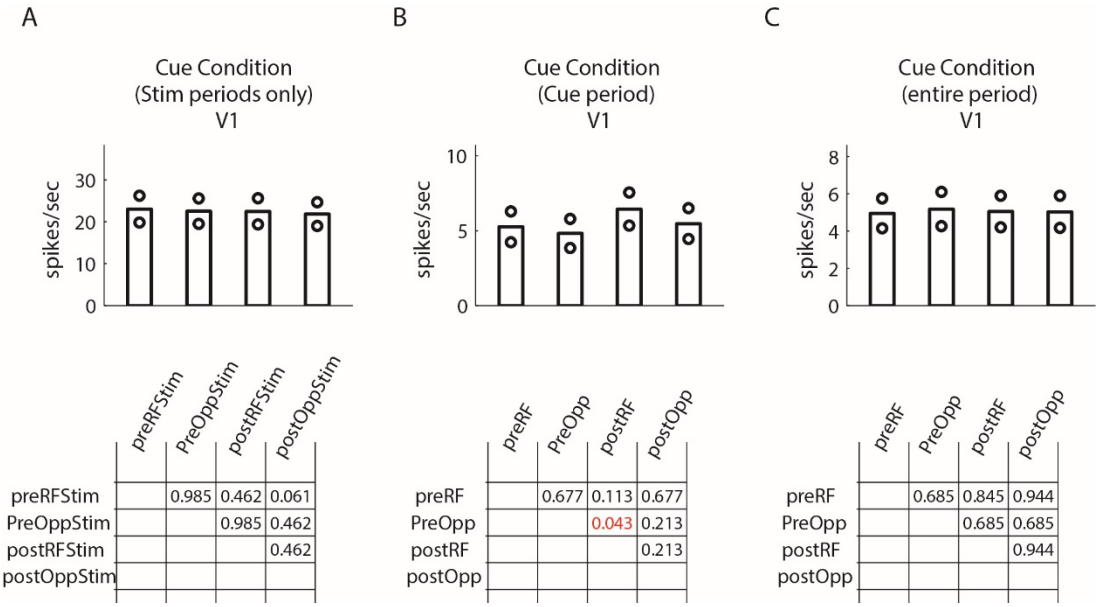

Figure 4-6. Comparison of Firing Rates for the Cuing Conditions in Different Time Periods Averaged Over Grating Orientations for Macaque V1

A. Mean firing rates for the population of V1 cells, during the stimulus time period for the 4 different cuing conditions (pre-cue RF [preRFStim], pre-cue opposite [preOppStim], post-cue RF [postRFStim], post-cue opposite [postOppStim]). **B.** Mean firing rates during the cuing time periods for the 4 different cuing conditions (pre-cue [preRF], pre-cue opposite [preOpp], post-cue RF [postRF], post-cue opposite [postOpp]). **C.** Mean firing rates during the entire time period (from pre-cue on until post-cue off) for the 4 different cuing conditions (pre-cue [preRF], pre-cue opposite [preOpp], post-cue RF [postRF], post-cue opposite [postOpp]). Tables below each subplot indicate pair wise differences (FDR corrected p-values based on Wilcoxon Signed Rank test). Bars show mean spiking activity, associated circles indicate 95% confidence intervals.

The pairwise analysis of cuing condition for the different analysis windows, only yielded on marginally significant effect (pre-cue in the opposite hemifield vs. post-cue RF) during the cuing time windows (p-value FDR corrected). No other effects were significant, as already suggested by the mixed model ANOVA analysis.

4.3.1.1.1.3.2 V4 Population Spiking Data

Firing rates of population V4 data significantly depended on cuing conditions, grating type, and time window analysed. The main effects and the interactions between different factors are summarised in Table 4-2. Significant interactions occurred between cuing conditions and time window analysed, as well as between grating type and time window analysed. The latter is trivial, as these effects (if any) were only expected during the stimulus time period.

Table 4-2. Repeated Measures Mixed Model Multi Factor ANOVA for the Population of Multiunits in Macaque V4

Term	FStat	DF1	DF2	pValue
Cuing Cnd	7.536	3	1152	<0.001
Grating Type	8.992	1	1152	0.003
Time Window	61.875	3	1152	<0.001
Cuing Cnd*Grating Type	0.641	3	1152	0.588
Cuing Cnd*Time Window	49.141	9	1152	<0.001
Grating Type*Time Window	2.947	3	1152	0.0031
Grating Type*Cuing Cnd*Time Window	0.371	9	1152	0.949

Figure 4-7 shows the main effects of time window and of grating type for the V4 data. Rates were highest during the stimulus window when compared to the cueing windows (Figure 4-7 A). No differences existed for the pre-cue vs. post-cue time window, when

averaged across all conditions. Rates were marginally (but significantly) higher for the vertical than for the horizontal grating (Figure 4-7 B).

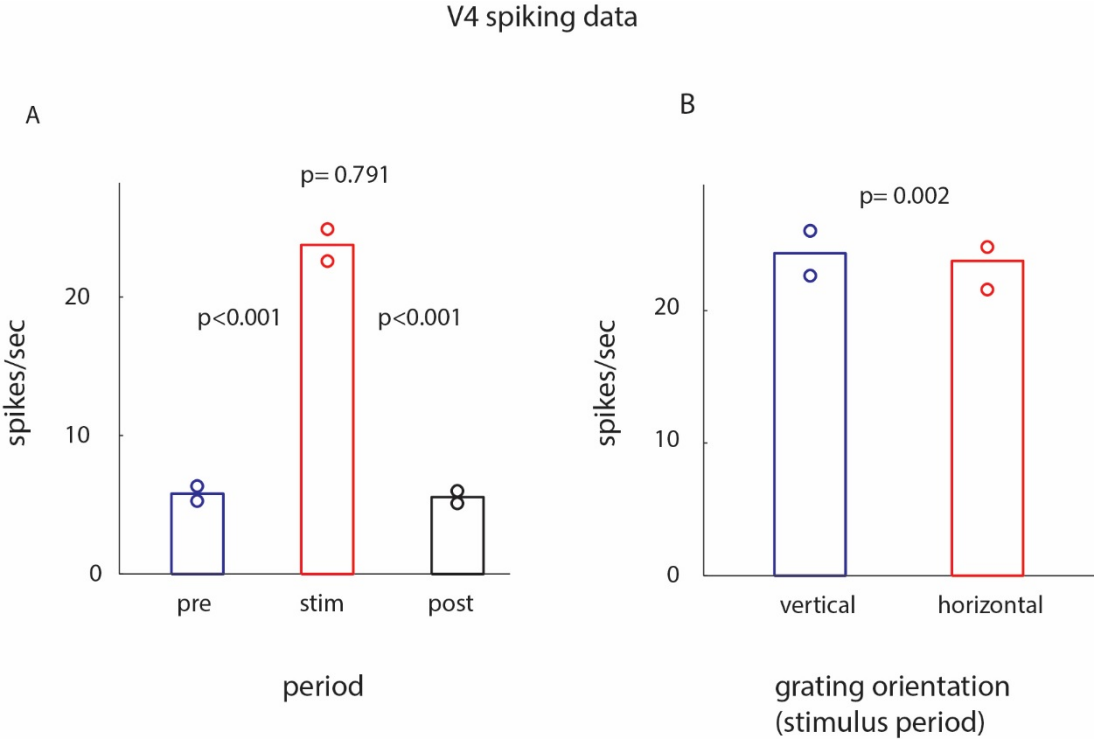

Figure 4-7. Comparison of Firing Rates for the Different Time Periods and the Two Grating Orientations for the V4 Spiking Data.

A. Mean firing rates for the population of V4 cells, during the different time periods (pre-cue [pre], stimulus [stim], and post-cue [post]). **B.** Mean firing rates for the population of V4 cells for the two different gratings, measured during the stimulus time period. P-values indicate pair wise differences (Wilcoxon Signed Rank test). Bars show mean activity, associated circles indicate 95% confidence intervals.

A detailed analysis of the effects of different cueing effects for the V4 spiking data is shown in Figure 4-8. The cuing conditions significantly affected the stimulus (grating) response, whereby it was significantly reduced when a pre-cue had been presented above the receptive field (Figure 4-8A). The pre-cue presented above the RF itself induced a

significantly larger response (during the cueing windows), when compared to the other cuing conditions (Figure 4-8B). This, was likely due to encroaching upon the classical receptive field of the recorded neurons. An increased response was also seen during the post-cue RF period, when compared to cuing conditions, where the cue appeared in the opposite hemifield, further supporting the idea that the cue above the RF encroached upon the classical RF. However, the post-cue RF yielded significantly smaller responses than the pre-cue RF. This could be due to response adaptation following stimulus presentation, or due to enduring normalisation mechanisms. The reduced stimulus response during pre-cue RF conditions (Figure 4-8A) could result from similar mechanisms (adaptation or normalization). An analysis of the entire response period did not show any significant differences (Figure 4-8C).

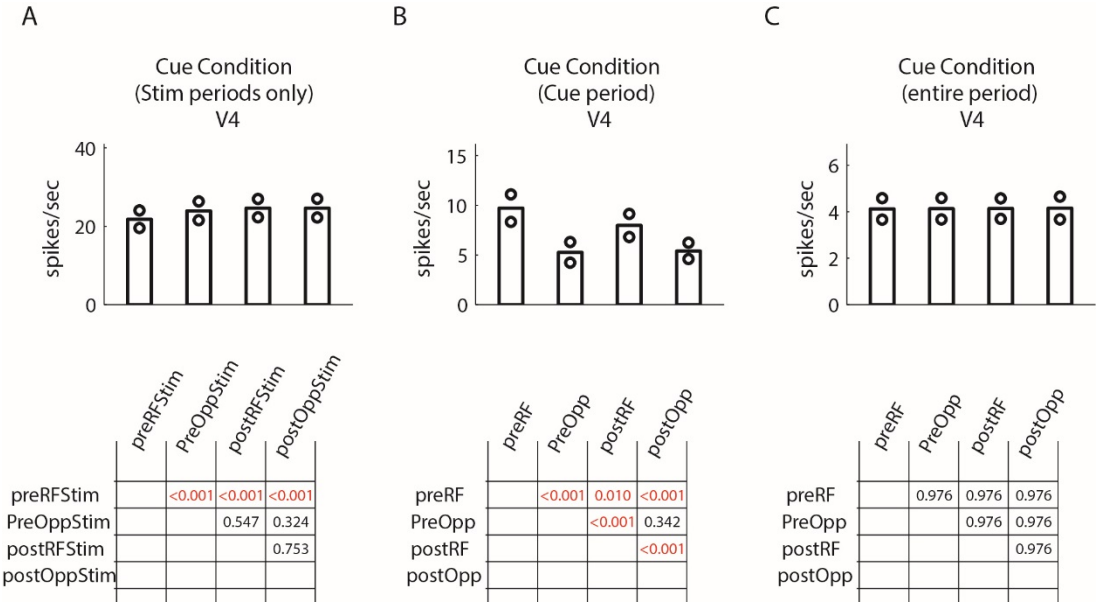

Figure 4-8. Comparison of Firing Rates for the Cuing Conditions in Different Time Periods Averaged Over Grating Orientations for Macaque V4.

A. Mean firing rates for the population of V4 cells, during the stimulus time period for the 4 different cuing conditions (pre-cue RF [preRFStim], pre-cue opposite [preOppStim], post-cue RF [postRFStim], post-cue opposite [postOppStim]). **B.** Mean firing rates during the cuing time periods for the 4 different cuing conditions (pre-cue [preRF], pre-cue opposite [preOpp], post-cue RF [postRF], post-cue opposite [postOpp]). **C.** Mean firing rates during the entire time period (from pre-cue on until post-cue off) for the 4 different cuing conditions (pre-cue [preRF], pre-cue opposite [preOpp], post-cue RF [postRF], post-

cue opposite [postOpp]). Tables below each subplot indicate pair wise differences (FDR corrected p-values based on Wilcoxon Signed Rank test). Bars show mean spiking activity, associated circles indicate 95% confidence intervals.

4.3.1.1.2 Multiunit Activity Envelope (MUAe) Data

For the analysis of MUAe activity the signal from 27 responsive V1 contacts and from 63 responsive V4 contacts was used. These numbers differed from the spiking data as the MUAe activity more often yielded z-score > 3 for stimulus induced activity than the spiking data did. Otherwise the analysis was equivalent to that described above, with the difference, that MUAe cannot be described in terms of spikes/second (i.e. firing rate), but it has to be normalised for every channel relative to baseline activity and relative to peak activity. An example of a single trial for a particular recording in macaque V1 and V4 with a 16 contact laminar electrode is shown below (Figure 4-9, Figure 4-10).

As done previously for spiking activity, population histograms will be shown first, with some description of the dominant features. This will be followed by quantitative analysis.

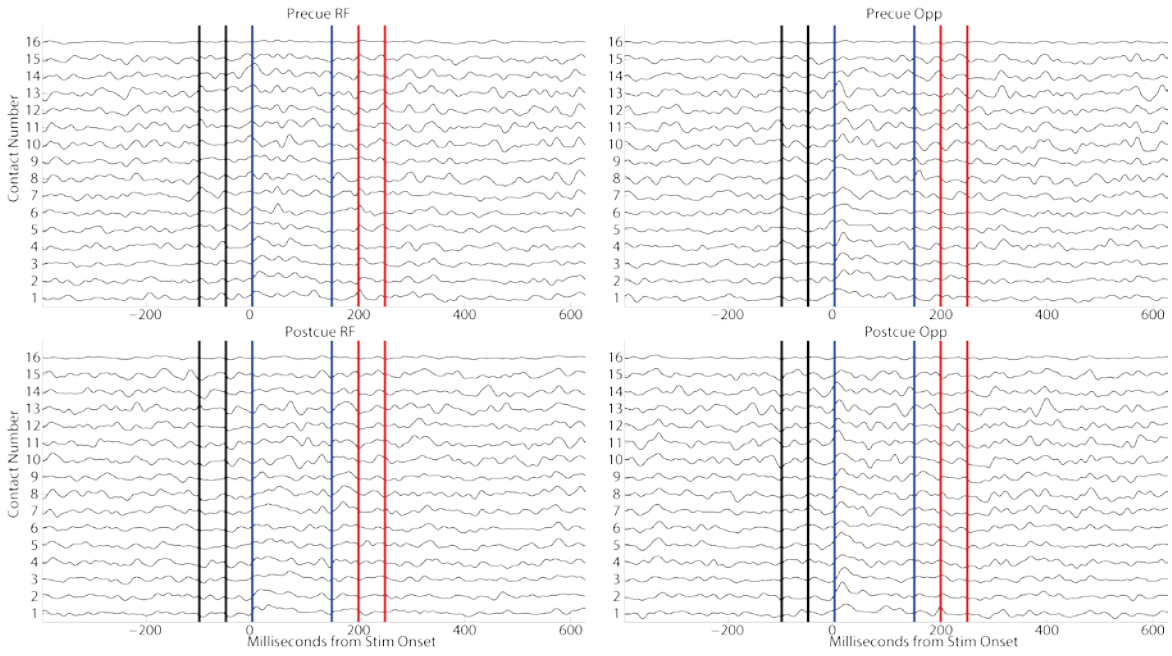

Figure 4-9. Raw Single Trial Example of MUAe Signal Recorded in Macaque V1 with a Laminar Electrode for the Vertical ‘Target’ Stimulus

Single trial traces for individual contacts along a laminar electrode in macaque V1. Contact number goes from most shallow to deepest. For this recording contact spacing

was 150µm. Vertical lines represent trial time epochs, black-pre-cue period, blue-grating stimulus period, red-post-cue period. Each panel displays a different trail for each cuing condition.

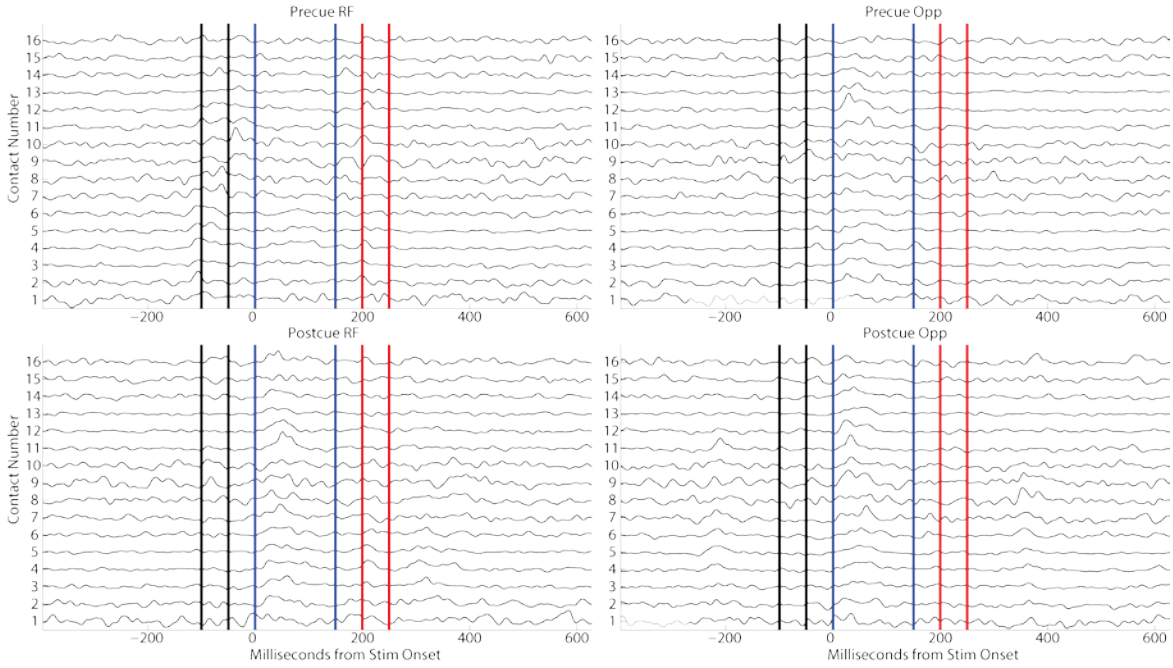

Figure 4-10. Raw Single Trial Example of MUAe Signal Recorded in Macaque V4 with a Laminar Electrode for the Vertical ‘Target’ Stimulus

Single trial traces for individual contacts along a laminar electrode in macaque V4. Contact number goes from most shallow to deepest. For this recording contact spacing was 150µm. Vertical lines represent trial time epochs, black-pre-cue period, blue-grating stimulus period, red-post-cue period. Each panel displays a different trail for each cuing condition.

4.3.1.1.2.1 MUAe Population Histograms

Figure 4-11 shows the MUAe population histogram when vertical stimuli were presented in V1 (and V4) receptive fields, along with the cumulative population histograms (right column). In V1 the pre-cue RF condition resulted in increased activity during the pre-cue period, when compared to pre-cue opposite and when compared to post-cue RF conditions. Additionally, the post-cue period showed higher activity when a post-cue was

presented above the RF, compared to when a pre-cue was presented above the RF. There were no obvious differences during the stimulus periods for the different cuing conditions. The increased activity for pre-cue RF conditions over pre-cue non-RF resulted in overall increased activity when the entire response period was analysed (cumulative activity, p=0.008, Wilcoxon Signed Rank test). The cumulative activity was not different for the pre-cue RF and the post-cue RF condition, as the activity differences described for the pre-cue and the post-cue period cancelled one another.

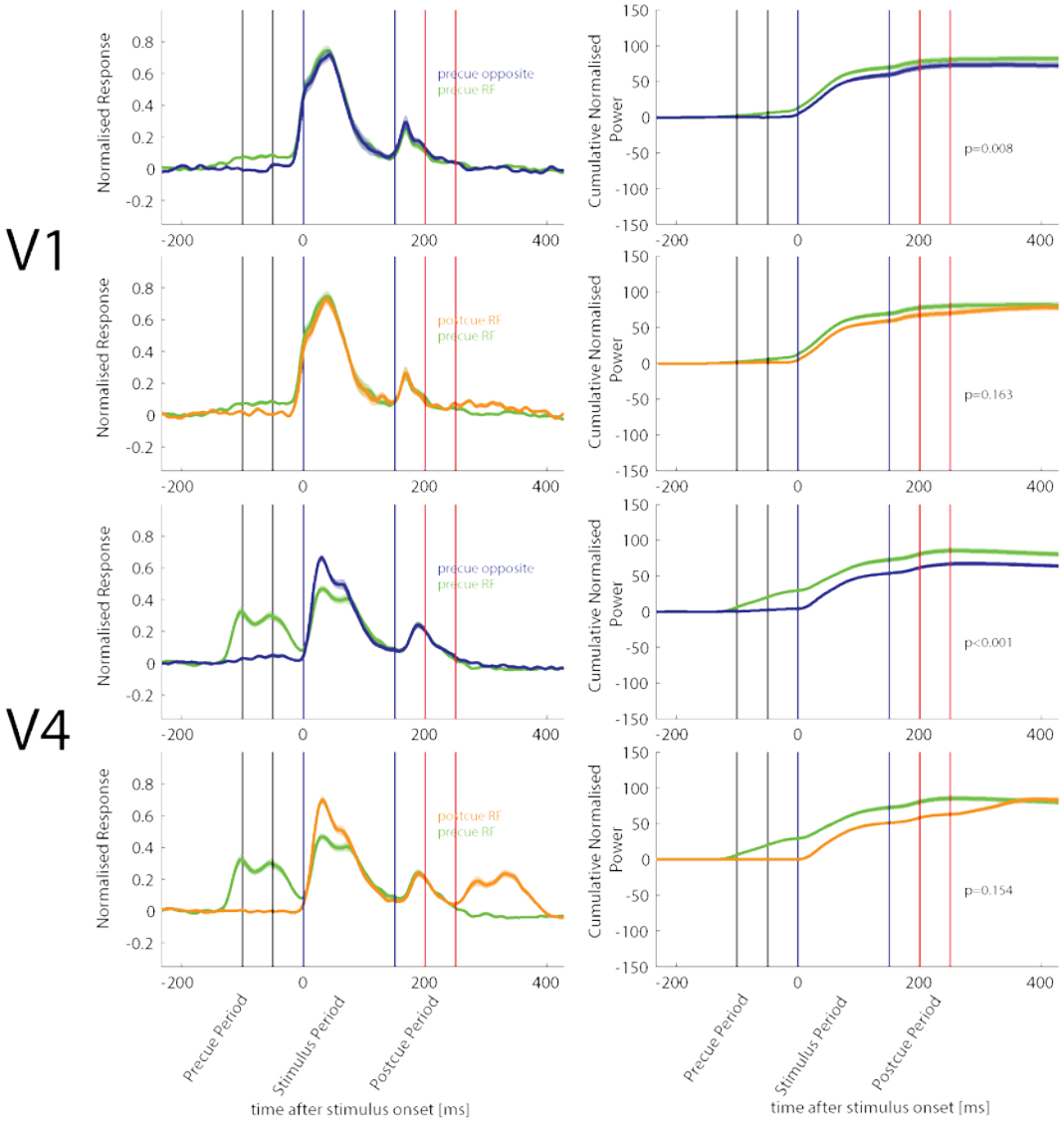

Figure 4-11. Comparison of Average Normalised MUAe Activity for the Vertical Stimuli in Macaque V1 and V4

Green lines show pre-cues presented above the RF location, blue lines show pre-cues presented in the non-receptive field location, orange lines show conditions where the post-cue was presented above the receptive field location. Vertical lines represent trial time epochs, black-pre-cue period, blue-grating stimulus period, red-post-cue period. In the left panels, the normalised multi-unit activity envelope (MUAe) for population of neurons in different conditions is presented. In the right panels, the cumulative activity across the trial is presented for different condition. P-value represents significance testing for the cumulative response (Wilcoxon Signed Rank test).

In V4 the pre-cue RF condition resulted in strongly enhanced activity in the pre-cue period, and reduced activity in the stimulus induced responses, as described for the spiking activity. However, the reduction in stimulus induced activity appeared smaller than the increase in pre-cue activity. No differences were found for the post-cue period when compared to pre-cue non-RF. As a consequence the cumulative activity differed significantly between pre-cue RF and pre-cue non-RF conditions. The post-cue RF condition elicited larger responses in the post-cue period than the pre-cue RF condition. Overall the cumulative activity did not differ between these two conditions.

Similar results were seen for the horizontal grating conditions (see Figure 4-12), which is why they are not described in detail here.

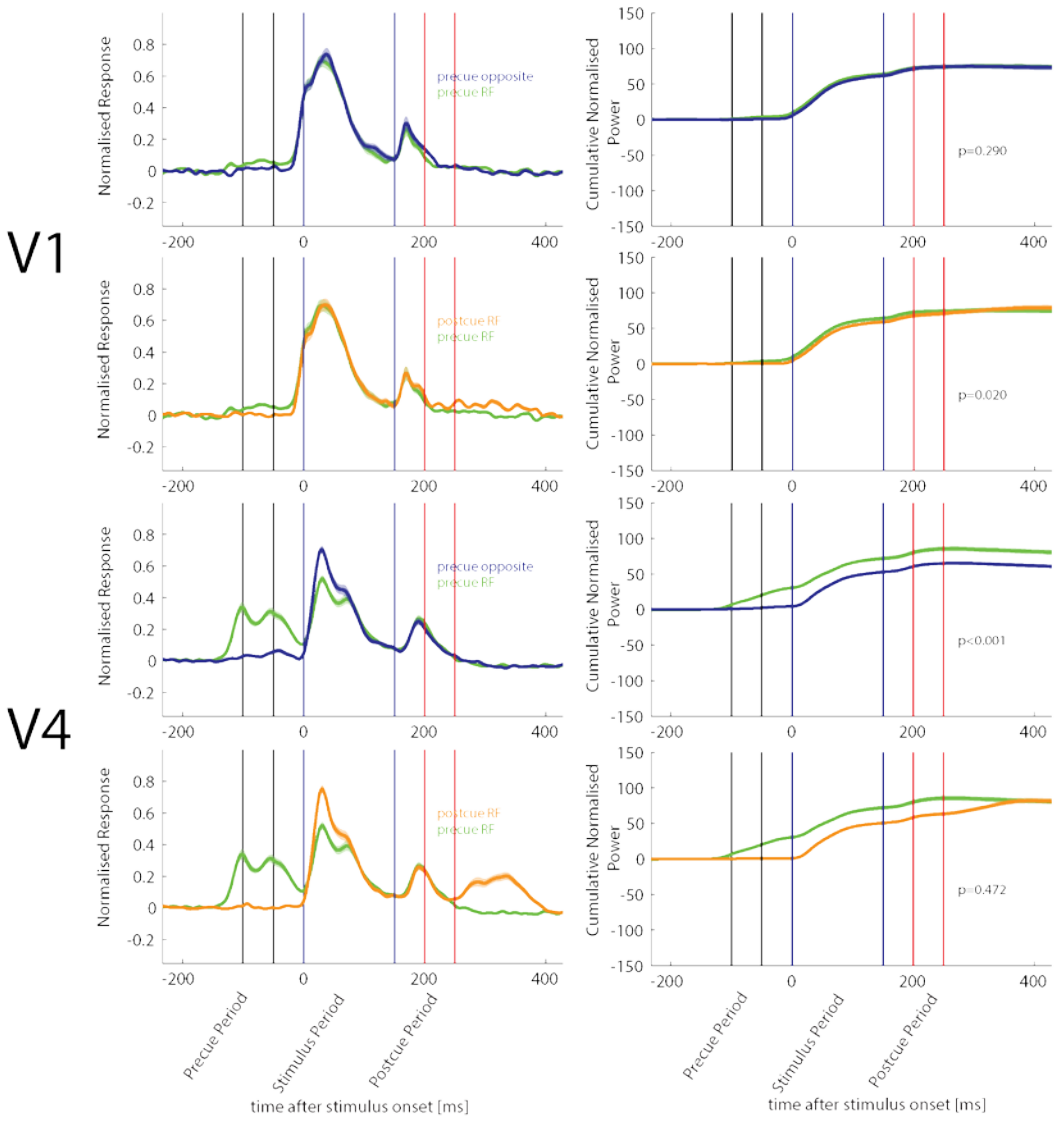

Figure 4-12. Comparison of Average Normalised MUAe Activity for the Horizontal 'Distractor' Stimuli in Macaque V1 and V4

Green lines show pre-cues presented in the RF location, blue lines show pre-cues presented in the non-receptive field location, orange lines show conditions where the post-cue was presented in the receptive field location. Vertical lines represent trial time epochs, black-pre-cue period, blue-grating stimulus period, red-post-cue period. In the left panels, the normalised multi-unit activity envelope (MUAe) for population of neurons in different conditions is presented. In the right panels, the cumulative activity across the trial is presented for different condition. P-value represents significance testing for the cumulative response, tested with Wilcoxon Signed Rank test.

4.3.1.1.2.2 Quantitative Analysis of V1 and V4 MUAe Data

The analysis pipeline for the MUAe data was identical to the spiking data. The first part describes how often single channel activity was affected by different cuing conditions. This was followed by an analysis of the effects at the population level.

4.3.1.1.2.2.1 Effects at the Level of Single Channels

To determine whether the different forms of (pre/post)-cuing and grating (vertical/horizontal) conditions affected the MUAe activity at the single channel level, a multi-factor 2x4x4 ANOVA was performed (described above in section 2.6.1). This ANOVA used the average normalised activity occurring in single trials over the time windows pre-cue (100ms-50m before stimulus onset), stimulus (0-150ms after stimulus onset), and the post-cue (50ms-100ms after stimulus offset) periods as the measured variable (note that the analysis windows had an offset of 40ms relative to the above described time periods to account for response latencies).

In general, a larger proportion of the single MUAe contacts were modulated by the different experimental conditions, than what had been found at the level of thresholded spiking activity). In V1 MUAe activity differed between time windows in all contacts, ($n=27/27$, $p<0.001$, ANOVA). Moreover, 12/27 of the contacts showed a significant effect of grating type ($p<0.001$). 7/27 of the contacts exhibited a significant effect of cuing condition ($p<0.05$). 22/27 contacts had a significant interaction between the grating type and the time window ($p<0.05$). 8/27 contacts showed a significant cue condition and time window interaction ($p<0.05$). Finally, grating type and cuing condition caused a significant interaction in 4/27 contacts.

In V4, MUAe activity different between time windows for all contacts ($n=63/63$, $p<0.001$, ANOVA). The cuing conditions caused a significant change in activity for 48/63 contacts ($p<0.001$). The grating type also caused 31/63 contacts to have significantly different activity ($p<0.05$). 53/63 contacts showed a significant interaction ($p<0.05$) between the cuing conditions and the time window. A significant interaction between the grating type and time window was found in 25/63 MUAe contacts ($p<0.05$). A significant difference between the grating type and the cuing condition ($p<0.05$) was found for 10/63 contacts. Finally, a single contact had a significant three way interaction between the grating type, the cuing condition and the time window.

4.3.1.1.2.2.2 Effects at the Level of Population Activity

A mixed model RM ANOVA was used to investigate whether cuing condition, time window analysed, or grating type significantly affected MUAe activity.

V1: The effects for MUAe activity in V1 are summarised in Table 4-3.

Table 4-3. Repeated Measures Mixed Model Multi Factor ANOVA for the MUAe Population in Macaque V1

Term	FStat	DF1	DF2	pValue
Cuing Cnd	8.459	3	848	<0.001
Grating Type	0.297	1	848	0.585
Time Window	4.850	3	848	0.027
Cuing Cnd*Grating Type	0.720	3	848	0.539
Cuing Cnd*Time Window	5.026	9	848	0.001
Grating Type*Time Window	0.009	3	848	0.920
Grating Type*Cuing Cnd*Time Window	0.442	9	848	0.723

The V1 MUAe activity was significantly affected by cuing condition, time window, and a significant interaction between cuing condition and time window was found (Table 4-3). Figure 4-13 and Figure 4-14 show these effects in more detail.

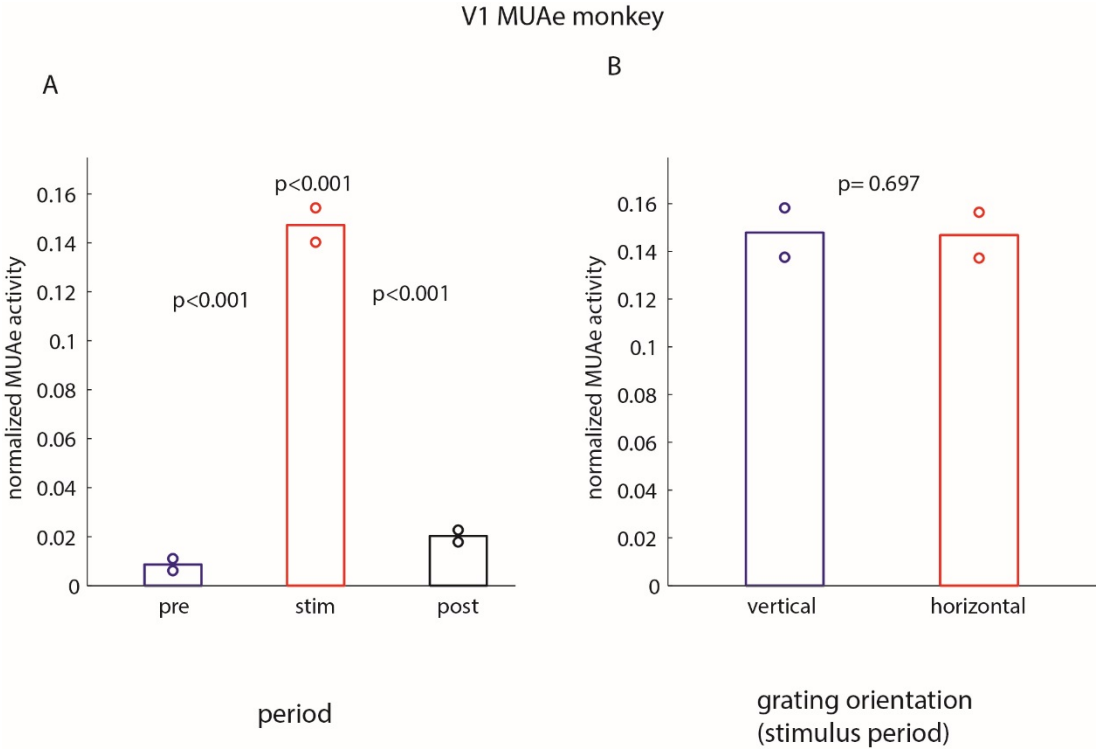

Figure 4-13. Comparison of MUAe Activity for the Different Time Periods and the Two Grating Orientations for V1

A. Mean normalised MUAe activity for the population of V1 channels, during the different time periods (pre-cue [pre], stimulus [stim], and post-cue [post]). **B.** Mean normalised MUAe activity for the population of V1 cells for the two different gratings, measured during the stimulus time period. FDR corrected p-values indicate pair wise differences (Wilcoxon Signed Rank test). Bars show mean activity, associated circles indicate 95% confidence intervals.

The lowest level of activity in V1 occurred during the pre-cue period, followed by the post-cue period (as already suggested by visual inspection of the population histograms (Figure 4-11 & Figure 4-12), while the highest activity occurred during the stimulus time period. The latter was expected, the differences between pre-cue and post-cue period were not necessarily expected given the results from the spiking analysis. Pairwise differences

were all significant ($p<0.001$, FDR corrected). No differences occurred between the different grating types.

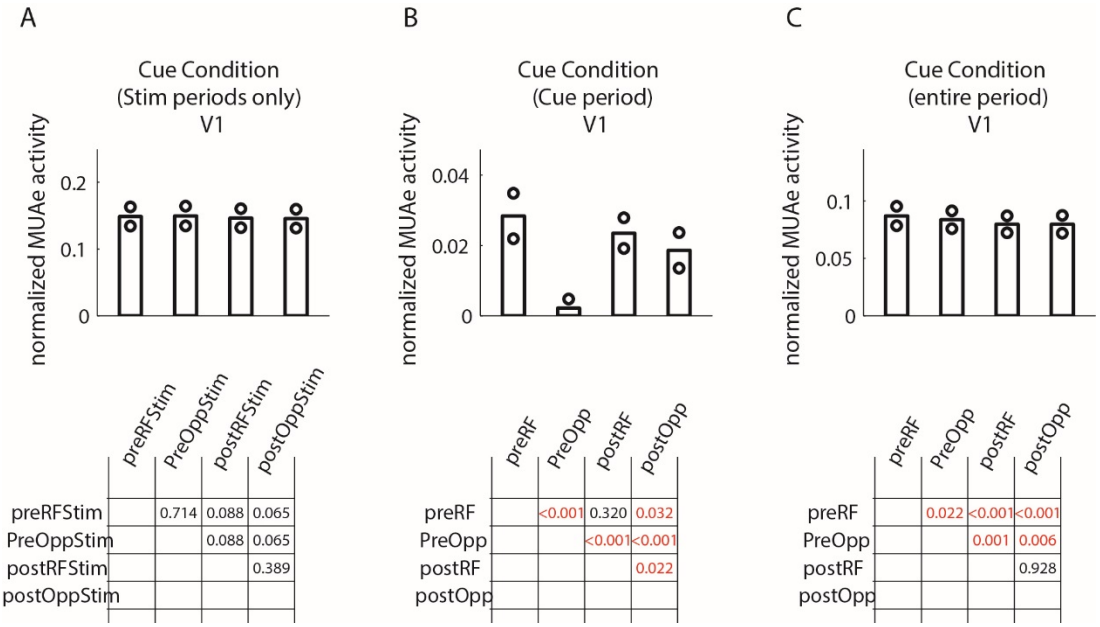

Figure 4-14. Comparison of Normalised MUAe Activity for the Cuing Conditions in Different Time Periods Averaged Over Grating Orientations for the V1 Data.

A. Normalised MUAe activity for the population of V1 contacts, during the stimulus time period for the 4 different cuing conditions (pre-cue RF [preRFStim], pre-cue opposite [preOppStim], post-cue RF [postRFStim], post-cue opposite [postOppStim]). **B.** Normalised MUAe activity during the cuing time periods for the 4 different cuing conditions (pre-cue [preRF], pre-cue opposite [preOpp], post-cue RF [postRF], post-cue opposite [postOpp]). **C.** Normalised MUAe activity during the entire time period (from pre-cue on until post-cue off) for the 4 different cuing conditions (pre-cue [preRF], pre-cue opposite [preOpp], post-cue RF [postRF], post-cue opposite [postOpp]). Tables below each subplot indicate pair wise differences (FDR corrected p-values based on Wilcoxon Signed Rank test). Bars show mean spiking activity, associated circles indicate 95% confidence intervals.

The largest V1 MUAe activity during the different cuing conditions occurred for the pre-cue RF condition (Figure 4-14B). It was significantly higher than the activity during pre- and post-cue opposite conditions. Pre-cue opposite conditions yielded significantly lower activity than any other conditions (FDR corrected pairwise comparisons, Figure 4-14B). The described results had the overall effect that significantly higher activity occurred for the pre-cue RF condition when the entire response period was taken into account than any of the other conditions, i.e. pre-cue RF conditions overall increased V1 MUAe activity (Figure 4-14C).

V4: The effects for MUAe activity in V4 are summarised in Table 4-4.

Table 4-4. Repeated Measures Mixed Model Multi Factor ANOVA for the MUAe Population in Macaque V4

Term	FStat	DF1	DF2	pValue
Cuing Cnd	129.5	3	2001	<0.001
Grating Type	0.095	1	2001	0.757
Time Window	9.234	3	2001	0.002
Cuing Cnd*Grating Type	0.080	3	2001	0.970
Cuing Cnd*Time Window	75.932	9	2001	<0.001
Grating Type*Time Window	0.010	3	2001	0.917
Grating Type*Cuing Cnd*Time Window	0.064	9	2001	0.978

MUAe V4 population activity was significantly affected cuing condition, and the time window analysed. Moreover, a significant interaction was found between cuing condition and time window. Figure 4-15 shows these effects in more detail. Post-hoc analysis revealed that pre-cue RF conditions significantly increased firing rates during the stimulus (grating) period (all pair-wise comparisons $p<0.05$ FDR corrected, Figure 4-16A). Moreover, post-cue period activity was larger than pre-cue period activity ($p<0.001$, Figure 4-16B), whereby pre-cue non-RF conditions resulted in the lowest 'cue' period activity (all pairwise comparisons $p<0.001$, Figure 4-15B). Analysis of the entire response period (pre-cue on until post-cue off), showed that the pre-cue RF condition yielded the

largest response (all pair-wise comparisons p<0.001). Additional details can be derived from the tables inFigure 4-15.

The lowest activity occurred during the pre-cue period, followed by the post-cue period (as already suggested by visual inspection of the population histograms (Figure 4-11 and Figure 4-12), while the highest activity occurred during the stimulus time period. The latter was expected. The differences between pre- and post-cue period were not necessarily expected given the results from the spiking analysis. Pairwise differences were all significant (p<0.001). No differences occurred between the different grating types.

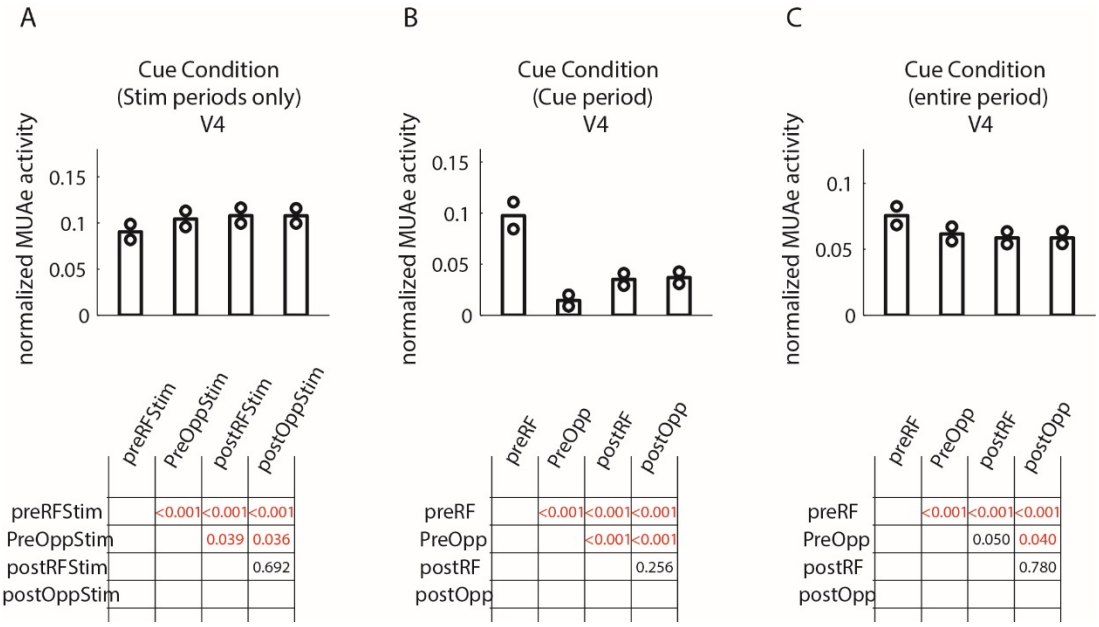

Figure 4-15. Comparison of Normalised MUAe Activity for the Cuing Conditions in Different Time Periods Averaged Over Grating Orientations for the V4 Data.

A. Normalised MUAe activity for the population of V4 cells, during the stimulus time period for the 4 different cuing conditions (pre-cue RF [preRFStim], pre-cue opposite [preOppStim], post-cue RF [postRFStim], post-cue opposite [postOppStim]). **B.** Normalised MUAe activity during the cuing time periods for the 4 different cuing conditions (pre-cue [preRF], pre-cue opposite [preOpp], post-cue RF [postRF], post-cue opposite [postOpp]). **C.** Normalised MUAe activity during the entire time period (from pre-cue on until post-cue off) for the 4 different cuing conditions (pre-cue [preRF], pre-cue opposite [preOpp], post-cue RF [postRF], post-cue opposite [postOpp]). Tables below each subplot indicate pair wise differences (p-values based on Wilcoxon Signed Rank

test). Bars show mean spiking activity, associated circles indicate 95% confidence intervals.

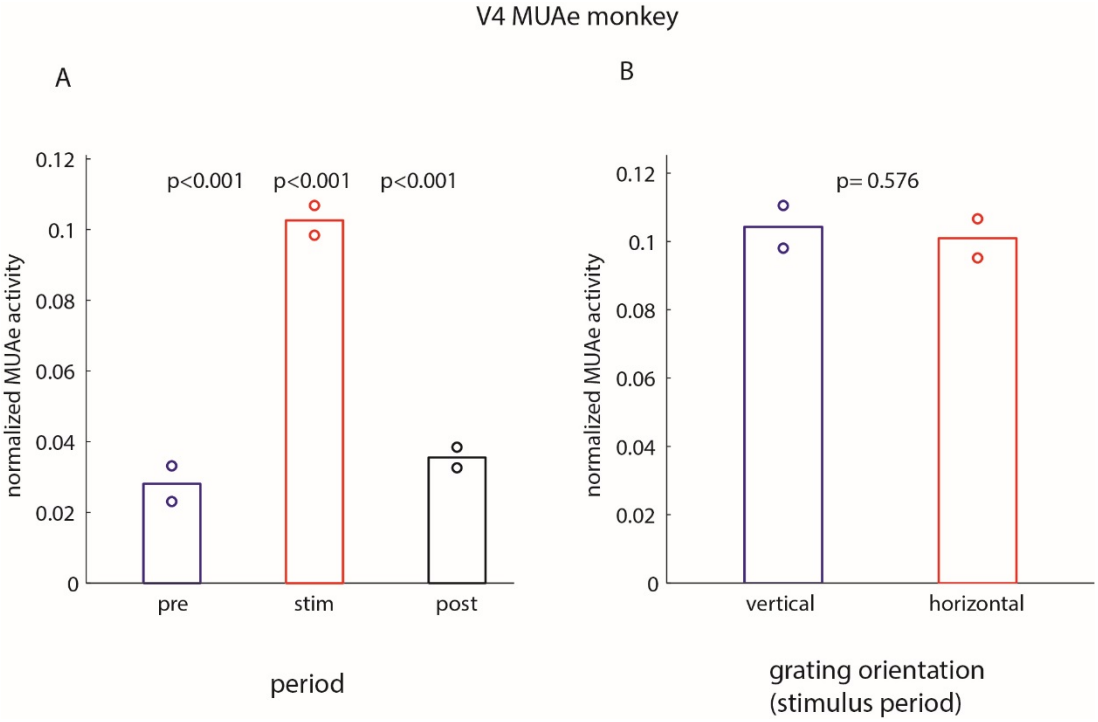

Figure 4-16. Comparison of MUAe Activity for the Different Time Periods and the Two Grating Orientations for V4.

A. Mean normalised MUAe activity for the population of V4 channels, during the different time periods (pre-cue [pre], stimulus [stim], and post-cue [post]). **B.** Mean normalised MUAe activity for the population of V4 cells for the two different gratings, measured during the stimulus time period. FDR corrected p-values indicate pair wise differences (Wilcoxon Signed Rank test). Bars show mean activity, associated circles indicate 95% confidence intervals.

Post-hoc analysis of effects of cuing condition on V4 MUAe activity revealed that pre-cue RF conditions significantly decreased firing rates during the stimulus (grating) period (all pair-wise comparisons $p<0.05$ FDR corrected, Figure 4-15A). Analysis of the cuing time periods, showed that pre-cue RF conditions yielded significantly higher firing rates during

the cue time period than any of the other conditions ($p<0.001$, Figure 4-15B), whereby pre-cue non-RF conditions resulted in the lowest 'cue' period activity (all pairwise comparisons $p<0.001$ FDR corrected, Figure 4-15B). Analysis of the entire response period (pre-cue on until post-cue off), showed that the pre-cue RF condition yielded the largest response (all pair-wise comparisons $p<0.001$ FDR corrected). Additional details can be derived from the tables in Figure 4-15.

4.3.1.1.3 LFP Matching Pursuit Analysis

For the LFP analysis the same electrode contacts were used as described in the MUAe section (V1: n=27, V4: n=63). Here we compare the pre-cue RF to the pre-cue non-RF, and to the post-cue RF condition, and plot difference spectrograms along with statistics (FDR corrected). The results for the conditions when the horizontal grating was presented are shown in Figure 4-17. The spectrogram data show difference maps, whereby the normalized (z-scored relative to pre-stimulus activity) time resolved spectral power differences for the conditions described above are shown. These difference maps were then averaged to obtain population data. Figure 4-17 shows population difference maps for all entries of the spectrogram, and it separately shows time frequency power differences that were significant (FDR corrected) at the population level. The data for the vertical grating were virtually identical, and are thus not shown separately.

4.3.1.1.3.1 Cuing Effects on the Horizontal 'Distractor' Stimulus

The presence of a pre-cue above the RF caused an increase in LFP spectral power in the 10-35Hz range with most of the power concentrated at ~25 Hz. Following stimulus onset, this changed, whereby the pre-cue RF condition resulted in higher low frequency (8-15Hz) compared to the pre-cue non-RF or post-cue RF conditions, combined with reduced power in the beta and gamma frequency range. Post-cue RF conditions also induced beta/gamma power during the post-cue period, and thus the difference spectrograms show a significant reduction in that frequency range during the post-cue period, when compared to the pre-cue RF condition.

The difference spectrograms seen in V4 differed from those seen in V1. The pre-cue above the RF resulted in a broad band increase in beta/gamma power, compared to the post-cue RF condition or the pre-cue non RF condition. The stimulus onset resulted in reduced

spectral power in the beta/gamma frequency band for the pre-cue RF condition, compared to the other conditions. The post-cue RF condition resulted in increased beta/gamma power during the post-cue period, similar to what was seen for the V1 data (Figure 4-17).

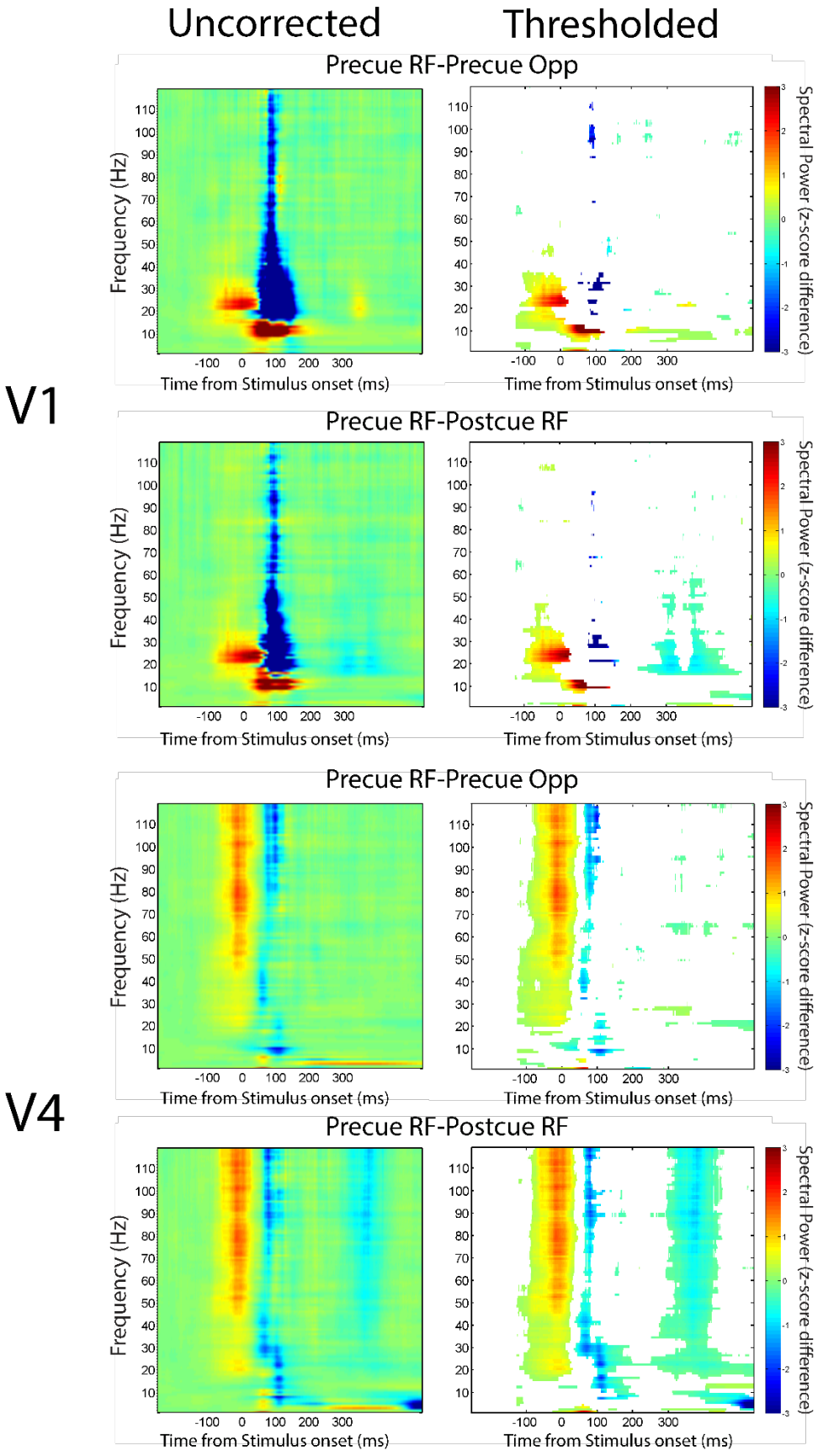

Figure 4-17. Spectrograms of Matching Pursuit LFP Analysis of Macaque V1 and V4 Data for the Horizontal 'Distractor' Stimulus.

Population pairwise spectrogram difference plots for both V1 and V4 macaque power spectrum data (z-scored for each channel). Time from stimulus onset is plotted against frequency for the pre-cue RF-pre-cue non-RF, and the pre-cue RF-post-cue RF conditions. Z-score differences are color coded. The left column displays the raw difference spectrograms. The right column shows spectrogram differences that were significant (t-test, with FDR correction, $p<0.05$). White entries of the right column plots were not significantly different.

4.3.1.1.4 Summary of Observable Effects in the Macaque

In general the macaque electrophysiological data was affected in some part by the different experimental conditions in the BU attentional task. Within the V1 data there was no observable bias for response to different gratings, however there was one observed in V4. Specifically there was an increase in activity for the vertical grating.

When summarising the effects of pre-cuing there were differential effects in V1. While there was no difference seen in the spiking data, the MUAe showed a noticeable increase in activity when the grating stimulus was pre-cued. Within the LFP, it was found that pre-cuing caused an increase beta band activity over the pre-cue period. Then during stimulus presentation there was a strong increase in theta band activity coupled with a large decrease in gamma band activation.

The experimental condition effects seen in macaque V4 were on the whole larger than those seen in V1. Precuing in both the spiking and MUAe data induced a large visual response. This resulted in a reduction of the stimulus induced response in comparison with the other conditions. Within the LFP, it was found that pre-cuing caused increase in beta/gamma power, whereas the stimulus onset reduced activity in this frequency range.

Taken together, these results show that pre-cuing causes differential effects in both macaque V1 and V4.

4.3.1.2 Mouse

18 recordings were performed in the mouse from 16 contact laminar electrodes in three animals (split as n= 4, n=2, and n=12). These used the passive bottom-up attention paradigm (see section 2.4.3), some without optogenetic stimulation (n=6) and some with optogenetic stimulation (n=12). This chapter separately analysed the basic effects of cuing, ignoring effects of optogenetic activation. The effects of optogenetic activation of Cg neurons on visual responses in V1 and SC will be described in the next chapter. For the analysis of the data, this chapter pooled all the recording data from V1 and from SC, but only used trials ***without*** the light activation. This yielded V1 (n=16) and SC recordings (n=4). The discrepancy of these numbers from the number listed above (n=18) arises because in two penetrations simultaneous recordings were performed from a single electrode in V1 and SC sites.

4.3.1.2.1 Spiking Data

Only a limited number of channel yielded adequate stimulus induced responses (z-score > 3 for stimulus response). Specifically, good multi-unit spiking activity was recorded in n=12 contacts in V1, and n=5 contacts in the SC. The multiunit spiking activity was analysed in an identical manner to that described in the macaque spiking activity section. As done previously, I will first describe some features of the population histograms, as these will prepare the way for the more quantitative analysis that follows thereafter.

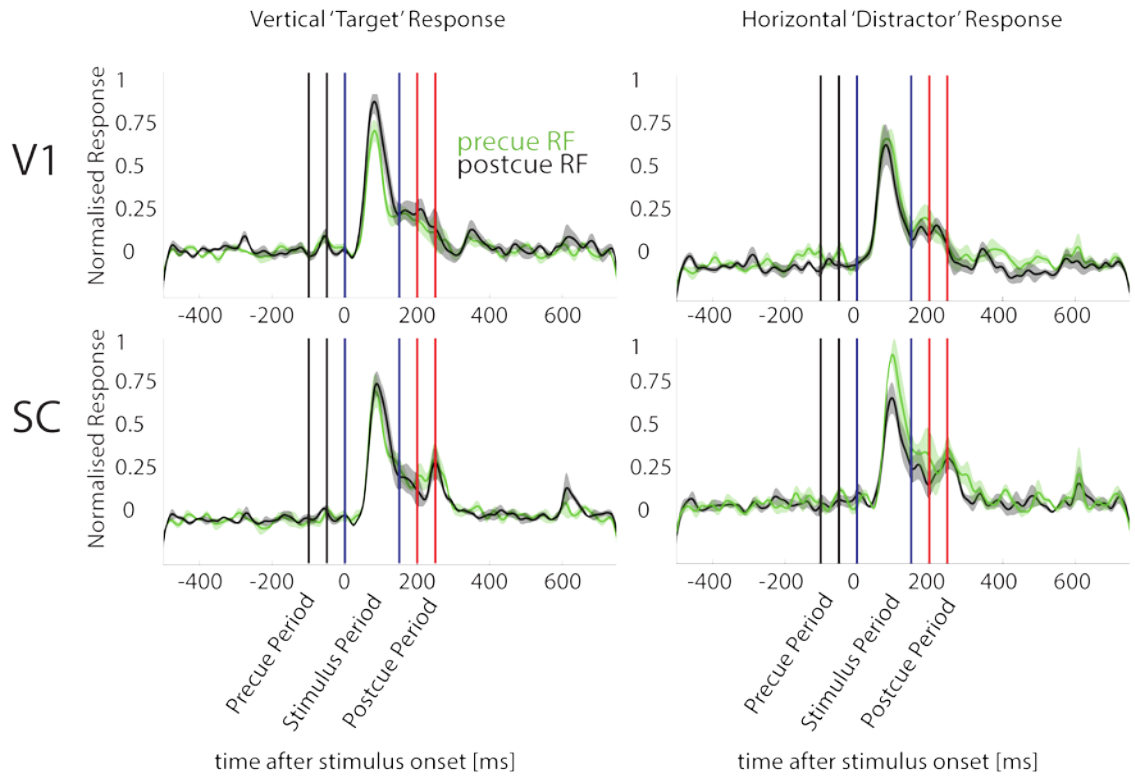

Figure 4-18. Average Normalised Firing Rates in Mouse V1 and SC for Pre-cue RF vs Post-cue RF Conditions.

Population histograms for the two grating types (vertical [left] and horizontal [right] grating) for V1 (upper row) and SC (lower row) data. Green histograms show the pre-cue RF conditions. Black histograms show the post-cue RF conditions. X-axis shows time relative to stimulus onset (time 0). Y-axis shows normalised activity. The different cuing, and stimulus periods are shown by vertical lines, demarcating onset and offset respectively. Solid lines of the histograms show means, shaded areas show S.E.M.

Neither the V1 nor the SC spiking population activity shows distinct differences between the two cue conditions (Figure 4-18). However, there may be hints that the pre-cue RF condition yielded higher horizontal grating responses in the SC data than the post-cue RF condition. The same was true when comparing pre-cue RF vs. pre-cue non-RF conditions (Figure 4-19).

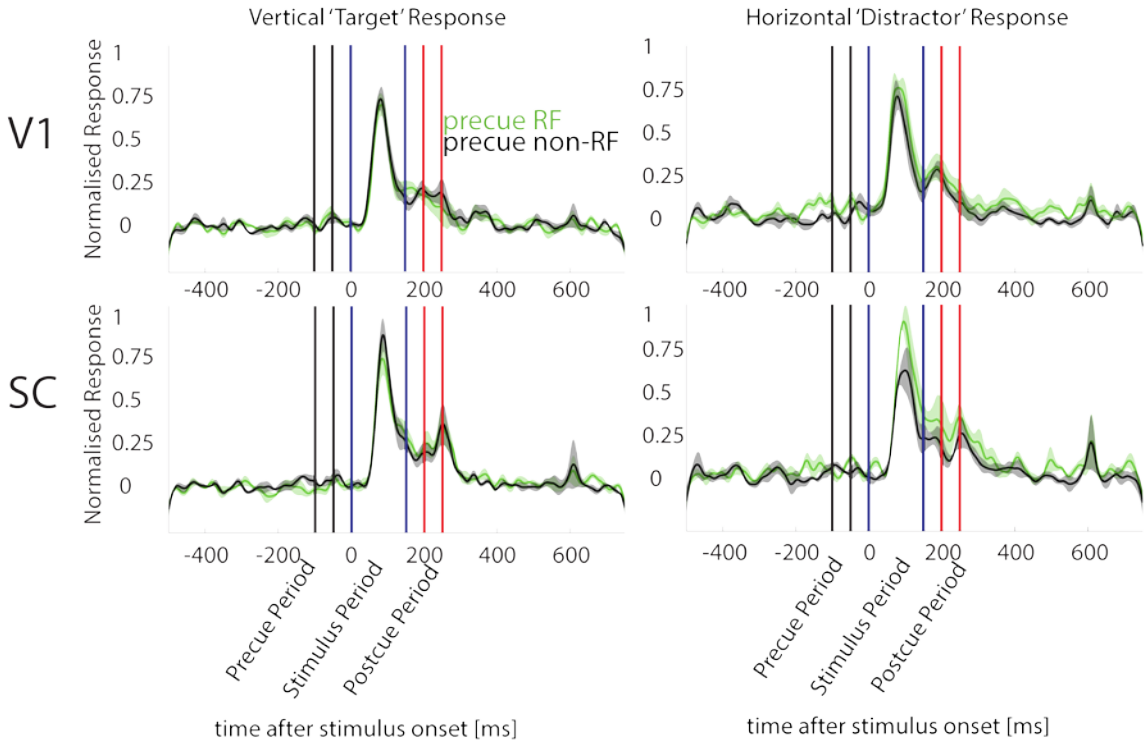

Figure 4-19. Average Normalised Firing Rates for the Visual Stimuli in Mouse V1 and SC Pre-cue RF vs Pre-cue non-RF.

Population histograms for the two stimulus types (vertical [left] and horizontal [right] grating) for V1 (upper row) and SC (lower row) data. Green histograms show the pre-cue RF conditions. Black histograms show the pre-cue non-RF conditions. X-axis shows time relative to stimulus onset (time 0). Y-axis shows normalised activity. The different cuing, and stimulus periods are shown by vertical lines, demarcating onset and offset respectively. Solid lines of the histograms show means, shaded areas show S.E.M.

4.3.1.2.1.1 Quantitative Analysis of Mouse Spiking Data

In V1 a significant main effect of time window was found in all contacts, (n=12/12, $p<0.001$, ANOVA). Moreover, 7/12 of the contacts showed a significant effect of grating type ($p<0.001$). 3/12 of the contacts exhibited a significant effect of cuing condition ($p<0.05$). 8/12 contacts showed a significant interaction between the grating type * the time window ($p<0.05$). A single contact showed a significant cue condition and time

window interaction ($p<0.05$). Finally, grating type and cuing condition caused a significant interaction in one contact ($p<0.05$). An example of a single neuron response in mouse V1 in the experiment is shown below (Figure 4-20).

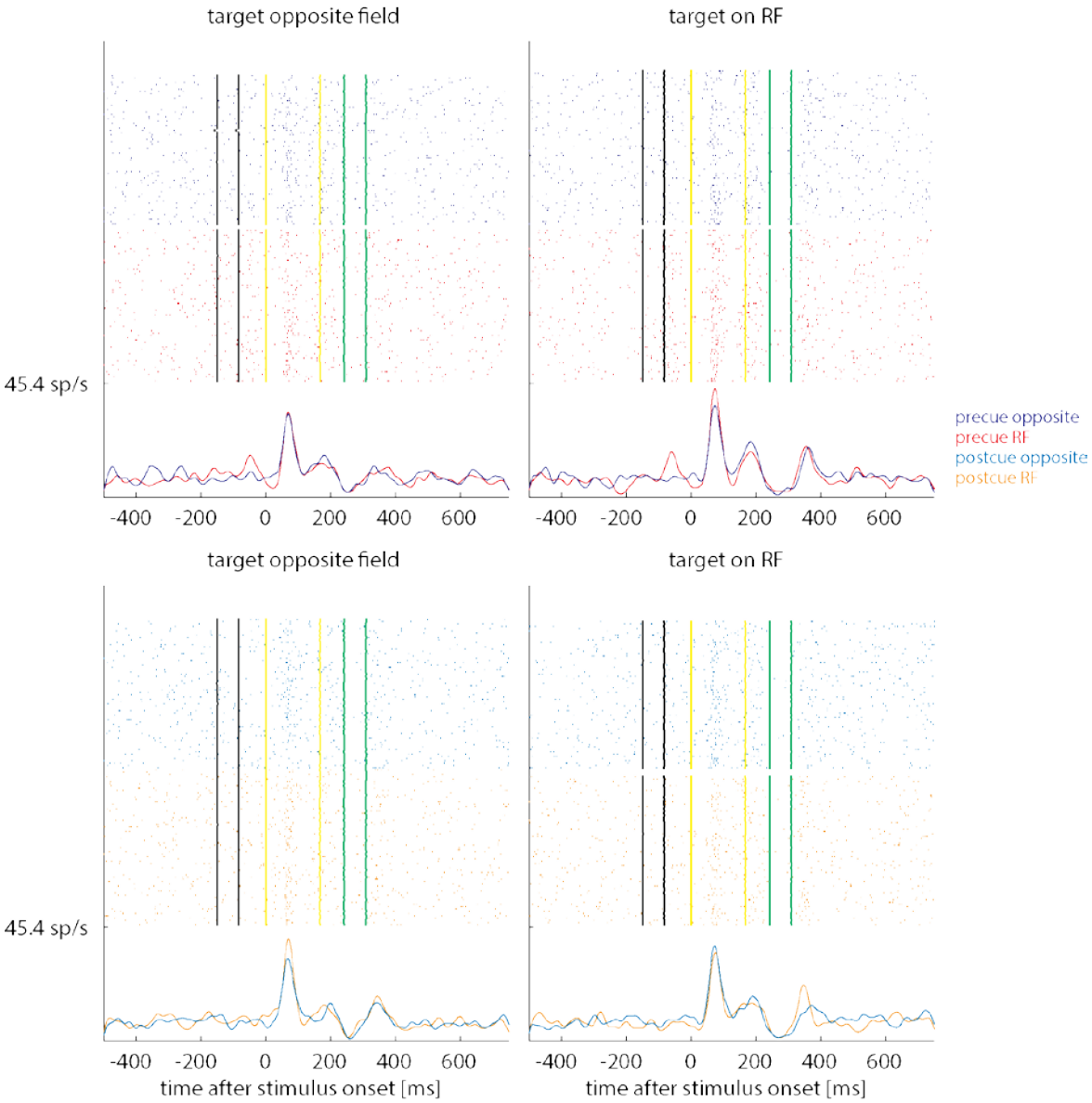

Figure 4-20. Raster Plots and Peristimulus Time Histograms for an Example Neuron in Mouse V1

Raster plots (upper panels) and histograms (lower panels) for the two grating types (horizontal [left] and vertical [right] grating) for a V1 neuron. Red ticks/trace equate to pre-cue RF condition, dark blue ticks/trace equate to pre-cue non-RF condition, orange ticks/trace equate to post-cue RF condition, light blue ticks/trace equate to post-cue non-

RF condition. X-axis shows time relative to stimulus onset (time 0). The different cuing, and stimulus analysis periods are shown by vertical lines, demarcating precue onset and offset (black), stimulus onset and offset (yellow), post-cue onset and offset (green) respectively. Solid lines of the histograms show means.

4.3.1.2.1.2 Mouse V1 Spiking Data

Firing rates of mouse population V1 data significantly depended on grating type and time window analysed. The main effects and the interactions between different factors are summarised in Table 4-5. Significant interactions occurred between grating type and time window. The latter is expected, as grating stimulus effects would only expected during the stimulus time period (if at all).

Table 4-5. Repeated Measures Mixed Model Multi Factor ANOVA for the Population of Multiunit Spiking Activity in Mouse V1

Term	FStat	DF1	DF2	pValue
Cuing Cnd	0.468	3	352	0.704
Grating Type	23.206	1	352	<0.001
Time Window	454.9	3	352	<0.001
Cuing Cnd*Grating Type	0.146	3	352	0.931
Cuing Cnd*Time Window	0.108	9	352	0.999
Grating Type*Time Window	15.872	3	352	<0.001
Grating Type*Cuing Cnd*Time Window	0.0819	9	352	0.999

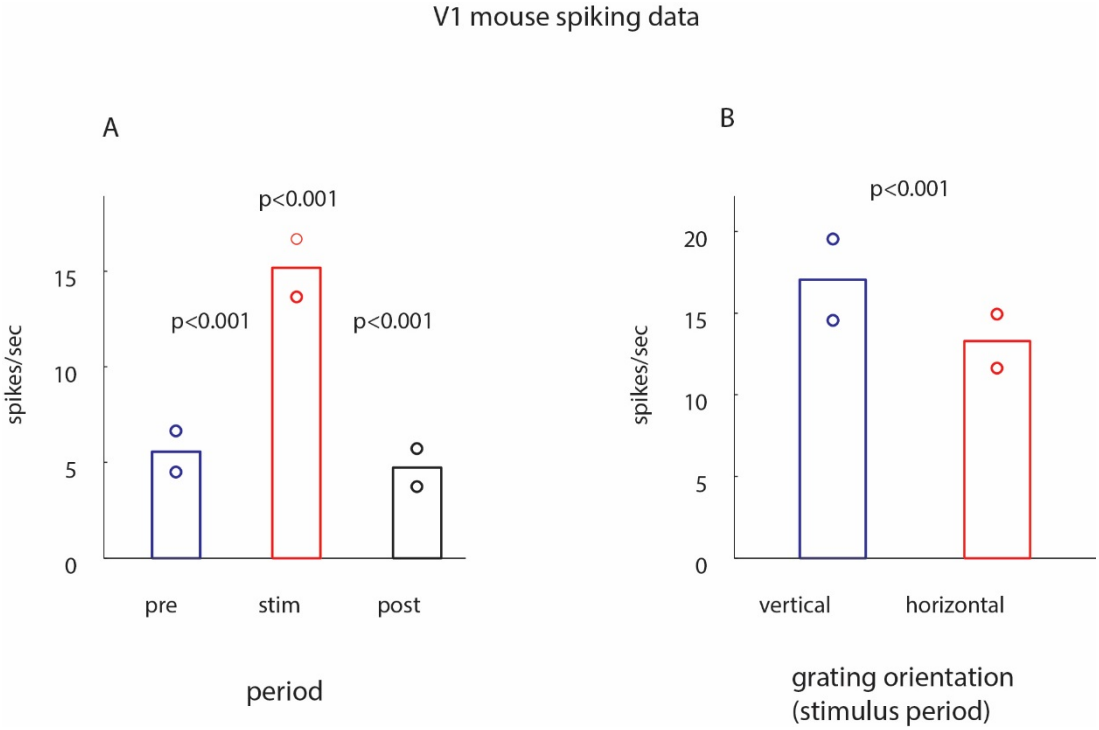

Figure 4-21. Comparison of Firing Rates for the different time periods and the two grating orientations.

A. Mean firing rates for the population of V1 cells, during the different time periods (pre-cue [pre], stimulus [stim], and post-cue [post]). **B.** Mean firing rates for the population of V1 cells for the two different gratings, measured during the stimulus time period. P-values indicate FDR corrected pair wise differences (Wilcoxon Signed Rank test). Bars show mean activity, associated circles indicate 95% confidence intervals.

Firing rates in mouse V1 were largest during the stimulus period, and smallest during the post-cue period (Figure 4-21A). Vertical gratings resulted in significantly higher firing rates than horizontal gratings in the mouse V1 data (Figure 4-21B).

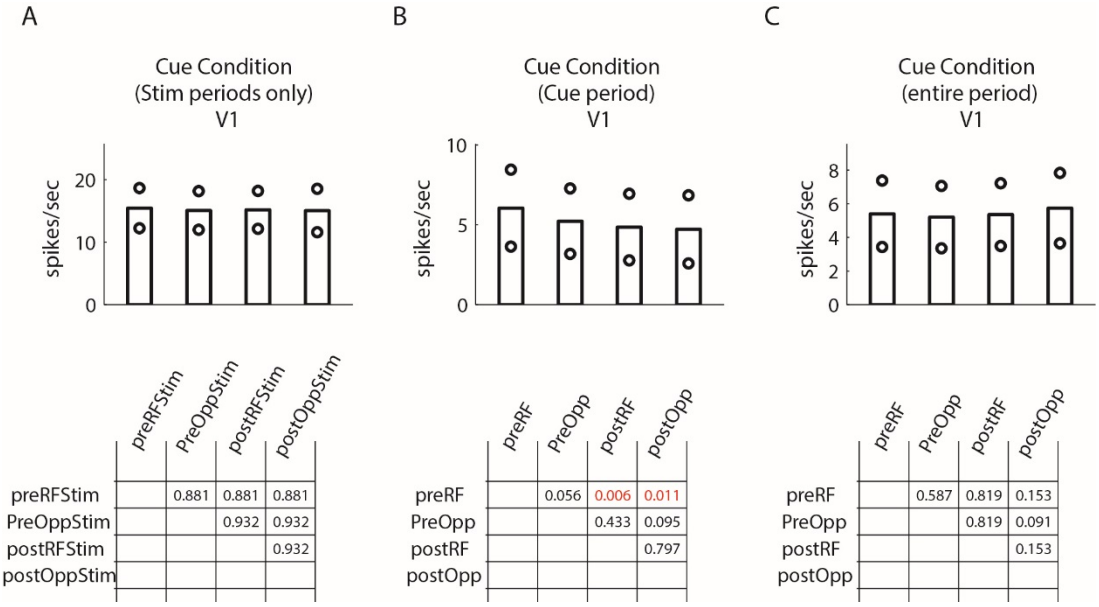

Figure 4-22. Comparison of Spiking Activity for the Cuing Conditions in Different Time Periods Averaged Over Grating Orientations for the Mouse V1 Data.

A. Spiking activity for the population of mouse V1 cells, during the stimulus time period for the 4 different cuing conditions (pre-cue RF [preRFStim], pre-cue opposite [preOppStim], post-cue RF [postRFStim], post-cue opposite [postOppStim]). **B.** Spiking activity during the cuing time periods for the 4 different cuing conditions (pre-cue [preRF], pre-cue opposite [preOpp], post-cue RF [postRF], post-cue opposite [postOpp]). **C.** Spiking activity during the entire time period (from pre-cue on until post-cue off) for the four different cuing conditions (pre-cue [preRF], pre-cue opposite [preOpp], post-cue RF [postRF], post-cue opposite [postOpp]). Tables below each subplot indicate pair wise differences (FDR corrected p-values based on Wilcoxon Signed Rank test). Bars show mean spiking activity, associated circles indicate 95% confidence intervals.

The different cuing conditions had no effect on the stimulus (grating) induced activity. However, significant differences were found for the different cueing periods, whereby post-cue periods showed lower responses than pre-cue RF periods ($p<0.05$ FDR corrected, Figure 4-22B). No other differences were found in the mouse V1 spiking data. There was

also a trend for pre-cue RF responses to be larger than pre-cue non-RF responses (p=0.056 adjusted FDR corrected, Figure 4-22B).

4.3.1.2.1.3 Mouse SC Spiking Data

Significant effects of time window were found in all contacts, (n=5/5, $p<0.001$, ANOVA). 3/5 contacts showed a significant effect of grating type on firing rates ($p<0.05$). Cuing conditions never had a significant main effect on firing rates. Significant interactions for grating type * time window were found in 3/5 contacts ($p<0.05$). One contact showed a significant interaction between cuing conditions and time window ($p<0.05$). One contact showed a significant interaction between grating type and cuing condition ($p<0.05$). An example neuronal response for spiking in mouse SC is shown below (Figure 4-23).

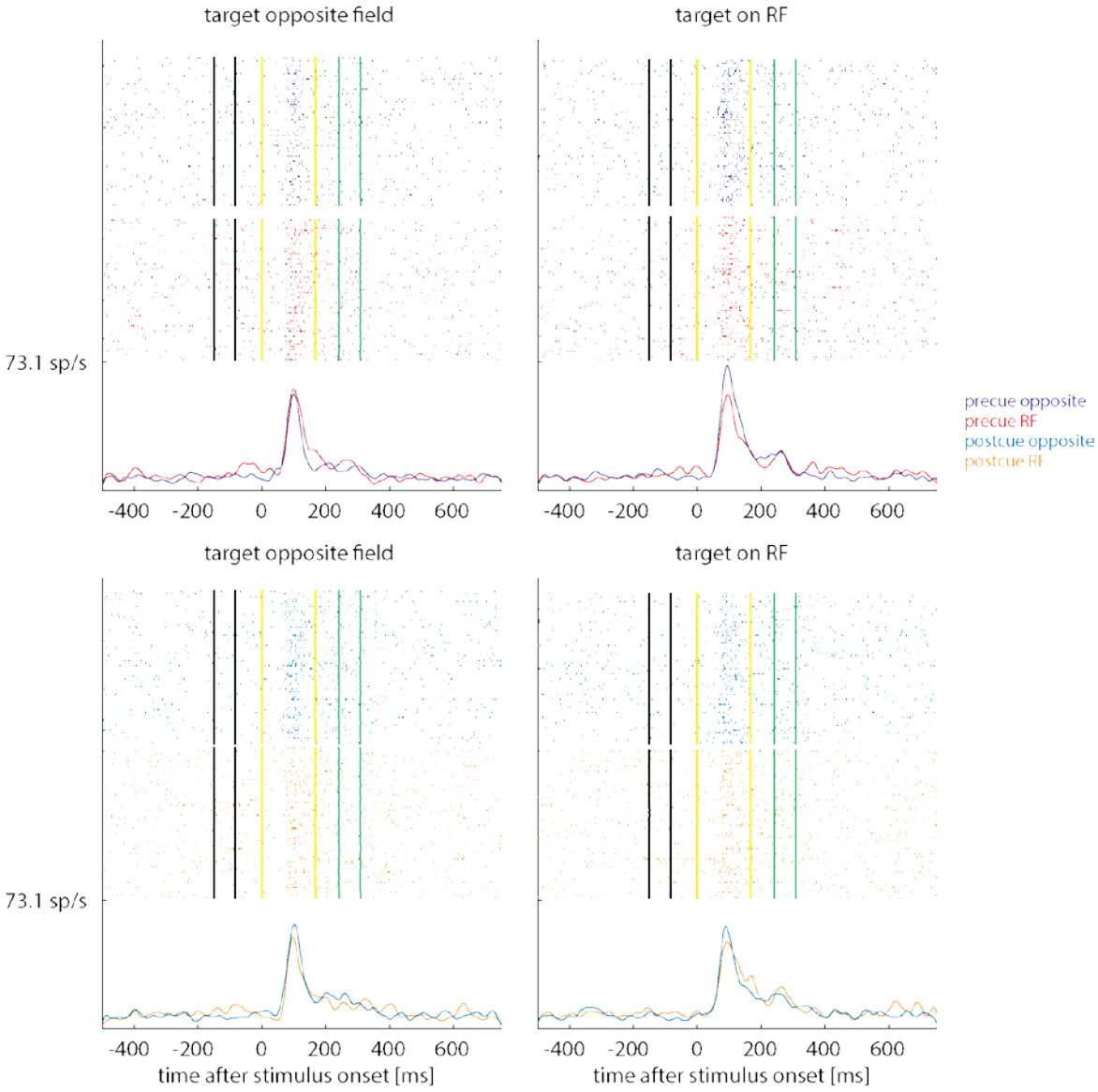

Figure 4-23. Raster Plots and Peristimulus Time Histograms for an Example Neuron in Mouse SC

Raster plots (upper panels) and histograms (lower panels) for the two grating types (horizontal [left] and vertical [right] grating) for a SC neuron. Red ticks/trace equate to pre-cue RF condition, dark blue ticks/trace equate to pre-cue non-RF condition, orange ticks/trace equate to post-cue RF condition, light blue ticks/trace equate to post-cue non-RF condition. X-axis shows time relative to stimulus onset (time 0). The different cuing, and stimulus analysis periods are shown by vertical lines, demarcating precue onset and offset (black), stimulus onset and offset (yellow), post-cue onset and offset (green) respectively. Solid lines of the histograms show means.

The main effects and interactions at the population level are summarised in Table 4-6. Significant interactions occurred between grating type and time window, similar to what was found in the mouse V1 spiking data.

Table 4-6. Repeated Measures Mixed Model Multi Factor ANOVA for the Population of Multiunit Spiking Data in Mouse SC

Term(Factor)	FStat	DF1	DF2	pValue
Cuing Cnd	0.293	3	129	0.830
Grating Type	8.129	1	129	0.005
Time Window	381.01	3	129	<0.001
Cuing Cnd*Grating Type	0.694	3	129	0.556
Cuing Cnd*Time Window	0.354	9	129	0.954
Grating Type*Time Window	4.204	3	129	0.007
Grating Type*Cuing Cnd*Time Window	0.695	9	129	0.712

Firing rates of mouse population SC data significantly depended on grating type and time window analysed. The main effects and the interactions between different factors are summarised in Table 4-6. As for the mouse V1, significant interactions occurred between grating type and time window.

Firing rates in mouse SC were largest during the stimulus period, and smallest during the pre-cue period (Figure 4-24A). Vertical gratings resulted in significantly higher firing rates than horizontal gratings in the mouse SC (Figure 4-24B).

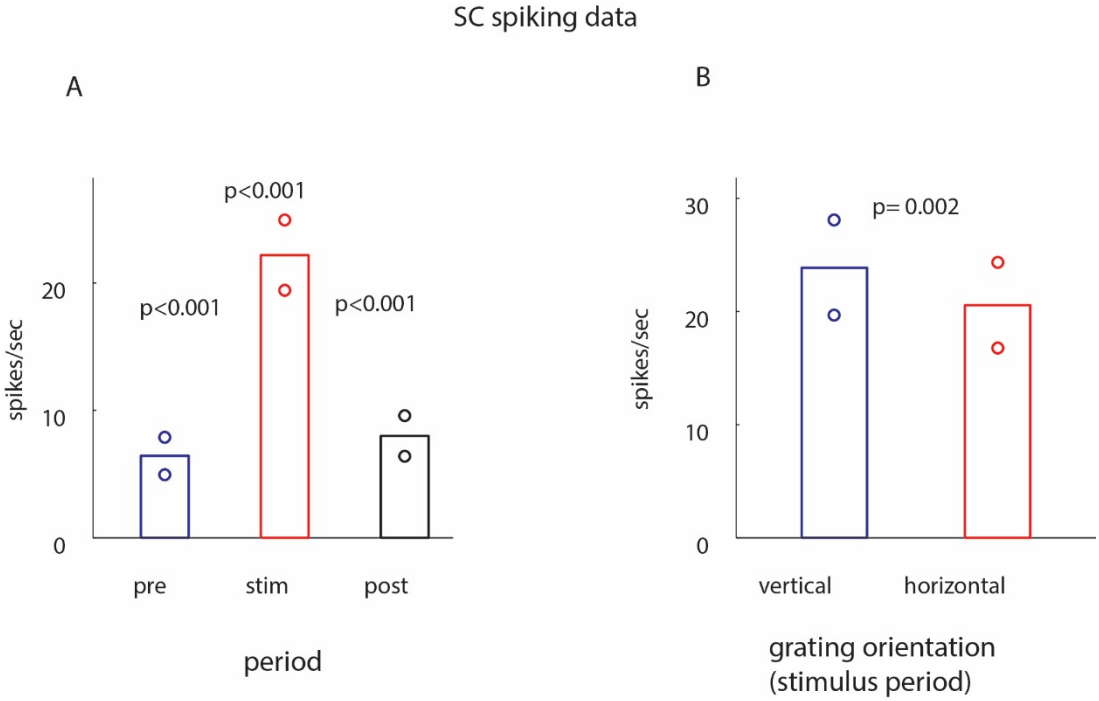

Figure 4-24. Comparison of Firing Rates for the different time periods and the two grating orientations.

A. Mean firing rates for the population of SC cells, during the different time periods (pre-cue [pre], stimulus [stim], and post-cue [post]). **B.** Mean firing rates for the population of SC cells for the two different gratings, measured during the stimulus time period. P-values indicate pair wise differences (FDR corrected and adjusted, Wilcoxon Signed Rank test). Bars show mean activity, associated circles indicate 95% confidence intervals.

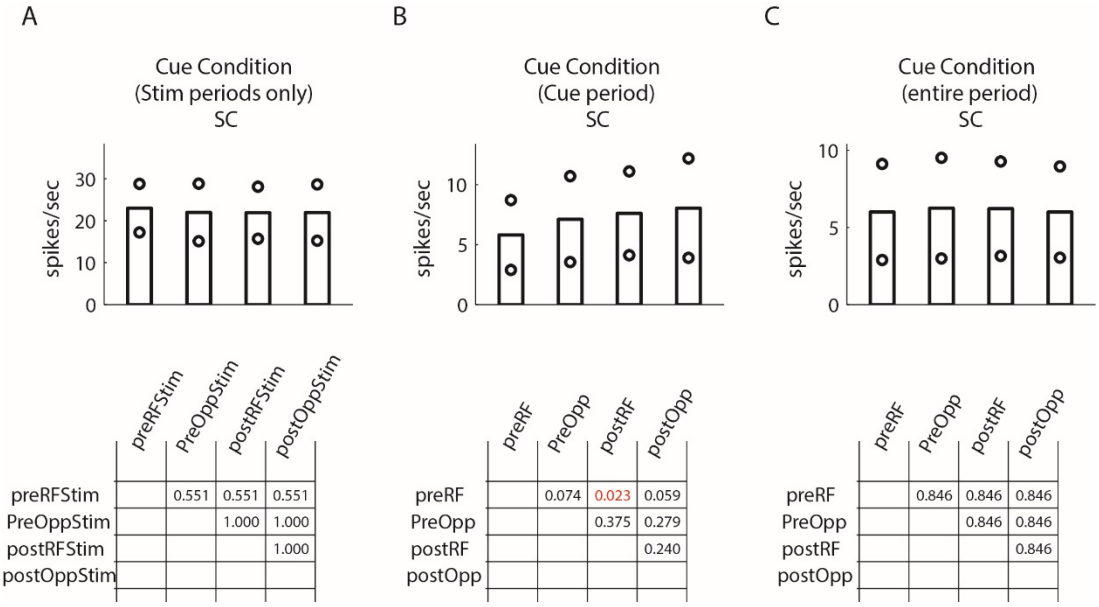

Figure 4-25. Comparison of Spiking Activity for the Cuing Conditions in Different Time Periods Averaged Over Grating Orientations for the Mouse SC Data.

A. Spiking activity for the population of mouse SC cells, during the stimulus time period for the 4 different cuing conditions (pre-cue RF [preRFStim], pre-cue opposite [preOppStim], post-cue RF [postRFStim], post-cue opposite [postOppStim]). **B.** Spiking activity during the cuing time periods for the 4 different cuing conditions (pre-cue [preRF], pre-cue opposite [preOpp], post-cue RF [postRF], post-cue opposite [postOpp]). **C.** Spiking activity during the entire time period (from pre-cue on until post-cue off) for the 4 different cuing conditions (pre-cue [preRF], pre-cue opposite [preOpp], post-cue RF [postRF], post-cue opposite [postOpp]). Tables below each subplot indicate pair wise differences (FDR corrected and adjusted p-values based on Wilcoxon Signed Rank test). Bars show mean spiking activity, associated circles indicate 95% confidence intervals.

The different cuing conditions had no effect on the stimulus (grating) induced activity. Significant differences were found for the different cueing periods, whereby pre-cue RF conditions resulted in lower activity than post-cue RF conditions (Figure 4-25B), and a trend of pre-cue RF conditions to be smaller than the pre-cue non-RF and the post-cue

non-RF condition (for adjusted FDR corrected p-values see Figure 4-25B). No other differences were found in the mouse SC spiking data.

4.3.1.2.2 Multiunit Activity Envelope (MUAe) Data

The multiunit channels used for the MUAe analysis were identical to those used for the spiking data (V1: n=12, SC: n=5), and the analysis was done in an identical manner as described above in relation to the macaque data.

4.3.1.2.2.1 General Effects at the Single Channel Level

To test whether different forms of (pre/post)-cuing and grating (vertical/horizontal) conditions affected the single channel MUAe activity, a multi-factor 2x4x4 ANOVA was used.

The dependant variable was the averaged normalised activity in single trials over the following time windows: pre-cue (100ms-50m before stimulus onset), stimulus (0-150ms after stimulus onset), and post-cue (50ms-100ms after stimulus offset) periods. 40ms offsets were added to all of these to account for visual response latencies.

In V1 the response depended on the factor time window in all contacts, (n=12/12, $p<0.001$, ANOVA). Moreover, 6/12 of the contacts showed a significant effect of grating type ($p<0.001$). 4/12 of the contacts exhibited a significant effect of cuing condition ($p<0.05$). 5/12 contacts had a significant interaction between the grating type and the time window ($p<0.05$). 3/12 contacts showed a significant cue condition * time window interaction ($p<0.05$). Finally, grating type and cuing condition caused a significant interaction in a single contact.

In the SC significant effects of time window were found on all contacts, (n=5/5, $p<0.001$, ANOVA). The grating type affected 4/5 contacts ($p<0.05$). The cuing conditions did not have a significant effects on any of the contacts. A significant interaction between time window and grating type was found for 2/5 contacts ($p<0.05$). No other significant interactions were found.

An example of a single trial for a particular recording in mouse V1 and SC with a 16 contact laminar electrode is shown below (Figure 4-26, Figure 4-27)

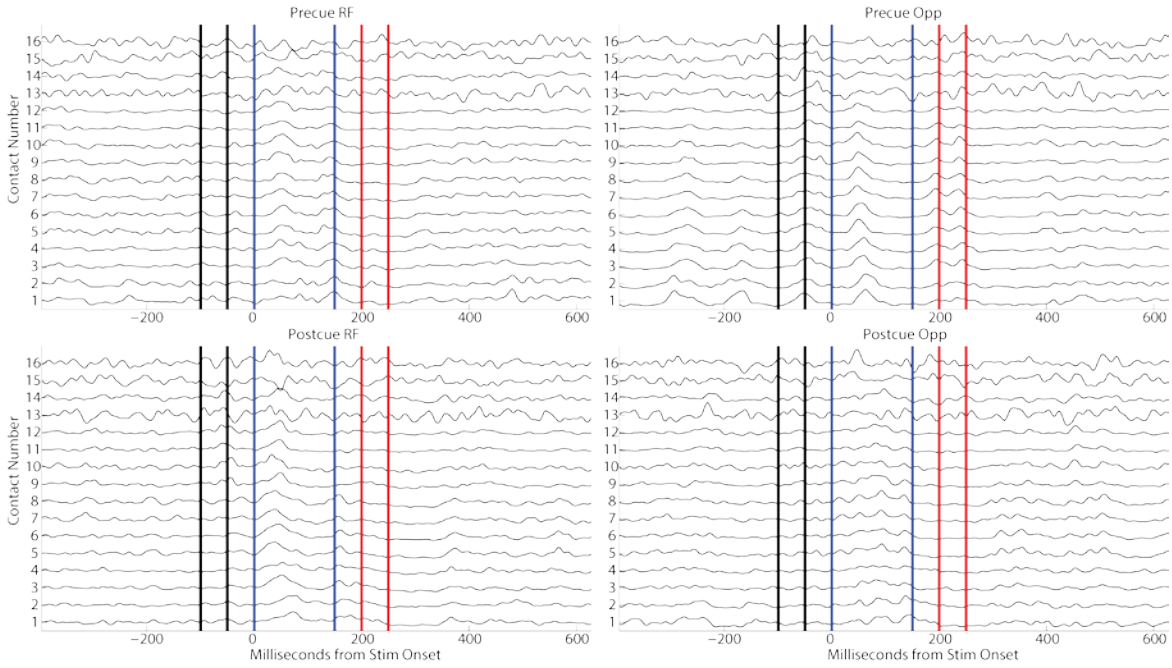

Figure 4-26. Raw Single Trial Example of MUAe Signal Recorded in Mouse V1 with a Laminar Electrode for the Vertical ‘Target’ Stimulus

Single trial traces for individual contacts along a laminar electrode in mouse V1. Contact number goes from most shallow to deepest. For this recording contact spacing was 50µm. Vertical lines represent trial time epochs, black-pre-cue period, blue-grating stimulus period, red-post-cue period. Each panel displays a different trail for each cuing condition.

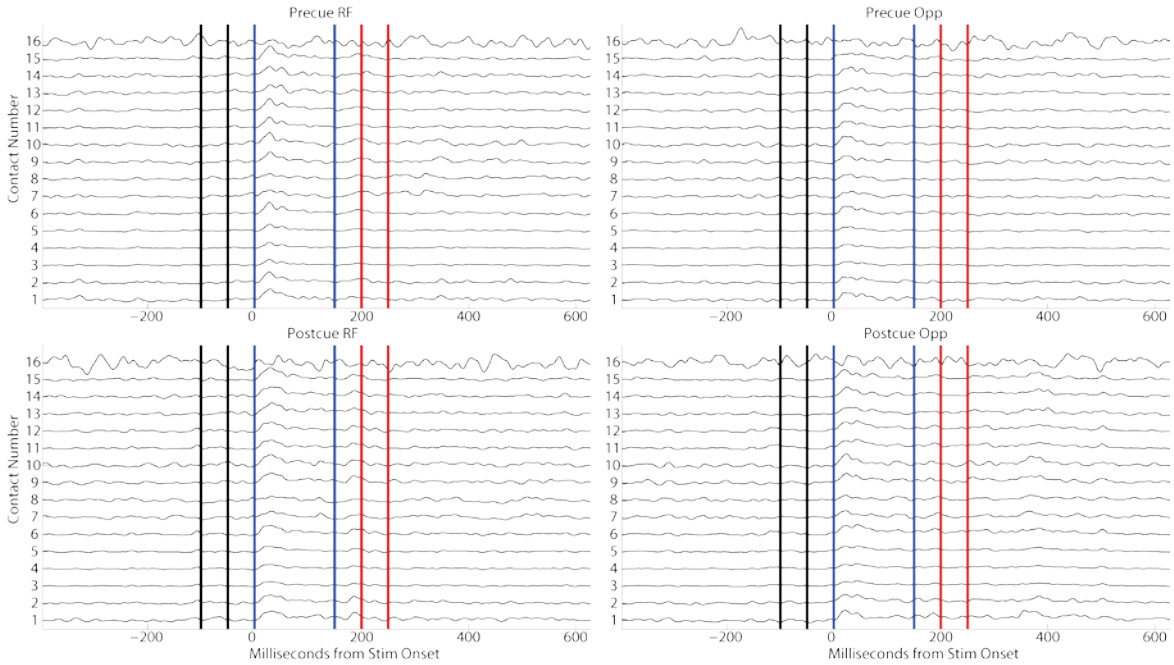

Figure 4-27. Raw Single Trial Example of MUAe Signal Recorded in Mouse SC with a Laminar Electrode for the Vertical 'Target' Stimulus

Single trial traces for individual contacts along a laminar electrode in mouse SC. Contact number goes from most shallow to deepest. For this recording contact spacing was 50µm. Vertical lines represent trial time epochs, black-pre-cue period, blue-grating stimulus period, red-post-cue period. Each panel displays a different trail for each cuing condition.

4.3.1.2.2.2 MUAe Population Histograms

Figure 4-28 shows how the different conditions affected MUAe population activity. In mouse V1 the presences of a pre-cue above the RF yielded slightly increased firing rates, when compared to pre-cue opposite or post-cue RF conditions (compare e.g. green and blue lines of the V1 data during the pre-cue window). No other obvious differences occurred. It is noteworthy that stimulus offset results in a strong response reduction below baseline activity for the V1 data set, which was not seen in any of the monkey data (and also did not occur for the SC data, see below).

Visual inspection of the mouse SC MUAe population histograms suggests that the different cueing conditions did not result in differential activity. The strong response suppression upon stimulus offset seen for the V1 data, was not present in the SC data. On

the contrary, stimulus offset induced a transient response on its own in the SC. Even though this appears to fall into the post-cue analysis time window, it cannot have been triggered by the post-cue as it was equally present on pre-cue trials.

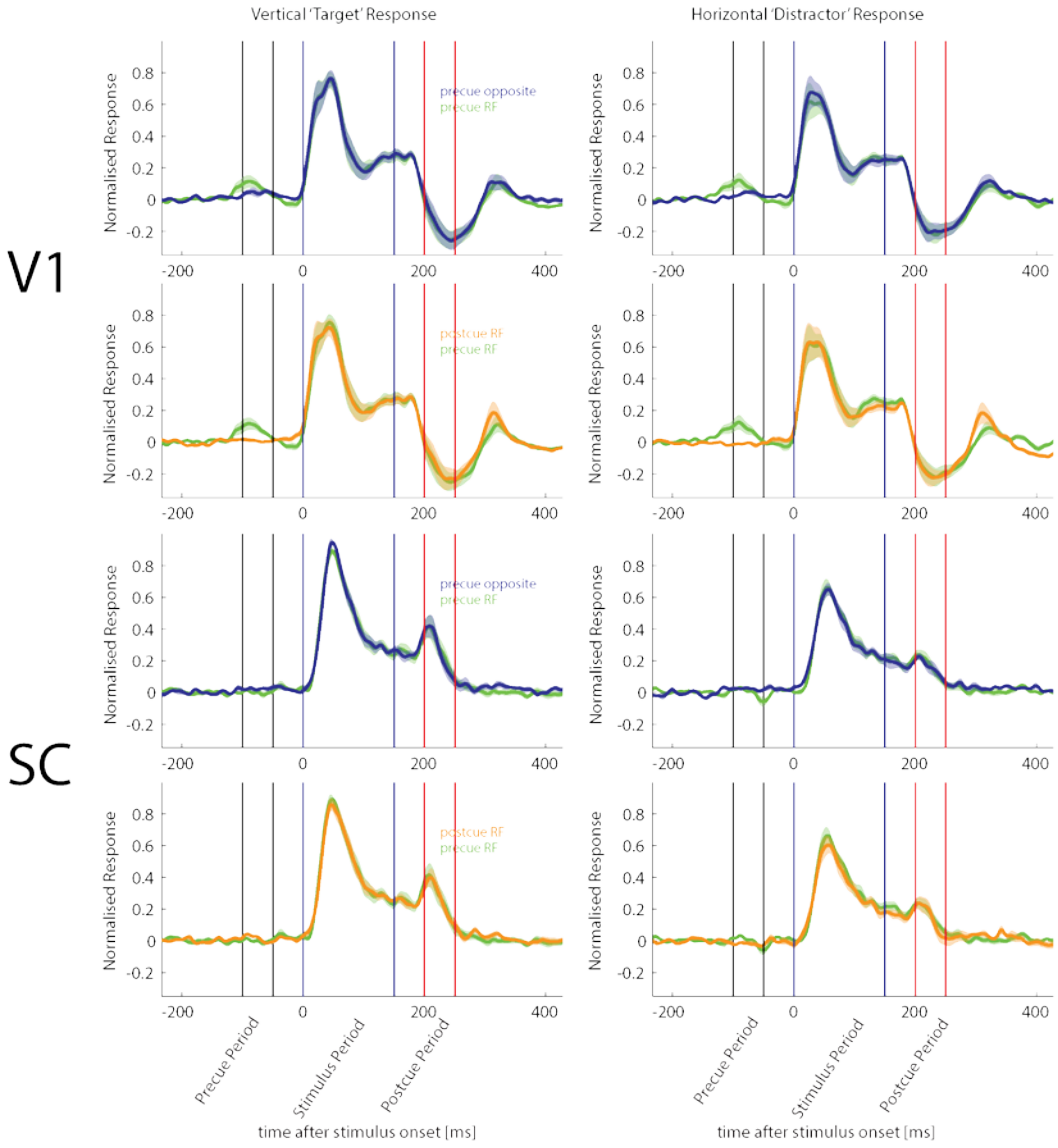

Figure 4-28. Comparison of Average Normalised MUAe Activity for the Bottom-Up Paradigm in Mouse V1 and SC.

Green-pre-cue presented in the RF location, blue-pre-cue presented in the non-RF location, orange-post-cue presented in the receptive field location. Vertical lines represent trial time epochs, black-pre-cue period, blue-grating stimulus period, red-post-cue period. Solid traces show population means, shaded areas show S.E.M.

4.3.1.2.2.3 Quantification of Mouse MUAe Response Differences

As previously, a mixed model multi-factor RM ANOVA was used to determine whether any of the conditions affected MUAe activity in the different response periods. The results of these analyses are shown in Table 4-7 (V1 data) and in Table 4-8 (SC data).

4.3.1.2.2.4 Mouse V1 MUAe Data

Table 4-7. Repeated Measures Mixed Model Multi Factor ANOVA for the MUAe Population of Mouse V1

Term	FStat	DF1	DF2	pValue
Cuing Cnd	3.133	3	369	0.025
Grating Type	6.197	1	369	0.013
Time Window	13.667	3	369	<0.001
Cuing Cnd*Grating Type	0.025	3	369	0.994
Cuing Cnd*Time Window	1.431	9	369	0.233
Grating Type*Time Window	2.775	3	369	0.09
Grating Type*Cuing Cnd*Time Window	0.079	9	369	0.970

In mouse V1, significant main effects were found for time window, cuing condition, and grating type. No other significant effects were found (Table 4-7).

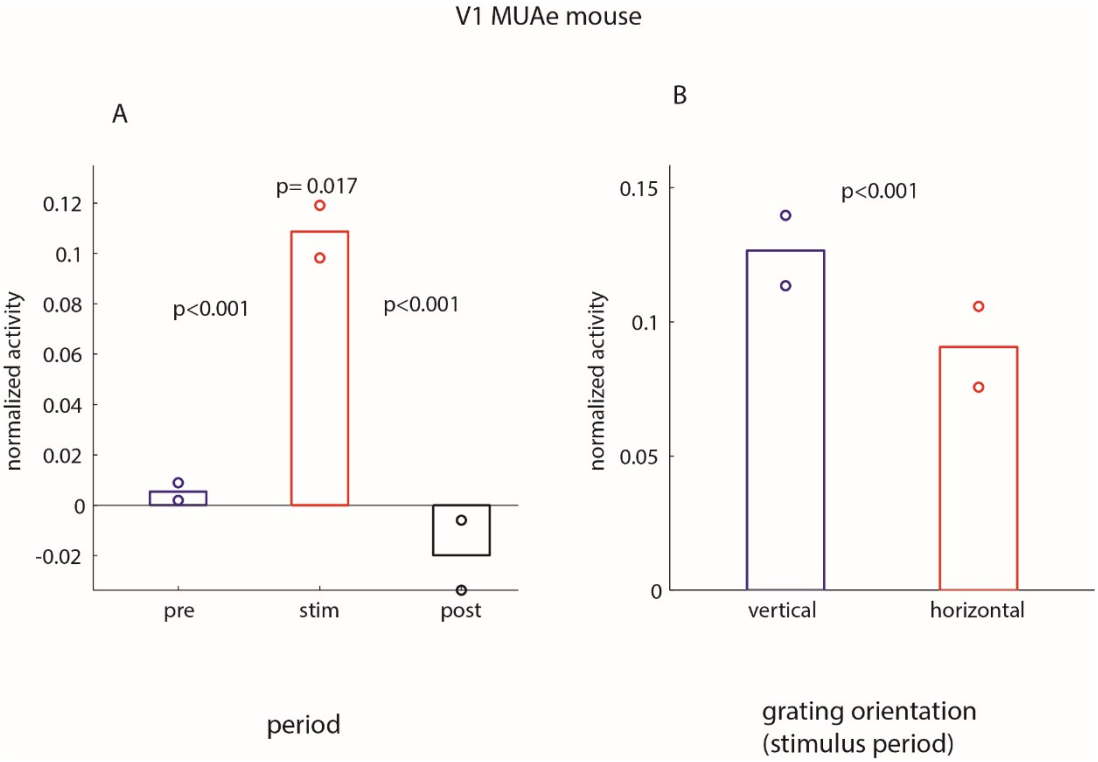

Figure 4-29. Comparison of V1 Normalised MUAe Activity for the Different Time Periods and the Two Grating Orientations.

A. Mean normalised MUAe activity for the population of mouse V1 cells, during the different time periods (pre-cue [pre], stimulus [stim], and post-cue [post]). **B.** Mean normalised MUAe activity for the population of mouse V1 cells for the two different gratings, measured during the stimulus time period. P-values indicate FDR corrected pair wise differences (Wilcoxon Signed Rank test). Bars show mean activity, associated circles indicate 95% confidence intervals. Middle p-value in A arises from the comparison between pre- and post-cue activity. The other p-values arise from the comparison between neighbouring bars.

Figure 4-29A shows that all pairwise comparisons for the different time periods were significant, when averaged across cuing conditions and grating types. As already outlined when describing the MUAe population histograms, in V1 the activity is reduced below baseline during the post-cue period, but this was induced by the temporal proximity of stimulus (grating) offset. Moreover, increased activity occurred for vertical grating responses, when compared to horizontal grating responses (Figure 4-29B). The differences between cuing conditions are shown in Figure 4-29. Even though the mixed model

ANOVA revealed a significant main effect of cuing condition, this was only significant in the post-hoc analysis when analysing the whole time period (see Figure 4-30C and associated table). Pre-cue opposite RF conditions resulted in significantly higher activity than post-cue conditions (for additional details see the tables in Figure 4-30).

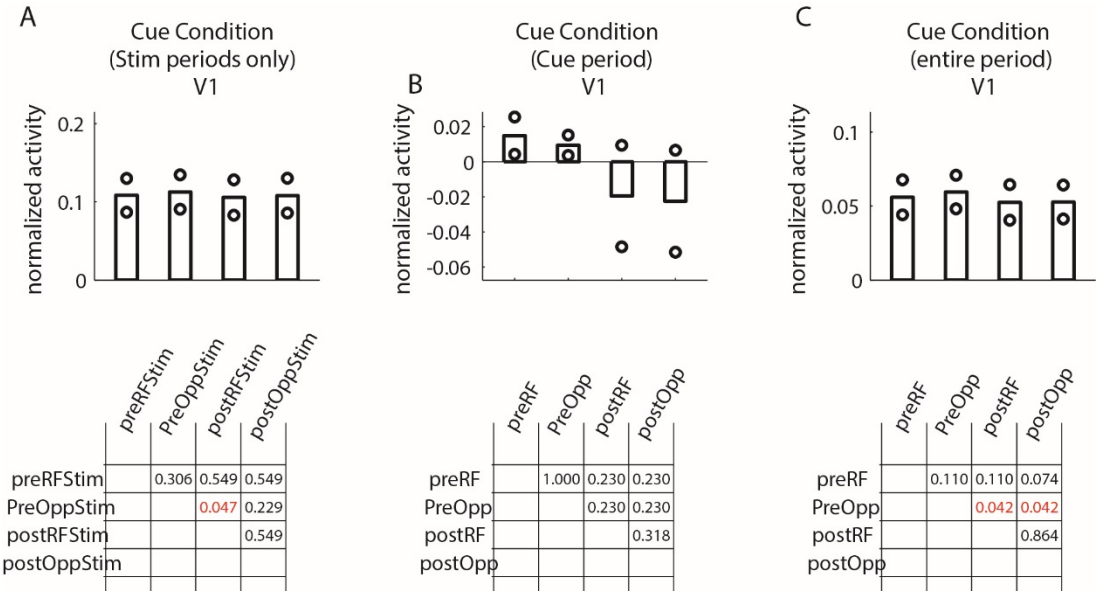

Figure 4-30. Comparison of Normalised MUAe Activity for the Cuing Conditions in Different Time Periods Averaged Over Grating Orientations for the Mouse V1 Data.

A. Normalised MUAe activity for the population of V1 channels, during the stimulus time period for the 4 different cuing conditions (pre-cue RF [preRFStim], pre-cue opposite [preOppStim], post-cue RF [postRFStim], post-cue opposite [postOppStim]). **B.** Normalised MUAe activity during the cuing time periods for the 4 different cuing conditions (pre-cue [preRF], pre-cue opposite [preOpp], post-cue RF [postRF], post-cue opposite [postOpp]). **C.** Normalised MUAe activity during the entire time period (from pre-cue on until post-cue off) for the 4 different cuing conditions (pre-cue [preRF], pre-cue opposite [preOpp], post-cue RF [postRF], post-cue opposite [postOpp]). Tables below each subplot indicate pair wise differences (p-values based on Wilcoxon Signed Rank test, FDR corrected and adjusted). Bars show mean spiking activity, associated circles indicate 95% confidence intervals.

4.3.1.2.2.5 Mouse SC MUAe Data

Table 4-8. Repeated Measures Mixed Model Multi Factor ANOVA for the MUAe Population Activity of Mouse SC

Term	FStat	DF1	DF2	pValue
Cuing Cnd	0.3454	3	145	0.792
Grating Type	0.837	1	145	0.361
Time Window	24.346	3	145	<0.001
Cuing Cnd*Grating Type	0.108	3	145	0.954
Cuing Cnd*Time Window	0.274	9	145	0.843
Grating Type*Time Window	9.594	3	145	0.002
Grating Type*Cuing Cnd*Time Window	0.1886	9	145	0.903

In the mouse SC significant effects occurred for time window and for grating type, and an interaction between the two. No other effects were found. These effects are further delineated in Figure 4-31 and Figure 4-32. Figure 4-31A shows that all pairwise comparisons for the different time periods were significant, when averaged across cuing conditions and grating types. Increased activity occurred for vertical grating responses, when compared to horizontal grating responses (Figure 4-31B), similar to what was found for V1 mouse data.

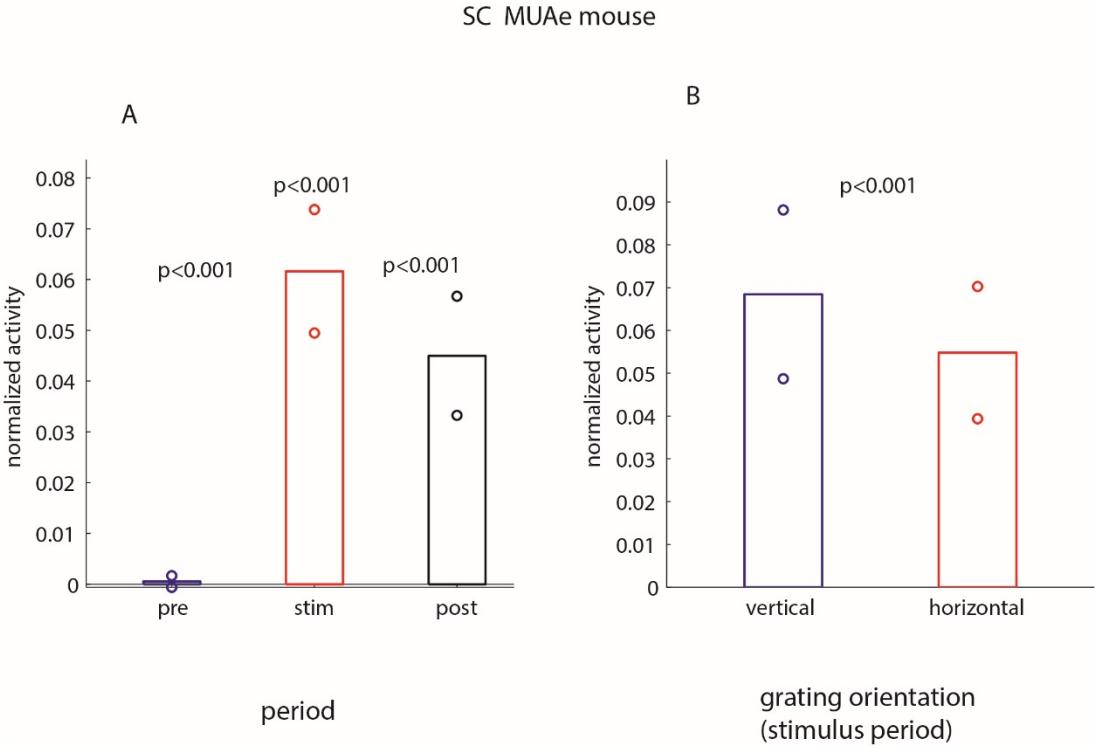

Figure 4-31. Comparison of SC Normalised MUAe Activity for the Different Time Periods and the Two Grating Orientations.

A. Mean normalised MUAe activity for the population of mouse SC channels, during the different time periods (pre-cue [pre], stimulus [stim], and post-cue [post]). **B.** Mean normalised MUAe activity for the population of mouse SC cells for the two different gratings, measured during the stimulus time period. P-values (FDR corrected and adjusted) indicate pair wise differences (Wilcoxon Signed Rank test). Bars show mean activity, associated circles indicate 95% confidence intervals. Middle p-value in A arises from the comparison between pre- and post-cue activity. The other p-values arise from the comparison between neighbouring bars.

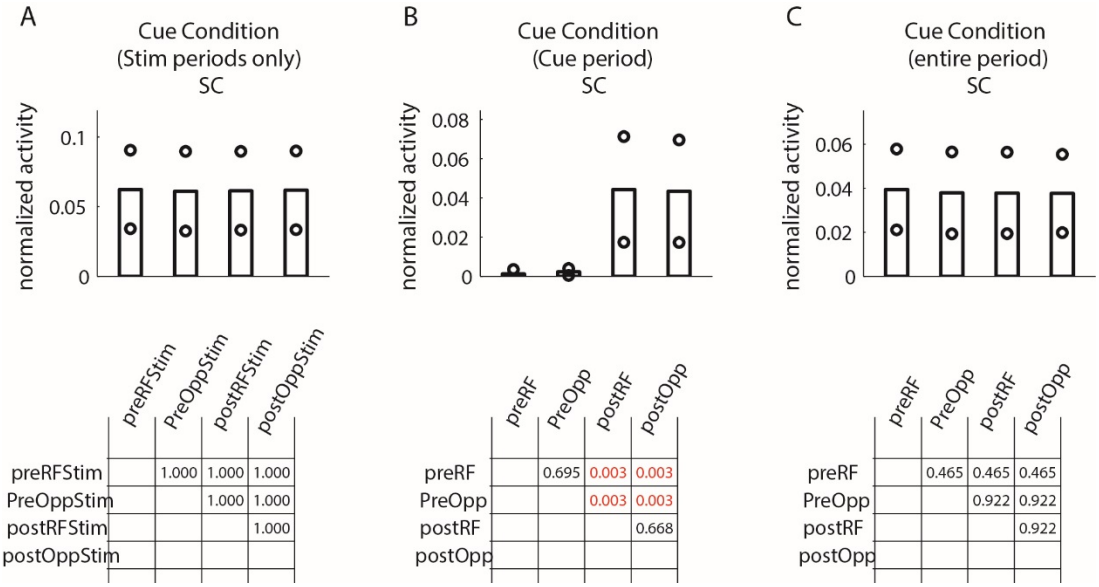

Figure 4-32. Comparison of Normalised MUAe Activity for the Cuing Conditions in Different Time Periods Averaged Over Grating Orientations for the Mouse SC Data.

A. Normalised MUAe activity for the population of SC channels, during the stimulus time period for the 4 different cuing conditions (pre-cue RF [preRFStim], pre-cue opposite [preOppStim], post-cue RF [postRFStim], post-cue opposite [postOppStim]). **B.** Normalised MUAe activity during the cuing time periods for the 4 different cuing conditions (pre-cue [preRF], pre-cue opposite [preOpp], post-cue RF [postRF], post-cue opposite [postOpp]). **C.** Normalised MUAe activity during the entire time period (from pre-cue on until post-cue off) for the 4 different cuing conditions (pre-cue [preRF], pre-cue opposite [preOpp], post-cue RF [postRF], post-cue opposite [postOpp]). Tables below each subplot indicate pair wise differences (p-values based on Wilcoxon Signed Rank test). Bars show mean spiking activity, associated circles indicate 95% confidence intervals.

Figure 4-32 shows that post-cue conditions resulted in higher activity during the post-cue period than pre-cue conditions. However, this was likely induced by the stimulus ‘off’ response, which occurred during the post-cue analysis period (see e.g. Figure 4-28).

4.3.1.2.3 LFP Matching Pursuit Analysis

To compare mouse LFP data the macaque data, LFPs were also analysed using the matching pursuit toolbox. Probably due to the small sample size, no trends or significant effect emerged. Therefore this paper does not show or discuss these data any further, as additional data would be required to gain meaningful insights.

4.3.1.2.4 Summary of Observable Effects in the Mouse

In general the mouse electrophysiological data was affected in some part by the different experimental conditions in the BU attentional task. However the effects observed were less noticeable than those seen in the macaque. Within both V1 the SC there an observable bias for response to different gratings. Specifically there was an increased response for the vertical grating.

When summarising the effects of pre-cuing there were differential effects in V1. While there was no difference seen in the spiking data, the MUAe showed that there was an increase in activity in pre-cue non-RF against post-cue conditions.

The effects seen in mouse SC were less pronounced than that seen in V1. Precuing in both the spiking and MUAe had no noticabe effect. However there was a trend foractivity in theafter the stimulus offset to be higher than that before stimulus onset.

Taken together, these results show that pre-cuing causes differential effects in both mouse V1 and SC. However the effects seen are very small compared to those seen in the macaque.

4.4 Discussion

Bottom-up attention is deployed when an unexpected stimulus suddenly appears in an animal's sensory field, which might have behavioural relevance (Posner, 1980, Nakayama and Mackeben, 1989). This then can cause an overt orienting response which brings the stimulus into a better position for sensory evaluation. In this manner bottom-up attention and orienting are intrinsically linked. However these mechanisms do not necessarily need to be externalised (Posner, 1980). Here this paper investigates possible neuronal signatures of bottom-up attention trough electrophysiological recordings in primary visual cortex in both macaque and mouse as well as macaque V4 and mouse SC.

4.4.1 Macaque Data

The macaque V1 thresholded spiking data were not affected by the cuing conditions. This result is somewhat in contrast with the existing literature concerning top-down attentional processing. Previously, external cuing has been shown to increasing spike firing rates in response to a visual stimulus (Wang et al., 2015). This lack of effect may be due to a number of reasons. Firstly, the cuing location may have been too far away from the RF location to induce spiking activity in the recorded neurons themselves, and may also have been too far, to cause other types of direct local network interactions. However, this argument is not really supported by our MUAe or LFP data (see below). If attention was automatically drawn to the cuing location, its focus might have been outside the receptive fields, thus not affecting the stimulus response either. A recent paper (published shortly after I acquired my data set for the thesis) showed that the effects of cuing on V1 responses depended on stimulus novelty and task engagement (Wang et al., 2015). Thus, the lack of a behavioural engagement in the passive conditions in our data set, and/or the repeated stimulation, could have caused habituation, and thereby resulted in suppression of potential effects. While this is a possible explanation, it is countered by the apparent lack of significant differences in the data between the active and the passive condition, which differs from the results reported by Wang et al.

A main difference between our data and those reported by Wang et al. is the type of cuing used. We used a bar that was presented above the neuron's RFs, while they used an annulus which flashed briefly around the V1 RFs, generally inducing a spiking response on its own (see e.g. their figure 2). Thus, the different types of cues used could also have contributed to the differences seen. All these arguments are, however, somewhat moot in light of the effects seen in the MUAe data (discussed below).

In contrast to the V1 data, pre-cuing affected macaque V4 thresholded spiking data. The pre-cue RF condition triggered a response of its own in our data, but at the same time it resulted in decreased stimulus induced responses. Despite this decrease, the activity over the entire trial period was increased, even if compared to the post-cue RF conditions. This reduction of the stimulus induced response in V4 is reminiscent of the effects seen with centre-surround suppression (Sundberg et al., 2009) or attention being drawn to a location outside of the RF (Reynolds and Desimone, 2003, Reynolds and Chelazzi, 2004). Finally, it could also be related to adaptation (Vogels, 2016). The design of my experiment does

not allow to differentiate between these possibilities, and they could all have contributed to some extent.

In contrast to the thresholded spiking V1 data, significant effects of cuing conditions were found in the macaque V1 MUAe activity. Pre-cuing RF conditions significantly increased the activity for the pre-cue period, as well as over the entire analysis period (from pre-cue onset to post-cue offset). The discrepancy between MUAe and thresholded spiking may arise from the pool of neurons that contribute to the two signals. The thresholded spiking activity data is likely from a relatively modest neuronal pool size (I would estimate about 3-8 neurons), while the MUAe is derived from ensembles of neurons that reside with ~100-200um from the electrode contact. Assuming that ~120,000 neurons exist within $1mm^3$ of V1 cortex (O'Kusky and Colonnier, 1982), it would mean that 120-960 neurons contribute to the MUAe signal, i.e. at least 1-2 orders of magnitude more neurons contributing to MUAe than to the thresholded spiking activity. Rather small effects of pre-cuing might result in measurable differences when averaging over large populations (MUAe), but they might not be detectable when smaller populations are analysed. Assuming that noise in the data is uncorrelated, the signal-to noise ratio would increase with the square root of the sample size, i.e. 2 orders of magnitude more neurons would increase SNR by a factor of 10, and would strongly improve the ability to detect even small differences. The pre-cue RF induced enhancement in V1 MUAe data is somewhat similar to that reported for the above mentioned bottom-up attention V1 study (Wang et al., 2015), but it was restricted to the pre-cuing period and did not affect stimulus responses. This might be due to the repetition of stimuli, which Wang et al. have reported for their spiking data.

The results we found for the MUAe V4 data were somewhat similar to the MUAe V1 data, but the pre-cue RF induced effects in V4 were enhanced, and significant effects were also seen when analysing the stimulus induced responses. The enhanced cuing effects were most pronounced when analysing the entire response period (pre-cue on until post-cue off). Larger attentional effects in V4 than in V1 have been reported previously when top-down attention was directed to the receptive field locations in V1 (Roelfsema et al., 1998, Roberts et al., 2007) and V4 (Moran and Desimone, 1985, Luck et al., 1997). Here it is shown that similar differences arise with bottom up attention induction.

Despite these similarities in terms of activity increases over the entire response period, there were differences in responses, when analysing shorter time epochs. For V1 there was

no significant difference in the stimulus induced response for the different cuing conditions, while in V4 there was a marked decrease in the peak response to the stimuli, after a pre-cue above the RF. Given this, why does the response increase in both areas when averaged across the entire period? In V4 the pre-cue above the RF induced a strong response on its own, which is stronger than the suppression it causes for the stimulus response. In V1 and in V4 the increased activity during the pre-cue period for the pre-cue RF condition is larger than the increase in activity during the post-cue RF period, and thus the summed activity increases for both over the entire time period.

These results can be compared to human fMRI data, which used essentially the same cuing paradigm used here (Liu et al., 2005). In fact we copied their cuing paradigm, to determine how neuronal signatures of bottom-up attention relate to fMRI signals. The authors of the fMRI study argued that pre- and post-cue conditions would result in identical fMRI signals (which are sluggish and average over long time periods due to the slow response time of the blood-oxygen-level dependent (BOLD) signal), unless cuing invoked some automatic attentional processing. The authors (Liu et al., 2005) found that in human cortex, pre-cueing altered responses in a graded manner across visual cortex, with virtually no effects (no increased BOLD signal) in area V1 and increasingly larger effects with cortical hierarchy (V1<V2<V3<V4). This mirrors the difference seen here. Despite this, the reduction in stimulus induced firing V4 with pre-cue RF, is hardly an expected signature of automatic attentional processing, even if the overall V4 activity increased, roughly mirroring the results in BOLD signal changes. Given the overall results from our V1 and V4 data, I would caution about the use of the word attention. Many of the effects seen might as parsimoniously be described in terms of local network effects including non-classical receptive field stimulation, normalization, and response habituation.

The latter is also supported by the LFP power spectra in V1. Pre cuing above the RF caused a distinct increase in power in the 20-30Hz band i.e. the beta and low gamma band. Increases in this frequency range these have been implicated with heightened top-down and bottom up attention (Fries et al., 2001, Buschman and Miller, 2007, Siegel et al., 2008). Despite this, the stimulus induced spectral power in these frequency bands was lower for the pre-cue RF condition, while it was enhanced in the alpha frequency band, a frequency band often associated with distractor suppression (Haegens et al., 2012). Thus, the stimulus induced spectral power, shows signatures opposite to those expected from ‘attentional’ processes (but see (Chalk et al., 2010)).

In V4 the LFP difference spectrograms showed somewhat different characteristics. The pre-cue RF itself triggered a large increase in spectral power across a wide frequency range (20-120Hz). This increase could be the forward drive to trigger bottom-up recruitment of attentional processing from higher cortical areas (Fries et al., 2001). During the stimulus, V4 spectral power was also reduced in the high gamma frequency range, compared to the other cuing conditions, and in the frequency bands below 40 Hz, with a notable reduction in the alpha frequency range (i.e. exactly the opposite to what was seen in V1). The traditional gamma frequency range (~40-60Hz) showed the least reduction, possibly a signature of the bottom-up attention induction.

Although bottom-up attentional processing is much less studied than top-down attentional processing at the electrophysiological level, some experiments have been performed using pop-out stimuli in multi stimulus displays. Here one stimulus has a different (more salient) colour to which the animal has to orient. Directing attention in this manner enhances visual activity in response to the salient stimulus within the receptive field. For the parietal cortex (area 7A) this response is highest when the salient stimulus is different from the surround stimuli (Constantinidis and Steinmetz, 2005). However in this area, cuing attention has also been shown to inhibit stimulus induced firing in the attended location (Steinmetz et al., 1994). Similar pop-out attentional studies have examined activity the frontal eye field (FEF). Here pop-out attentional priming increased neuronal responses to the salient stimulus, while inhibiting responses and increasing saccade latencies to the previously attended location through an inhibition of return. (Bichot and Schall, 2002). These brain regions are hierarchically higher than the macaque visual areas studied in this research. The effects seen in these higher areas might well, influence the activity as seen in V1 and V4 in my study through feedback connections.

4.4.2 Mouse Data

In the mouse visual areas cuing effects were limited. This is possibly a result of the small sample size.

In mouse V1, pre-cue RF conditions resulted in significantly larger responses than post-cue conditions for the cueing periods for the spiking and the MUAe data, which is qualitatively similar to the macaque data. Moreover, a slight trend for an increase in peak and sustained visual response occurred in the presence of a pre-cue vs a post-cue, but only

for the horizontal stimulus. This preference for stimuli of specific orientation could mean a number of things. Firstly, it could be that our sample size was too small to rule out the random sampling effects for stimulus orientation preference. Or it could be that within the small region of visual cortex sample, which tended to be in the upper lateral portion of the visual field, there is a tendency for gratings which are orientated parallel to the animals body length are preferentially processed for exogenous cuing. A similar type of stimulus/location specific processing has been shown previously to exist in the direct projections from the retina for looming stimuli (Yilmaz and Meister, 2013). A noticeable difference of the mouse V1 data was the pronounced response suppression after stimulus offset in the MUAe data. This response reduction resulted in overall decreased activity for post-cue conditions, as the post-cue presentation (even if above the RF) was not able to counter the reduction.

In comparison the trends in SC spiking and MUAe activity were different. Specifically, pre-cue RF and pre-cue opposite conditions resulted in lower activity than post-cue conditions. No differences were found for stimulus induced activities, which differs from work done in the macaque where exogenous peripheral cuing caused an increase in visual stimulus induced response (Ignashchenkova et al., 2004).

No differences were found for the SC activity when averaged across the entire response period. The only additional noticeable feature of the SC response, which occurred for all cuing conditions, was the marked sustained stimulus response, with a response offset enhancement, i.e. the opposite response to that seen in mouse V1. This may aid an animal in initiating short latency orienting response like saccades (Munoz et al., 1991), attentional deployment (Müller et al., 2005), stimulus orienting (Dean et al., 1986), or approach/avoidance mechanism (Sahibzada et al., 1986).

While pre-cue induced alterations of neuronal activity have been studied to some small extent in the macaque, virtually no meaningful comparison is possible to existing rodent literature. A few studies have used visually cues to inform behavioural choice responses or response locations to increase SC choice preferences and visually induced firing (Duan et al., 2015, Ngan et al., 2015). But these served rather different purpose, namely active decision making, and results can thus not be compared in a meaningful manner.

Chapter 5. Optogenetic Perturbation of Prefrontal Areas in Mouse and its Effect on Visual Related Activity and Bottom-up Attention

5.1 Introduction

So far the focus of this thesis has been on the anatomical segregation of different orienting behaviours in the mouse and the effect of bottom-up (BU) attentional signals on early visual processing. This final chapter expands on this, aiming to incorporate the role of prefrontal areas in this BU modulation. In Chapter 3, the differential connectivity strength of two prefrontal regions, the cingulate area (Cg) and motor cortex area 2 (M2), were described in terms of connectivity to subregions of the superior colliculus (SC) (medial vs lateral) and the rest of the brain. It was found that the Cg projected preferentially to the medial SC and regions involved in avoidance behaviours. Conversely, M2 projected preferentially to the lateral SC and regions involved in approach behaviours. Both regions do project to the primary visual cortex, which can be seen from this research and others (Miller and Vogt, 1984, Zhang et al., 2014). It is also known that these prefrontal regions produce signals which are able to modulate upcoming behavioural orienting and decisions in rodents, as described in Chapter 1.

The behavioural outputs for orienting behaviours and those seen in BU attention are very similar. Both can be elicited by temporally transient focal peripheral stimuli, which may or may not be behaviourally relevant. The briefness of such stimuli and their location in the visual field requires animals to reorient their sensory apparatus (e.g. eyes, pinnae, head) to better evaluate the stimuli for behavioural response. This action, by definition, is an orienting response which in higher primates is usually a saccade, but can also include head movements (Monteon et al., 2010). In rodents due to the lack of high density photoreceptor foci in the eye, this action brings the stimulus into the binocular field in the frontal/central visual field (Wallace et al., 2013). These behaviours almost always include a head or body movement (Dean et al., 1986, Sahibzada et al., 1986, Dean et al., 1988a). Therefore any region that is involved in orienting behaviours in the rodent may be involved in the underlying covert BU attentional behaviour that precede it. In fact stimulation of Cg neuron axon terminals in mouse V1 has been shown to increase neuronal responses and improve visual discrimination (Zhang et al., 2014).

The anatomical connectivity delineated in Chapter 3 and the results from Chapter 4 in BU modulation in V1, bring about the following question. Are the BU effects seen in V1 triggered (or modulated) by prefrontal areas? To investigate this, the same BU attentional paradigm as in Chapter 4 were used, but with optogenetically transfected animals. These mice were injected with channelrhodopsin 2 into the prefrontal control regions of Cg or M2. This then allowed for optogenetic activation of the transfected region during the presentation of the visual stimuli. Unfortunately, due to the time constraints of this thesis only a few animals were tested in this manner, and all of them were from the Cg injection cohort. The effects of stimulation on M2 region will have to be conducted at a future date.

5.2 Methodology

In general the methodologies utilised for viral injection have been described previously (see Chapter 2.1). Furthermore the experimental design for this section has also be described above in Chapter 4. This methodology section covers the specific procedures employed to analyse the effects of optogenetic stimulation of prefrontal regions in the mouse and their effect on activity in murine visual areas.

5.2.1 Efficacy of Optogenetic Transfection in Injected Regions

In order to explore the effects of optogenetic innervation of visual areas in the mouse through projections from higher cognitive areas a number of steps were taken. To test the efficacy of the optogenetic transfection before the implantation of a cranial window, test penetrations were conducted. This entailed sedating and headfixing the animal, and preforming a craniotomy as has been described previous in Chapter 2. Then a laminar electrode (Atlas Neuroenginering) was advanced into the area of prior transfection.

The region was stimulated with pulses of blue light from one of the previously stated light sources (see

Table 2-2). There were two interleaved conditions in this paradigm, one with light stimulation and one without any stimulation. The activity for each contact was data was collected and analysed as described above in section 2.6.

5.3 Results

12 laminar electrode recordings were performed in one animal. These were split into V1 (n=8) and SC recordings (n=4). The animal in question had been transfected with channel rhodopsin 2 under a calmodulin-dependent kinase II promotor with a yellow florescent protein marker (AAV5-CamKII-ChR2-eYFP). The virus was injected into the cingulate area (Cg) of mouse cortex and was left to express for 3 months prior to the start of recording. Further details of these procedures can be found in section 2.5.

5.3.1 Histology of AAV5 CAMKII Channelrhodopsin Animal

In order to verify the transfection of the experimental animal the brain was collected after the experiments were concluded. The brain was sectioned and examined under fluorescence microscopy to examine to the pattern of fibres. It was found that the injection location was centred over the Cg region, however there was some overlap into the M2 region (see Figure 5-1). It was interesting that within the viral injection site labelled neurons were not easily discernible. However labelled fibres were found in abundance.

The projection pattern to the recording sites was also investigated. The fibres found in V1 were concentrated in layer 1 and 6. However, there were fibres found throughout layers 4/5. This can be seen in the figures below (Figure 5-2, Figure 5-3). In general the labelling to V1 was light in comparison to the labelling seen with the SC.

The SC pattern of neuronal fibres was restricted to the intermediate and deep layers (Figure 5-3). Interestingly the medial/lateral bias observed in the previous chapter was not as obviously shown here. This may be due to the injection site overlap in the prefrontal cortex.

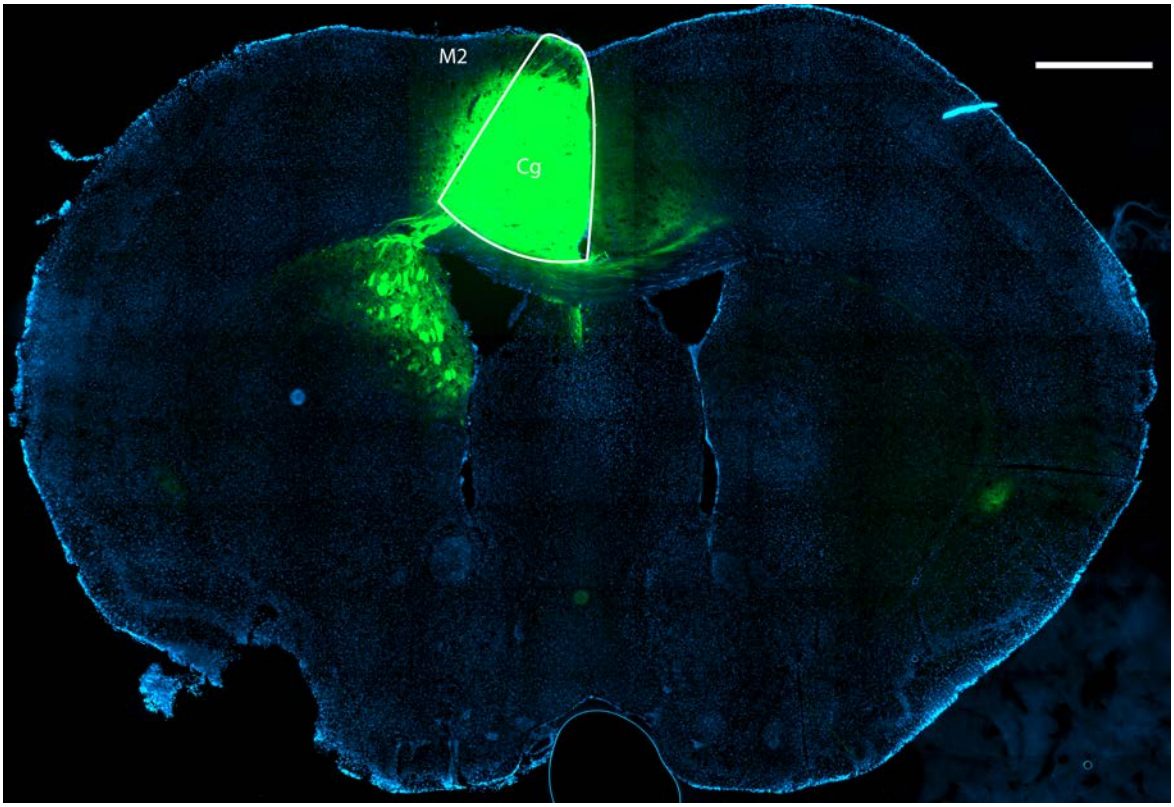

Figure 5-1. Example Photomicrograph of the Injection Site for AAV5 CAMKII Channelrhodopsin Injected into the Cingulate Region Brain

Green labelling represents endogenous CAMKII ChR2 neuronal fibres. Cyan colur represents DAPI nuclei labelling. Scale bar equate to 500µm. Nomenclature is derived from Franklin, K.B.J. & Paxinos, G. 2012. For abbreviations see list.

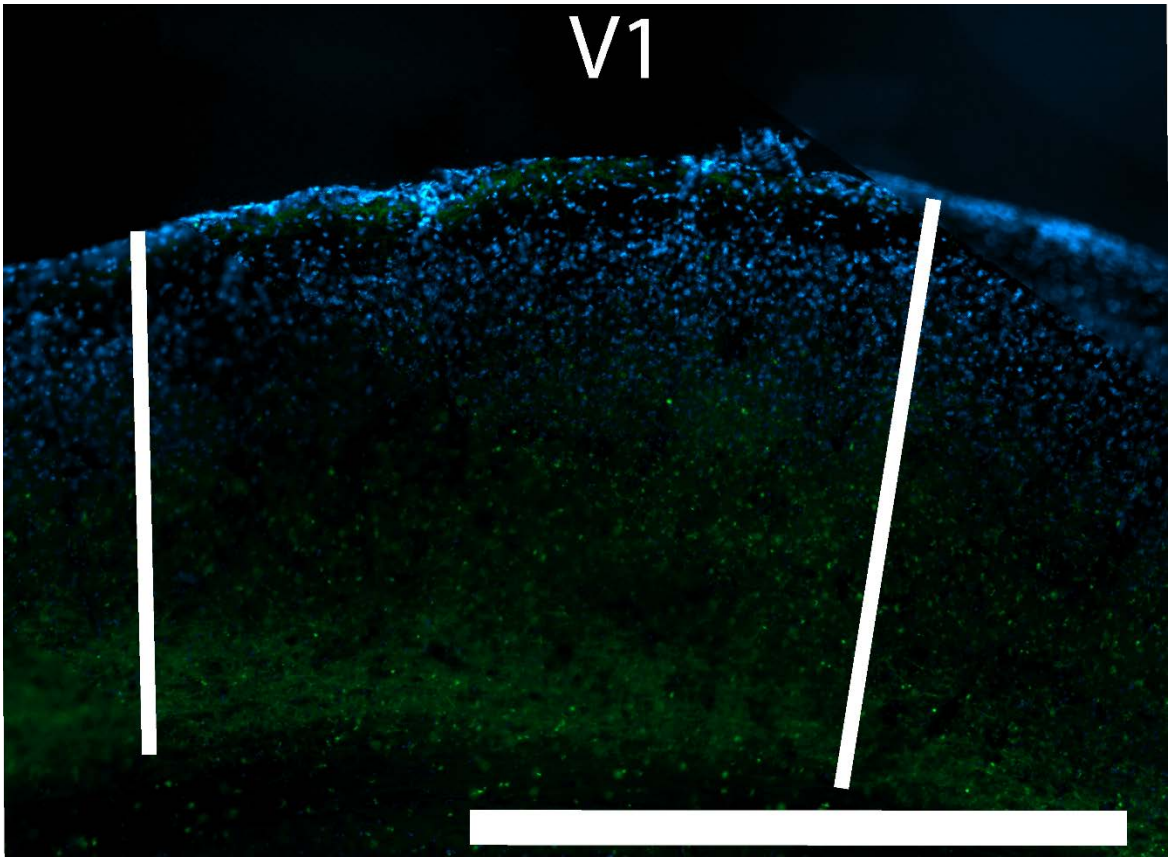

Figure 5-2. Example Photomicrograph of the Labelled Fibres in the Posterior Section of Mouse Primary Viusal Cortex

Green labelling represents endogenous CAMKII ChR2 neuronal fibres. Cyan colur represents DAPI nuclei labelling. Scale bar equate to 500µm. Nomenclature is derived from Franklin, K.B.J. & Paxinos, G. 2012. For abbreviations see list.

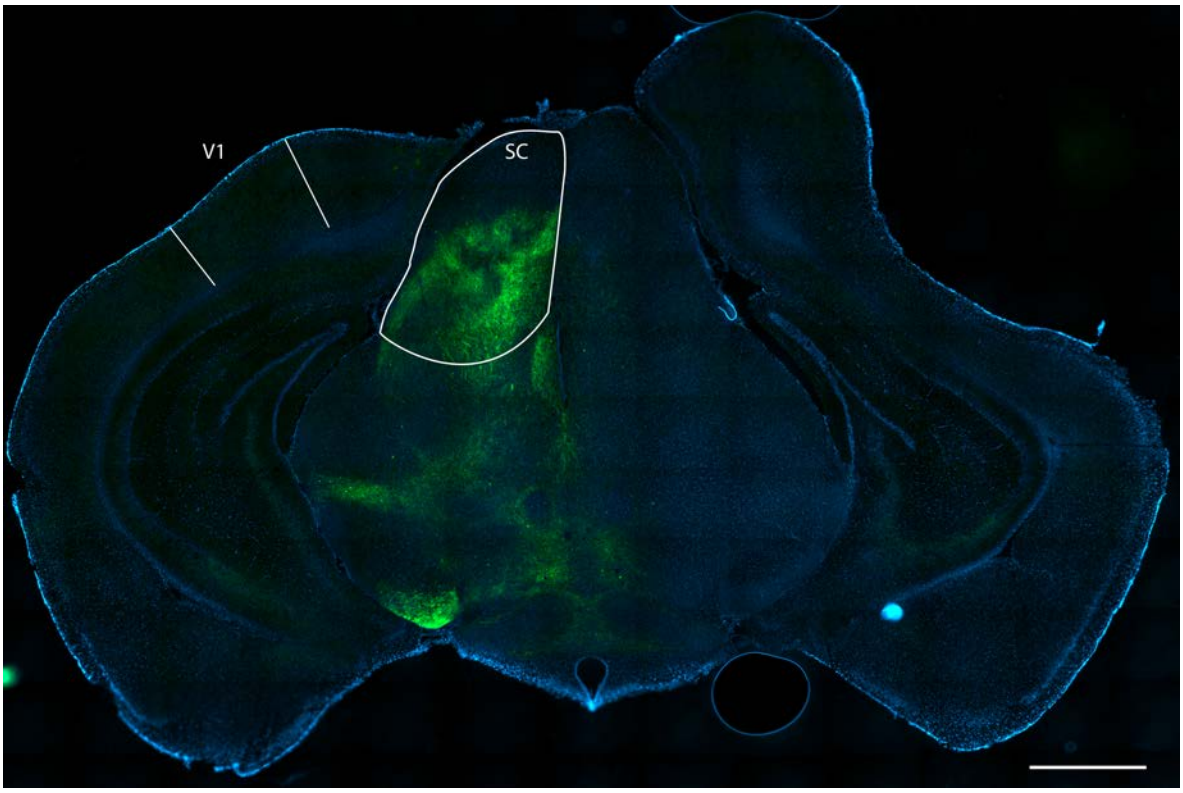

Figure 5-3. Example Photomicrograph of the Labelled Fibres in Mouse Primary Viusal Cortex and Superior Colliculus

Green labelling represents endogenous CAMKII ChR2 neuronal fibres. Cyan colour represents DAPI nuclei labelling. Scale bar equate to 500µm. Nomenclature is derived from Franklin, K.B.J. & Paxinos, G. 2012. For abbreviations see list.

5.3.2 Spiking Data

5.3.2.1 Optogenetic Stimulation of the Transfected Brain Areas

Before electrophysiological recordings began, it was necessary to test the efficacy of the optogenetic transfection. To do so, a single laminar multielectrode recording was conducted in the anaesthetised animal within the originally transfected region. In this manner it was possible to gain an indication of the effect of optogenetic stimulation within the transfected area. Two example optogenetic responsive contacts are displayed below (Figure 5-4, Figure 5-5**)**.

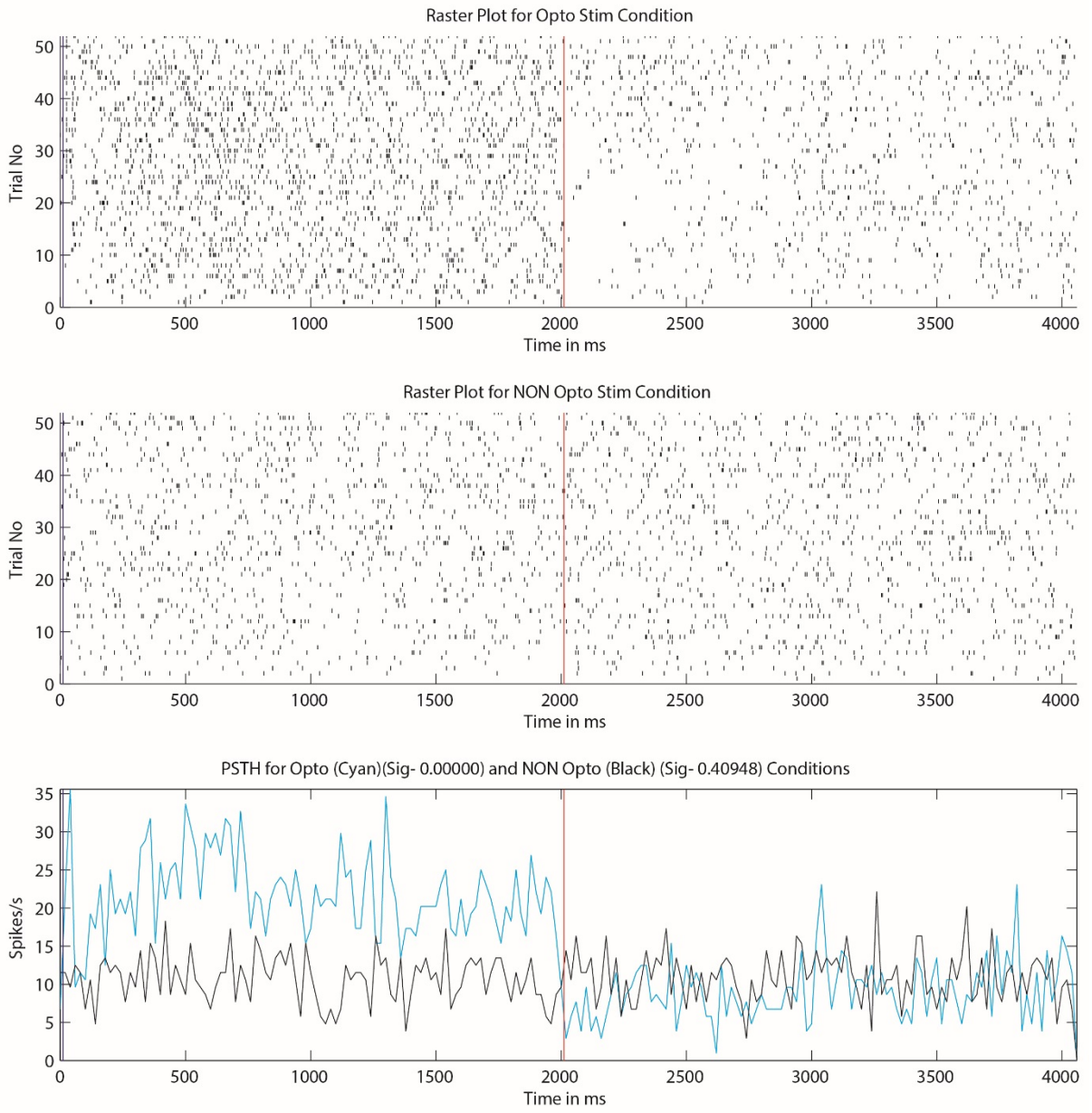

Figure 5-4. Example Cell/Contact Which Displayed Optogenetic Stimulation in the Viral Vector Transfection Site

Top panel displays a raster plot for the optogenetic stimulated condition for single contact. Middle panel displays a raster plot for the control condition with no optogenetic stimulation for single contact. Bottom panel displays peri-stimulus time histograms for both the optogenetically stimulation condition (cyan) and the control condition (black).

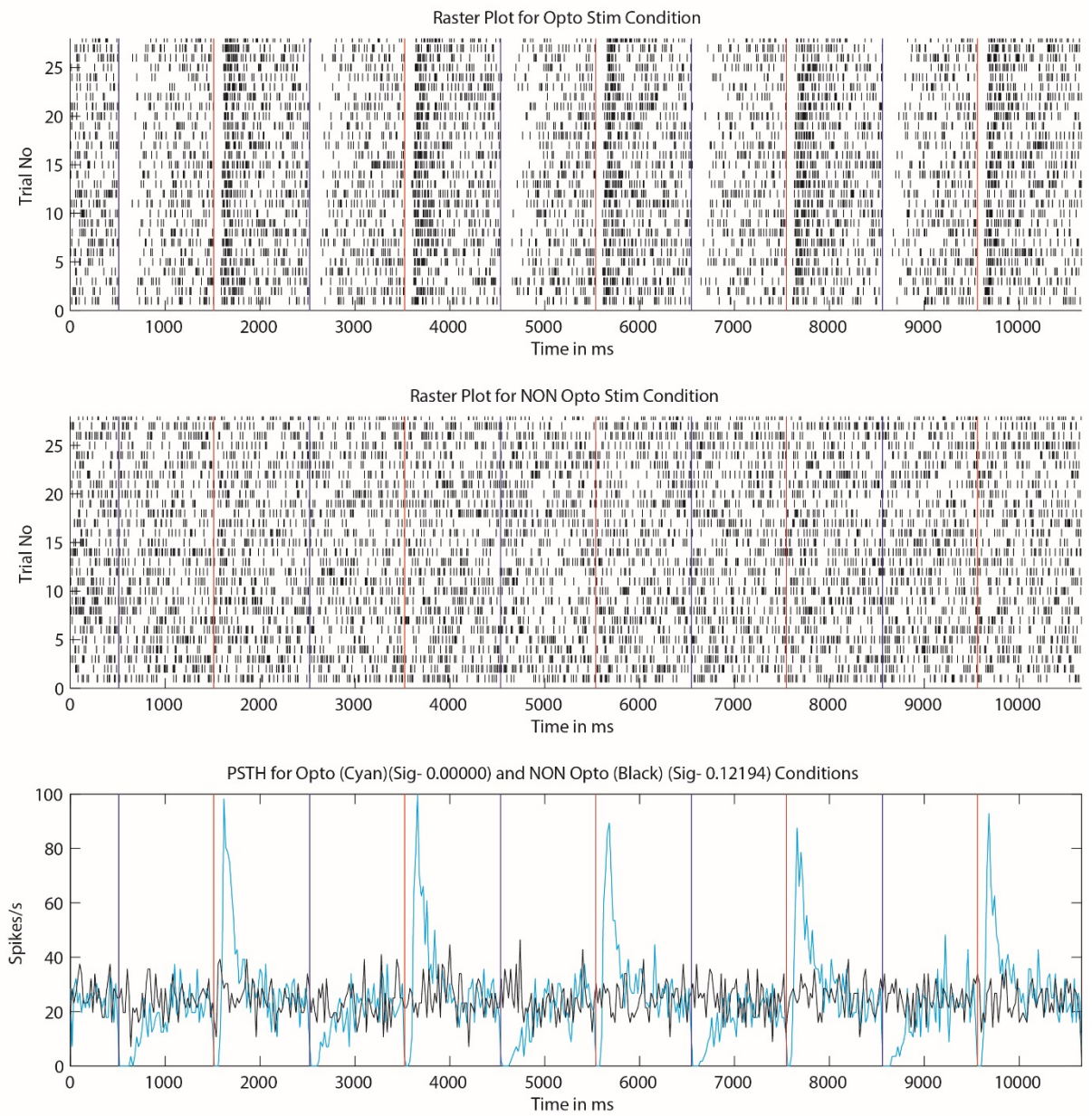

Figure 5-5. Example Cell/Contact Which Displayed Optogenetic Inhibition in the Viral Vector Transfection Site

Top panel displays a raster plot for the optogenetic stimulated condition for single contact. Middle panel displays a raster plot for the control condition with no optogenetic stimulation for single contact. Bottom panel displays peri-stimulus time histograms for both the optogenetically stimulation condition (cyan) and the control condition (black).

As has been reported previously, two main effects of light stimulation were observed. This included both an excitation in firing rates and a decrease in firing rates. In Figure 5-4, a recording location in which stimulation with a 2 second pulse increased firing rates significantly between stimulation and non-stimulation times (cyan, $p<0.0001$, Wilcoxon Signed Rank test) is shown. The interleaved no stimulation trials (black) show no modulation of firing rate. Conversely, in Figure 5-5, a recording location is shown, which showed a marked decrease in firing when stimulation occurred, as well as a large increase in firing once the stimulation was removed. This effect was significant (cyan, $p<0.0001$, Wilcoxon Signed Rank test).

5.3.2.2 Cuing Effects in the Bottom-Up Attentional Paradigm with Optogenetic Stimulation

5.3.2.2.1 Stimulation through the Cingulate Area

n=7 (V1) and n=5 (SC) responsive (z-score>3 for stimulus induced activity) multiunits were recorded, in separate session, with and without concurrent optogenetic stimulation of area Cg neurons using the bottom-up attention task. Data were analysed as described previously, with a focus on potential effects of optogenetic stimulation.

5.3.2.2.1.1 Single Contact Effects of Cuing and Optogenetic Stimulation

To test whether different forms of (pre/post)-cuing, grating (vertical/horizontal) and optogenetic conditions affected neuronal spiking activity, a mixed model multi-factor 2x2x4x4 ANOVA was used, as is described above in section 2.6.1.

V1: For the V1 recordings, no contacts showed a significant main effect of optogenetic stimulation, but 2/7 contacts showed a significant interaction of optogenetic stimulation and experimental time window ($p< 0.05$). 2/7 contacts showed a significant interaction of optogenetic stimulation and cuing condition ($p<0.05$). One contact showed a significant interaction of optogenetic stimulation, grating type, and cuing condition ($p<0.05$). Finally, grating type and cuing condition, experimental time window, and optogenetic stimulation condition caused a significant interaction in one contact ($p<0.05$). No other effects related to optogenetic stimulation were found.

SC: 2/5 contacts showed a significant main effect of optogenetic stimulation ($p<0.05$). A single contact showed a significant interaction of optogenetic stimulation and grating type ($p< 0.05$). One contact showed a significant interaction of optogenetic stimulation, grating type, and cuing condition ($p<0.05$). One contact had a significant interaction of optogenetic stimulation, grating type and time window ($p<0.05$). One contact had a significant interaction of optogenetic stimulation, cuing condition and time window ($p<0.05$). Finally, grating type and cuing condition, experimental time window, and optogenetic stimulation condition caused a significant interaction in one contact ($p<0.05$).

5.3.2.2.2 Population Spiking Histograms

Visual inspection of the spiking population data suggests that optogenetic stimulation might have affected (reduced) stimulus induced responses in V1 when vertical gratings were present (Figure 5-6). However, these hints did not occur when horizontal gratings were presented (Figure 5-7). More consistent effects (across conditions seemed to be present in the SC activity. Here optogenetic stimulation appeared to increase the late (sustained) stimulus induced response and the post-cue response period**.**

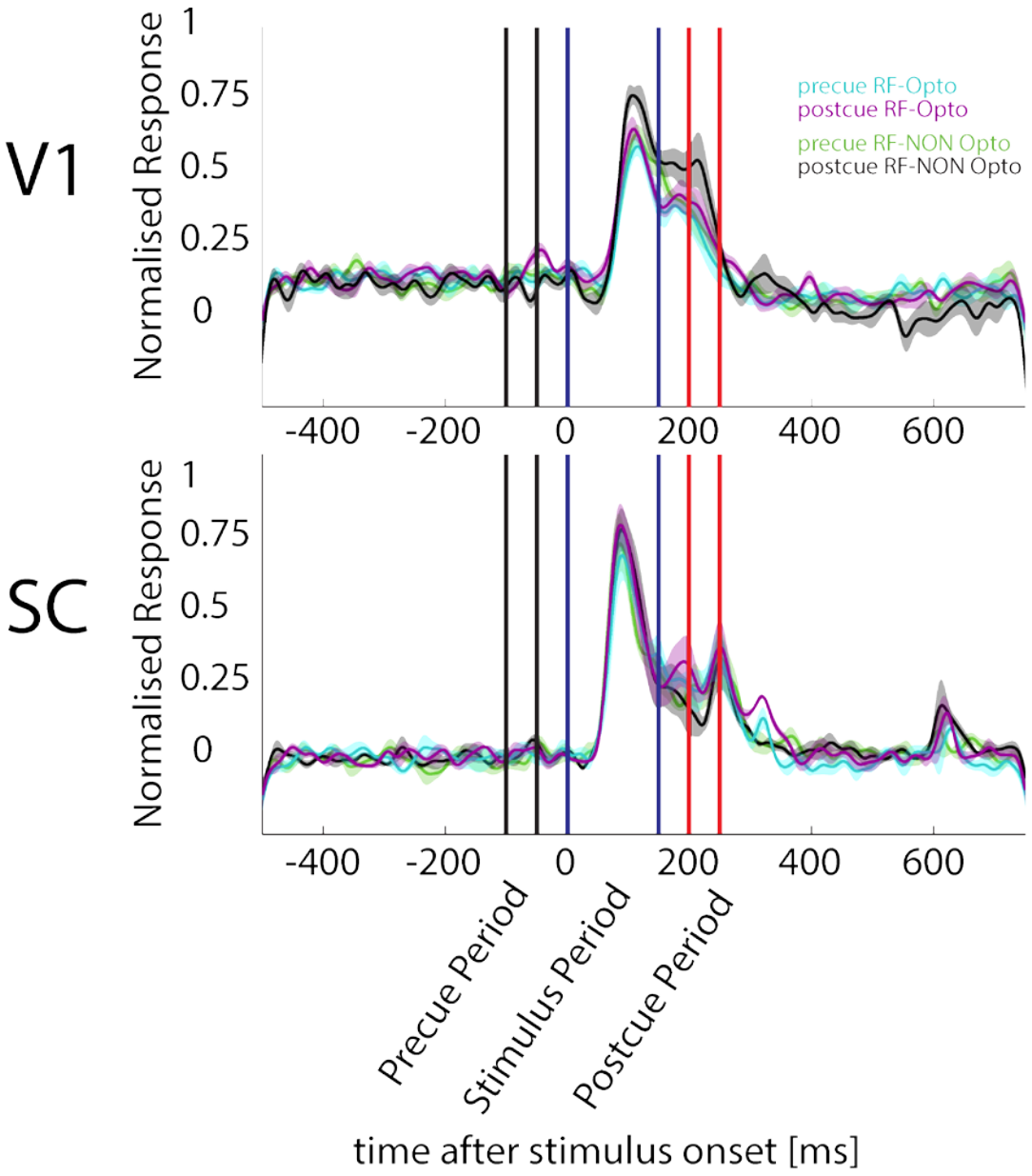

Figure 5-6. Comparison of Average Normalised Firing Rates in Mouse V1 and SC, When Vertical Gratings Were Presented During the Stimulus Period.

Pre-cue RF vs post-cue RF with and without optogenetic stimulation. Green-pre-cue presented in the receptive field location, black-post-cue presented in the receptive field location. Solid lines show trials with optogenetic stimulation, dashed line show trials without optogenetic stimulation. Vertical lines represent trial time epochs, black-pre-cue period, blue-grating stimulus period, red-post-cue period.

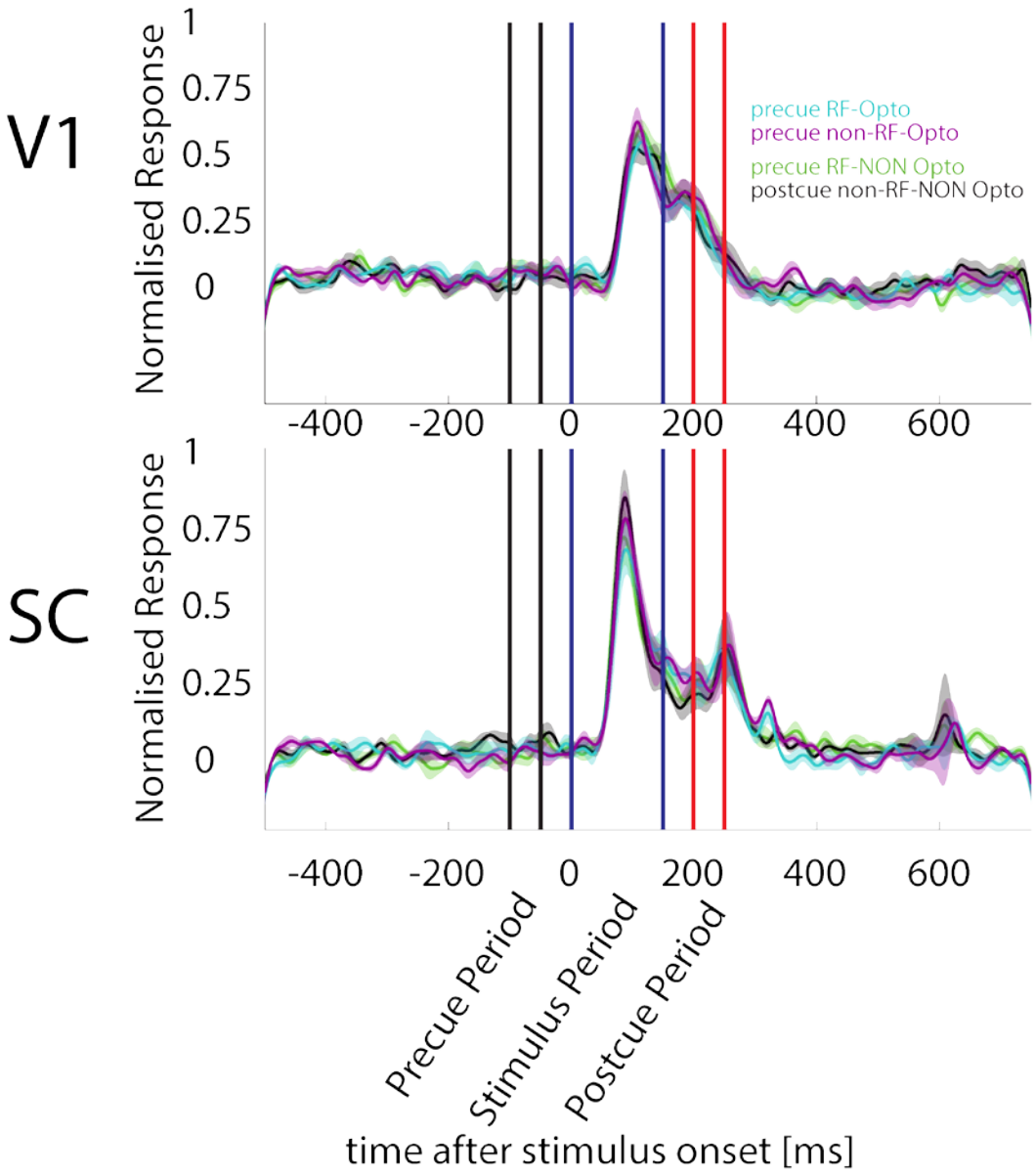

Figure 5-7. Comparison of Average Normalised Firing Rates in Mouse V1 and SC, When Horizontal Gratings Were Presented During the Stimulus Period.

Pre-cue RF vs pre-cue non-RF with and without optogenetic stimulation. Green-pre-cue presented in the receptive field location, black-post-cue presented in the receptive field location. Solid lines show trials with optogenetic stimulation, dashed line show trials without optogenetic stimulation. Vertical lines represent trial time epochs, black-pre-cue period, blue-grating stimulus period, red-post-cue period.

5.3.2.2.3 Quantification of Optogenetic Stimulation Effects at the Population Level

To quantify these effects (or absence thereof) we performed the previously described mixed model RM ANOVA, with the added factor of 'optogenetic stimulation'. An overview of the results for our V1 data is given in Table 5-1. While many factors affected the V1 spiking activity (as described in detail in previous chapters), optogenetic stimulation had no significant main effect (or interaction effect) on spiking activity in V1. Given the absence of an effect of optogenetic stimulation in this dataset, no more detailed analysis of the spiking activity for the different stimulus, cue, time period, and optogenetic conditions will be shown, as this has been dealt with previously. The FDR corrected pair-wise comparison for relevant pairs of baseline versus optogenetic conditions did equally not show any significance, corroborating the results from the mixed model RM ANOVA.

Table 5-1. Repeated Measures Mixed Model Multi Factor ANOVA for the Population of Multiunit Spiking Activity in Mouse V1 for Optogenetic Data

Term	FStat	DF1	DF2	pValue
Cuing Cnd	0.523	3	385	0.666
Grating Type	115.2	1	385	<0.001
Time Window	584.1	3	385	<0.001
Opto Stim	1.246	1	385	0.264
Grating Type*Cuing Cnd	0.242	3	385	0.866
Cuing Cnd*Time Window	0.358	9	385	0.954
Grating Type*Time Window	46.06	3	385	<0.001
Opto Stim*Cuing Cnd	0.343	3	385	0.793
Opto Stim*Grating Type	0.043	1	385	0.834
Opto Stim*Time Window	1.036	3	385	0.376
Grating Type*Cuing Cnd*Time Window	0.4164	9	385	0.926
Opto Stim*Grating Type*Cuing Cnd	0.239	3	385	0.868
Opto Stim*Cuing Cnd*Time Window	0.280	9	385	0.9798
Opto Stim*Grating Type*Time Window	0.1384	3	385	0.936
Opto Stim*Grating Type*Cuing Cnd*Time Window	0.267	9	385	0.982

An overview of the results for our SC data is given in Table 5-2. Contrary to V1, optogenetic stimulation had a significant main effect and a significant interaction with time window on spiking activity in SC.

Table 5-2. Repeated Measures Mixed Model Multi Factor ANOVA for the Population of Multiunit Spiking Activity in Mouse SC for Optogenetic Data

Term	FStat	DF1	DF2	pValue
Cuing Cnd	0.453	3	257	0.714
Grating Type	24.914	1	257	<0.001
Time Window	572.425	3	257	<0.001
Opto Stim	5.079	1	257	0.025
Grating Type*Cuing Cnd	1.414	3	257	0.239
Cuing Cnd*Time Window	0.166	9	257	0.997
Grating Type*Time Window	7.801	3	257	<0.001
Opto Stim*Cuing Cnd	0.443	3	257	0.721
Opto Stim*Grating Type	0.761	1	257	0.383
Opto Stim*Time Window	4.300	3	257	0.005
Grating Type*Cuing Cnd*Time Window	0.610	9	257	0.787
Opto Stim*Grating Type*Cuing Cnd	0.012	3	257	0.998
Opto Stim*Cuing Cnd*Time Window	0.203	9	257	0.993
Opto Stim*Grating Type*Time Window	0.328	3	257	0.804
Opto Stim*Grating Type*Cuing Cnd*Time Window	0.253	9	257	0.985

The significant effects of optogenetic stimulation above area Cg on SC firing rates, raises the question which time periods were affected by the manipulation. This is delineated in Figure 5-8, Figure 5-9, and Figure 5-10

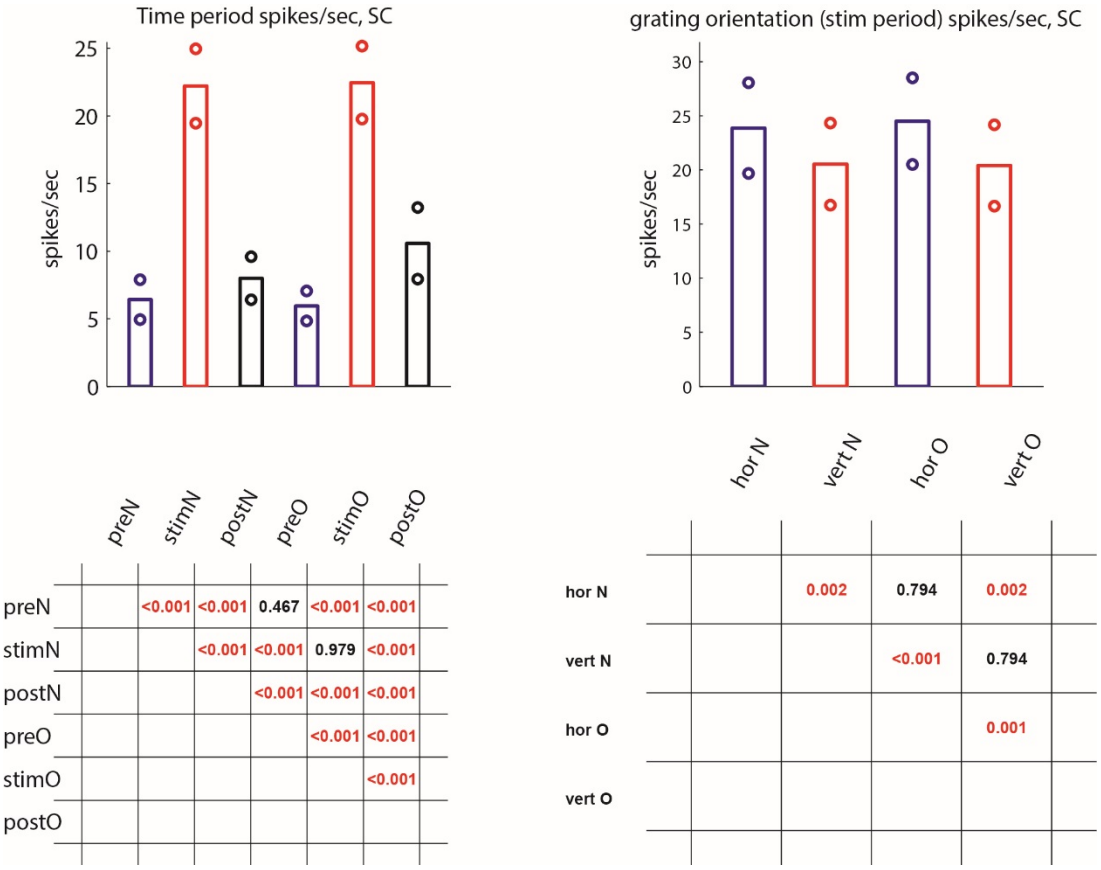

Figure 5-8. Comparison of SC Spiking Activity for the Different Time Periods, the Two Grating Orientations, and the Baseline Condition vs. Optogenetic Stimulation Condition.

Left. Mean spiking activity for the population of mouse SC cells, during the different time periods (pre-cue [pre], stimulus [stim], and post-cue [post]). An added 'N' and 'O' to every label indicates whether optogenetic stimulation was applied: ='O'. Right. Mean spiking activity for the population of mouse SC cells for the two different gratings, measured during the stimulus time period. P-values in the tables below main plots indicate FDR corrected pair wise differences (Wilcoxon Signed Rank test). Bars show mean activity, associated circles indicate 95% confidence intervals.

Figure 5-8 shows that the main differences between baseline and optogenetic stimulation appear during the post-cue period (when averaged over all stimulus conditions and the two

different post-cue conditions). The optogenetic stimulation did not affect the pre-cue or the stimulus period (relevant pairwise comparisons in Figure 5-8 e.g. stimN vs. stimO p=0.979). The optogenetic stimulation equally did not affect the strength of responses to the two grating orientations.

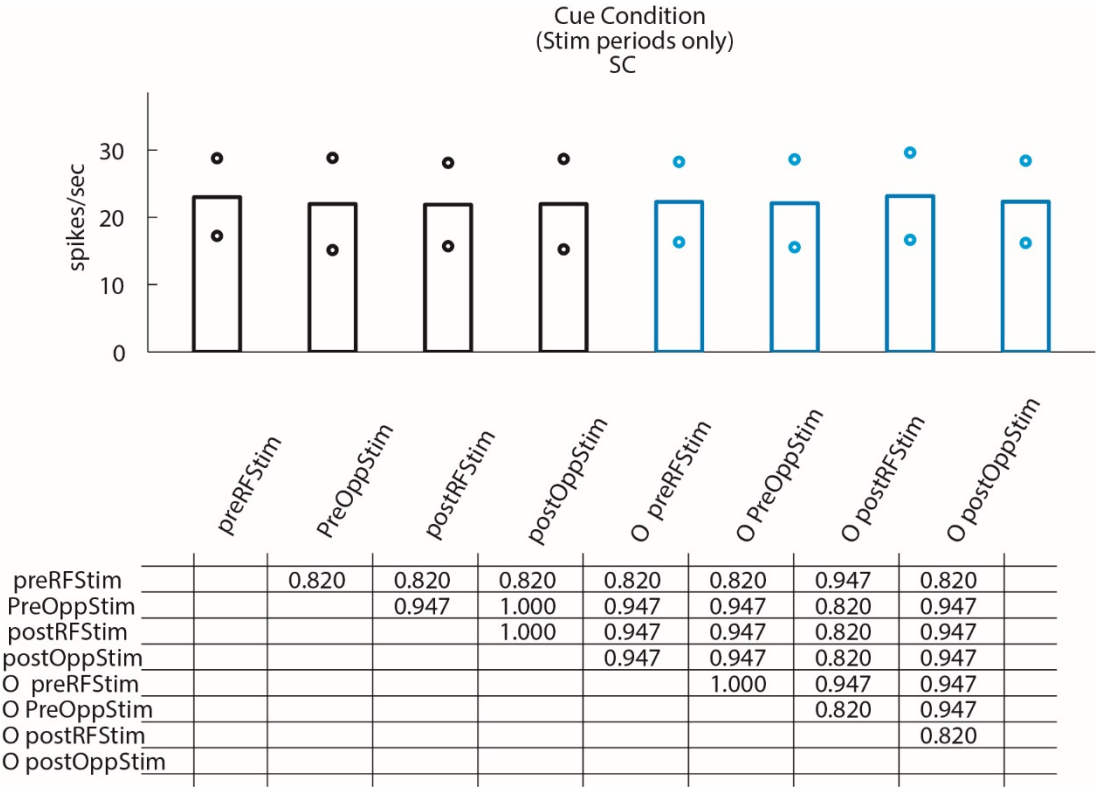

preRFStim		0.820	0.820	0.820	0.820	0.820	0.947	0.820
PreOppStim			0.947	1.000	0.947	0.947	0.820	0.947
postRFStim				1.000	0.947	0.947	0.820	0.947
postOppStim					0.947	0.947	0.820	0.947
O preRFStim						1.000	0.947	0.947
O PreOppStim							0.820	0.947
O postRFStim								0.820
O postOppStim								

Figure 5-9. Comparison of Population Spiking Activity for the Cuing Conditions in the Stimulus Time Period for the Mouse SC Data With and Without Optogenetic Stimulation.

Mean spiking activity for the population of SC cells, during the stimulus time period for the 4 different cuing conditions (pre-cue RF [preRFStim], pre-cue opposite [preOppStim], post-cue RF [postRFStim], post-cue opposite [postOppStim]), separately for the baseline condition (black bars) and the optogenetic stimulation condition (cyan bars, and added label 'O'). Activity was averaged across the two grating orientations, but separated according to cue condition. Tables below each subplot indicate pair wise differences (FDR corrected p-values based on Wilcoxon Signed Rank test). Bars show mean spiking activity, associated circles indicate 95% confidence intervals.

Figure 5-9 shows that the optogenetic stimulation did not affect the stimulus induced responses, irrespective of which cuing condition was analysed.

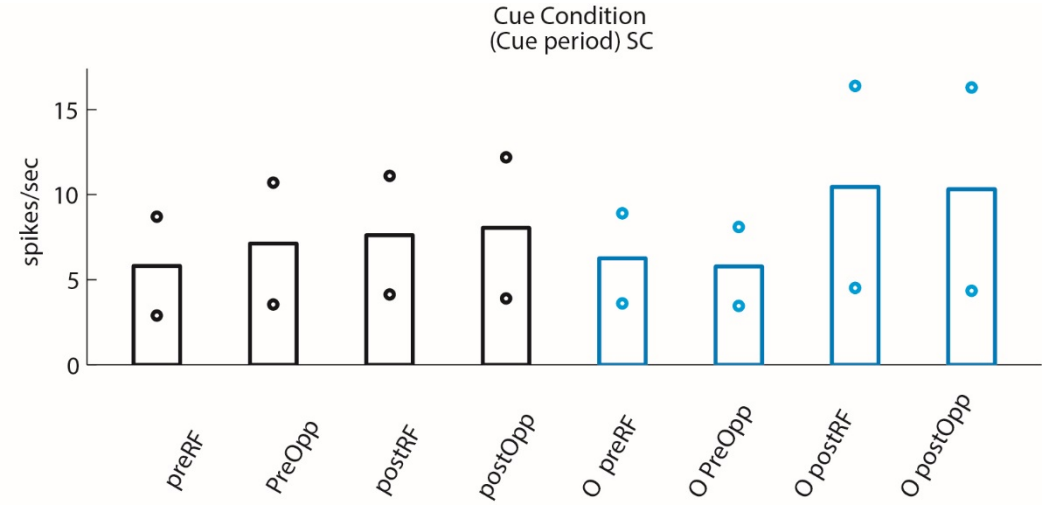

preRF		0.080	0.018	0.055	0.465	0.922	0.014	0.014
PreOpp			0.438	0.310	0.465	0.350	0.055	0.034
postRF				0.224	0.204	0.080	0.106	0.080
postOpp					0.224	0.106	0.091	0.091
O preRF						0.392	0.014	0.014
O PreOpp							0.023	0.018
O postRF								0.648
O postOpp								

Figure 5-10. Comparison of Population Spiking Activity During the Cue Period for the Mouse SC Data With and Without Optogenetic Stimulation.

Mean spiking activity during the cuing time periods for the 4 different cuing conditions (pre-cue [preRF], pre-cue opposite [preOpp], post-cue RF [postRF], post-cue opposite [postOpp]) plotted separately for the baseline condition (black bars) and the optogenetic stimulation condition (cyan bars, and added label ‘O’). Tables below each subplot indicate pair wise differences (FDR corrected p-values based on Wilcoxon Signed Rank test). Bars show mean spiking activity, associated circles indicate 95% confidence intervals.

While Figure 5-10 suggests that SC activity during the post-cue periods was higher with optogenetic stimulation, than without optogenetic stimulation, these effects were not significant in the FDR corrected direct pairwise comparison. The discrepancy to the

findings shown in Figure 5-8 are likely due to the diminished sample size, as data in Figure 5-8 (left column) were pooled across the two post-cue conditions. However, the data shown in Figure 5-10, show a trend in the FDR corrected p-values, and uncorrected p-values were 0.064 and 0.049 respectively.

No effects (or trends) of optogenetic stimulation were found when analysing the entire response period, separated for cue conditions. All FDR corrected p-values were >0.7, and thus data are not shown.

5.4 Discussion

In this chapter the effect of optogenetic stimulation on bottom-up attentional processing in mouse primary visual cortex and superior colliculus (SC) was examined. This was achieved through optogenetic transfection of mouse brain area Cg by injection of a projection neuron specific excitatory optogenetic compound. Cg was chosen due to its previously documented role in attention and orienting processes in rodents and primates (Kvitsiani et al., 2013, Blanchard and Hayden, 2014). Furthermore, from our data (see Chapter 3) and others, it is known that this region directly projects to both cortical visual areas such as primary visual cortex (V1) (Zhang et al., 2014) and to the main subcortical visually responsive region, the SC (Vogt and Miller, 1983).

Firstly, to test the efficacy of optogenetic transfection we recorded from area Cg in the transfection location, with and without blue light exposure. Light stimulation of the region caused both excitation and inhibition of neurons within that region. These results are equivalent to previous literature reports (Han, 2012). Response inhibition would normally not immediately expected with ChR2, but it may be caused by indirect effects of the optogenetic stimulation. Light stimulation might have excited neurons which project to inhibitory cells. These inhibitory cells could then then inhibit the neuron that are recorded from, provided the recorded neurons themselves did not express ChR2.

Optogenetic stimulation did not affect any of the experimental BU condition responses for our V1 data. This may seem surprising, as other have successfully activated V1 following area Cg ChR2 injection (Zhang et al., 2014). This group recorded from the Cg and V1 after transfection CAMKII channelrhodopsin 2 into Cg. However, they directly activated the Cg fibres terminating in V1, by shining light onto V1, not onto Cg. Optogenetic stimulation of these Cg fibres increased V1 firing rates in general, and caused a

potentiation of orientation selectivity of the neurons. Furthermore, optogenetic stimulation of the fibres in V1 was able to increase the experimental animals' performance in a visual discrimination task. The differences in experimental approach might be the reason why outcomes were different. At the same time, our current data sample is rather small, and strong conclusion cannot be drawn just yet.

Optogenetic stimulation did cause significant changes in SC neuronal activity. Here, light activation of Cg neurons resulted in increased SC activity during the post-cue period, but it is difficult to exclude an effect on the stimulus induced sustained response, which may simply have lasted longer, than when Cg was not activated. The temporal proximity of the post-cue period to stimulus offset makes a distinction difficult, but the population histograms suggest effects to be present during the late sustained period already. I would argue that the optogenetic stimulation prolonged the sustained visual stimulus response but additional data will be necessary to prove this.

The presence of both excited and inhibited neurons within the Cg region raises some questions on the effects seen in the SC. The increase in activity during the post-cue period may be caused by an increase in activity in excitatory neurons within Cg which excite cells within the SC region. Or there may be more complex network interactions, whereby excitation of neurons causes indirect inhibition of neurons which in turn disinhibit the SC, thereby causing an increase in activity. Under the current experimental setup it may be difficult to disentangle these issues. Although it may be possible with the aid of specific immunohistochemical labelling to get a finer scale picture of specific neuronal subtype interaction. As well the usage of a CAMKII specific promoter for the ChR2 expression should limit the optogenetic transfection to pyramidal projection neurons.

Few studies have investigated how optogenetic transfection affects SC neuronal firing. The studies that did, have employed transfection and stimulation of the SC itself, rather than remote areas (Stubblefield et al., 2013). One study was able to bias the response in a sensory cued decision task to the side contralateral to stimulation. The other was able to trigger aversive freezing behaviours in rodents as well as abolish normal freezing behaviours. To the best of my knowledge no published work to date has looked at the modulation of neuronal firing in the SC with optogenetic stimulation in a visually cued paradigm such as we have employed.

Chapter 6. General Discussion

6.1 Overview

The biological basis of attention and orienting behaviours has been a central focus of neuroscientific research for many years. The most widely used animal for the more complex problem of visual attention is the non-human primate (NHP). The organism's complexity and distinct similarities to the human make it an ideal choice for the study of visual based attention.

However, attention (or at least orienting) is not restricted to these animals. All mammals, and indeed most animals, perform orienting which allows the animal to navigate the world and extract behaviourally relevant cues from the environment. An animal model, which is one of the mostly widely utilised animal in biological research, is the mouse (Bockamp et al., 2002). The mouse brain shows similarities, but also differences to the primate brain, which asks for the type of comparative work done here.

In Chapter 3 a neuroanatomical characterisation of the networks involved in rodent orienting was conducted. The first target was the superior colliculus (SC). In line with previous work done in the rat (Comoli et al., 2012), I found that subregions of the SC receive projections from partially segregated networks in the brain. The main prefrontal inputs to the medial and lateral SC differed. The medial SC received the majority of its projections from the cingulate area (Cg), whereas the lateral SC receives the majority of its prefrontal input from the motor area 2 (M2) region. The Cg region has been implicated in the control of pain processing, aversion learning and mediation of aversion behaviours (Gabriel et al., 1991, Calejesan et al., 2000). Whereas the M2 region has been implicated in the control of orienting behaviours and goal based decision making (Reep et al., 1987, Duan et al., 2015). The M2 has also been suggested as the rodent homologue of the frontal eye field in macaque (Erlich et al., 2011). This result then led to the second part of the study were the anterograde connectivity of these prefrontal regions was investigated to examine whether the subregions of the SC and the relevant prefrontal regions were parts of wider segregated orienting networks. The anterograde data cemented the hypothesis that these specific prefrontal regions (Cg/M2) interact with their efferent brain networks including the medial and lateral SC, respectively. These partially segregated networks then may preferentially process aversive (Cg-medial SC) and approach (M2-lateral SC) related

orienting behaviours. In this manner, this chapter adds to the literature in setting out the fine scale anatomical networks which may control attentional based orienting in the mouse model.

In Chapter 4 a direct comparison of attentional processing in the macaque and mouse was conducted. This was done through laminar multi-electrode recordings in multiple visual areas of both the macaque (V1 and V4) and the mouse (V1 and SC). The animals completed a passive visual bottom-up attentional paradigm whereby an ambiguous pre-cue or post-cue was presented either 100ms before or 100ms after the onset of a sinusoidal grating. This was adapted from a human paradigm (Liu et al., 2005). By using such a trial structure an investigation of the bottom-up influences of exogenous attention on visual stimulus induced activity could be achieved.

In the macaque and mouse data, there was no effect of cuing condition on stimulus induced V1 neuronal firing, but the macaque MUAe data showed an overall increased activity, when averaged across the entire response period. This is somewhat at odds with the literature which has shown there to be an enhancement of neuronal firing after precuing the visual stimulus (Luck et al., 1997, Roberts et al., 2007). In V4 there was a significant increase in spiking and MUAe activity over the entire trial period. This increase in overall firing rate is similar to that seen in the literature (Moran and Desimone, 1985, Luck et al., 1997). However, there was a contrasting reduction in stimulus induced firing in the pre-cue conditions, likely due to temporally delayed centre surround inhibition (Sundberg et al., 2009).

In mouse SC there were no changes in the firing rates in the response to the visual stimulus, but there were changes in the post-cue period. These were unlikely to be due to cuing itself. By and large the effects in the mouse were smaller than those seen in the monkey, but a final verdict requires a larger sample size.

Finally in Chapter 5 we investigated the role of the prefrontal areas identified in Chapter 3 in modulating the bottom-up attentional processing discussed in the Chapter 4 within the mouse data. This was achieved by optogenetic stimulation a of CAMKII channelrhodopsin 2 transfected neurons in area Cg of mouse. The Cg is assumed to process and trigger aversive behaviours, pain and orienting responses. As such activation of the Cg might modulate visual responses in V1 and the SC, areas that processes the relevance of salient stimuli. Light activation of Cg did not alter responses in area V1 but there was an effect of optogenetic stimulation within the SC. This stimulation did not depend upon the cuing

condition. In fact the modulation was only apparent in the late response phase of visual stimulus activation, and during the offset response period. It shows that Cg can directly affect responses in SC, but the exact role thereof remains to be determined. It certainly did not do it in a manner specific to our cuing conditions.

6.2 Limitations of this Research

An issue worth consideration when comparing the effects seen in the mouse and the macaque is the role that bottom-up attention has in the specific animals' ethological niche. For a mouse, sudden onsets of visual stimuli often signals danger. It is most likely to be a cue relating to a predator or at the very least something that will cause the animal to hide or avoid the source of the stimulus. Therefore, for the rodent localization of the stimulus and its movement would be the highest priority. It would allow any orienting (reflexive aversion/shelter seeking) response to occur faster, if the activity to the ensuing stimulus was enhanced and preferably processed. In contrast, the onset of a sudden visual stimulus for the macaque may not necessarily be as aversive. So the highest priority for this animal may be to further evaluate the details of the object itself.

In Chapter 3, with hindsight (and more time available) a yet more quantitative approach could have been taken, specifically a stereological approach would have been useful. This methodology takes accounts for the complete brain region volume by the use of statistical inference. This garners a better estimation of the total numbers of labelled cells in the brain volumes of interest. However, this methodology is extremely time intensive and it would be very difficult to complete the amount of tracing work presented here considering the time limits of PhD. Furthermore in a more definite quantification of the anterograde labelling conducted in Chapter 3 would have benefited the research. However this would have entailed using a method like densitometry or synaptic bouton counting. Both of which, again are extremely time consuming and may not have been possible during the course of this PhD.

When critically examining Chapter 4, the inclusion of more data from different animals, i.e. a second macaque and additional mouse recordings, would have be beneficial. This might have increased the significance of certain experimental effects. In addition, the active behavioural task which was conducted in the macaque did not produce enough data to be certain of the absence or presence of significant differences in the population response, when compared to passive viewing conditions. Furthermore in the macaque,

paired recordings in both V1 and V4 were attempted, but they did not yield a large enough sample with matching receptive fields to warrant any inter areal analysis of information flow. Finally, some form of active perception task in the rodent would fully compliment the macaque data and allow a better comparison of the effects of bottom-up attention in a goal directed task.

6.3 Future Work

Due to the time constraints of a 3 year PhD some interesting avenues of research were not fully explored. First and foremost, although our hypothesis regarding the optogenetic manipulation of bottom-up attentional processing attempted to investigate the mechanisms behind cingulate area and motor cortex area 2 innervation; the M2 transfected CAMKII cohort was not tested. Conducting these tests would uncover any differences between the modulations of both prefrontal areas in visual processing in the mouse. Additionally, increasing the sample size of the optogenetic cohort would be a necessity before drawing any stronger conclusions from the data.

Furthermore it might be relevant to investigate whether the optogenetic stimulation from prefrontal regions had any effect in changing orientation preferences or receptive field properties within V1 and SC. Also, since activation in the prefrontal regions resulted in a noticeable effect on visual stimulus induced firing, it might be worthwhile examining what optogenetic inhibition of the area might yield.

6.4 Conclusion

The main goal of this work was to at least partially bridge the gap between our understanding of the processes behind the control of sensory orienting behaviours in the mouse and the processes involved in bottom-up visual attention in the macaque. Comparisons of this sort are difficult to make considering the differences in brain structure and fundamental cognitive functioning in these animals. However in this work a detailed neuroanatomical some brain regions involved in sensory orienting in the mouse was conducted. This furthers our understanding of the networks involved with specific types of sensory orienting in the mouse model. A direct investigation of bottom-up attentional processing was done in both the macaque and the model using the same paradigm. One, which had been created for human subjects. This allowed a clear comparison between the

early visual system processing in these two animals. In general, the visual processing of sinusoidal gratings between monkeys and mice is similar, with a short term transient peak followed by a longer term sustained response. There were some differences in the sustained response in V1; for the macaque there was a positive sustained/off response. For the mouse the off response was highlighted by a large reduction in overall activity. Furthermore the effects of precuing the grating were far larger in the macaque than that seen in the mouse. This may reflect the larger visual sensitivity seen in the macaque species. Finally by linking together the findings of the previous two chapters, an investigation of the neural influences of one of the partial segregated prefrontal inputs to the visual system in mouse was conducted. It was found that one of the main prefrontal inputs to the superior colliculus increases the sustained response to a visual stimulus. This furthered the understanding of the top-down influences in the mouse brain in terms of basis visual processing.

Bibliography

ADRIAN, E. 1928. *The Basis of Sensation: The Action of the Sense Organs*, London.

AHMADLOU, M. & HEIMEL, J. A. 2015. Preference for concentric orientations in the mouse superior colliculus. *Nature Communications,* 6.

ALBANO, J. E., MISHKIN, M., WESTBROOK, L. E. & WURTZ, R. H. 1982. Visuomotor deficits following ablation of monkey superior colliculus. *Journal of Neurophysiology,* 48**,** 338-351.

ANASTASSIOU, C. A., PERIN, R., MARKRAM, H. & KOCH, C. 2011. Ephaptic coupling of cortical neurons. *Nat Neurosci,* 14**,** 217-223.

ASTAFIEV, S. V., SHULMAN, G. L. & CORBETTA, M. 2006. Visuospatial reorienting signals in the human temporo-parietal junction are independent of response selection. *European Journal of Neuroscience,* 23**,** 591-596.

BARTFELD, E. & GRINVALD, A. 1992. Relationships between orientation-preference pinwheels, cytochrome oxidase blobs, and ocular-dominance columns in primate striate cortex. *Proc Natl Acad Sci U S A,* 89**,** 11905-9.

BECKER, W. 1989. The neurobiology of saccadic eye movements. Metrics. *Rev Oculomot Res,* 3**,** 13-67.

BENJAMINI, Y. & HOCHBERG, Y. 1995. Controlling the False Discovery Rate: A Practical and Powerful Approach to Multiple Testing. *Journal of the Royal Statistical Society. Series B (Methodological),* 57**,** 289-300.

BEZDUDNAYA, T. & CASTRO-ALAMANCOS, M. A. 2014. Neuromodulation of whisking related neural activity in superior colliculus. *Journal of Neuroscience,* 34**,** 7683-7695.

BICHOT, N. P. & SCHALL, J. D. 2002. Priming in Macaque Frontal Cortex during Popout Visual Search: Feature-Based Facilitation and Location-Based Inhibition of Return. *The Journal of Neuroscience,* 22**,** 4675-4685.

BISLEY, J. W. & GOLDBERG, M. E. 2003. Neuronal Activity in the Lateral Intraparietal Area and Spatial Attention. *Science,* 299**,** 81-86.

BJERRE, L., ANDERSEN, A. T., HAGELSKJAER, M. T., GE, N., MORCH, C. D. & ANDERSEN, O. K. 2011. Dynamic tuning of human withdrawal reflex receptive fields during cognitive attention and distraction tasks. *Eur J Pain,* 15**,** 816-21.

BLANCHARD, T. C. & HAYDEN, B. Y. 2014. Neurons in dorsal anterior cingulate cortex signal postdecisional variables in a foraging task. *J Neurosci,* 34**,** 646-55.
BLASDEL, G. & LUND, J. 1983. Termination of afferent axons in macaque striate cortex. *The Journal of Neuroscience,* 3**,** 1389-1413.
BOCKAMP, E., MARINGER, M., SPANGENBERG, C., FEES, S., FRASER, S., ESHKIND, L., OESCH, F. & ZABEL, B. 2002. Of mice and models: improved animal models for biomedical research. *Physiological Genomics,* 11**,** 115-132.
BRECHT, M., KRAUSS, A., MUHAMMAD, S., SINAI-ESFAHANI, L., BELLANCA, S. & MARGRIE, T. W. 2004. Organization of rat vibrissa motor cortex and adjacent areas according to cytoarchitectonics, microstimulation, and intracellular stimulation of identified cells. *J Comp Neurol,* 479**,** 360-73.
BUSCHMAN, T. J. & MILLER, E. K. 2007. Top-Down Versus Bottom-Up Control of Attention in the Prefrontal and Posterior Parietal Cortices. *Science,* 315**,** 1860-1862.
CAJAL, S. R. 1909. *Histologie du système nerveux de l'homme et des vertébrés* [Online]. New York: Oxford University Press.
CALEJESAN, A. A., KIM, S. J. & ZHUO, M. 2000. Descending facilitatory modulation of a behavioral nociceptive response by stimulation in the adult rat anterior cingulate cortex. *European Journal of Pain,* 4**,** 83-96.
CALLAWAY, E. M. 1998. Local circuits in primary visual cortex of the macaque monkey. *Annu Rev Neurosci,* 21**,** 47-74.
CARRASCO, M., PENPECI-TALGAR, C. & ECKSTEIN, M. 2000. Spatial covert attention increases contrast sensitivity across the CSF: support for signal enhancement. *Vision Res,* 40**,** 1203-15.
CARRETIE, L. 2014. Exogenous (automatic) attention to emotional stimuli: a review. *Cogn Affect Behav Neurosci*.
CHALK, M., HERRERO, J. L., GIESELMANN, M. A., DELICATO, L. S., GOTTHARDT, S. & THIELE, A. 2010. Attention reduces stimulus-driven gamma frequency oscillations and spike field coherence in V1. *Neuron,* 66**,** 114-25.
CHALUPA, L. M. & THOMPSON, I. 1980. Retinal ganglion cell projections to the superior colliculus of the hamster demonstrated by the horseradish peroxidase technique. *Neurosci Lett,* 19**,** 13-9.
CHANDRAN KS, S., MISHRA, A., SHIRHATTI, V. & RAY, S. 2016. Comparison of Matching Pursuit Algorithm with Other Signal Processing Techniques for Computation of

the Time-Frequency Power Spectrum of Brain Signals. *The Journal of Neuroscience,* 36**,** 3399-3408.
CHEN, J. L., CARTA, S., SOLDADO-MAGRANER, J., SCHNEIDER, B. L. & HELMCHEN, F. 2013. Behaviour-dependent recruitment of long-range projection neurons in somatosensory cortex. *Nature,* 499**,** 336-340.
CHEN, J. L., MARGOLIS, D. J., STANKOV, A., SUMANOVSKI, L. T., SCHNEIDER, B. L. & HELMCHEN, F. 2015. Pathway-specific reorganization of projection neurons in somatosensory cortex during learning. *Nat Neurosci,* 18**,** 1101-1108.
CHICA, A. B., BARTOLOMEO, P. & LUPIANEZ, J. 2013. Two cognitive and neural systems for endogenous and exogenous spatial attention. *Behav Brain Res,* 237**,** 107-23.
COLEMAN, J. E., LAW, K. & BEAR, M. F. 2009. Anatomical origins of ocular dominance in mouse primary visual cortex. *Neuroscience,* 161**,** 561-571.
COMOLI, E., DAS NEVES FAVARO, P., VAUTRELLE, N., LERICHE, M., OVERTON, P. G. & REDGRAVE, P. 2012. Segregated anatomical input to sub-regions of the rodent superior colliculus associated with approach and defense. *Front Neuroanat,* 6**,** 9.
CONSTANTINIDIS, C. & STEINMETZ, M. A. 2005. Posterior Parietal Cortex Automatically Encodes the Location of Salient Stimuli. *The Journal of Neuroscience,* 25**,** 233-238.
CORBETTA, M., PATEL, G. & SHULMAN, G. L. 2008. The Reorienting System of the Human Brain: From Environment to Theory of Mind. *Neuron,* 58**,** 306-324.
CORBETTA, M. & SHULMAN, G. L. 2002. Control of goal-directed and stimulus-driven attention in the brain. *Nat Rev Neurosci,* 3**,** 201-215.
COWEY, A. & BOZEK, T. 1974. Contralateral 'neglect' after unilateral dorsomedial prefrontal lesions in rats. *Brain Res,* 72**,** 53-63.
CROWNE, D. P. & PATHRIA, M. N. 1982. Some attentional effects of unilateral frontal lesions in the rat. *Behavioural Brain Research,* 6**,** 25-39.
CROWNE, D. P., RICHARDSON, C. M. & DAWSON, K. A. 1986. Parietal and frontal eye field neglect in the rat. *Behavioural Brain Research,* 22**,** 227-231.
DEAN, P., MITCHELL, I. J. & REDGRAVE, P. 1988a. Contralateral head movements produced by microinjection of glutamate into superior colliculus of rats: Evidence for mediation by multiple output pathways. *Neuroscience,* 24**,** 491-500.

DEAN, P., MITCHELL, I. J. & REDGRAVE, P. 1988b. Responses resembling defensive behaviour produced by micoinjection of glutamate into superior colliculus of rats. *Neuroscience,* 24**,** 501-510.
DEAN, P., REDGRAVE, P., SAHIBZADA, N. & TSUJI, K. 1986. Head and body movements produced by electrical stimulation of superior colliculus in rats: Effects of interruption of crossed tectoreticulospinal pathway. *Neuroscience,* 19**,** 367-380.
DEAN, P., REDGRAVE, P. & WESTBY, G. W. M. 1989. Event or emergency? Two response systems in the mammalian superior colliculus. *Trends in Neurosciences,* 12**,** 137-147.
DIELENBERG, R. A., HUNT, G. E. & MCGREGOR, I. S. 2001. 'When a rat smells a cat': The distribution of Fos immunoreactivity in rat brain following exposure to a predatory odor. *Neuroscience,* 104**,** 1085-1097.
DOMESICK, V. B. 1969. Projections from the cingulate cortex in the rat. *Brain Research,* 12**,** 296-320.
DONAHUE, R. R., LAGRAIZE, S. C. & FUCHS, P. N. 2001. Electrolytic lesion of the anterior cingulate cortex decreases inflammatory, but not neuropathic nociceptive behavior in rats. *Brain Res,* 897**,** 131-8.
DRAGER, U. C. & HUBEL, D. H. 1976. Topography of visual and somatosensory projections to mouse superior colliculus. *Journal of Neurophysiology,* 39**,** 91-101.
DUAN, C. A., ERLICH, J. C. & BRODY, C. D. 2015. Requirement of Prefrontal and Midbrain Regions for Rapid Executive Control of Behavior in the Rat. *Neuron,* 86**,** 1491-1503.
ERLICH, J., BIALEK, M. & BRODY, C. 2011. A cortical substrate for memory-guided orienting in the rat. *Neuron,* 72**,** 330-343.
FAVARO, P. D., GOUVEA, T. S., DE OLIVEIRA, S. R., VAUTRELLE, N., REDGRAVE, P. & COMOLI, E. 2011. The influence of vibrissal somatosensory processing in rat superior colliculus on prey capture. *Neuroscience,* 176**,** 318-27.
FELLEMAN, D. J., BURKHALTER, A. & VAN ESSEN, D. C. 1997. Cortical connections of areas V3 and VP of macaque monkey extrastriate visual cortex. *The Journal of Comparative Neurology,* 379**,** 21-47.
FELSEN, G. & MAINEN, Z. F. 2008. Neural Substrates of Sensory-Guided Locomotor Decisions in the Rat Superior Colliculus. *Neuron,* 60**,** 137-148.
FELSEN, G. & MAINEN, Z. F. 2012. Midbrain contributions to sensorimotor decision making. *Journal of Neurophysiology,* 108**,** 135-147.

FEREZOU, I., HAISS, F., GENTET, L. J., ARONOFF, R., WEBER, B. & PETERSEN, C. C. H. 2007. Spatiotemporal Dynamics of Cortical Sensorimotor Integration in Behaving Mice. *Neuron,* 56**,** 907-923.

FRANKLIN, K. B. J. & PAXINOS, G. 2008. *The mouse brain in stereotaxic coordinates,* Amsterdam, Elsevier.

FRANKLIN, K. B. J. & PAXINOS, G. 2012. *The mouse brain in stereotaxic coordinates,* Amsterdam, Elsevier.

FREEDMAN, E. G., STANFORD, T. R. & SPARKS, D. L. 1996. Combined eye-head gaze shifts produced by electrical stimulation of the superior colliculus in rhesus monkeys. *Journal of Neurophysiology,* 76**,** 927-952.

FREEMAN JR, J. H., CUPPERNELL, C., FLANNERY, K. & GABRIEL, M. 1996. Context-specific multi-site cingulate cortical, limbic thalamic, and hippocampal neuronal activity during concurrent discriminative approach and avoidance training in rabbits. *Journal of Neuroscience,* 16**,** 1538-1549.

FRIES, P., REYNOLDS, J. H., RORIE, A. E. & DESIMONE, R. 2001. Modulation of Oscillatory Neuronal Synchronization by Selective Visual Attention. *Science,* 291**,** 1560-1563.

FURIGO, I. C., DE OLIVEIRA, W. F., DE OLIVEIRA, A. R., COMOLI, E., BALDO, M. V. C., MOTA-ORTIZ, S. R. & CANTERAS, N. S. 2010. The role of the superior colliculus in predatory hunting. *Neuroscience,* 165**,** 1-15.

GABBOTT, P. L. A., WARNER, T. A., JAYS, P. R. L., SALWAY, P. & BUSBY, S. J. 2005. Prefrontal cortex in the rat: Projections to subcortical autonomic, motor, and limbic centers. *Journal of Comparative Neurology,* 492**,** 145-177.

GABRIEL, M., KUBOTA, Y., SPARENBORG, S., STRAUBE, K. & VOGT, B. A. 1991. Effects of cingulate cortical lesions on avoidance learning and training-induced unit activity in rabbits. *Experimental Brain Research,* 86**,** 585-600.

GARRETT, M. E., NAUHAUS, I., MARSHEL, J. H. & CALLAWAY, E. M. 2014. Topography and areal organization of mouse visual cortex. *Journal of Neuroscience,* 34**,** 12587-12600.

GIESELMANN, M. A. & THIELE, A. 2008. Comparison of spatial integration and surround suppression characteristics in spiking activity and the local field potential in macaque V1. *European Journal of Neuroscience,* 28**,** 447-459.

GOLDBERG, M. E. & WURTZ, R. H. 1972a. ACTIVITY OF SUPERIOR COLLICULUS IN BEHAVING MONKEY .2. EFFECT OF ATTENTION ON NEURONAL RESPONSES. *Journal of Neurophysiology,* 35**,** 560-&.

GOLDBERG, M. E. & WURTZ, R. H. 1972b. Activity of superior colliculus in behaving monkey. I. Visual receptive fields of single neurons. *J Neurophysiol,* 35**,** 542-59.

GOODALE, M. A. & MURISON, R. C. 1975. The effects of lesions of the superior colliculus on locomotor orientation and the orienting reflex in the rat. *Brain Res,* 88**,** 243-61.

GOTTLIEB, J. P., KUSUNOKI, M. & GOLDBERG, M. E. 1998. The representation of visual salience in monkey parietal cortex. *Nature,* 391**,** 481-484.

GROVES, P. M. & THOMPSON, R. F. 1970. Habituation: A dual-process theory. *Psychological Review,* 77**,** 419-450.

GUANDALINI, P. 1998. The corticocortical projections of the physiologically defined eye field in the rat medial frontal cortex. *Brain Research Bulletin,* 47**,** 377-385.

GUO, Z. V., LI, N., HUBER, D., OPHIR, E., GUTNISKY, D., TING, J. T., FENG, G. & SVOBODA, K. 2014. Flow of cortical activity underlying a tactile decision in mice. *Neuron,* 81**,** 179-94.

HAEGENS, S., LUTHER, L. & JENSEN, O. 2012. Somatosensory anticipatory alpha activity increases to suppress distracting input. *J Cogn Neurosci,* 24**,** 677-85.

HAN, X. 2012. Optogenetics in the nonhuman primate. *Prog Brain Res,* 196**,** 215-33.

HANKS, T. D., KOPEC, C. D., BRUNTON, B. W., DUAN, C. A., ERLICH, J. C. & BRODY, C. D. 2015. Distinct relationships of parietal and prefrontal cortices to evidence accumulation. *Nature,* 520**,** 220-223.

HARRIS, L. R. 1980. The superior colliculus and movements of the head and eyes in cats. *Journal of Physiology,* VOL. 300**,** 367-391.

HARVEY, C. D., COEN, P. & TANK, D. W. 2012. Choice-specific sequences in parietal cortex during a virtual-navigation decision task. *Nature,* 484**,** 62-8.

HARVEY, C. D., COLLMAN, F., DOMBECK, D. A. & TANK, D. W. 2009. Intracellular dynamics of hippocampal place cells during virtual navigation. *Nature,* 461**,** 941-6.

HENDRICKSON, A. E., WILSON, J. R. & OGREN, M. P. 1978. The neuroanatomical organization of pathways between the dorsal lateral geniculate nucleus and visual cortex in Old World and New World primates. *J Comp Neurol,* 182**,** 123-36.

HENDRY, S. H. C. & REID, R. C. 2000. The Koniocellular Pathway in Primate Vision. *Annual Review of Neuroscience,* 23**,** 127-153.

HIKOSAKA, O. & WURTZ, R. H. 1985. Modification of saccadic eye movements by GABA-related substances. I. Effect of muscimol and bicuculline in monkey superior colliculus. *Journal of Neurophysiology,* 53**,** 266-291.
HILL, DANIEL N., CURTIS, JOHN C., MOORE, JEFFREY D. & KLEINFELD, D. 2011. Primary Motor Cortex Reports Efferent Control of Vibrissa Motion on Multiple Timescales. *Neuron,* 72**,** 344-356.
HO, J. W., POETA, D. L., JACOBSON, T. K., ZOLNIK, T. A., NESKE, G. T., CONNORS, B. W. & BURWELL, R. D. 2015. Bidirectional Modulation of Recognition Memory. *J Neurosci,* 35**,** 13323-35.
HOFBAUER, A. & DRÄGER, U. C. 1985. Depth segregation of retinal ganglion cells projecting to mouse superior colliculus. *The Journal of Comparative Neurology,* 234**,** 465-474.
HOFFMAN, G. E. & LE, W. W. 2004. Just cool it! Cryoprotectant anti-freeze in immunocytochemistry and in situ hybridization. *Peptides,* 25**,** 425-31.
HOFFMAN, J. E. & SUBRAMANIAM, B. 1995. The role of visual attention in saccadic eye movements. *Percept Psychophys,* 57**,** 787-95.
HOGLUND, E., WELTZIEN, F. A., SCHJOLDEN, J., WINBERG, S., URSIN, H. & DOVING, K. B. 2005. Avoidance behavior and brain monoamines in fish. *Brain Res,* 1032**,** 104-10.
HOOVER, W. B. & VERTES, R. P. 2007. Anatomical analysis of afferent projections to the medial prefrontal cortex in the rat. *Brain Structure and Function,* 212**,** 149-179.
HUBEL, D. H. & WIESEL, T. N. 1959. Receptive fields of single neurones in the cat's striate cortex. *The Journal of Physiology,* 148**,** 574-591.
HUBEL, D. H. & WIESEL, T. N. 1962. Receptive fields, binocular interaction and functional architecture in the cat's visual cortex. *The Journal of Physiology,* 160**,** 106-154.2.
HUBEL, D. H. & WIESEL, T. N. 1972. Laminar and columnar distribution of geniculo-cortical fibers in the macaque monkey. *The Journal of Comparative Neurology,* 146**,** 421-450.
HUBER, D., GUTNISKY, D. A., PERON, S., O/'CONNOR, D. H., WIEGERT, J. S., TIAN, L., OERTNER, T. G., LOOGER, L. L. & SVOBODA, K. 2012. Multiple dynamic representations in the motor cortex during sensorimotor learning. *Nature,* 484**,** 473-478.

IGNASHCHENKOVA, A., DICKE, P. W., HAARMEIER, T. & THIER, P. 2004. Neuron-specific contribution of the superior colliculus to overt and covert shifts of attention. *Nat Neurosci,* 7**,** 56-64.

INGLE, D. 1970. Visuomotor Functions of the Frog Optic Tectum. *Brain, Behavior and Evolution,* 3**,** 57-71.

INGLE, D. 1975. Focal attention in the frog: behavioral and physiological correlates. *Science,* 188**,** 1033-1035.

JAVAL, L. E. 1879. Essai sur la physiologie de la lecture. *Annales d'Oculistique,* 82 242 - 253.

JAY, M. F. & SPARKS, D. L. 1987. Sensorimotor integration in the primate superior colliculus. II. Coordinates of auditory signals. *Journal of Neurophysiology,* 57**,** 35-55.

JEONG, M., KIM, Y., KIM, J., FERRANTE, D. D., MITRA, P. P., OSTEN, P. & KIM, D. 2016. Comparative three-dimensional connectome map of motor cortical projections in the mouse brain. *Scientific Reports,* 6**,** 20072.

JI, W., GĂMĂNUȚ, R., BISTA, P., D'SOUZA, RINALDO D., WANG, Q. & BURKHALTER, A. 2015. Modularity in the Organization of Mouse Primary Visual Cortex. *Neuron,* 87**,** 632-643.

JOHANSEN, J. P. & FIELDS, H. L. 2004. Glutamatergic activation of anterior cingulate cortex produces an aversive teaching signal. *Nat Neurosci,* 7**,** 398-403.

JOHANSEN, J. P., FIELDS, H. L. & MANNING, B. H. 2001. The affective component of pain in rodents: direct evidence for a contribution of the anterior cingulate cortex. *Proc Natl Acad Sci U S A,* 98**,** 8077-82.

JOHNSON, E. N., HAWKEN, M. J. & SHAPLEY, R. 2001. The spatial transformation of color in the primary visual cortex of the macaque monkey. *Nat Neurosci,* 4**,** 409-416.

JOSHUA, I. G. & MICHAEL, N. S. 2007. The Neural Basis of Decision Making. *Annual Review of Neuroscience,* 30**,** 535-574.

KATSUKI, F. & CONSTANTINIDIS, C. 2012. Early involvement of prefrontal cortex in visual bottom-up attention. *Nat Neurosci,* 15**,** 1160-6.

KING, A. J. 2004. The superior colliculus. *Current Biology,* 14**,** R335-R338.

KIRVEL, R. D., GREENFIELD, R. A. & MEYER, D. R. 1974. Multimodal sensory neglect in rats with radical unilateral posterior isocortical and superior collicular ablations. *Journal of Comparative and Physiological Psychology,* 87**,** 156-162.

KISS, J. Z., HERTEL, R. & SACK, F. D. 1989. Amyloplasts are necessary for full gravitropic sensitivity in roots of Arabidopsis thaliana. *Planta,* 177**,** 198-206.

KLEIN, C., EVRARD, H. C., SHAPCOTT, K. A., HAVERKAMP, S., LOGOTHETIS, N. K. & SCHMID, M. C. 2016. Cell-Targeted Optogenetics and Electrical Microstimulation Reveal the Primate Koniocellular Projection to Supra-granular Visual Cortex. *Neuron,* 90**,** 143-51.

KNUDSEN, E. I., KNUDSEN, P. F. & MASINO, T. 1993. Parallel pathways mediating both sound localization and gaze control in the forebrain and midbrain of the barn owl. *J Neurosci,* 13**,** 2837-52.

KOPEC, C. D., ERLICH, J. C., BRUNTON, B. W., DEISSEROTH, K. & BRODY, C. D. 2015. Cortical and Subcortical Contributions to Short-Term Memory for Orienting Movements. *Neuron,* 88**,** 367-377.

KOWLER, E., ANDERSON, E., DOSHER, B. & BLASER, E. 1995. The role of attention in the programming of saccades. *Vision Res,* 35**,** 1897-916.

KVITSIANI, D., RANADE, S., HANGYA, B., TANIGUCHI, H., HUANG, J. Z. & KEPECS, A. 2013. Distinct behavioural and network correlates of two interneuron types in prefrontal cortex. *Nature,* advance online publication.

LEVAY, S., HUBEL, D. H. & WIESEL, T. N. 1975. The pattern of ocular dominance columns in macaque visual cortex revealed by a reduced silver stain. *The Journal of Comparative Neurology,* 159**,** 559-575.

LI, N., CHEN, T.-W., GUO, Z. V., GERFEN, C. R. & SVOBODA, K. 2015. A motor cortex circuit for motor planning and movement. *Nature,* 519**,** 51-56.

LIU, T., PESTILLI, F. & CARRASCO, M. 2005. Transient attention enhances perceptual performance and FMRI response in human visual cortex. *Neuron,* 45**,** 469-77.

LIVINGSTONE, M. & HUBEL, D. 1984. Anatomy and physiology of a color system in the primate visual cortex. *The Journal of Neuroscience,* 4**,** 309-356.

LIVINGSTONE, M. S. & HUBEL, D. H. 1982. Thalamic inputs to cytochrome oxidase-rich regions in monkey visual cortex. *Proc Natl Acad Sci U S A,* 79**,** 6098-101.

LU, Z. L. & DOSHER, B. A. 1998. External noise distinguishes attention mechanisms. *Vision Res,* 38**,** 1183-98.

LUCK, S. J., CHELAZZI, L., HILLYARD, S. A. & DESIMONE, R. 1997. Neural Mechanisms of Spatial Selective Attention in Areas V1, V2, and V4 of Macaque Visual Cortex. *Journal of Neurophysiology,* 77**,** 24-42.

MANITA, S., SUZUKI, T., HOMMA, C., MATSUMOTO, T., ODAGAWA, M., YAMADA, K., OTA, K., MATSUBARA, C., INUTSUKA, A., SATO, M., OHKURA, M., YAMANAKA, A., YANAGAWA, Y., NAKAI, J., HAYASHI, Y., LARKUM,

MATTHEW E. & MURAYAMA, M. 2015. A Top-Down Cortical Circuit for Accurate Sensory Perception. *Neuron,* 86**,** 1304-1316.
MARSHEL, J. H., GARRETT, M. E., NAUHAUS, I. & CALLAWAY, E. M. 2011. Functional specialization of seven mouse visual cortical areas. *Neuron,* 72**,** 1040-1054.
MCMAINS, S. & KASTNER, S. 2011. Interactions of Top-Down and Bottom-Up Mechanisms in Human Visual Cortex. *The Journal of neuroscience : the official journal of the Society for Neuroscience,* 31**,** 587-597.
MEEK, J. 1983. Functional anatomy of the tectum mesencephali of the goldfish. An explorative analysis of the functional implications of the laminar structural organization of the tectum. *Brain Research Reviews,* 6**,** 247-297.
MELCHER, D. & KOWLER, E. 2001. Visual scene memory and the guidance of saccadic eye movements. *Vision Research,* 41**,** 3597-3611.
MEREDITH, M. A. & STEIN, B. E. 1990. The visuotopic component of the multisensory map in the deep laminae of the cat superior colliculus. *Journal of Neuroscience,* 10**,** 3727-3742.
MEREDITH, M. A., WALLACE, M. T. & STEIN, B. E. 1992. Visual, auditory and somatosensory convergence in output neurons of the cat superior colliculus: multisensory properties of the tecto-reticulo-spinal projection. *Experimental Brain Research,* 88**,** 181-186.
MIDGLEY, G. C. & TEES, R. C. 1981. Orienting behavior by rats with visual cortical and subcortical lesions. *Experimental Brain Research,* 41**,** 316-328.
MILLER, M. W. 1987. The origin of corticospinal projection neurons in rat. *Exp Brain Res,* 67**,** 339-51.
MILLER, M. W. & VOGT, B. A. 1984. Direct connections of rat visual cortex with sensory, motor, and association cortices. *The Journal of Comparative Neurology,* 226**,** 184-202.
MONTEON, J. A., CONSTANTIN, A. G., WANG, H., MARTINEZ-TRUJILLO, J. & CRAWFORD, J. D. 2010. Electrical stimulation of the frontal eye fields in the head-free macaque evokes kinematically normal 3D gaze shifts. *J Neurophysiol,* 104**,** 3462-75.
MOORE, T. & ARMSTRONG, K. M. 2003. Selective gating of visual signals by microstimulation of frontal cortex. *Nature,* 421**,** 370-373.
MOORE, T. & FALLAH, M. 2001. Control of eye movements and spatial attention. *Proceedings of the National Academy of Sciences of the United States of America,* 98**,** 1273-1276.

MOORE, T. & FALLAH, M. 2004. Microstimulation of the Frontal Eye Field and Its Effects on Covert Spatial Attention. *Journal of Neurophysiology,* 91**,** 152-162.
MORAN, J. & DESIMONE, R. 1985. Selective attention gates visual processing in the extrastriate cortex. *Science,* 229**,** 782-784.
MUIR, J. L., EVERITT, B. J. & ROBBINS, T. W. 1996. The Cerebral Cortex of the Rat and Visual Attentional Function: Dissociable Effects of Mediofrontal, Cingulate, Anterior Dorsolateral, and Parietal Cortex Lesions on a Five-Choice Serial Reaction Time Task. *Cerebral Cortex,* 6**,** 470-481.
MÜLLER, J. R., PHILIASTIDES, M. G. & NEWSOME, W. T. 2005. Microstimulation of the superior colliculus focuses attention without moving the eyes. *Proceedings of the National Academy of Sciences of the United States of America,* 102**,** 524-529.
MUNOZ, D. P., PELISSON, D. & GUITTON, D. 1991. Movement of neural activity on the superior colliculus motor map during gaze shifts. *Science,* 251**,** 1358-1360.
NAGEL, G., SZELLAS, T., HUHN, W., KATERIYA, S., ADEISHVILI, N., BERTHOLD, P., OLLIG, D., HEGEMANN, P. & BAMBERG, E. 2003. Channelrhodopsin-2, a directly light-gated cation-selective membrane channel. *Proceedings of the National Academy of Sciences,* 100**,** 13940-13945.
NAKAYAMA, K. & MACKEBEN, M. 1989. Sustained and transient components of focal visual attention. *Vision Res,* 29**,** 1631-47.
NEAFSEY, E. J., HURLEY-GIUS, K. M. & ARVANITIS, D. 1986. The topographical organization of neurons in the rat medial frontal, insular and olfactory cortex projecting to the solitary nucleus, olfactory bulb, periaqueductal gray and superior colliculus. *Brain research,* 377**,** 561-570.
NEWMAN, E. A., GRUBERG, E. R. & HARTLINE, P. H. 1980. The infrared trigemino-tectal pathway in the rattlesnake and in the python. *J Comp Neurol,* 191**,** 465-77.
NGAN, N. H., MATSUMOTO, J., TAKAMURA, Y., TRAN, A. H., ONO, T. & NISHIJO, H. 2015. Neuronal correlates of attention and its disengagement in the superior colliculus of rat. *Frontiers in Integrative Neuroscience,* 9**,** 9.
O'KUSKY, J. & COLONNIER, M. 1982. A laminar analysis of the number of neurons, glia, and synapses in the adult cortex (area 17) of adult macaque monkeys. *J Comp Neurol,* 210**,** 278-90.
OH, S. W., HARRIS, J. A., NG, L., WINSLOW, B., CAIN, N., MIHALAS, S., WANG, Q., LAU, C., KUAN, L., HENRY, A. M., MORTRUD, M. T., OUELLETTE, B., NGUYEN, T. N., SORENSEN, S. A., SLAUGHTERBECK, C. R., WAKEMAN, W., LI,

Y., FENG, D., HO, A., NICHOLAS, E., HIROKAWA, K. E., BOHN, P., JOINES, K. M., PENG, H., HAWRYLYCZ, M. J., PHILLIPS, J. W., HOHMANN, J. G., WOHNOUTKA, P., GERFEN, C. R., KOCH, C., BERNARD, A., DANG, C., JONES, A. R. & ZENG, H. 2014. A mesoscale connectome of the mouse brain. *Nature,* 508**,** 207-214.

OHKI, K. & REID, R. C. 2007. Specificity and randomness in the visual cortex. *Curr Opin Neurobiol,* 17**,** 401-7.

OLCESE, U., IURILLI, G. & MEDINI, P. 2013. Cellular and Synaptic Architecture of Multisensory Integration in the Mouse Neocortex. *Neuron,* 79**,** 579-593.

PANIZZA, B. 1855. *Osservazioni sul nervo ottico,* Milano, Bernardoni.

PARÉ, M., CROMMELINCK, M. & GUITTON, D. 1994. Gaze shifts evoked by stimulation of the superior colliculus in the head-free cat conform to the motor map but also depend on stimulus strength and fixation activity. *Experimental Brain Research,* 101**,** 123-139.

PASTORIZA, L. N., MORROW, T. J. & CASEY, K. L. 1996. Medial frontal cortex lesions selectively attenuate the hot plate response: possible nocifensive apraxia in the rat. *Pain,* 64**,** 11-7.

PAVLOV, I. P. 1927. *Conditioned reflexes: an investigation of the physiological activity of the cerebral cortex,* Oxford, England, Oxford Univ. Press.

PAXINOS, G. & WATSON, C. 1986. *The rat brain in stereotaxic coordinates: hard cover edition.,* London, Academic Press.

PECK, C. K., BARO, J. A. & WARDER, S. M. 1995. Effects of eye position on saccadic eye movements and on the neuronal responses to auditory and visual stimuli in cat superior colliculus. *Exp Brain Res,* 103**,** 227-42.

PERRY, V. H. & COWEY, A. 1984. Retinal ganglion cells that project to the superior colliculus and pretectum in the macaque monkey. *Neuroscience,* 12**,** 1125-37.

PETROS, T. J., REBSAM, A. & MASON, C. A. 2008. Retinal Axon Growth at the Optic Chiasm: To Cross or Not to Cross. *Annual Review of Neuroscience,* 31**,** 295-315.

PISULA, W., TURLEJSKI, K. & CHARLES, E. P. 2013. Comparative psychology as unified psychology: The case of curiosity and other novelty-related behavior. *Review of General Psychology,* 17**,** 224-229.

POSNER, M. I. 1980. Orienting of attention. *Q J Exp Psychol,* 32**,** 3-25.

POSNER, M. I. & COHEN, Y. 1984. Components of visual orienting. *Attention and performance X: Control of language processes,* 32**,** 531-556.

REDGRAVE, P., DEAN, P., MITCHELL, I. J., ODEKUNLE, A. & CLARK, A. 1988. The projection from superior colliculus to cuneiform area in the rat - I. Anatomical studies. *Experimental Brain Research,* 72**,** 611-625.

REDGRAVE, P., DEAN, P. & WESTBY, G. W. M. 1990. Organization of the crossed tecto-reticulo-spinal projection in rat-I. Anatomical evidence for separate output channels to the periabducens area and caudal medulla. *Neuroscience,* 37**,** 571-584.

REDGRAVE, P., ODEKUNLE, A. & DEAN, P. 1986. Tectal cells of origin of predorsal bundle in rat: location and segregation from ipsilateral descending pathway. *Experimental Brain Research,* 63**,** 279-293.

REEP, R. L., CORWIN, J. V., HASHIMOTO, A. & WATSON, R. T. 1984. Afferent connections of medial precentral cortex in the rat. *Neurosci Lett,* 44**,** 247-52.

REEP, R. L., CORWIN, J. V., HASHIMOTO, A. & WATSON, R. T. 1987. Efferent Connections of the Rostral Portion of Medial Agranular Cortex in Rats. *Brain Research Bulletin,* 19**,** 203-221.

REYNOLDS, J. H. & CHELAZZI, L. 2004. Attentional modulation of visual processing. *Annu Rev Neurosci,* 27**,** 611-47.

REYNOLDS, J. H. & DESIMONE, R. 2003. Interacting Roles of Attention and Visual Salience in V4. *Neuron,* 37**,** 853-863.

RINGACH, D. L., MINEAULT, P. J., TRING, E., OLIVAS, N. D., GARCIA-JUNCO-CLEMENTE, P. & TRACHTENBERG, J. T. 2016. Spatial clustering of tuning in mouse primary visual cortex. *Nat Commun,* 7.

RIZZOLATTI, G., RIGGIO, L., DASCOLA, I. & UMILTÁ, C. 1987. Reorienting attention across the horizontal and vertical meridians: Evidence in favor of a premotor theory of attention. *Neuropsychologia,* 25**,** 31-40.

ROBERTS, M., DELICATO, L. S., HERRERO, J., GIESELMANN, M. A. & THIELE, A. 2007. Attention alters spatial integration in macaque V1 in an eccentricity-dependent manner. *Nat Neurosci,* 10**,** 1483-1491.

ROBINSON, D. A. 1972. Eye movements evoked by collicular stimulation in the alert monkey. *Vision Res,* 12**,** 1795-808.

ROELFSEMA, P. R., LAMME, V. A. F. & SPEKREIJSE, H. 1998. Object-based attention in the primary visual cortex of the macaque monkey. *Nature,* 395**,** 376-381.

RUDEBECK, P. H., WALTON, M. E., SMYTH, A. N., BANNERMAN, D. M. & RUSHWORTH, M. F. S. 2006. Separate neural pathways process different decision costs. *Nat Neurosci,* 9**,** 1161-1168.

RUNYAN, C. A. & SUR, M. 2013. Response Selectivity Is Correlated to Dendritic Structure in Parvalbumin-Expressing Inhibitory Neurons in Visual Cortex. *The Journal of Neuroscience,* 33**,** 11724-11733.

SAHIBZADA, N., DEAN, P. & REDGRAVE, P. 1986. Movements resembling orientation or avoidance elicited by electrical stimulation of the superior colliculus in rats. *Journal of Neuroscience,* 6**,** 723-733.

SCHALL, J. D. 2004. On the role of frontal eye field in guiding attention and saccades. *Vision Research,* 44**,** 1453-1467.

SCHILLER, P. H. 1977. The effect of superior colliculus ablation on saccades elicited by cortical stimulation. *Brain Research,* 122**,** 154-156.

SCHILLER, P. H., SANDELL, J. H. & MAUNSELL, J. H. 1987. The effect of frontal eye field and superior colliculus lesions on saccadic latencies in the rhesus monkey. *Journal of Neurophysiology,* 57**,** 1033-1049.

SCHILLER, P. H. & STRYKER, M. 1972. Single-unit recording and stimulation in superior colliculus of the alert rhesus monkey. *J Neurophysiol,* 35**,** 915-24.

SCHINDELIN, J., ARGANDA-CARRERAS, I., FRISE, E., KAYNIG, V., LONGAIR, M., PIETZSCH, T., PREIBISCH, S., RUEDEN, C., SAALFELD, S., SCHMID, B., TINEVEZ, J.-Y., WHITE, D. J., HARTENSTEIN, V., ELICEIRI, K., TOMANCAK, P. & CARDONA, A. 2012. Fiji: an open-source platform for biological-image analysis. *Nat Meth,* 9**,** 676-682.

SCHMUED, L. C. & HEIMER, L. 1990. Iontophoretic injection of fluoro-gold and other fluorescent tracers. *Journal of Histochemistry and Cytochemistry,* 38**,** 721-723.

SCHÜTZ, A. C., BRAUN, D. I. & GEGENFURTNER, K. R. 2009. Object recognition during foveating eye movements. *Vision Research,* 49**,** 2241-2253.

SCOTT, B. B., CONSTANTINOPLE, C. M., ERLICH, J. C., TANK, D. W. & BRODY, C. D. 2015. Sources of noise during accumulation of evidence in unrestrained and voluntarily head-restrained rats. *eLife,* 4**,** e11308.

SHANG, C., LIU, Z., CHEN, Z., SHI, Y., WANG, Q., LIU, S., LI, D. & CAO, P. 2015. A parvalbumin-positive excitatory visual pathway to trigger fear responses in mice. *Science,* 348**,** 1472-1477.

SHIPP, S. & ZEKI, S. 1985. Segregation of pathways leading from area V2 to areas V4 and V5 of macaque monkey visual cortex. *Nature,* 315**,** 322-5.

SHYU, B. C., CHEN, W. F. & SHIH, H. C. 2008. Electrically and mechanically evoked nociceptive neuronal responses in the rat anterior cingulate cortex. *Acta Neurochir Suppl,* 101**,** 23-5.
SIEGEL, M., DONNER, T. H., OOSTENVELD, R., FRIES, P. & ENGEL, A. K. 2008. Neuronal Synchronization along the Dorsal Visual Pathway Reflects the Focus of Spatial Attention. *Neuron,* 60**,** 709-719.
SIKES, R. W. & VOGT, B. A. 1992. Nociceptive neurons in area 24 of rabbit cingulate cortex. *Journal of Neurophysiology,* 68**,** 1720-1732.
SIKES, R. W., VOGT, L. J. & VOGT, B. A. 2008. Distribution and properties of visceral nociceptive neurons in rabbit cingulate cortex. *PAIN®,* 135**,** 160-174.
SINNAMON, H. M. & GALER, B. S. 1984. Head movements elicited by electrical stimulation of the anteromedial cortex of the rat. *Physiology and Behavior,* 33**,** 185-190.
SMITH, N. J., HORST, N. K., LIU, B., CAETANO, M. S. & LAUBACH, M. 2010. Reversible Inactivation of Rat Premotor Cortex Impairs Temporal Preparation, but not Inhibitory Control, During Simple Reaction-Time Performance. *Frontiers in Integrative Neuroscience,* 4**,** 124.
SPRENGER, W. W., HOFF, W. D., ARMITAGE, J. P. & HELLINGWERF, K. J. 1993. The eubacterium Ectothiorhodospira halophila is negatively phototactic, with a wavelength dependence that fits the absorption spectrum of the photoactive yellow protein. *Journal of Bacteriology,* 175**,** 3096-3104.
STEIN, B. E. 1981. Organization of the rodent superior colliculus: Some comparisons with other mammals. *Behavioural Brain Research,* 3**,** 175-188.
STEIN, B. E. & CLAMANN, H. P. 1981. Control of pinna movements and sensorimotor register in cat superior colliculus. *Brain, Behavior and Evolution,* 19**,** 180-192.
STEIN, B. E. & GAITHER, N. S. 1981. Sensory representation in reptilian optic tectum: Some comparisons with mammals. *The Journal of Comparative Neurology,* 202**,** 69-87.
STEIN, B. E., STANFORD, T. R. & ROWLAND, B. A. 2014. Development of multisensory integration from the perspective of the individual neuron. *Nature reviews. Neuroscience,* 15**,** 520-535.
STEINMETZ, M. A., CONNOR, C. E., CONSTANTINIDIS, C. & MCLAUGHLIN, J. R. 1994. Covert attention suppresses neuronal responses in area 7a of the posterior parietal cortex. *J Neurophysiol,* 72**,** 1020-3.

STRYKER, M. P. & SCHILLER, P. H. 1975. Eye and head movements evoked by electrical stimulation of monkey superior colliculus. *Experimental Brain Research,* 23**,** 103-112.
STUBBLEFIELD, E. A., COSTABILE, J. D. & FELSEN, G. 2013. Optogenetic investigation of the role of the superior colliculus in orienting movements. *Behavioural Brain Research,* 255**,** 55-63.
STUPHORN, V., BAUSWEIN, E. & HOFFMANN, K.-P. 2000. Neurons in the Primate Superior Colliculus Coding for Arm Movements in Gaze-Related Coordinates. *Journal of Neurophysiology,* 83**,** 1283-1299.
SUL, J. H., JO, S., LEE, D. & JUNG, M. W. 2011. Role of rodent secondary motor cortex in value-based action selection. *Nat Neurosci,* 14**,** 1202-1208.
SUNDBERG, K. A., MITCHELL, J. F. & REYNOLDS, J. H. 2009. Spatial Attention Modulates Center-Surround Interactions in Macaque Visual Area V4. *Neuron,* 61**,** 952-963.
SUPER, H. & ROELFSEMA, P. R. 2005. Chronic multiunit recordings in behaving animals: advantages and limitations. *Prog Brain Res,* 147**,** 263-82.
TANG, J., KO, S., DING, H. K., QIU, C. S., CALEJESAN, A. A. & ZHUO, M. 2005. Pavlovian fear memory induced by activation in the anterior cingulate cortex. *Mol Pain,* 1**,** 6.
TAYLOR, A. M., JEFFERY, G. & LIEBERMAN, A. R. 1986. Subcortical afferent and efferent connections of the superior colliculus in the rat and comparisons between albino and pigmented strains. *Experimental Brain Research,* 62**,** 131-142.
THEEUWES, J. 1991. Exogenous and endogenous control of attention: The effect of visual onsets and offsets. *Perception & Psychophysics,* 49**,** 83-90.
THIELE, A., DELICATO, L. S., ROBERTS, M. J. & GIESELMANN, M. A. 2006. A novel electrode-pipette design for simultaneous recording of extracellular spikes and iontophoretic drug application in awake behaving monkeys. *J Neurosci Methods,* 158**,** 207-11.
THIELE, A., RÜBSAMEN, R. & HOFFMANN, K. P. 1996. Anatomical and physiological investigation of auditory input to the superior colliculus of the echolocating megachiropteran bat Rousettus aegyptiacus. *Experimental Brain Research,* 112**,** 223-236.
THIELE, A., VOGELSANG, M. & HOFFMANN, K. P. 1991. Pattern of retinotectal projection in the megachiropteran bat Rousettus aegyptiacus. *Journal of Comparative Neurology,* 314**,** 671-683.

THOMSON, A. M. & BANNISTER, A. P. 2003. Interlaminar Connections in the Neocortex. *Cerebral Cortex,* 13**,** 5-14.
THORNDIKE, E. L. 1927. The Law of Effect. *The American Journal of Psychology,* 39**,** 212-222.
TOOTELL, R., SWITKES, E., SILVERMAN, M. & HAMILTON, S. 1988. Functional anatomy of macaque striate cortex. II. Retinotopic organization. *The Journal of Neuroscience,* 8**,** 1531-1568.
TU, T. A. & KEATING, E. G. 2000. Electrical stimulation of the frontal eye field in a monkey produces combined eye and head movements. *Journal of Neurophysiology,* 84**,** 1103-1106.
UNGERLEIDER, L. G., GALKIN, T. W., DESIMONE, R. & GATTASS, R. 2008. Cortical Connections of Area V4 in the Macaque. *Cerebral Cortex,* 18**,** 477-499.
VANEY, D. I., PEICHL, L., WÄSSLE, H. & ILLING, R. B. 1981. Almost all ganglion cells in the rabbit retina project to the superior colliculus. *Brain Research,* 212**,** 447-453.
VOGELS, R. 2016. Sources of adaptation of inferior temporal cortical responses. *Cortex,* 80**,** 185-195.
VOGT, B. A. & MILLER, M. W. 1983. Cortical connections between rat cingulate cortex and visual, motor, and postsubicular cortices. *Journal of Comparative Neurology,* 216**,** 192-210.
VON HELMHOLTZ, H. 1867. *Treatise on Physiological Optics Vol. III*, Dover.
WADHAMS, G. H. & ARMITAGE, J. P. 2004. Making sense of it all: bacterial chemotaxis. *Nat Rev Mol Cell Biol,* 5**,** 1024-1037.
WAGOR, E., MANGINI, N. J. & PEARLMAN, A. L. 1980. Retinotopic organization of striate and extrastriate visual cortex in the mouse. *The Journal of Comparative Neurology,* 193**,** 187-202.
WALLACE, D. J., GREENBERG, D. S., SAWINSKI, J., RULLA, S., NOTARO, G. & KERR, J. N. D. 2013. Rats maintain an overhead binocular field at the expense of constant fusion. *Nature,* 498**,** 65-69.
WALLACE, M. T., MEREDITH, M. A. & STEIN, B. E. 1993. Converging influences from visual, auditory, and somatosensory cortices onto output neurons of the superior colliculus. *Journal of Neurophysiology,* 69**,** 1797-1809.
WALLACE, M. T., WILKINSON, L. K. & STEIN, B. E. 1996. Representation and integration of multiple sensory inputs in primate superior colliculus. *Journal of Neurophysiology,* 76**,** 1246-1266.

WANG, F., CHEN, M., YAN, Y., ZHAOPING, L. & LI, W. 2015. Modulation of Neuronal Responses by Exogenous Attention in Macaque Primary Visual Cortex. *The Journal of Neuroscience,* 35**,** 13419-13429.
WANG, Q. & BURKHALTER, A. 2007. Area map of mouse visual cortex. *The Journal of Comparative Neurology,* 502**,** 339-357.
WATSON JR, R. E., WIEGAND, S. J., CLOUGH, R. W. & HOFFMAN, G. E. 1986. Use of cryoprotectant to maintain long-term peptide immunoreactivity and tissue morphology. *Peptides,* 7**,** 155-159.
WEI, P., LIU, N., ZHANG, Z., LIU, X., TANG, Y., HE, X., WU, B., ZHOU, Z., LIU, Y., LI, J., ZHANG, Y., ZHOU, X., XU, L., CHEN, L., BI, G., HU, X., XU, F. & WANG, L. 2015. Processing of visually evoked innate fear by a non-canonical thalamic pathway. *Nature Communications,* 6.
WESTBY, G. W. M., KEAY, K. A., REDGRAVE, P., DEAN, P. & BANNISTER, M. 1990. Output pathways from the rat superior colliculus mediating approach and avoidance have different sensory properties. *Experimental Brain Research,* 81**,** 626-638.
WHIPPO, C. W. & HANGARTER, R. P. 2006. Phototropism: Bending towards Enlightenment. *The Plant Cell,* 18**,** 1110-1119.
WURTZ, R. H. & ALBANO, J. E. 1980. Visual-motor function of the primate superior colliculus. *Annual Review of Neuroscience,* 3**,** 189-226.
WYLIE, D. R., GUTIERREZ-IBANEZ, C., PAKAN, J. M. & IWANIUK, A. N. 2009. The optic tectum of birds: mapping our way to understanding visual processing. *Can J Exp Psychol,* 63**,** 328-38.
YAMAMURA, H., IWATA, K., TSUBOI, Y., TODA, K., KITAJIMA, K., SHIMIZU, N., NOMURA, H., HIBIYA, J., FUJITA, S. & SUMINO, R. 1996. Morphological and electrophysiological properties of ACCx nociceptive neurons in rats. *Brain Research,* 735**,** 83-92.
YARBUS, A. L. 1967. *Eye Movements and Vision.* , New York, Plenum Press.
YILMAZ, M. & MEISTER, M. 2013. Rapid innate defensive responses of mice to looming visual stimuli. *Current biology : CB,* 23**,** 10.1016/j.cub.2013.08.015.
YUSTE, R. 2015. The Discovery of Dendritic Spines by Cajal. *Frontiers in Neuroanatomy,* 9.
ZAGHA, E., CASALE, AMANDA E., SACHDEV, ROBERT N. S., MCGINLEY, MATTHEW J. & MCCORMICK, DAVID A. 2013. Motor Cortex Feedback Influences Sensory Processing by Modulating Network State. *Neuron,* 79**,** 567-578.

ZEMELMAN, B. V., LEE, G. A., NG, M. & MIESENBÖCK, G. 2002. Selective Photostimulation of Genetically ChARGed Neurons. *Neuron,* 33**,** 15-22.
ZERNICKI, B. 1987. Pavlovian orienting reflex. *Acta Neurobiol Exp (Wars),* 47**,** 239-47.
ZHANG, F., WANG, L. P., BRAUNER, M., LIEWALD, J. F., KAY, K., WATZKE, N., WOOD, P. G., BAMBERG, E., NAGEL, G., GOTTSCHALK, A. & DEISSEROTH, K. 2007. Multimodal fast optical interrogation of neural circuitry. *Nature,* 446**,** 633-9.
ZHANG, S., XU, M., KAMIGAKI, T., HOANG DO, J. P., CHANG, W. C., JENVAY, S., MIYAMICHI, K., LUO, L. & DAN, Y. 2014. Selective attention. Long-range and local circuits for top-down modulation of visual cortex processing. *Science,* 345**,** 660-5.
ZHAO, Z. & DAVIS, M. 2004. Fear-Potentiated Startle in Rats Is Mediated by Neurons in the Deep Layers of the Superior Colliculus/Deep Mesencephalic Nucleus of the Rostral Midbrain through the Glutamate Non-NMDA Receptors. *The Journal of Neuroscience,* 24**,** 10326-10334.
ZILLES, K. 1985. *The cortex of the rat : a stereotaxic atlas,* Berlin, Springer-Verlag.
ZINGG, B., HINTIRYAN, H., GOU, L., SONG, MONICA Y., BAY, M., BIENKOWSKI, MICHAEL S., FOSTER, NICHOLAS N., YAMASHITA, S., BOWMAN, I., TOGA, ARTHUR W. & DONG, H.-W. 2014. Neural Networks of the Mouse Neocortex. *Cell,* 156**,** 1096-1111.